

# **Upgrading a pyrolytic side stream by utilization as substrate for fungal L-malic acid production**

Zur Erlangung des akademischen Grades einer

DOKTORIN DER NATURWISSENSCHAFTEN (DR. RER. NAT.)

von der KIT-Fakultät für Chemieingenieurwesen und Verfahrenstechnik des  
Karlsruher Instituts für Technologie (KIT)

genehmigte

DISSERTATION

von

M. Sc. Christin Kubisch

aus Haldensleben, Sachsen-Anhalt

Tag der mündlichen Prüfung: 27.01.2023

Erstgutachter: Prof. Dr.-Ing. Matthias Franzreb

Zweitgutachterin: PD Dr.-Ing. Katrin Ochsenreither



# Acknowledgements

In the following, I want to thank all the people who accompanied me on my journey to the completion of this thesis and who contributed to the success of my work.

First of all, I would like to express my utmost gratitude to Prof. Dr. Christoph Syldatk for offering me the opportunity to become a part of his research group. Furthermore, I deeply thank my supervisor, Dr.-Ing. Katrin Ochsenreither for the conceptualization of this interesting project, her tireless support and for helping me to recognize my own achievements.

I'm also very grateful to Dr. Habibu Aliyu for his patience in guiding me through the process of writing my transcriptome paper and for sharing his extensive knowledge in this research area with me. Without your help, this part of the work would undoubtedly not have been possible.

Moreover, I would like to thank all TeBi employees for the great time and the pleasant working atmosphere they created by their presence. Special thanks to Susanne and Beate for their help in overcoming all bureaucratic hurdles and to Pascal for his great support in the lab. There is probably no HPLC problem that you cannot solve.

Thanks also to my current and former PhD colleagues Alba, Alberto, André, Caro, Fei, Flavio, Jens, Magda, Marcus, Nebyat, Olga, Rebecca, Teresa and Vanessa for their company and many interesting professional and private conversations. To my dear colleague and friend Aline: I am very grateful that we went through these years together and that I could always rely on you both as a lab partner and as a person.

Many thanks also to my students Manuel Brislinger, Steven Leonhardt, David Müller and Manuel Müller as well as to my research assistants Julia Hagemeister and Carmen Mandel. You all did an excellent job and made an important contribution to my research.

Furthermore, I am grateful for the financial support from the Federal Ministry of Education and Research.

Last but not least, I would like to express my love and deepest gratitude to my family and partner. Thank you for always providing me with a place to forget my worries and concerns.

# List of publications

## Peer reviewed original publications

**Kubisch, C.** & Ochsenreither, K. (2022). Detoxification of a pyrolytic aqueous condensate from wheat straw for utilization as substrate in *Aspergillus oryzae* DSM 1863 cultivations. *Biotechnology for Biofuels and Bioproducts*, 15(1), 18.

**Kubisch C.** & Ochsenreither K. (2022) Valorization of a Pyrolytic Aqueous Condensate and Its Main Components for L-Malic Acid Production with *Aspergillus oryzae* DSM 1863. *Fermentation*, 8(3), 107.

**Kubisch, C.**, Kövilein, A., Aliyu, H., Ochsenreither, K. (2022) RNA-Seq Based Transcriptome Analysis of *Aspergillus oryzae* DSM 1863 Grown on Glucose, Acetate and an Aqueous Condensate from the Fast Pyrolysis of Wheat Straw. *Journal of Fungi*, 8(8), 765.

## Review

Kövilein, A.\*, **Kubisch, C.\***, Cai, L., Ochsenreither, K. (2020). Malic acid production from renewables: a review. *Journal of chemical technology & biotechnology*, 95(3), 513-526.

\*Co-first authorship

## Conference Posters

**Kubisch C.** & Ochsenreither K. (2021). Microbial utilization of process waters derived from thermochemical biomass conversion processes, DECHEMA Himmelfahrtstagung

**Kubisch C.** & Ochsenreither K. (2022). Valorization of an aqueous pyrolytic condensate for L-malic acid production with *Aspergillus oryzae* DSM 1863, Annual conference of the association for general and applied microbiology (VAAM)

# Preamble

As a cumulative thesis, this work is largely based on peer-reviewed research articles. All articles were published during this work and describe the main findings on the valorization of a pyrolytic aqueous condensate by utilizing it as a substrate for L-malic acid production with the filamentous fungus *Aspergillus oryzae*. The text of chapters that are based on these articles is therefore partly identical to the content of the publications, but layout, citation style, figures and formatting have been adjusted to the style of this dissertation. The following chapters contain contents of previously published work:

**Chapter 1** describes the theoretical background of this thesis. The chapter on malic acid contained therein is largely based on the following publication:

Kövilein, A., Kubisch, C., Cai, L., and Ochsenreither, K. (2020). Malic acid production from renewables: a review. *Journal of chemical technology & biotechnology*, 95(3), 513-526.

**Chapter 2** provides an overview of the materials and methods used for this dissertation and therefore includes sections from all three research articles published during this work.

In **chapter 3**, the transcriptional stress response of *A. oryzae* to using the pyrolysis condensate as substrate in shake flasks was examined and potential targets for an improvement of the fungal tolerance by genetic modification were identified. The content of this chapter can be found in:

Kubisch, C., Kövilein, A., Aliyu, H., Ochsenreither, K. (2022) RNA-Seq Based Transcriptome Analysis of *Aspergillus oryzae* DSM 1863 Grown on Glucose, Acetate and an Aqueous Condensate from the Fast Pyrolysis of Wheat Straw. *Journal of Fungi*, 8(8), 765.

**Chapter 4** addressed the improvement of the fungal tolerance to the pyrolysis condensate by applying appropriate detoxification methods and is based on the following publication:

Kubisch, C. & Ochsenreither, K. (2022). Detoxification of a pyrolytic aqueous condensate from wheat straw for utilization as substrate in *Aspergillus oryzae* DSM 1863 cultivations. *Biotechnology for Biofuels and Bioproducts*, 15(1), 18.

**Chapter 5** focused on malate production from the detoxified condensate and its major constituents and was previously published as:

Kubisch C. & Ochsenreither K. (2022) Valorization of a Pyrolytic Aqueous Condensate and Its Main Components for L-Malic Acid Production with *Aspergillus oryzae* DSM 1863. *Fermentation*, 8(3), 107.

# Abstract

Climate change, an increasing world population and the associated scarcity of resources are among the key challenges of the 21st century and require a transformation of the fossil-based economy towards an intensified use of renewable feedstocks in resource-conserving processes. Lignocellulosic waste streams from agriculture and forestry are ideally suited as such feedstocks, as they are cost-effective owing to their high availability and also offer the advantage of not competing with the food industry.

The aqueous condensate formed during the pyrolytic conversion of wheat straw into liquid biofuels currently accumulates as such a lignocellulose-based waste stream due to its high water content and low calorific value. However, it still contains a variety of organic carbons that render it an interesting candidate for utilization as a substrate in microbial fermentations. Its use for biotechnological L-malic acid production with the filamentous fungus *Aspergillus oryzae* appears particularly promising, as this natural acid producer is capable of metabolizing acetate, one of the main components of the pyrolytic condensate. Since malic acid is currently produced mainly by chemical synthesis from fossil resources, this approach could simultaneously avoid the accumulation of a waste stream and enable a bio-based acid production process that is more economically competitive with conventional synthesis due to the low substrate costs.

The main objective of this work was therefore to establish a process for the production of this industrially relevant organic acid based on the pyrolytic aqueous condensate (PAC). However, in addition to utilizable carbon sources, PAC also contains several substances that impede microbial growth. Hence, the present work also involved the evaluation of potential approaches to increase the fungal PAC tolerance.

For this purpose, transcriptome analysis was performed in the 3rd chapter of this thesis to identify genes that show highly altered expression levels when using PAC as a substrate in shake flask cultures compared to glucose or acetate. Such genes may be of interest as future targets for genetic modification of *A. oryzae* aimed at improving the fungal usability of the pyrolysis condensate. Since acetate is a major component of PAC, rather similar changes in gene expression were observed, when both substrates were compared to the glucose control. The central transcriptional response to growth in the acetate-containing cultures was the upregulation of genes related to the glutathione system and the biosynthesis of the amino acids arginine, serine, cysteine, and tryptophan. Such changes in expression have already been described as typical cellular reactions to external stressors and thus show that even the use of acetate as the sole substrate induces a general stress response. Direct comparison of gene

expression during growth on acetate and PAC also provided insight into the transcriptional response of *A. oryzae* to inhibitors present in the pyrolysis condensate. Pyruvate metabolism proved to be the only significantly differentially expressed pathway between these two conditions and primarily included genes encoding various alcohol dehydrogenases and enzymes involved in the degradation of methylglyoxal. Furthermore, a strongly increased expression of a so-called "old yellow enzyme" was observed during growth on the pyrolysis condensate. All these enzymes are of great importance for improving the fungal tolerance by genetic modification, as they might be associated with the conversion of the partially toxic PAC components furfural, acetol, and 2-cyclopenten-1-one. However, targeted changes in the expression of genes related to the glutathione system and amino acid synthesis may also positively affect the overall stress resistance of the fungus, thus facilitating growth on the pyrolysis condensate.

Since the *A. oryzae* DSM1863 wild-type strain is unable to utilize PAC as a substrate without prior removal of inhibitory components, detoxification of the pyrolysis condensate by overliming, rotary evaporation, and subsequent activated carbon treatment was required before performing transcriptome analysis. However, the resulting increase in the fungal PAC tolerance was not sufficient to enable malate production, so further optimization of the pretreatment procedure was pursued in Chapter 4 of this thesis. In addition to the detoxification methods already mentioned, enzymatic treatment with laccase from the white rot fungus *Trametes versicolor* was studied, which is mainly aimed at the removal of phenolic components. For each pretreatment method, diverse reaction conditions were investigated and detoxification efficiency was assessed by growth tests and analysis of selected PAC components. Despite the removal of phenolic substances, laccase treatment did not significantly improve fungal tolerance towards the pyrolysis condensate, as the growth limit of 1.25 % PAC was comparable to the untreated control. By contrast, under optimized conditions, activated carbon, overliming, and rotary evaporation treatment allowed fungal growth on PAC concentrations up to 1.625 %, 12.5 %, and 30 %, respectively. A carbon load of 10 % and a treatment duration of 10 min were determined as optimal for the activated carbon treatment, whereas the overliming should ideally be performed at 100 °C and an initial pH of 12 adjusted with NaOH. The best detoxification results were obtained after 4 h of rotary evaporation at 200 mbar, as a complete removal of guaiacol and a strong reduction in the concentrations of acetol, furfural, 2-cyclopenten-1-one and phenol by 84.9 %, 95.4 %, 97.7 % and 86.2 %, respectively, were observed. After determining the optimal reaction conditions, all possible combinations of the individual detoxification methods were performed and it was found that

sequential treatment of the pyrolysis condensate using rotary evaporation, overliming, and activated carbon allowed the use of 100 % PAC as the sole substrate for growth of *A. oryzae*. Finally, in chapter 5 of this dissertation, it was evaluated whether treatment with the optimized detoxification procedure would allow fungal L-malic acid production from the carbon sources contained in the pyrolysis condensate. However, based on the indications that emerged from the results of the transcriptome analysis, it was first investigated whether acetol, the second main component of the PAC, might also serve as a potential carbon source (C-source) for *A. oryzae* cultivations. Therefore, the suitability of different acetol concentrations for fungal biomass formation and malate production was studied in shake flask cultures containing the ketone as the only C-source or in simple PAC model mixtures with 40 g/L acetate. It was found that acetol levels up to 40 g/L could be used as sole substrate for growth of *A. oryzae*, but increasing inhibition was observed with higher acetol concentrations. However, a formation of malic acid solely on the basis of the ketone did not seem feasible. An increasing inhibitory effect of acetol was also observed in the cultivations with PAC model mixtures, and a concentration of 20 g/L was found to be the upper limit for both growth and malate production. Accordingly, the removal of the ketone from the pyrolysis condensate by appropriate pretreatment methods seems indeed essential to ensure effective malic acid production. Using the optimized detoxification procedure from the previous chapter, the acetol concentration in the PAC was reduced to approximately 3 g/L, which allowed the formation of a maximum malate titer of  $3.37 \pm 0.61$  g/L in a first shake flask cultivation. In this experiment, the high pH of the cultures was identified as a critical factor preventing the production of even higher malic acid concentrations. Therefore, an optimization of the initial medium pH was performed using 96 % sulfuric acid and 100 % acetic acid, resulting in an increase in malate titers to  $8.29 \pm 0.26$  g/L and  $9.77 \pm 0.55$  g/L, respectively. Finally, the optimized process was successfully transferred to 500 mL bioreactors, achieving a total malate productivity of  $0.051 \pm 0.002$  g/(L·h), which was the highest value among all PAC cultivations performed in this work.

In summary, it was shown that the choice of appropriate detoxification methods allows the use of the pyrolysis condensate as a substrate for malate production with *A. oryzae*. However, in order to strive for a complete utilization of the condensate and to keep the costs for pretreatment as low as possible, approaches to increase the fungal PAC tolerance by genetic modification should also be pursued in the future. This work has provided a good basis for such approaches by identifying genes involved in the fungal response to the presence of the pyrolysis condensate and the inhibitors it contains.

# Zusammenfassung

Der Klimawandel, das zunehmende Bevölkerungswachstum sowie die damit verbundene Verknappung von Ressourcen zählen zu den zentralen Herausforderungen des 21. Jahrhunderts und erfordern langfristig eine Umstrukturierung der auf fossilen Energieträgern basierenden Wirtschaft hin zu einem verstärkten Einsatz nachwachsender Rohstoffe in ressourcenschonenden, kreislauffähigen Prozessen. Lignocellulosehaltige Restströme aus der Land- und Forstwirtschaft eignen sich in besonderem Maße als solche Rohstoffe, da sie dank ihrer hohen Verfügbarkeit kostengünstig sind und zudem den Vorteil bieten, nicht in Konkurrenz zur Lebensmittelindustrie zu stehen.

Das wässrige Kondensat, das bei der pyrolytischen Umwandlung von Weizenstroh zu flüssigen Biokraftstoffen entsteht, fällt aufgrund seines hohen Wassergehalts und niedrigen Heizwertes derzeit als ein solcher lignocellulosebasierter Reststrom an. Es enthält jedoch diverse organische Kohlenstoffverbindungen, die es für eine stoffliche Verwertung als Substrat in mikrobiellen Fermentationen interessant machen. Als besonders vielversprechend ist dabei der Einsatz für eine biotechnologische L-Äpfelsäureproduktion mit dem Schimmelpilz *Aspergillus oryzae* anzusehen, da der natürliche Säureproduzent in der Lage ist, mit Acetat einen der Hauptbestandteile des Pyrolysekondensats zu verstoffwechseln. Da Äpfelsäure aktuell weitestgehend über chemische Synthese aus fossilen Rohstoffen gewonnen wird, könnte mit diesem Vorhaben gleichzeitig das Anfallen eines ungenutzten Reststromes vermieden und ein bio-basierter Säureproduktionsprozess etabliert werden, der aufgrund der geringen Substratkosten wirtschaftlich konkurrenzfähiger zu herkömmlichen Herstellungsverfahren ist. Das Hauptziel dieser Arbeit bestand daher in der Etablierung eines Verfahrens zur Herstellung dieser vor allem für die Lebensmittelindustrie bedeutsamen organischen Säure auf Basis des Pyrolysekondensats. Da das sogenannte Schwelwasser neben verwertbaren Kohlenstoffen jedoch auch eine Vielzahl an Komponenten enthält, die das mikrobielle Wachstum erschweren, wurden in der aktuellen Arbeit auch potentielle Ansätze zur Erhöhung der pilzlichen Toleranz gegenüber dem Pyrolysekondensat untersucht.

Mittels Transkriptom-Analyse sollten dafür im 3. Kapitel dieser Dissertation Gene identifiziert werden, die bei der Verwendung von Schwelwasser als Substrat in Schüttelkolbenkulturen eine stark veränderte Expression im Vergleich zu Glucose und Acetat aufweisen. Solche Gene könnten in Zukunft als Ansatzpunkte für Manipulationen des Genoms von *A. oryzae* interessant sein, die auf die Verbesserung der Schwelwasserverwertbarkeit abzielen.

Da Acetat ein Hauptbestandteil des Schwelwassers ist, zeigten sich für beide Substrate verglichen mit Glukose teilweise ähnliche Änderungen in der Genexpression. Als zentrale transkriptionelle Reaktion auf das Wachstum in den acetathaltigen Kulturen wurde dabei die Hochregulierung von Genen beobachtet, die mit dem Glutathion-System sowie der Biosynthese der Aminosäuren Arginin, Serin, Cystein und Tryptophan assoziiert sind. Solche Expressionsänderungen wurden bereits als typische Reaktion auf externe Stressoren beschrieben und zeigen demnach, dass selbst der Einsatz von Acetat als alleiniges Substrat eine pilzliche Stressantwort induziert. Über den direkten Vergleich der Genexpression bei Wachstum auf Acetat und Schwelwasser konnte zudem ein Einblick in die transkriptionelle Antwort von *A. oryzae* auf die im Pyrolysekondensat vorhandenen Inhibitoren gewonnen werden. Der Pyruvat-Metabolismus erwies sich dabei als der einzige Stoffwechselweg mit einer signifikant unterschiedlichen Expression und umfasste in erster Linie Gene, die für verschiedene Alkoholdehydrogenasen sowie für am Abbau von Methylglyoxal beteiligte Enzyme kodieren. Zudem hatte sich bei Wachstum auf Schwelwasser eine stark erhöhte Expression eines sogenannten „old yellow enzymes“ ergeben. All diese Enzyme sind von großem Interesse für die Erhöhung der pilzlichen Schwelwassertoleranz mittels genetischer Modifikation, da sie mit dem Abbau der teils toxisch wirkenden Schwelwasserkomponenten Furfural, Acetol und 2-Cyclopenten-1-on in Verbindung stehen. Aber auch eine gezielte Variation des Expressionslevels von Genen des Glutathion-Systems und der Aminosäuresynthese können sich positiv auf die allgemeine Stressresistenz des Pilzes auswirken und zukünftig das Wachstum auf Schwelwasser erleichtern.

Da der *A. oryzae* DSM1863 Wildtypstamm ohne eine vorherige Entfernung inhibierender Komponenten nicht in der Lage ist, das Schwelwasser als Substrat zu nutzen, musste bereits im Vorfeld der Transkriptom-Analyse eine Detoxifizierung des Pyrolysekondensats mittels Overliming, Rotationsverdampfen und anschließender Aktivkohlebehandlung erfolgen. Die dadurch erzielte Steigerung der pilzlichen Schwelwassertoleranz war jedoch nicht ausreichend, um eine Malatproduktion zu gewährleisten, so dass im Kapitel 4 dieser Arbeit eine weitere Optimierung der Vorbehandlungsprozedur angestrebt wurde. Neben den bereits genannten Methoden zur Detoxifizierung des Schwelwassers wurde auch eine enzymatische Behandlung mit Laccase aus dem Weißfäulepilz *Trametes versicolor* durchgeführt, die sich vor allem gegen phenolische Komponenten des Kondensats richtet. Für jede einzelne Vorbehandlungsmethode wurden diverse Reaktionsbedingungen untersucht und die Detoxifizierungseffizienz anhand von Wachstumstests und der Analyse ausgewählter Schwelwasserkomponenten beurteilt. Dabei zeigte sich für die Laccasebehandlung trotz der Entfernung phenolischer Substanzen mit

einem Wachstum auf maximal 1,25 % Schwelwasser keine nennenswerte Verbesserung der pilzlichen Toleranz im Vergleich zur unbehandelten Kontrolle. Im Gegensatz dazu ermöglichten die Behandlungen mit Aktivkohle, Overliming und Rotationsverdampfung unter optimierten Bedingungen ein pilzliches Wachstum auf Schwelwasserkonzentrationen von bis zu 1,625 %, 12,5 % bzw. 30 %. Als optimal wurde dabei für die Aktivkohlebehandlung eine Kohlenstoffkonzentration von 10 % und eine Behandlungsdauer von 10 min ermittelt, während die Overlimingbehandlung idealerweise bei einem mit NaOH eingestellten initialen pH-Wert von 12 und 100 °C durchgeführt werden sollte. Die besten Detoxifizierungsergebnisse wurden mit der 4-stündigen Rotationsverdampfung bei 200 mbar erzielt, da eine vollständige Entfernung von Guajakol und eine starke Verringerung der Konzentrationen von Acetol, Furfural, 2-Cyclopenten-1-on und Phenol um 84,9 %, 95,4 %, 97,7 % bzw. 86,2 % beobachtet wurden. Nach der Identifizierung der optimalen Reaktionsbedingungen wurden Kombinationen der einzelnen Detoxifizierungsmethoden durchgeführt und festgestellt, dass eine sequentielle Behandlung des Pyrolysekondensats mittels Rotationsverdampfung, Overliming und Aktivkohle die Nutzung von 100 % Schwelwasser als alleiniges Substrat für das Wachstum von *A. oryzae* ermöglicht.

In Kapitel 5 dieser Dissertation wurde schließlich evaluiert, inwieweit sich das Kondensat aus der Schnellpyrolyse nach einer Behandlung mit dem optimierten Detoxifizierungsverfahren auch für die pilzliche L-Äpfelsäureproduktion eignet. Nachdem die Transkriptom-Analyse bereits erste Hinweise darauf ergeben hatte, sollte jedoch zuvor geprüft werden, ob mit Acetol auch der zweite Hauptbestandteil des Schwelwassers von *A. oryzae* als Substrat verwertet werden kann. Es wurden daher verschiedene Konzentrationen des Ketons als alleinige C-Quelle sowie in einfachen Schwelwassermodellmischungen mit 40 g/L Acetat auf ihre Eignung für die pilzliche Biomassebildung und Malatproduktion untersucht. Dabei zeigte sich, dass Acetolgehalte von bis zu 40 g/L für das Wachstum von *A. oryzae* eingesetzt werden können, wobei jedoch mit steigender Konzentration eine zunehmende Inhibierung festgestellt wurde. Eine Äpfelsäureproduktion alleine auf Basis des Ketons schien hingegen nicht möglich. Auch in den Kultivierungen mit Modellschwelwässern war eine zunehmende inhibierende Wirkung des Ketons zu beobachten, so dass für Konzentrationen über 20 g/L Acetol weder Wachstum noch eine Malatproduktion verzeichnet werden konnten. Demnach erscheint eine Entfernung des Ketons aus dem Schwelwasser über entsprechende Vorbehandlungen in der Tat notwendig, um eine effektive Säureproduktion zu gewährleisten. Mithilfe der optimierten Detoxifizierungsprozedur aus dem vorherigen Kapitel konnte die Acetolkonzentration im Schwelwasser auf ca. 3 g/L herabgesetzt und so in einer ersten Schüttelkolbenkultivierung ein

maximaler Malattiter von  $3,37 \pm 0,61$  g/L erzielt werden. Der hohe pH-Wert der Kulturen wurde dabei als ein kritischer Faktor identifiziert, der die Produktion noch höherer Äpfelsäurekonzentrationen verhinderte. Es erfolgte daher nachfolgend eine Optimierung des Anfangs-pH-Wertes unter Verwendung von 96 % Schwefelsäure und 100 % Essigsäure, die eine Steigerung der Malatproduktion auf  $8,29 \pm 0,26$  g/L bzw.  $9,77 \pm 0,55$  g/L ermöglichte. Abschließend wurde ein Scale-up des optimierten Prozesses in 500 mL Bioreaktoren vorgenommen und dabei mit einer Gesamtproduktivität von  $0,051 \pm 0,002$  g/(L·h) der bisher höchste Wert unter allen in dieser Arbeit durchgeführten Schwelwasserkultivierungen erzielt. Zusammenfassend konnte gezeigt werden, dass eine Verwendung des Pyrolysekondensats als Substrat für die Malatproduktion mit *A. oryzae* durch die Wahl geeigneter Detoxifizierungsmethoden grundsätzlich realisierbar ist. Um jedoch eine möglichst ganzheitliche Verwertung des Schwelwassers zu gewährleisten und die Kosten und den Aufwand für Vorbehandlungen so gering wie möglich zu halten, sollte auch der Ansatz einer genetischen Modifikation des Pilzes zukünftig weiterverfolgt werden. Mit dieser Arbeit wurde eine gute Grundlage für solche Ansätze geschaffen, da Gene identifiziert wurden, die an der Reaktion des Pilzes auf das Vorhandensein von Schwelwasser und den darin enthaltenen Inhibitoren beteiligt sind.

# Table of content

Acknowledgements .....	I
List of publications.....	II
Preamble.....	III
Abstract .....	V
Zusammenfassung.....	VIII
Table of content.....	XII
1. Theoretical background and research proposal .....	1
1.1. Malic acid.....	3
1.1.1. Microbial malic acid production routes.....	4
1.1.2. Fungi as natural malic acid producers.....	6
1.1.3. Alternative substrates for fungal malic acid production .....	7
1.2. (De-) composition of lignocellulosic biomass .....	9
1.2.1. Fast pyrolysis.....	12
1.3. Pyrolytic aqueous condensate (PAC).....	14
1.3.1. Composition .....	15
1.3.2. Detoxification.....	25
1.4. Research proposal .....	28
2. Materials and methods .....	29
2.1. Microorganism .....	29
2.2. Media and cultivation conditions .....	29
2.2.1. Conidia preparation .....	29
2.2.2. PAC tolerance tests on agar plates .....	30
2.2.3. Pre-cultures.....	30
2.2.4. Main cultures in shake flasks .....	31
2.2.5. Main culture in bioreactors .....	32
2.3. PAC formation and detoxification .....	33
2.3.1. Detoxification procedure for the transcriptome analysis .....	33
2.3.2. Optimization of the detoxification procedure .....	34
2.4. Transcriptome analysis.....	36
2.4.1. RNA isolation, library preparation and sequencing .....	36
2.4.2. RNA-seq data analysis .....	36

2.5.	Analytics.....	37
2.5.1.	Quantification of the fungal biomass formation.....	37
2.5.2.	High pressure liquid chromatographic (HPLC) analysis .....	37
2.5.3.	Gas chromatographic (GC) analysis of inhibiting PAC components .....	37
2.5.4.	Folin-Ciocalteu (FC) analysis .....	38
2.5.5.	Spectrometric quantification of ammonia .....	38
2.5.6.	Quantification of acetate by enzyme assays.....	38
3.	Variations in the fungal gene expression in response to growth on the pyrolytic aqueous condensate .....	39
3.1.	Introduction .....	41
3.2.	Results and discussion.....	42
3.2.1.	Characterization of fungal growth on the different carbon sources .....	42
3.2.2.	General characteristics of the RNA-seq data .....	44
3.2.3.	Differential gene expression during growth on the different carbon sources .....	45
3.2.4.	Functional enrichment and pathway analyses .....	47
4.	Optimization of the pretreatment procedure for detoxification of the pyrolytic aqueous condensate .....	75
4.1.	Introduction .....	77
4.2.	Results .....	78
4.2.1.	Single methods .....	78
4.2.2.	Combinations of methods.....	89
4.2.3.	<i>Aspergillus oryzae</i> pre-culture cultivation on detoxified PAC .....	92
4.3.	Discussion .....	94
4.3.1.	Single methods .....	94
4.3.2.	Combination of detoxification methods and <i>A. oryzae</i> cultivation.....	101
5.	Malic acid production from the pyrolytic aqueous condensate and its main components .....	103
5.1.	Introduction .....	105
5.2.	Results .....	106
5.2.1.	Utilization of acetol as substrate for biomass formation of <i>A. oryzae</i> .....	106
5.2.2.	Acetate-acetol mixtures as substrates for fungal growth .....	108
5.2.3.	L-malic acid production with acetate-acetol mixtures.....	111
5.2.4.	PAC as sole substrate for L-malic acid formation .....	114
5.3.	Discussion .....	121

5.3.1. Acetol utilization in <i>A. oryzae</i> pre-culture .....	121
5.3.2. Malic acid production on artificial and authentic PAC.....	123
6. Summary and conclusions.....	127
List of references .....	XV
List of figures .....	XLIX
List of tables .....	LII
Appendix .....	LIII

# 1. Theoretical background and research proposal

This chapter is partly based on the publication:

## **Malic acid production from renewables: a review**

Aline Kövilein\*, Christin Kubisch\*, Liyin Cai and Katrin Ochsenreither

\*Co-first authorship

Institute of Process Engineering in Life Science 2: Technical Biology, Karlsruhe Institute of  
Technology, Karlsruhe, Germany

## **Publication details:**

*Journal of chemical technology & biotechnology*

Volume: 95, Issue 3 765, Pages 513-526.

Publication date: 6 November 2019

DOI: 10.1002/jctb.6269

**Author's contribution:**

**Aline Kövilein** performed the conceptualization, writing of the original draft and the editing of the final manuscript.

**Christin Kubisch** performed the conceptualization, writing of the original draft and the editing of the final manuscript.

**Liyin Cai** constructively contributed to the content of this work and reviewed the final manuscript.

**Katrin Ochsenreither** performed the conceptualization, participated in writing the original draft and reviewed the final manuscript.

## 1.1. Malic acid

Malic acid is an aliphatic organic acid with a chain length of four carbon atoms (C-atoms), whose chemical structure is characterized by two carboxyl and one hydroxyl group. The presence of the latter results in the formation of a stereocenter at the alpha-C atom and thus the existence of two isoforms: L- and D-malic acid (**Figure 1**). In nature, however, the acid occurs exclusively in its L-form and is found in a variety of fruits [1–4]. Furthermore, the dicarboxylic acid is artificially added to foods and beverages as an acidifier and flavor enhancer (labelled as E 296) [5, 6], which currently accounts for the majority of its industrial application. Other potential fields of application include cosmetics [7], pharmaceutical [8] and feed industry [9], as well as metal leaching [10] and semiconductor cleaning [11]. Moreover, due to its functional groups, malic acid can be converted into a variety of high-value chemicals and was therefore selected by the U.S. Department of Energy as one of the top 12 building blocks that can be derived from biomass [12]. Especially its ability to serve as a raw material for the synthesis of various biopolymers [13] may become increasingly important in the future.

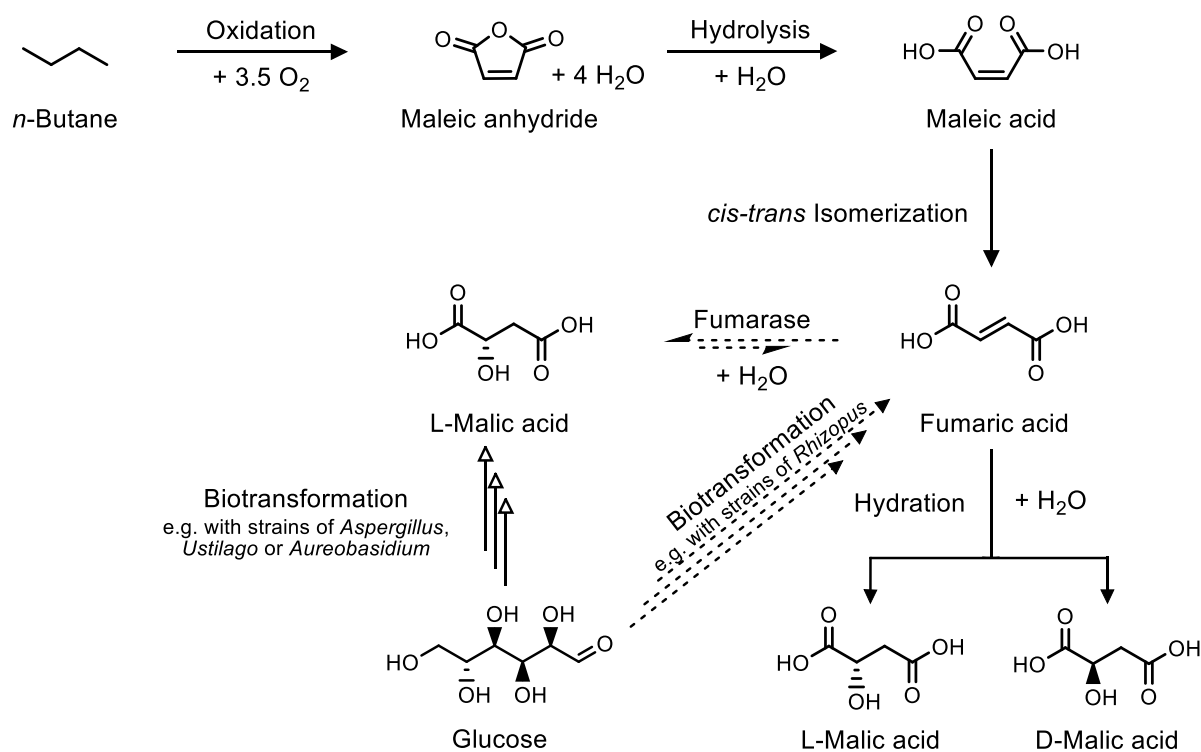


**Figure 1:** Overview of the different malic acid production routes. Solid arrows = chemical synthesis of a racemic DL-malic acid mixture; dashed arrows = enzymatic L-malate synthesis; hollow arrows = microbial L-malate formation

Currently, malic acid is mainly produced by chemical synthesis from maleic anhydride, which in turn is derived from the fossil hydrocarbon *n*-butane [14]. The first step in this malic acid synthesis process involves the hydrolysis of maleic anhydride to maleic acid followed by an isomerization to fumaric acid (**Figure 1**). The final hydration of fumaric acid leads to the formation of a crude malic acid liquor that contains a racemic mixture of D- and L-malic acid but also fumaric acid and small amounts of maleic acid. Although most fumaric acid can be separated from the reaction mixture by crystallization due to its low solubility, the remaining crude malic acid usually still contains between 1 and 3 % of fumaric and maleic acid each [15]. Pure DL-malic acid is therefore only obtained after further purification by liquid-liquid extraction and subsequent crystallization or chromatography.

The racemic mixture of D- and L-malic acid formed during chemical synthesis can be readily used for most food, beverage, cosmetics and cleaning products. However, some specific applications in the pharmaceutical or polymer industries, may require the production of enantiopure malic acid [13]. For this purpose, bio-based processes are preferable as they allow the formation of pure L-malate under milder reaction conditions than those used for chemical synthesis. One possible approach for bio-based malic acid production is the enzymatic hydration of fumaric acid (**Figure 1**). This biotransformation is catalyzed by fumarase and can be performed with purified enzyme [16, 17] or whole cells [17–20], both of which are usually immobilized to allow recycling of the catalyst [16, 21, 22]. However, since the fumaric acid required for this process is currently exclusively obtained via chemical synthesis from maleic anhydride [23], this process cannot be considered entirely bio-based. Therefore, microbial production of L-malic acid using renewable substrates represents a more sustainable alternative (**Figure 1**).

### 1.1.1. Microbial malic acid production routes

Since malic acid is an intermediate of the tricarboxylic acid (TCA) cycle, many aerobic microorganisms are naturally capable of producing this compound. In this so called oxidative TCA cycle (**Figure 2**, green), that takes place in the mitochondrion, acetyl-CoA condenses with oxaloacetate to form one molecule of citrate. The citrate is then further oxidized to L-malate in multiple enzymatic reaction steps accompanied by the release of two molecules of CO<sub>2</sub>. Due to the CO<sub>2</sub> losses, the maximum molar yield of this pathway is restricted to 1 mol malate per mol of glucose [24]. However, the presence of multiple isoforms of TCA cycle enzymes located either in the cytosol or in mitochondria [25, 26] suggests the existence of an additional cytosolic

L-malate production pathway. This pathway is referred to as the reductive TCA cycle (**Figure 2**, red) and involves the carboxylation of pyruvate to oxaloacetate catalyzed by pyruvate carboxylase (pyc) and the subsequent conversion of oxaloacetate to L-malate by malate dehydrogenase (mdh). If pyruvate is produced via glycolysis, this nonoxidative pathway is ATP neutral and involves a net fixation of CO<sub>2</sub>, resulting in a maximum theoretical L-malate yield of 2 mol/mol [24].

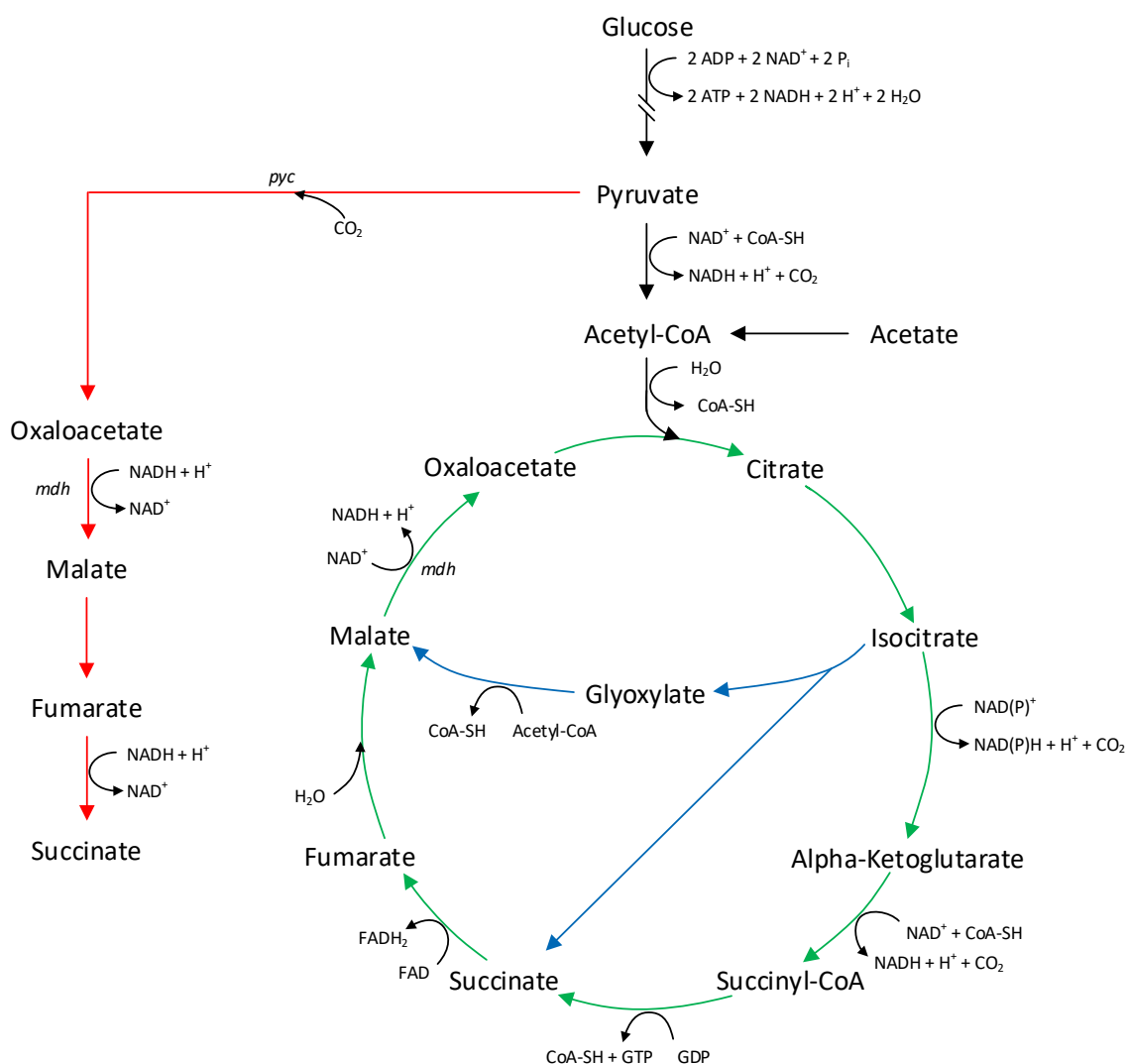


**Figure 2:** The three key pathways of L-malic acid production in microorganisms. Green = Oxidative tricarboxylic acid (TCA) cycle, red = Reductive TCA cycle, blue = Glyoxylate cycle

The citrate formed in the oxidative TCA cycle can also serve as an intermediate for the third malic acid production route, the glyoxylate cycle (**Figure 2**, blue). In this metabolic pathway, citrate is converted to succinate and glyoxylate followed by condensation of the latter with acetyl CoA to form L-malate. As the acetyl-CoA synthesis from pyruvate is accompanied by a CO<sub>2</sub> release, the maximum molar L-malate yield for the glyoxylate pathway is limited to

1 mol/mol. However, when the oxaloacetate used for citrate formation is replenished by the carboxylation of pyruvate, the maximum yield increases to 1.33 mol/mol [24].

### 1.1.2. Fungi as natural malic acid producers

The first patent dealing with the microbial production of L-malic acid was filed in 1962 and identified *Aspergillus flavus* as the most promising species among the genus *Aspergillus* since it formed up to 58.4 g/L malate after nine days of shake flask cultivation, corresponding to a molar yield of 0.79 mol/mol (glucose) and a productivity of 0.27 g/(L·h) [27]. Almost 30 years later, its outstanding natural L-malic acid production potential could be further enhanced by process optimization using a mineral salt medium containing glucose, a limiting amount of nitrogen and high concentrations of CaCO<sub>3</sub> for pH regulation and CO<sub>2</sub> supply. The implementation of the optimized conditions resulted in an almost complete conversion of 120 g/L glucose to 113 g/L malic acid with an overall productivity of 0.59 g/(L·h) after 190 h of cultivation in a 16-L fermenter [28]. However, *A. flavus* was found to be an aflatoxin producer in the 1960s [29] and has no longer been applicable for food-related malic acid production. Consequently, alternative production strains needed to be identified. Among these, *Aspergillus oryzae* appeared to be the most promising candidate, as it lacks aflatoxin biosynthesis [30], but shares high genetic sequence similarity with *A. flavus* [31]. The comparable L-malic acid production potential of *A. oryzae* indicated in the first patent [27] was confirmed by Knuf et al., when a maximum L-malate yield of 1.09 mol/mol (glucose) was obtained after 48 h of batch cultivation in 2-L reactors using the strain NRRL3488 [32]. Another *A. oryzae* wild-type strain (DSMZ1863) was evaluated for its malic acid production potential in 1.5-L bioreactor batch fermentations. After 168 h of cultivation, the strain had utilized 62.5 % of the 120 g/L glucose provided for the production of 43.5 g/L malate, resulting in a molar yield of 0.85 mol/mol [33]. In addition to *Aspergillus* species, there are other representatives of the fungal kingdom that are suitable for efficient natural L-malic acid production. For example, *Ustilago trichophora* TZ1 formed an L-malate titer of 195 ± 15 g/L within 264 h of CaCO<sub>3</sub>-buffered fed-batch cultivation on glycerol [34] and a *Rhizopus delemar* isolate showed the natural potential to produce 60 g/L malate from corn straw hydrolyte (**Table 1**) [35].

### 1.1.3. Alternative substrates for fungal malic acid production

Currently, microbial fermentation processes are largely based on glucose as an easily metabolized carbon source. However, the use of this edible sugar competes with the food industry and is furthermore comparatively expensive [36]. Therefore, glucose does not appear to be a suitable substrate for microbial processes aimed at replacing conventional chemical malate synthesis and more cost-effective, non-food alternatives need to be identified. As indicated by the fermentations with *U. trichophora* and *R. delemar* mentioned in the previous section, fungal organisms are capable of utilizing a variety of substrates for malate production (Table 1).

**Table 1:** Comparison of L-malic acid production from various renewable substrates

Substrate	Microorganism	Malate titer [g/L]	Yield [g/g]	Productivity [g/(L·h)]	Reference
Glycerol (crude)	<i>A. niger</i> ATCC 9142	16.5	0.17	0.09	[37, 38]
	<i>A. niger</i> ATCC 10577	20.3	0.20	0.11	[37, 38]
	<i>A. niger</i> ATCC 12846	23.5	0.24	0.12	[37, 38]
	<i>A. niger</i> PJR1	83.2	0.18 <sup>1</sup>	0.43	[39]
	<i>U. trichophora</i> TZ1	120	0.26	0.75	[34]
Glycerol (pure)	<i>U. trichophora</i> TZ1	195	0.43	0.74	[34]
	<i>A. oryzae</i> DSM 1863	45.4	0.54	0.13	[33]
Thin stillage	<i>A. niger</i> ATCC 9142	16.9	0.79	0.09	[38, 40]
	<i>A. niger</i> ATCC 10577	16.4	0.79	0.09	[38, 40]
Beech wood cellulose hydrolysate	<i>A. oryzae</i> DSM 1863	37.9	0.97	0.23	[41]
Beech wood hemicellulose fraction	<i>A. oryzae</i> DSM 1863	5.8	-	0.03	[41]
Miscanthus cellulose hydrolysate	<i>A. oryzae</i> DSM 1863	30.8	0.32	0.18	[41]
Corn straw hydrolysate	<i>R. delemar</i> HF-119	60	0.48	1.00	[35]
	<i>R. delemar</i> HF-121	120.5	0.96	2.01	[35]

<sup>1</sup> In the present author's opinion, the yield of 0.18 g/g as indicated in the publication is too low; from the data available the yield is estimated at  $\approx 0.6$  g/g.

This includes crude glycerol, which is the main by-product generated during biodiesel production and accounts for up to 10 % (w/w) of the final product [42]. Due to the expanding global demand for biodiesel, the market for crude glycerol is oversaturated, making it a

comparatively cost-effective feedstock [43]. Although glycerol is an important chemical used primarily for food, pharmaceutical, cosmetic and other personal care products [44], impurities in the crude glycerol hinder its utilization for these applications. Since purification involves additional costs, its use as a substrate for microbial malate production might be an alternative for the valorization of this by-product. Even though it has already been reported that impurities in crude glycerol may affect microbial viability [45], malate titers ranging from 16.5 g/L to 120 g/L were obtained with *U. trichophora* TZ1 and several *A. niger* strains (**Table 1**), highlighting the robustness of fungal organisms. A direct comparison of malate formation from crude and purified glycerol was performed for *U. trichophora* and resulted in comparable productivities [34]. However, the malate titer increased from 120 g/L to 195 g/L, when pure glycerol was used, suggesting that even higher malic acid concentrations are achievable if inhibition by impurities can be overcome. This has already been achieved by Iyyappan et al. who adapted *A. niger* to methanol, an important impurity in crude glycerol, and generated a strain that achieved 4.4-folds higher malate yield compared to the wild type [46].

Thin stillage, a by-product of bioethanol production from corn and grain, represents another potential substrate for microbial fermentations, that is also based on glycerol as a major constituent. In addition, it contains lactic acid and residual oligosaccharides, which may serve as additional carbon sources [47]. Its suitability to be converted to L-malate has already been proven by West et al. for several *Aspergillus* species, and a maximum titer of 16.9 g/L was obtained with *A. niger* ATCC 9142 (**Table 1**) [38, 40]. However, since the whole process of bioethanol production from corn and grain competes with the food and feed industry, it would be preferable to make use of the non-edible components of the plant.

This was done by Li et al. when they used corn straw hydrolysate as substrate for *R. delemar* HF-119 and achieved a malate titer of approximately 60 g/L after 60 h of cultivation. Mutation of the strain by exposure to soft-X ray greatly reduced the formation of ethanol as a by-product, and the maximum titer achieved by the newly generated strain *R. delemar* HF-121 was thus significantly increased to 120.5 g/L [35]. Accordingly, yield and productivity doubled to values of 0.96 g/g and 2.01 g/(L·h), respectively. Dörsam et al. also investigated different biomass hydrolysates and demonstrated their applicability as substrate for malate production with *A. oryzae* DSM 1863 [41]. They obtained the best results with beechwood cellulose hydrolysate, which allowed the formation of 37.9 g/L of malate with a yield of 0.97 g/g. Both studies show the great potential of lignocellulosic biomass to serve as a substrate for microbial fermentations, as the malate yields were in a comparable range to those obtained with glucose (0.68-1.11 g/g) [36]. In fact, the productivity of 2.01 g/(L·h) determined

for the cultivation with *R. delemar* HF-121 even represented the highest value ever achieved for microbial malate production processes. However, despite yielding high malate titers and productivities, the use of lignocellulosic substrates usually has the drawback that the biomass needs to be processed by methods like the aforementioned hydrolysis in order to be decomposed into metabolizable substances.

## 1.2. (De-) composition of lignocellulosic biomass

Lignocellulose is mainly composed of the three polymers cellulose ( $\approx 30-50\%$ ), hemicellulose ( $\approx 20-40\%$ ) and lignin ( $\approx 15-25\%$ ), with their proportion varying greatly depending on the plant species [48]. In addition, the plant matter contains various extractives like lipids, waxes, terpenoids and flavonoids as well as minerals (e.g. Na, Mg, K, Ca and Si), which are also referred to as ash [49]. Cellulose is a homopolymer consisting of linear chains of  $\beta$ -D-glucose units, that are linked by  $\beta$ -1,4-glycosidic bonds (**Figure 3**).

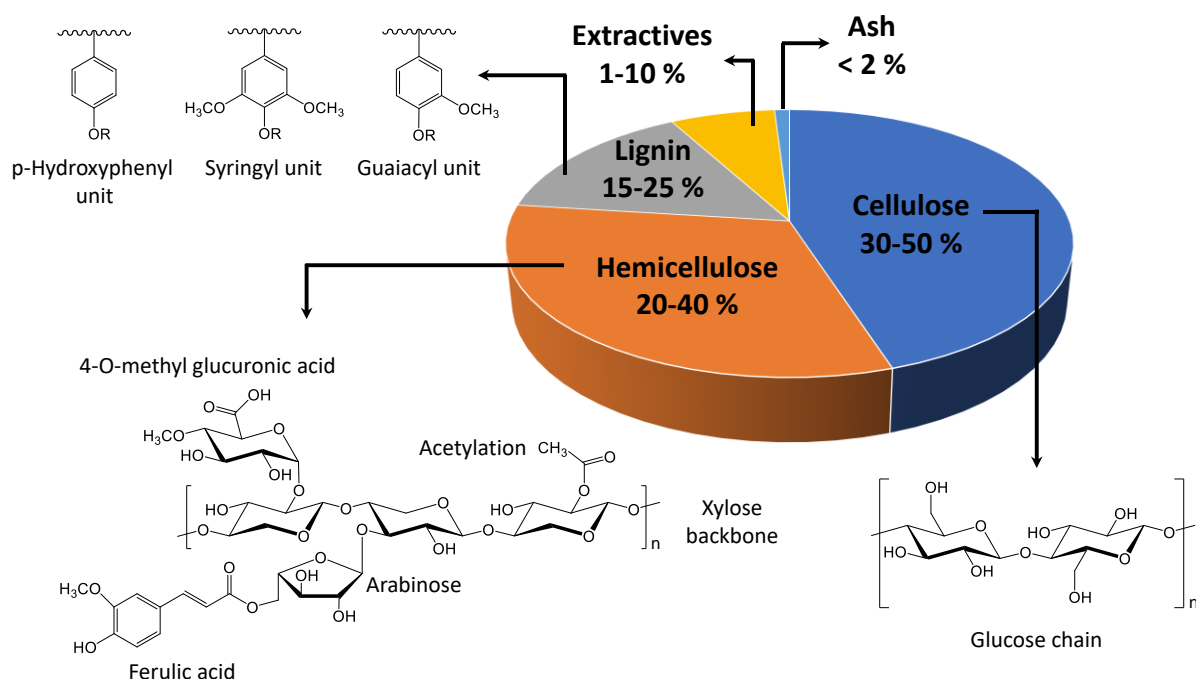


**Figure 3:** Composition of lignocellulosic biomass. The depicted structure for hemicellulose is only one possible example and represents a xylan molecule

These chains aggregate to cellulose fibers that occur predominantly as crystalline (ordered) structures, but may also contain amorphous (less ordered) regions [48]. Compared to cellulose, hemicellulose is characterized by a lower degree of polymerization [50] and greater structural

diversity. It is a branched heteropolymer consisting of different types of sugars including pentoses (xylose and arabinose) and hexoses (e.g. glucose, mannose and galactose). Moreover, several acids such as glucuronic acid, ferulic acid and acetic acid may also be incorporated into the molecular structure (**Figure 3**) [51]. Even though lignocellulose thus offers large quantities of fermentable sugars, its complex tertiary structure impairs a microbial utilization. For example, the crystalline regions in the cellulose polymer are only hardly accessible to enzymatic hydrolysis [52]. In addition, the cellulose fibers are embedded in an amorphous, heteromatrix structure of hemicellulose and lignin [53], with the individual components being cross-linked by a variety of different bonds [54]. Especially the phenylpropane polymer lignin, which is composed of guaiacyl (G), syringyl (S) and p-hydroxyphenyl (H) units (**Figure 3**), has been reported to provide the plant cell wall with rigidity, impermeability and resistance to microbial attack. [55]

Therefore, pretreatment is usually required to modify the structure of the lignocellulose in such a way that the carbohydrate polymers are more accessible for conversion into fermentable sugars and ultimately into the bioproduct of interest. The main objectives of such pretreatments include removing lignin, reducing the degree of polymerization and crystallinity of cellulose, and increasing the overall surface area and porosity of the biomass to allow for a better penetration of enzymes [54]. In addition to effective biomass decomposition, pretreatments should ideally result in limited formation of degradation products that inhibit enzymatic hydrolysis and fermentation, while also being cost-effective [54]. The pretreatments described in the literature can be divided into biological, physical, and chemical methods as well as combinations thereof (e.g. physicochemical treatments) (**Figure 4**), with all procedures having advantages and disadvantages [56, 57].

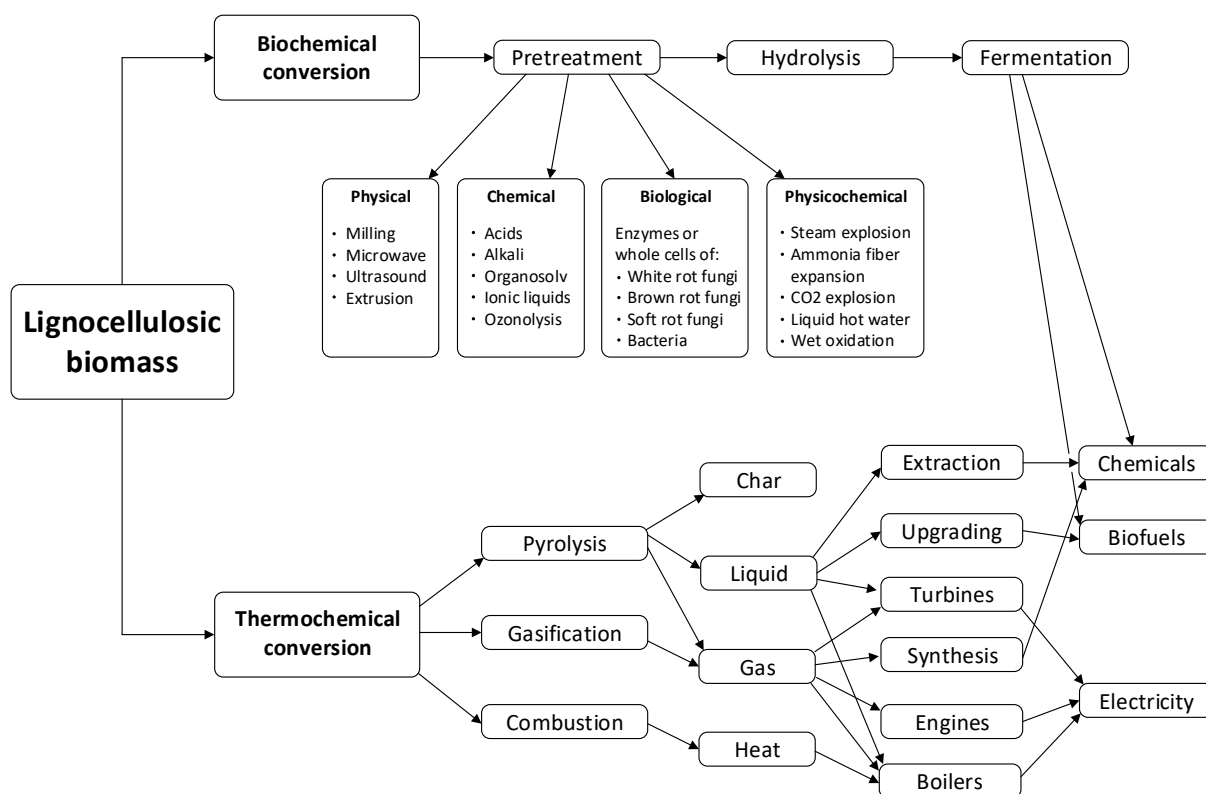


**Figure 4:** The two key routes for the conversion of lignocellulosic biomass. The illustration of the thermochemical route is based on Bridgwater et al. [58].

Subsequent enzymatic cleavage of the carbohydrates into sugar monomers is accomplished by the use of cellulases and hemicellulases, which can be naturally produced by a variety of fungal and bacterial microorganisms [59]. While the conversion of cellulose to glucose monomers requires the cooperative action of endo-1,4- $\beta$ -glucanases, exo-1,4- $\beta$ -glucanases, and  $\beta$ -glucosidases [59], a variety of different enzymes are needed for the complete degradation of hemicellulose due to its more complex structure [60]. The sugars released from the polymers can subsequently be utilized as carbon sources in microbial fermentations, with bioethanol production by *Saccharomyces cerevisiae* probably being the most extensively studied process [61]. Hydrogen [62, 63] and biogas [64, 65] are two other potential bio-fuels that can be obtained from lignocellulosic sugars. Moreover, the production of several chemicals such as solvents [66, 67], lipids [68, 69] and organic acids [41, 70] has been reported, illustrating the wide range of value-added bioproducts that can be derived from plant biomass.

In addition to the biochemical route, there are also several processes that use heat and/or chemical catalysts for the conversion of lignocellulosic biomass [57]. These so called thermochemical processes differ mainly in their oxygen demand and the primary products formed. Combustion is probably the simplest and the most commonly used method and involves the conversion of the plant feedstock to heat at an excess of air/oxygen [71]. This heat can in

turn be used to generate electricity (**Figure 4**). In contrast, gasification is a process in which the carbon contained in the plant material is transformed to synthesis gas (syngas) under a controlled supply of oxygen and/or steam [72]. Syngas is a mixture of carbon monoxide (CO), hydrogen (H<sub>2</sub>), methane (CH<sub>4</sub>) and carbon dioxide (CO<sub>2</sub>) as well as some light and heavier hydrocarbons [73]. The pyrolytic conversion of lignocellulosic biomass occurs under complete oxygen exclusion and leads to the formation of liquids, gases and char [74]. Unlike combustion, pyrolysis and gasification thus yield lignocellulosic degradation products that, in addition to generating electricity and heat, have the potential of being processed into biofuels and chemicals (**Figure 4**).

### 1.2.1. Fast pyrolysis

Although pyrolysis has been used for centuries to produce charcoal, current research is mainly focused on an increased formation of pyrolysis liquids (bio-oils), as they can be easily stored and transported and offer a wide range of potential applications [75]. The yield of bio-oils can be controlled by selecting suitable pyrolysis conditions. Moderate temperatures, high heating rates, short residence times, and immediate quenching of pyrolysis vapors have been reported to favor the production of liquids [76]. Accordingly, processes aimed at enhanced formation of bio-oils are commonly referred to as fast pyrolysis.

Such a fast pyrolysis represent the first step of the bioliq® process developed at KIT for the conversion of lignocellulosic biomass into synthetic fuels and chemicals (**Figure 5**). During this process, dried and shredded biomass is mixed with hot sand in a twin-screw reactor and heated to temperatures of about 500 °C in the absence of oxygen [77]. Within 2-3 seconds the solid lignocellulosic feedstock is decomposed into char and vapors, that are partly condensed to form the bio-oil and non-condensable pyrolysis gases [78]. In addition to the selected process parameters, the ratio of pyrolysis products (char, liquids, gas) also depends on the type of biomass feedstock. For the bioliq® process at KIT, wheat straw is primarily used as substrate, which is characterized by a comparatively high ash content [79]. This high amount of minerals in the biomass lowers the yield of condensate as solid particles can have a catalytic effect on the pyrolysis vapors and promote their further conversion into char and non-condensable gases [80]. Moreover, condensates derived from ash-rich feedstocks have a high water content, which can lead to spontaneous or delayed phase separation of the bio-oil [81]. Therefore, condensation at KIT is carried out as a two-stage process in which the organic bio-oil and an aqueous condensate are formed separately (**Figure 5**) [82].

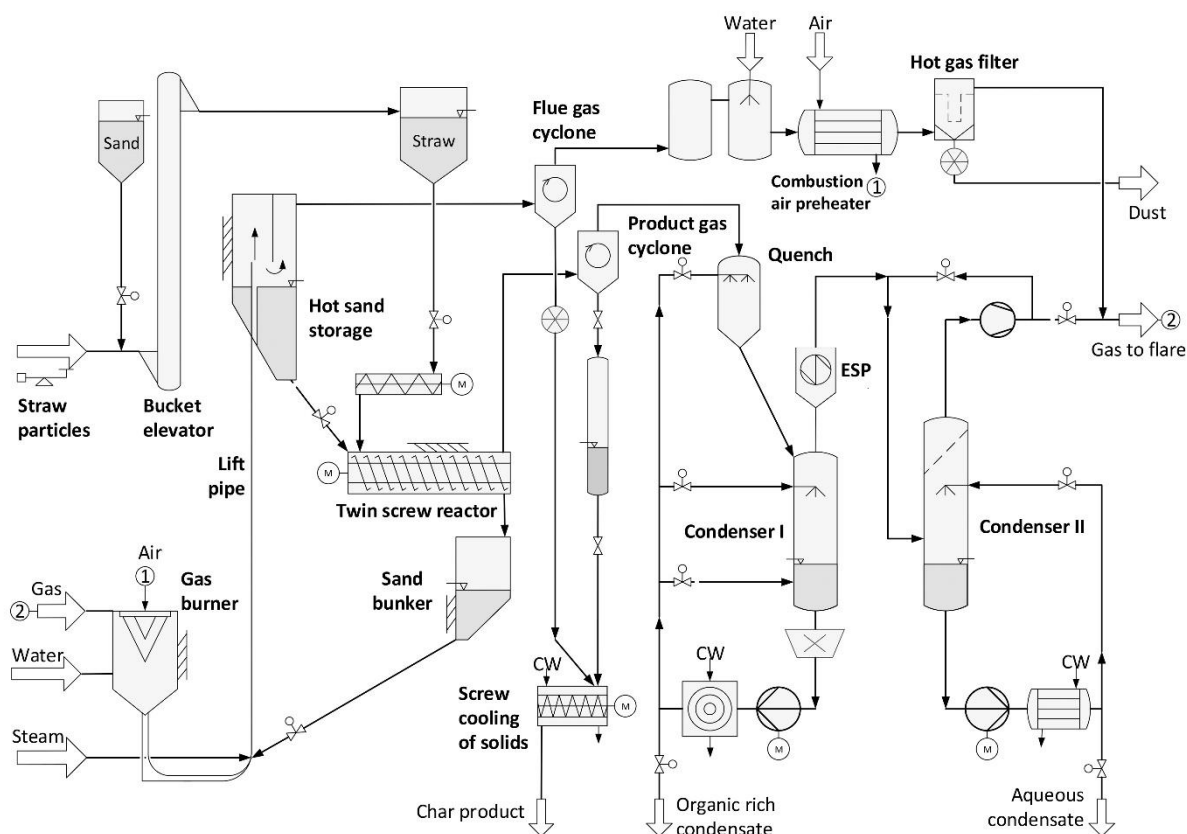


**Figure 5:** Process diagram of fast pyrolysis as a central part of the bioliq® process performed at KIT. (According to Niebel et al. [83]) CW = Cooling water, ESP = Electrostatic precipitator

However, before condensation the product gas stream that leaves the pyrolysis reactor at a temperature of 500 °C has to pass through a hot gas cyclone to remove entrained char particles. Afterwards, the pyrolysis vapors and gases enter a quench cooler, in which the first condensation step is performed by injecting an excess of recirculated bio-oil of 80–100 °C (condenser I) [77]. An electrostatic precipitator (ESP) prevents aerosols from entering the second condensation system, where the aqueous condensate is obtained at a temperature of about 30 °C (condenser II). The remaining non-condensable gases (mainly CO<sub>2</sub> and CO) are currently burnt in a flare, but could potentially be used to cover the process energy demand in commercial applications [77, 84].

The bio-oil formed during pyrolysis has many drawbacks that hinder its direct utilization as a transportation fuel. These include low heating value due to the high oxygen and water content, ignition delay, high acidity, low thermal stability, high viscosity, poor lubrication, and the formation of engine deposits [85]. Improving the fuel properties by blending is also limited due to the low miscibility with diesel or gasoline, so the pyrolysis oil can only be used directly as a fuel in boilers for electricity or heat generation without prior processing [85]. In the bioliq® process conducted at KIT, the pyrolysis oil is therefore upgraded by conversion into syngas in

order to achieve a significant expansion of its potential applications (**Figure 6**). The heating value of the pyrolysis oil (about 23 MJ/kg [83]) is high enough to allow direct gasification. However, it contains only 50-70 % of the initial bioenergy of the feedstock and is therefore mixed with up to 20 % of the pyrolysis char to obtain a dense bio-slurry, that makes about 90 % of the bioenergy accessible for syngas production [78, 86].

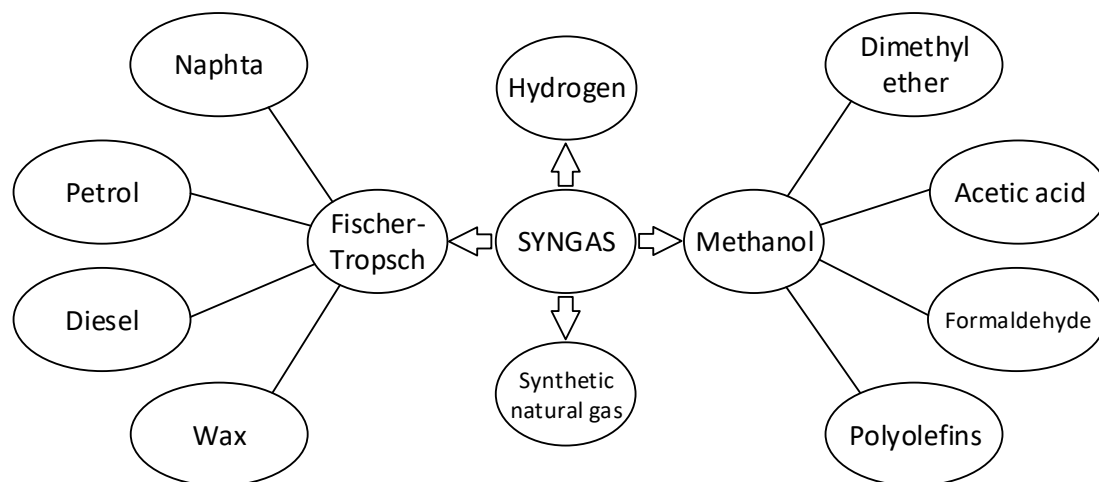


**Figure 6:** Potential applications of synthesis gas (syngas)

### 1.3. Pyrolytic aqueous condensate (PAC)

Due to its high water content of more than 80 %, the aqueous condensate formed during fast pyrolysis at KIT has a very low heating value of only about 4 MJ/kg (**Table 2**).

**Table 2:** Properties of the PAC formed during the bioliq® Campaign in 2018 [83]

Property	Dimension	Value
water content	wt. %	81 ± 2
pH value (20 °C)	-	2.8 ± 0.1
density (20 °C)	kg/m <sup>3</sup>	1013 ± 3
higher heating value (HHV)	MJ/kg	4.1 ± 0.3
total organic carbon (TOC)	mg/L	90000 ± 5000
chemical oxygen demand (COD)	mg/L	280000 ± 20000

Although there have been attempts to enable its gasification by mixing it with up to 40 % of pyrolysis char [80], an energetic use of the condensate seems therefore rather unlikely. Extraction of industrially relevant chemicals such as phenols or furans from the PAC is usually

also impractical due to the low content of these substances. Therefore, using the condensate as a substrate for microbial fermentations could be a promising alternative for the valorization of this pyrolysis side stream. Even though the PAC does not contain any sugars (**Appendix 1**), some of its organic constituents have already been described as potential carbon sources for microbial growth and production of bio-based chemicals. However, pyrolytic conversion of lignocellulosic biomass also leads to the formation of several fermentation inhibitors, making detoxification of the PAC a prerequisite for its utilization as a substrate.

### **1.3.1. Composition**

#### *1.3.1.1. Acetic acid*

Acetic acid is a two-carbon monocarboxylic acid and an important commodity chemical with a broad spectrum of industrial applications. As the main ingredient in vinegar (5-15 %), it was already used by the cultures of ancient Egypt, Babylon, India, Greece and Rome for beverage and food production as well as for medical purposes [87]. Nowadays, acetic acid is mainly required for the production of vinyl acetate, acetic anhydride, acetate esters, monochloroacetic acid and as a solvent in the synthesis of terephthalic acid [88], which in turn serves as a starting material for polyethylene terephthalate (PET) production [89]. The carboxylic acid can be obtained by both biotechnological and petrochemical routes, with the former being almost exclusively applied for the production of vinegar [90]. This process involves the alcoholic fermentation of sugars by yeasts and the subsequent incomplete oxidation of ethanol by bacteria of the *Acetobacteraceae* family [87]. Further possible processes for microbial acetic acid production include methane fermentation, anaerobic digestion of various organic wastes (e.g. animal manure, sewage sludge, and food waste), carbon fixation from syngas and microbial electrosynthesis [90, 91]. The most common chemical routes for acetic acid synthesis are metal-catalyzed carbonylation of methanol [92] and liquid-phase oxidation of butane, naphtha, ethylene or acetaldehyde [88]. However, methanol carbonylation is the preferred method for large-scale production and was first patented by BASF SE (Ludwigshafen, Germany) as early as 1913 [93].

Moreover, acetic acid can also be formed during the pyrolytic degradation of lignocellulosic biomass, mainly through deacetylation of the hemicellulose fraction (**Figure 7**) [94].

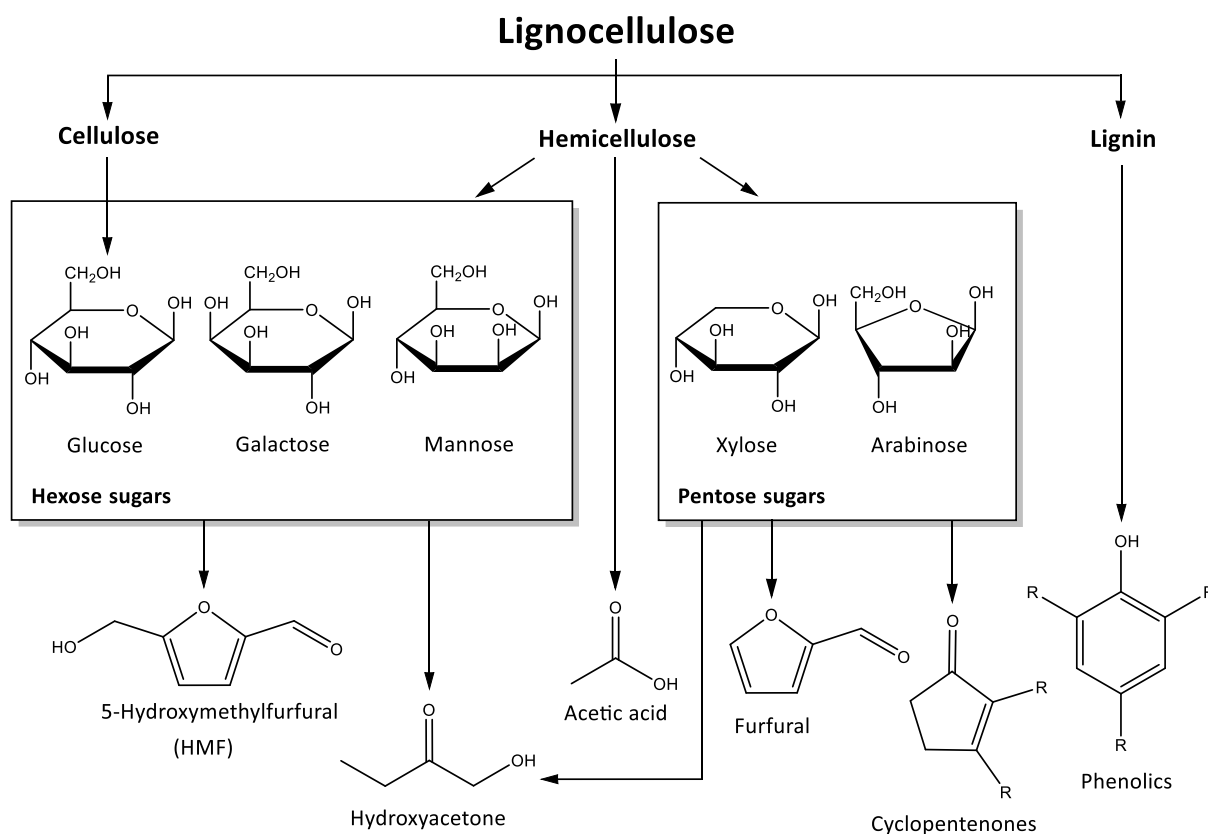


**Figure 7:** Main routes for the formation of selected PAC components

The content of acetic acid in pyrolysis oils has been reported to range from 0.5-17 wt.% [95], but due to its high volatility, the acid is also present in the aqueous condensate [77]. Depending on the batch, its concentration amounts to about 3-5 wt.%, which makes it a major contributor to the acidity of the condensate (**Table 2**). However, neutralization allows acetic acid to be converted to the acetate anion, which has been repeatedly described as a suitable substrate for microbial fermentations and is therefore considered the most promising C-source in PAC.

The metabolization of acetate involves its uptake into the cell by transport proteins [96–98] and a subsequent conversion to acetyl-CoA [91]. Although acetyl-CoA is usually oxidized in the TCA cycle to generate energy and reduction equivalents, it has been reported that the metabolization of acetate occurs largely through the glyoxylate cycle (**Figure 2**, blue) [99].

The ability of bacterial microorganisms to metabolize acetate as a sole C-source was previously investigated by Arnold et al. [100]. In this study, *Pseudomonas putida* and *Corynebacterium glutamicum* proved to be the best-performing strains as they grew on acetate concentrations of up to 15 g/L and 30 g/L, respectively. *Escherichia coli* was also able to use at least 10 g/L acetate as sole C-source for growth. Moreover, a genetically optimized strain could even convert this substrate into 3.57 g/L of itaconic acid after 84 h of fed-batch fermentation [101]. Regarding eukaryotic organisms, it has been repeatedly shown that *Aspergillus oryzae* is

capable of utilizing acetate for biomass formation [102, 103] and L-malate production [104, 105]. Of particular note is that the acetate used in these fungal fermentations was partly derived from microbial synthesis. For instance, Uwineza et al. used the volatile fatty acid (VFA) solution derived from anaerobic digestion of cow manure and food wastes as the sole nutrient source to obtain a maximum fungal biomass yield of  $0.26 \pm 0.03$  g/g VFA [103]. In contrast, the acetate in the study by Oswald et al. was derived from syngas fermentation with *Clostridium ljungdahlii* and was converted to L-malate with a yield of 0.37 g/g acetate or 0.22 g/g syngas [105]. Especially the latter example demonstrates the potential of coupling microbial acetate synthesis processes with subsequent fermentations to upgrade the acetate into value-added bioproducts. Moreover, various oleaginous yeasts like *Yarrowia lipolytica* [106], *Rhodospiridium toruloides* [107], *Cryptococcus albidus* [108] and *Cryptococcus curvatus* [109] have been reported to be capable of acetate-based lipid production. Using the latter, it was also demonstrated for the first time, that a pyrolytic aqueous condensate containing 20 g/L acetate could be converted to 6.9 g/L dry biomass and 2.2 g/L lipid [110]. Although prior neutralization and detoxification was required, this study successfully demonstrates that PAC can serve as a substrate for microbial fermentations.

#### 1.3.1.2. Acetol

Acetol (or hydroxyacetone) is the simplest representative of hydroxyketones and accounts for the largest proportion of the organic components present in the pyrolytic aqueous condensate used in this work ( $\approx 5$  wt. %, **Appendix 1**). It was identified as one of the major oxygenated C2-4 products arising from the pyrolysis of cellulose [111], and several possible reaction mechanisms have been proposed for its formation by direct conversion of cellulose units as well as by secondary decomposition reactions of levoglucosan [111–113]. Furthermore, the ketone was also reported to be an important product of hemicellulose pyrolysis (**Figure 7**) [114, 115]. The first chemical synthesis of the hydroxyketone was achieved by reacting bromoacetone with potassium hydroxide and ethyl formate in methanolic solution [116]. However, due to the current low market price of glycerol, there have also been various attempts to obtain acetol by catalytic dehydration of this polyol [117]. The acetol formed from glycerol can further react with hydrogen to produce 1,2-propanediol [118], which is an important commodity chemical with a variety of industrial applications [119]. Moreover, the hydroxyketone has been reported to be a potential starting material for the synthesis of renewable diesel and jet fuels [120] and to play a role in Maillard reactions [121, 122].

Acetol furthermore represents an intermediate in the metabolism of propane- and acetone-utilizing bacteria [123, 124]. This metabolic pathway involves subterminal hydroxylation of propane to 2-propanol followed by oxidation of the secondary alcohol to acetone (**Figure 8**).

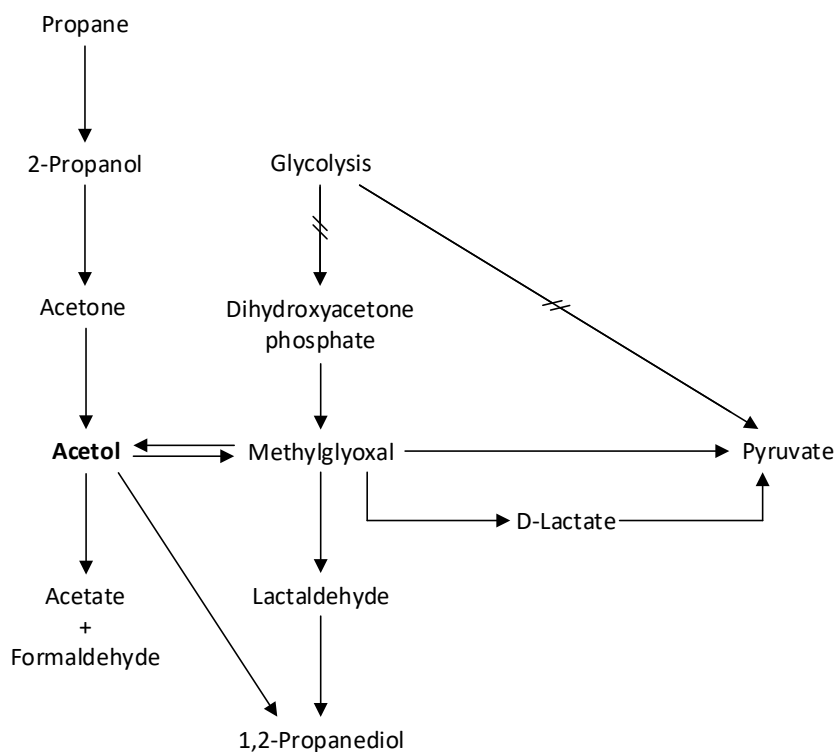


**Figure 8:** Possible pathways for the microbial formation of acetol and its conversion into other metabolites

Although there are several routes for the further conversion of this ketone, in most aerobic bacteria it is hydroxylated to acetol in an  $O_2$ -dependent reaction [125]. Similarly, the subsequent metabolization of acetol may also occur via different metabolic pathways. In *Mycobacterium*, the presence of an acetol monooxygenase has been reported, which converts the hydroxyketone to hydroxymethylene acetate in an oxygen- and NADPH-consuming reaction. However, since this substance is unstable it spontaneously decomposes to acetate and formaldehyde [126]. Another route, which has been proposed for example by Taylor et al. for *Corynebacterium* strains, is the reaction of acetol to methylglyoxal by an acetol dehydrogenase [123]. Since methylglyoxal is a cytotoxic substance [127], it is usually rapidly degraded to D-lactate by the glyoxalase system [128], but also a direct oxidation to pyruvate has been reported for *Bacillus subtilis* [129] and some *Pseudomonas* species [130, 131]. The D-lactate formed by the glyoxalase system can also be converted to pyruvate via a D-lactate dehydrogenase [132].

However, research interest focused primarily on the reverse reaction of methylglyoxal to acetol, since this reduction represents an important step in the formation of 1,2-propanediol from glucose [133]. As mentioned above, this compound is an important commodity chemical, and the development of a bio-based alternative to its conventional chemical synthesis could thus contribute to reducing reliance on fossil resources. Microbial production of the diol involves either acetol or lactaldehyde as an intermediate and has been described for several bacteria [134, 135]. There have also been approaches in yeast to enable the conversion of acetol to 1,2-propanediol, but these mostly required genetic modifications [136, 137] or occurred as simple biotransformations using acetate or ethanol as primary substrates [138, 139]. However, in a study by Lian et al. it was reported for the first time that some yeast strains are able to use concentrations of 1 wt.% of acetol as the sole C-source for growth [110]. Therefore, the acetol contained in the PAC may also be considered as a potential substrate for the microbial valorization of the pyrolysis condensate.

#### *1.3.1.3. Potential inhibitors*

Even though acetate and acetol appear to be suitable feedstocks for microbial fermentations, these compounds may also negatively affect cell viability under certain conditions. For example, growth inhibition by the acid variant of the former is well known and deliberately used in the preservation of foods [140], thus highlighting the need for neutralization of the PAC prior to its utilization as a substrate. However, with increasing PAC concentration in the growth medium, larger amounts of hydroxide are required for neutralization, which in turn leads to an increased salinity of the medium. High external salt concentrations have been reported to induce osmotic stress and can therefore also impair microbial growth [141–143]. Moreover, although at a neutral medium pH most of the acetic acid contained in the PAC ( $pK_a = 4.75$ ) is present in the form of acetate, the amount of undissociated acid increases with increasing PAC concentrations. Unlike acetate, the lipid-permeable acid can freely diffuse into the cytosol of the cell until an equilibrium between internal and external concentrations is reached. Since the intracellular pH is usually neutral or slightly alkaline, the acid dissociates to form an acetate anion and a proton, with the latter causing an acidification of the cytosol [90]. An acidic internal pH has been reported to cause a decrease in the activity of several enzymes of the central carbon metabolism in *A. niger* [144]. Moreover, to prevent acidification, microorganisms like *S. cerevisiae* use a transmembrane ATPase to actively transport protons out of the cell [145], leaving the ATP required for this process unavailable for microbial growth. Negative effects of

acetate accumulation were also observed in *E. coli* and included perturbation of other anion pools (e.g. glutamate) [146] and interference with methionine biosynthesis [147].

Despite the usability by some yeast strains [110], an inhibitory effect of acetol on microbial growth has also been described in the literature. For example, Lian et al. examined 18 model substances typically found in pyrolysis condensates for their toxicity to the growth and ethanol production of *S. cerevisiae* and found that concentrations of 2.16 wt.% acetol caused reductions by 80.07 % and 99.08 %, respectively [148]. Comparable findings were also reported for *Aspergillus oryzae*, as Dörsam et al. determined the limits for fungal growth and L-malic acid production to be 1.5 wt.% and 2.5 wt.% acetol, respectively (**Table 3**).

**Table 3:** Maximum concentration of selected inhibitors from pyrolysis condensates that can be tolerated by *A. oryzae* (according to Dörsam et al. [149] but supplemented by the inhibitor concentration in PAC)

Tested substances	Concentration in pyrolysis oil [% w/w]	Concentration in PAC [% w/w]	Growth limit [% (w/w)] <sup>1</sup>	Malic acid production limit [% (w/w)] <sup>1</sup>
Propionic acid	1.302	1.041	0.07	> 1.3
Ethylene glycol	1.258	0.327	> 1.25	> 1.25
$\gamma$ -butyrolactone	0.335	0.073	> 0.335	> 0.335
Hydroxyacetone	4.463	5.146	1.5	2.5
Syringol <sup>2</sup>	0.556	0.017	0.27	0.3
Guaiacol	0.469	0.180	0.1	0.1
Furfural	0.281	0.294	0.03	0.07
Phenol	0.384	0.064	0.07	0.07
Isoeugenol <sup>2</sup>	0.524	–	0.03	0.06
<i>o</i> -, <i>m</i> -, <i>p</i> -cresol <sup>3</sup>	0.17	0.046 ( <i>o</i> -Cresol) 0.021 ( <i>m</i> -Cresol)	0.05	0.03
2-cyclopenten-1-one	0.308	0.340	0.00625	0.0125

<sup>1</sup> Values represent the highest tested concentrations for which growth/ production was still detectable

<sup>2</sup> Analysis indicates a degradation of these substances during cultivation

<sup>3</sup> The concentration of the individual cresols contained in the PAC was analyzed separately and not as a mixture. No *p*-cresol could be detected.

Unlike acetic acid, the mechanism underlying the toxicity of acetol is not well understood. However, it was hypothesized that the solvent properties of the hydroxyketone might cause disorganization of the cellular membrane [149].

Besides these major constituents, pyrolysis condensates contain smaller amounts of a variety of other substances that may inhibit microbial growth and have even led to pyrolysis products being used as wood preservatives [150–152].

### Cyclic ketones

In addition to the aliphatic acetol, numerous cyclic ketones of different chemical structure are present in the aqueous condensate (**Appendix 1**). The exact pathways for the formation of these cyclic ketones during the pyrolytic conversion of lignocellulosic biomass have not yet been extensively studied. However, Stefanidis et al. reported that especially various cyclopentenones with methyl- and ethyl- substitutes belong to the main products of the pyrolysis of xylan [114]. They suggested these cyclic ketones to be derived from the xylan main stem by cleavage of the o-glucosidic bonds and subsequent removal of the hydroxyl groups of the xylose ring [114]. The formation of minor amounts of cyclic ketones during cellulose pyrolysis was also observed and appeared to be promoted by elevated reaction temperatures [153].

So far, cyclic ketones have received little attention in studies on the inhibitory effects of pyrolysis products on microbial growth. However, the need to consider such compounds is highlighted by the toxicity tests performed by Dörsam et al. as they showed that concentrations above 0.00625 wt.% and 0.0125 wt.% 2-cyclopenten-1-one already resulted in complete inhibition of the growth and malate production of *A. oryzae* (**Table 3**) [149]. Although the underlying mechanism of inhibition is unknown, it can probably be attributed to the unsaturated nature of this compound. For example, Lee et al. studied various sesquiterpene lactone derivatives for their antimicrobial and antitumor activity, and although these compounds had a far more complex structure than 2-cyclopenten-1-one, their cytotoxicity was primarily attributed to the cyclopentenone ring moiety [154, 155]. The importance of the double bond for the inhibitory effect is further highlighted by the fact that a 32-fold higher fungal growth limit of more than 0.2 wt.% was determined for the corresponding saturated 2-cyclopentanone (**Table 4**). Similarly, Lian et al. showed that this compound was only weakly inhibitory and in low amounts even partially beneficial to the growth and ethanol production of *S. cerevisiae* [148].

**Table 4:** Toxicity tests on agar plates containing glucose as main carbon source and different concentrations of cyclic ketones present in PAC

Tested substances	Concentration in PAC	Growth limit
	[% (w/w)]	[% (w/w)]
2-cyclopenten-1-one	0.340	0.00625 <sup>1</sup>
2-cyclopentanone	0.112	> 0.2 <sup>2</sup>
2-methyl-2-cyclopenten-1-one	0.135	> 0.15 <sup>2</sup>
2-cyclohexen-1-one	0.011	> 0.025 <sup>2</sup>

<sup>1</sup> determined by Dörsam et al. [149]

<sup>2</sup> previously unpublished data obtained in collaboration with Aline Kövilein

Moreover, Lee et al. reported that substituents bound to the cyclopentenone ring structure may attenuate the cytotoxic effect of the antimicrobial agents [155]. This is reflected in the observations that *A. oryzae* tolerates 2-methyl-2-cyclopenten-1-one concentrations that were at least 24 times higher than for the unmethylated derivative. The number of carbon atoms contained in the ring structure also appears to affect the cytotoxicity of cyclic ketones with the C6 compound 2-cyclohexen-1-one being less harmful compared to the corresponding C5 variant (**Table 4**). However, the exact correlations between the structural features of cyclic ketones and their inhibitory effect on microorganisms still require further investigation.

### Furans

Among the furan compounds formed during pyrolytic degradation of lignocellulosic materials, 5-hydroxymethyl-2-furfural (HMF) and furfural are probably the most relevant and best studied substances. The C6 furan HMF is mainly derived from hexose sugars (**Figure 7**) and possible reaction mechanisms for its formation from cellulose units or levoglucosan have been described to involve ring-opening to the C6 aliphatic intermediate, followed by intramolecular dehydrations and an acetal reaction between the C2 and C5 atom [111]. A similar mechanism is assumed for furfural (C5 compound), but with pentose sugars like xylose serving as the precursor [156].

Due to their potential to be converted into a variety of industrially relevant substances [157–159], both furans were recently included in the revised list of the most promising chemicals that can be derived from biomass published by the U.S. Department of Energy [160]. Consequently, there have been studies aiming at a selective formation of these compounds during pyrolysis by choosing a suitable catalyst [161, 162]. However, this conflicts with microbial utilization of the pyrolysis condensate, as furans have been repeatedly described to

impede the growth of various organisms including *A. oryzae* (**Table 3**). Reported inhibitory effects of furfural include DNA damage in *Salmonella typhimurium* [163] and *E. coli* [164], as well as accumulation of reactive oxidative species (ROS) and a resulting damage to mitochondria, vacuoles, actin, and nuclear chromatin in *S. cerevisiae* [165]. Furthermore, furfural has also been shown to inhibit various enzymes of the central carbon metabolism [166, 167] and to interfere with sulfur assimilation in *E. coli* [168]. However, at least some of the observed inhibitory effects may be related to furan defense mechanisms that have evolved in several microorganisms and involve the conversion of these compounds into less harmful alcohols or acids (**Figure 9**).

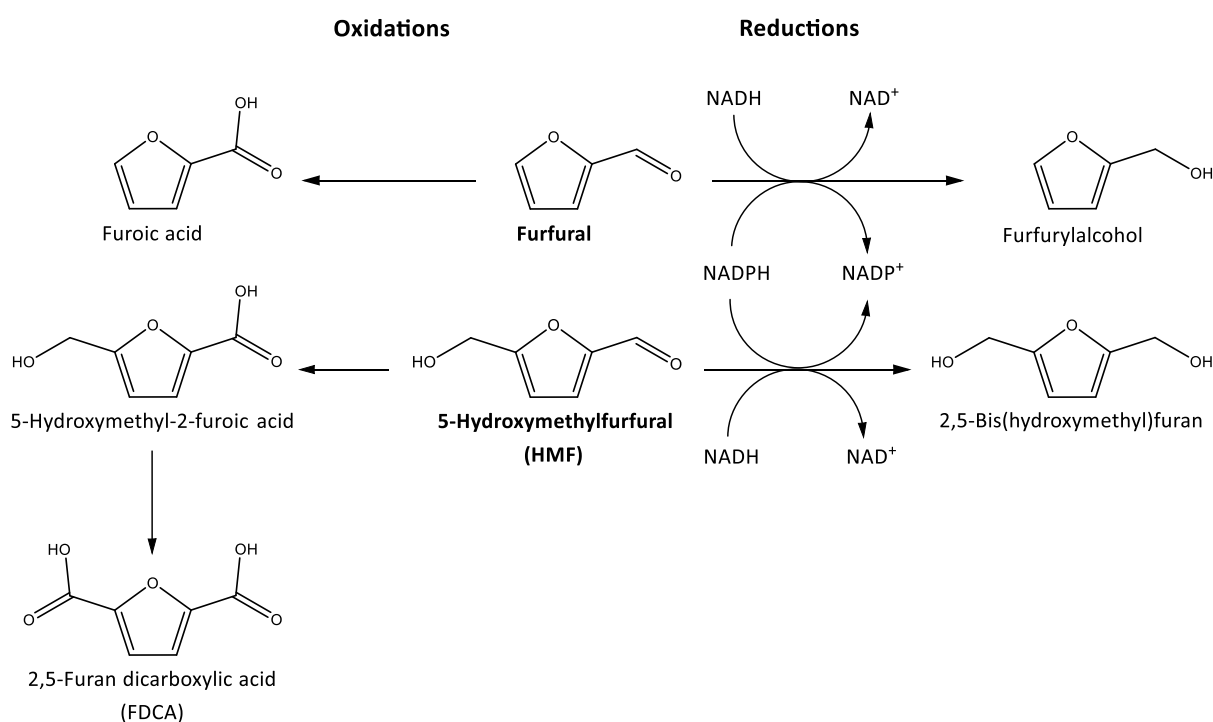


**Figure 9:** Oxidative and reductive furan conversion routes.

Various oxidoreductases in *E. coli* [168, 169] and *S. cerevisiae* [170–174] have been reported to be capable of catalyzing the reductive reactions of furfural and HMF to furan alcohols but require NADH or NADPH. This results in an intracellular imbalance of these reductions equivalents [175] and restricts their availability for other fundamental metabolic reactions. However, NADPH in particular is an important co-factor for enzymes involved in the oxidative stress defense [176] and is also essential for the above-mentioned sulfur assimilation [168]. Effective approaches to increase the furfural tolerance in *E. coli* therefore included deletions of NADPH-dependent oxidoreductases [169] and substitution with NADH-dependent enzyme variants [177, 178] as well as overexpression of the transhydrogenase *pntA* [168], which is

capable of converting NADH to NADPH [179]. Similar modification in the expression of oxidoreductases [170, 180–182] and genes involved in the balance of reduction equivalents [181, 183] have also been investigated in yeast to achieve increased furan tolerance and conversion.

Various fungal organisms that can naturally transform furans into alcohols and acids have also been identified [184, 185], including the industrially relevant strains *Trichoderma reesei* [186] and *Aspergillus terreus* [187]. However, while these biotransformations usually require the presence of an additional substrate, some fungi [188, 189] and bacteria [190, 191] also seem to be capable of utilizing furans as a sole C-source. The first biochemical route for the metabolization of furfural was already proposed by Trudgill et al. in 1969 for the aerobic bacterium *P. putida* F2 [192] This pathway involves a multistep enzymatic conversion of the furan to  $\alpha$ -ketoglutarate, which can enter the TCA cycle [193]. Moreover, Koopmann et al. identified the gene cluster responsible for the metabolization of furans in *Cupriavidus basilensis* HMF14, paving the way for the construction of HMF and furfural-utilizing strains via genetic modifications [194–196]. Besides its ability to metabolize toxic components present in lignocellulosic hydrolysates, *C. basilensis* HMF14 has been reported to be unable to utilize the most abundant (hemi-)cellulose sugars glucose, xylose, and arabinose, thus making it a particularly interesting candidate for biological detoxifications of lignocellulosic degradation products [191].

### Phenolics

The phenolic substances contained in liquid pyrolysis products are primarily derived from the lignin fraction of the lignocellulosic substrate (**Figure 7**) [114]. However, formation during pyrolysis of cellulose and hemicellulose has also been reported and likely occurs through secondary polymerization reactions of unsaturated species such as propylene, butadiene and butene contained in the gas phase [197]. The amount and type of phenolic compounds formed depends on the biomass source, as lignin in different feedstocks varies in its monolignol composition (G, S, H units), intramolecular linkages, and association with hemicellulose and cellulose [198]. Total lignin content is also an important factor and is usually lower for wheat straw than for softwood or hardwood [199]. However, the comparatively low overall content of <0.5 wt. % phenolics in the PAC used in this work (**Appendix 1**) is mainly due to the fact that most of these substances are already separated from the vapor stream in the first condensation step of the pyrolysis process and are thus mainly found in the bio-oil (**Table 3**). Nevertheless, the pyrolysis condensate still contains phenolic derivatives that can adversely

affect microbial viability. For example, the content of guaiacol in the PAC (0.18 wt.%) exceeds the maximum limit for biomass and malate formation in *A. oryzae*, which was reported to be 0.1 wt.% by Dörsam et al. (**Table 3**) [149]. The mechanisms underlying the inhibition by phenolics are not yet fully understood due to the heterogeneity of this group of substances. However, the structure of the compounds seems to play a crucial role in their toxic effects on microorganisms. For example, experiments with vanillin showed that the hydroxy substituent in ortho position was far more toxic to *S. cerevisiae* than in meta or para position and resulted in a complete inhibition of growth at a concentration of 0.2 g/L [200]. In a comprehensive study that included 34 aromatic compounds, Sierra-Alvarez further revealed that the nature of the substituent is also of great importance for microbial viability. Examining the activity of acetoclastic methanogenic bacteria, they found that toxicity increased with increasing number and length of alkyl substitutions, indicating a correlation between the hydrophobicity of a phenolic compound and the level of inhibition [201]. The strong impact of hydrophobicity suggests that the membranes are the primary site of toxic action of these substances. This assumption is further supported by two studies on *E. coli* showing that phenol addition to the growth medium causes changes in the protein-to-lipid ratio in the membrane [202] as well as an efflux of potassium ions from the cell [203]. However, given the structural diversity of phenolic substances formed during biomass degradation, it is reasonable to assume that there are other mechanisms of inhibition that are still unknown.

### **1.3.2. Detoxification**

Due to the presence of these toxic substances, which may even reinforce each other in their inhibitory effect [204, 205], detoxification is required before the PAC can be used as substrate for microbial fermentations. Numerous biological, physical and chemical methods have already been described in the literature to enable the removal of inhibitory compounds from lignocellulose degradation products [206].

Biological detoxification involves the use of microorganisms that are capable of either converting the inhibitors into less harmful substances or even metabolizing them as carbon source. Although there are a few studies on biological detoxification with bacteria [207] and yeast [208, 209], fungal organisms such as *Coniochaeta ligniaria* [188, 210], *T. reesei* [211], *A. nidulans* [212] are usually preferred and proved to be effective in removing furans, organic acids, and some aromatic compounds. In addition to whole cells, pure enzymes like peroxidases and laccases from several white rot fungi have also been reported to reduce the toxicity of

lignocellulose degradation products [213]. These enzymes act selectively on phenolic compounds by generating unstable phenoxy radicals that polymerize to less toxic aromatic substances [213]. However, this selectivity results in the disadvantage that non-phenolic inhibitors formed during the degradation of lignocellulose remain largely unaffected.

In contrast, chemical methods such as extraction with different solvents [214, 215], ion exchange [216, 217], overliming [218–220] or activated carbon treatment [218, 221] have proven to be effective for the simultaneous removal of several toxic substances. For example, a trialkylamine extraction performed by Zhu et al. resulted in the removal of 73.3 % of acetic acid, 45.7 % of HMF and even a complete elimination of furfural from a corn stover prehydrolyzate [214]. Detoxification by overliming is typically accomplished by the use of high amounts of  $\text{Ca}(\text{OH})_2$  (lime), but other metal hydroxides and  $\text{NH}_4\text{OH}$  have also been investigated [220]. As indicated by a study of Zhao et al. the effectiveness of the different alkaline agents appears to vary depending on the nature of the inhibitory substance [222]. They treated an acetic acid rich fraction from the pyrolysis of soft wood with  $\text{KOH}$ ,  $\text{NaOH}$  or  $\text{Ca}(\text{OH})_2$  and found furfural to be equally removed by all three hydroxides, whereas elimination of phenols and acetol was more effective with  $\text{Ca}(\text{OH})_2$ . Chi et al. also used  $\text{Ca}(\text{OH})_2$  to examine the removal of phenols from a pyrolytic sugar syrup and found a concentration- and pH-dependent reduction of these substances, with a  $\text{pH} \geq 10$  being required to achieve a maximum elimination of 72 % [219]. While Zhao et al. were able to confirm the pH dependence of phenol removal, they found methanol and organic acids to be completely unaffected by overliming treatments regardless of the pH-value [223]. In contrast, the pH of the suspension proved to be particularly important for the removal of organic acids by adsorption to activated carbon, with an acidic pH being preferable [221]. Moreover, contact time, carbon concentration and temperature were also reported to affect the overall detoxification efficiency of this treatment method [206]. Nevertheless, activated carbon has repeatedly been described as effective in the removal of furans and phenols [218, 221] and is widely used due to its ease of application.

Physical methods for the detoxification of lignocellulose degradation products include membrane filtration processes [224–226] and evaporation [216, 227, 228]. While the separation of inhibitors by the former depends largely on the membrane material [224], detoxification by evaporation is based on the vapor pressure making it particularly suitable for reducing the contents of volatile compounds like acetic acid, acetol and furfural. However, this method may also lead to an increase in the concentration of non-volatile toxins (e.g. lignin derivatives) and consequently to fermentation inhibition [206, 229]. The problem can be avoided by refilling the concentrated solution to the initial volume, as performed by Larsson et al. after an evaporation

treatment in which they reduced the volume of a spruce hydrolysate by 90 %. This detoxification procedure resulted in a removal of acetic and formic acid by 65 % and 74 %, respectively, while furfural was even completely eliminated [216].

In addition to the use of individual methods, there are also various reports on combinations of detoxification methods to further improve the elimination of inhibitors [230–232]. For example, Parajó et al. performed a comprehensive study on combinations of alkaline and activated carbon treatments with extraction processes using different organic solvents [232]. They evaluated their effect on the removal of phenols from an eucalyptus wood hydrolysate and found that overliming followed by extraction with ethyl acetate and subsequent activated carbon treatment was the most effective combination, resulting in a 78.7 % reduction in phenol concentration. The detoxification procedure described in the study by Lian et al. also involved three different methods as they conducted sequential treatment of a pyrolytic aqueous phase by neutralization, rotary evaporation, and activated carbon [110]. Although they did not analyze the removal of inhibitors, the detoxification appeared to be sufficient to allow a utilization of the pyrolysis product for lipid production in a fermentation with *C. curvatus*.

It therefore seems possible that by establishing a suitable detoxification procedure, the concentrations of inhibitors in the PAC from the bioliq® process at KIT may also be reduced to such an extent that utilization for L-malate production with *A. oryzae* becomes feasible. However, the current literature does not provide any information on the efficacy of the different detoxification methods for the removal of highly inhibitory cyclic ketones, highlighting the need for further investigation. By combining detailed detoxification studies and transcriptome analyses, this work provides comprehensive insight into the effects of PAC and its inhibitors on *A. oryzae* at both physiological and gene regulatory levels.

## 1.4. Research proposal

Reducing substrate costs is an important step towards making bio-based processes for the production of platform chemicals more economically competitive with conventional petrochemical synthesis routes. Therefore, this work aimed at utilizing pyrolytic aqueous condensate, a waste stream generated during the fast pyrolysis of wheat straw, for the microbial production of L-malic acid with the filamentous fungus *Aspergillus oryzae*. While usable components like acetate generally render PAC a promising renewable substrate, the inhibitors it contains interfere with fungal growth.

The following aspects were therefore addressed in the chapters of this thesis to increase the fungal tolerance towards the condensate and to enable its utilization by the fungus:

### Chapter 3:

- What kind of stress response is induced at the transcriptional level by using PAC as a substrate in *A. oryzae* cultivations?
- Which changes in transcription can actually be attributed to the inhibitors contained in the PAC and which are also observed when pure acetate is used?
- Which potential targets for a genetic modification of *A. oryzae* aimed at increasing its PAC tolerance can be derived from these findings?

### Chapter 4:

- To what extent can the fungal PAC tolerance be increased by removing inhibitory substances from the pyrolysis condensate?
- What are the optimal reaction conditions for individual detoxification methods and which improvements can be achieved by combining them?
- Does the optimized detoxification method allow fungal growth on pure PAC?

### Chapter 5:

- Is acetol also a suitable substrate for fungal growth and malic acid production?
- Does a treatment with the optimized detoxification procedure allow malate production based on the pyrolysis condensate?
- And if so, how can the acid production process be further improved and possibly transferred to the reactor scale?

## 2. Materials and methods

### 2.1. Microorganism

*Aspergillus oryzae* DSM 1863 was obtained from the DSMZ German Collection of Microorganisms and Cell Cultures (Deutsche Sammlung von Mikroorganismen und Zellkulturen GmbH, Braunschweig, Germany).

### 2.2. Media and cultivation conditions

Malic acid production with *A. oryzae* is a two-step process in which biomass growth and acid formation are decoupled from each other. First, a pre-culture is inoculated by adding spore suspension, and the cultures are then incubated until a sufficient amount of biomass is formed. After filtration and thorough washing with sterile ultrapure water, the biomass is transferred to the main culture medium, which is characterized by a reduced nitrogen concentration to stimulate acid formation. In addition, CaCO<sub>3</sub> is added to the main cultures as pH buffering agent and for CO<sub>2</sub> supply.

#### 2.2.1. Conidia preparation

For inoculation of agar plates and shake flask pre-cultures, glycerol stocks of *A. oryzae* conidia were prepared. For this purpose, the fungus was cultivated on minimal medium according to Barratt et al. containing 10 g/L glucose, 6 g/L NaNO<sub>3</sub>, 0.52 g/L KCl, 0.52 g/L MgSO<sub>4</sub>·7H<sub>2</sub>O, and 1.52 g/L KH<sub>2</sub>PO<sub>4</sub> [233] and 2 mL/L 1000 × Hutner's Trace Elements. The pH of the medium was adjusted to 6.5 with NaOH and 20 g/L agar were added before autoclaving for 20 min at 121 °C. The 1000 × Hutner's Trace Element solution was composed of 5 g/L FeSO<sub>4</sub>·7H<sub>2</sub>O, 50 g/L EDTA-Na<sub>2</sub>, 22 g/L ZnSO<sub>4</sub>·7H<sub>2</sub>O, 11 g/L H<sub>3</sub>BO<sub>3</sub>, 5 g/L MnCl<sub>2</sub>·4H<sub>2</sub>O, 1.6 g/L CoCl<sub>2</sub>·6H<sub>2</sub>O, 1.6 g/L CuSO<sub>4</sub>·5H<sub>2</sub>O, and 1.1 g/L (NH<sub>4</sub>)<sub>6</sub>Mo<sub>7</sub>O<sub>24</sub>·4H<sub>2</sub>O, pH 6.5 [234]. After incubation at 30 °C for 7 days, the conidia were harvested by suspension in 50 % glycerol and filtered through a sterile Miracloth (Merck KGaA, Darmstadt, Germany). The final concentration of the suspension was adjusted to 3·10<sup>7</sup> spores/mL. Aliquots were prepared and stored at -80 °C until use.

### 2.2.2. PAC tolerance tests on agar plates

The medium for tolerance tests was similar to that used for conidia preparation, but additional defined amounts of untreated or detoxified PAC were added after autoclaving to prevent heat-induced changes of the PAC composition. For inoculation, 5  $\mu$ L of spore suspension ( $c = 1 \cdot 10^7$  spores/mL) were dropped onto the middle of the plate. After 5 days of incubation at 30 °C the colony diameters were determined as the mean value of two measurements at an angle of 90 °. All growth tests were performed as quadruplicates.

### 2.2.3. Pre-cultures

The general medium composition for all pre-cultures performed in this thesis was 4 g/L  $(\text{NH}_4)_2\text{SO}_4$ , 0.75 g/L  $\text{KH}_2\text{PO}_4$ , 0.98 g/L  $\text{K}_2\text{HPO}_4$ , 0.1 g/L  $\text{MgSO}_4 \cdot 7\text{H}_2\text{O}$ , 0.1 g/L  $\text{CaCl}_2 \cdot 2\text{H}_2\text{O}$ , 5 mg/L NaCl, 5 mg/L  $\text{FeSO}_4 \cdot 7\text{H}_2\text{O}$  [33] and 2 mL/L Hutner's Trace Element solution. All cultivations were performed in 500 mL baffled shake flasks, each containing 100 mL of medium and 1 mL of a 10 % Tween® 80 solution to prevent the fungus from adhering to the flask walls. The pre-cultures were inoculated by adding 1 mL of spore suspension with a concentration of  $3 \cdot 10^7$  conidia/mL and incubated at 30 °C and 100 rpm for 96 h (unless otherwise stated). To follow substrate consumption and pH change during cultivation, a daily sampling of 1.9 mL was performed from all cultures that were not intended for inoculation of main cultures. The remaining contents of these flasks were used for biomass quantification. All growth experiments were performed as biological triplicates.

#### 2.2.3.1. Pre-culture cultivations for the transcriptome analysis

Pre-cultures using glucose, pure acetate or 20 % detoxified PAC as C-sources were performed to characterize the growth of *A. oryzae* on these substrates and to isolate RNA from the biomass formed. The concentration of the first two C-sources was chosen according to the amount of acetate present in PAC to ensure comparability between the cultures. Glucose and acetate were added directly to the corresponding media and the pH of the latter was adjusted to 6.5 with NaOH pellets before both media were autoclaved at 121 °C for 20 min. By contrast, the PAC medium was prepared without the C-source as a 2 $\times$  concentrated stock solution. After autoclaving, it was supplemented to 1 $\times$  concentration by adding sterile ultrapure water and 20 % sterile-filtered (Nalgene Rapid-Flow, 0.2  $\mu$ m PES membrane, Thermo Scientific) detoxified PAC. The glucose cultivation was performed for 48 h, whereas the cultures with acetate and PAC were incubated for 72 h.

### 2.2.3.2. *Pre-cultures containing acetol and acetol-acetate mixtures*

To investigate whether *A. oryzae* is able to utilize acetol as a C-source, shake flask pre-cultures containing the above mentioned medium components and 3, 5, 10, 20, 30, 40 and 50 g/L acetol were prepared. The media were autoclaved at 121 °C for 20 min and a subsequent pH adjustment to 6.5 was performed using 10 M NaOH. The media for the cultivations with acetate-acetol mixtures were prepared in a similar manner, but the components were dissolved in a 40 g/L acetate solution and only acetol concentrations of 0-40 g/L were tested. The pH of the media was set to a value of 7 before autoclaving using NaOH pellets, but was readjusted with 10 M NaOH afterwards if necessary.

### 2.2.3.3. *Pre-culture for characterization of the fungal growth on 100 % detoxified PAC*

In order to evaluate whether treatment with the optimized detoxification procedure would allow *A. oryzae* to grow on pure pyrolysis condensate, pre-culture media were prepared by dissolving the media components directly in the detoxified PAC followed by sterile filtration.

### 2.2.3.4. *Pre-cultures for main culture inoculation*

Pre-cultures were not only needed to study fungal growth, but also to inoculate main cultures for malic acid production. For all main culture experiments with 100 % detoxified PAC, the condensate was also used as the sole C-source in the pre-cultures. The corresponding medium were prepared as described in the previous section. In contrast, the biomass used for inoculation of main cultures containing acetate, i.e., the mixtures with acetol in shake flasks as well as the bioreactor fermentations, was grown in pre-cultures containing 40 g/L acetate as sole substrate. For these pre-cultures, basically the same cultivation conditions were used as for the growth experiments. However, no sampling was performed and the cultivation time was shortened to 48 h to allow the cells to be transferred to the main culture in their exponential growth phase.

## 2.2.4. **Main cultures in shake flasks**

In general, all main culture media consisted of 1.2 g/L (NH<sub>4</sub>)<sub>2</sub>SO<sub>4</sub>, 0.1 g/L KH<sub>2</sub>PO<sub>4</sub>, 0.17 g/L K<sub>2</sub>HPO<sub>4</sub>, 0.1 g/L MgSO<sub>4</sub>·7H<sub>2</sub>O, 0.1 g/L CaCl<sub>2</sub>·2H<sub>2</sub>O, 5 mg/L NaCl, and 60 mg/L FeSO<sub>4</sub>·7H<sub>2</sub>O. The media for the main cultures with mixtures of 40 g/L acetate and 3-20 g/L acetol were prepared similarly to the pre-cultures, but the pH was adjusted to 5.5 with NaOH pellets. Afterwards the media were autoclaved at 121 °C for 20 min. In contrast, for all main cultures containing PAC, the medium was sterile filtered after dissolving the above components in the

condensate. While the pH of the medium was not adjusted in the first PAC cultivation, for the experiment on the effect of the initial medium pH on malic acid production, the pH was lowered to 5.5 before sterile filtration using 96 % H<sub>2</sub>SO<sub>4</sub> or 100 % acetic acid. A concentration of 90 g/L CaCO<sub>3</sub> was added to each shake flask and inoculation was performed by transferring 0.75 g of filtered (Miracloth) and thoroughly washed biomass from the corresponding pre-cultures. The main cultures were incubated for 240 h at 32 °C and 120 rpm and samples of 4 mL were taken every 48 h to determine substrate consumption, product formation and pH. All experiments were performed as biological quadruplicates.

### **2.2.5. Main culture in bioreactors**

Four parallel *A. oryzae* batch fermentations were performed in the sixfors bioreactor (Infors AG, Switzerland), a multi-fermenter system that allows for simultaneous cultivation in up to six 500 mL vessels. Each vessel can be controlled independently via a shared control unit equipped with IRIS software for online monitoring of the cultivation parameters. The media for the bioreactor cultures consisted of the same components already listed in the section on the main culture experiments in shake flasks. To prepare the medium for the control reactors, these components were dissolved in a solution of 40 g/L acetic acid and the mixture was adjusted to a pH of 5.5 with NaOH pellets. A volume of 350 mL of the medium was added to each of the reactors, which were then autoclaved at 121 °C for 20 min. As in the shake flask main cultures, the medium containing PAC was sterilized via filtration and 350 mL of the medium was filled into each of the previously autoclaved reactors. A concentration of 90 g/L CaCO<sub>3</sub> was sterilely added to all bioreactors. For inoculation, the contents of two pre-culture flasks were filtered together through a Miracloth filter, washed thoroughly with sterile ultrapure water and resuspended in 50 mL of the corresponding main culture medium. The suspension was added to the bioreactor, resulting in a final working volume of 400 mL. Throughout the fermentation, the temperature and stirrer speed were kept constant at 32 °C and 800 rpm, respectively, and aeration was performed at a rate of 10 L/h. Immediately after the start of aeration, 0.1 mL of anti-foam solution (Contraspum A 4050 HAC (Zschimmer und Schwarz GmbH und Co KG, Lahnstein, Germany) was sterilely added to the bioreactors to prevent foam formation. The total cultivation time was 144 h, and samples of 4 mL were taken from each reactor once a day to quantify substrate consumption and product formation. Starting at 72 h of cultivation, the pH was manually adjusted to a value < 7.5 with 72 % H<sub>2</sub>SO<sub>4</sub> after each sampling. Fermentations were performed as biological duplicates.

## 2.3. PAC formation and detoxification

The PAC used in this work is derived from the fast pyrolysis of wheat straw, which is part of the bioliq® process performed at KIT. A detailed description of the whole process was given by Pfitzer et al. [77]. Condensation of the vapors released during pyrolysis takes place in two successive stages, with the aqueous condensate being formed in the second condensation step at a temperature of about 30°C. The composition of the PAC was analyzed via GC/MS by the Thünen Institute of Wood Research in Hamburg and can be found in the **Appendix 1**.

### 2.3.1. Detoxification procedure for the transcriptome analysis

Prior to use as a substrate in the cultivations performed for transcriptome analysis, the PAC was detoxified using a pretreatment procedure according to Lian et al. [110]. However, the initial neutralization step with NaOH included in this procedure was replaced by overliming with Ca(OH)<sub>2</sub>. For this overliming treatment, the pH of the PAC was increased to a value of 10 and the condensate was then incubated in an oil bath at 80 °C for 4 h with continuous stirring. After incubation, the PAC was centrifuged at 4700 × g for 10 min to remove precipitates and the supernatant was filtered using a filter paper (Macherey-Nagel, type MN615, cellulose). The pH of the filtrate was adjusted to 6.5 using 96 % H<sub>2</sub>SO<sub>4</sub> and the condensate was then further processed via rotary evaporation. For this treatment, the PAC was heated to 80 °C in an oil bath under constant rotation at 90 rpm. The pressure was gradually reduced to 40 mbar and the PAC was refilled with ultrapure water to the initial volume to prevent concentration of non-volatile toxins. Finally, 10 % (w/v) activated carbon was added to the PAC, and the suspension was incubated for 1 h at room temperature with continuous stirring. The carbon was then separated by centrifugation using the aforementioned parameters and the supernatant was further purified by two successive vacuum filtration steps to remove residual carbon particles. The first step, using a Büchner funnel and two layers of filter paper (Whatman, type 595), was followed by bottle top filtration. The GC/MS analysis of the PAC composition after the treatment was performed by the Thünen Institute of Wood Research and is included in **Appendix 1**.

### 2.3.2. Optimization of the detoxification procedure

**Table 5** gives a summary of the different parameters investigated for each pretreatment method in order to improve the PAC detoxification procedure that was used prior to transcriptome analysis (2.3.1.). A more detailed description of the individual optimization experiments is given in the following sections.

**Table 5:** Summary of the experiments for optimization of the pretreatment procedure

Detoxification method	Parameter	Tested values
<b>Laccase</b>	Enzyme concentration [U/mL]	0, 1.25, 2.5, 5, 10, 25
	Treatment duration [h]	0, 0.5, 1, 2, 4, 8, 24
<b>Activated carbon</b>	Carbon loading [% (w/v)]	0, 1.25, 2.5, 5, 10
<b>Overliming</b>	Temperature [°C] <sup>1</sup>	20, 40, 60, 80, 100
	pH <sup>2</sup>	pH 10 not adjusted, pH 12 not adjusted, pH 10 adjusted
	Hydroxide <sup>3</sup>	NaOH, Ca(OH) <sub>2</sub>
<b>Rotary evaporation</b>	Pressure [mbar]	200, 300, 400

<sup>1</sup> performed at pH 10

<sup>2</sup> performed at 80 °C

<sup>3</sup> all overliming experiments were performed with both hydroxides

#### 2.3.2.1. Laccase treatments

The enzymatic treatment of the pyrolysis condensate was performed using *T. versicolor* laccase (38429, Sigma Aldrich) with a specific activity of >0.5 U/mg. To determine the optimum enzyme amount and duration for PAC detoxification enzyme concentrations of 0, 1, 2.5, 5, 10 and 25 U/mL were added to 5 mL of the PAC and the mixtures were incubated for 24 h at 30 °C and 180 rpm. Samples of 200 µL were taken after 0, 0.5, 1, 2, 4, 8 and 24 h and diluted 1:10 in 10 % acetic acid immediately to perform a pH induced halt in the enzymatic reaction [235]. The experiments were performed in duplicates. For the growth test on agar plates, the PAC was treated with 25 U/mL for 24 h.

#### 2.3.2.2. Activated carbon

To optimize the activated carbon treatment, carbon loads of 0, 1.25, 2.5, 5 and 10 % (w/v) were added to 100 mL PAC and the suspension was constantly stirred for 1 h at room temperature. To track changes in the PAC composition 5 mL samples were taken every 15 min and

centrifuged immediately. The supernatant was then filtered through a 0.2  $\mu\text{m}$  syringe filter and stored at 4 °C until analysis. After the incubation, the remaining mixture was centrifuged and filtered as previously described in 2.3.1. The experiment was performed in duplicates, but both batches were combined after filtration and used for the *A. oryzae* growth test.

#### 2.3.2.3. *Overliming*

The use of the two hydroxides NaOH or  $\text{Ca}(\text{OH})_2$  at different pH-values and temperatures was investigated to optimize the overliming process outlined in 2.3.1. To evaluate the influence of the latter on the detoxification efficiency oil bath temperatures of 20, 40, 60, 80 and 100 °C were tested. For this experiment, the initial pH values were set to 10. The alkaline PAC was incubated for 4 h and samples of 3 mL were taken at hourly intervals. The experiment was performed in duplicates at 100 mL scale. For the pH experiments, the temperature was set to 80 °C and the incubation time was shortened to 90 min. In addition to the standard procedure, two alternative pH strategies were applied: increasing the initial pH to 12 and regulating the pH to a value of 10 throughout the overliming process. The experiment was performed at 500 mL scale and 15 mL samples were taken every 15 min. The pH of the regulated batch was manually adjusted after every sampling, using the same hydroxide that was applied for the initial pH increase.

#### 2.3.2.4. *Rotary evaporation*

To ensure more stable evaporation conditions compared to the procedure described in 2.4.1, the PAC was preheated for 10 min in the 80 °C oil bath at atmospheric pressure and a rotation speed of 90 rpm. Following the preheating phase, the pressure was decreased gradually to values of 400, 300 and 200 mbar and was kept constant for 4 h. After the evaporation, the condensate was refilled with ultrapure water to the initial volume to avoid a concentration of residual inhibitors. The experiments were performed in duplicates.

#### 2.3.2.5. *Combination of pretreatment methods*

In the combination experiments, the activated carbon treatment was performed using a carbon load of 10 % (w/v) for 10 min. The overliming in this experiment was carried out at 100 °C and an initial pH of 12 using NaOH pellets as alkaline agent. For the rotary evaporation, a pressure of 200 mbar was held for 4 h at the temperature and rotary speed already mentioned above.

## 2.4. Transcriptome analysis

### 2.4.1. RNA isolation, library preparation and sequencing

To ensure comparable growth phases for all substrates tested, cell harvest for RNA isolation was performed at different time points of the cultivation. While sampling for glucose and pure acetate was performed after 24 h, biomass of the PAC cultures was harvested after 48 h. For the biomass harvest, the content of the entire shake flask was poured through a Miracloth filter and then rinsed with ultrapure water. The washed biomass was snap frozen with liquid nitrogen and stored at -80 °C until further use. Total RNA isolation, poly A enrichment of mRNA, construction of Illumina-stranded TruSeq RNA libraries as well as the actual mRNA sequencing (Illumina NextSeq, 75 bp, paired-end) were performed by Microsynth AG (Balgach, Switzerland).

### 2.4.2. RNA-seq data analysis

Quality control of raw reads was performed with fastQC v0.11.9 [236] and fastp v 0.20.1 using the default settings, except the cut window size (-W), the minimum length (-l) and the qualified quality Phred (-q) set at 16, 50 and 30, respectively. We mapped the high quality reads against the *A. oryzae* RIB40 genome [237] using STAR v 2.7.10a [238] and generated read counts with RSEM v1.2.28 [239] under default settings. The gene count data were filtered (minimal counts per million (CPM) = 0.5 in at least one library) and transformed based on the regularized logarithm (rlog) transformation method implemented in iDEP.95 [240]. iDEP.95 was also used to perform and visualize the principal component analysis (PCA) of the transformed read data as well as for the differential gene expression (DGE) analysis using the DESeq2 package [241]. For the DGE analysis, the  $\log_2$  fold change ( $\log_2$ FC) and false discovery rate (FDR) thresholds were set at >2 and <0.05, respectively. To gain insights into the functional implication of the observed DGE, we performed gene ontology (GO) term enrichment analysis in iDEP.95 and KEGG pathway analysis using Pathview Web [242]. Additional annotation of *A. oryzae* RIB40 predicted proteins was performed with eggNOG mapper v2.1.7 [243] and uniprot [244].

## 2.5. Analytics

### 2.5.1. Quantification of the fungal biomass formation

For determination of the fungal cell dry weight (CDW) the culture broth of a whole shake flask was filtered through pre-weighed paper filters. After thorough washing with ultrapure water, the biomass containing filters were dried in an oven at 70 °C until a constant weight was reached. The weight of the filters was measured using a precision scale and the CDW was expressed in g/L after subtraction of the filter blank weight.

### 2.5.2. High pressure liquid chromatographic (HPLC) analysis

With the exception of the acetate content in the pre-cultures that contained 20 % detoxified PAC, all substrate concentrations in the fungal fermentations were determined by reversed-phase HPLC (Agilent 1100 Series, Agilent, Germany). Prior to analysis, samples were centrifuged at 4700 x g for 10 min to spin down the biomass and residual CaCO<sub>3</sub> and 10 µL of the supernatant was injected into the HPLC after appropriate dilution. Measurements were performed using a Rezex ROA organic acid H+ (8%) column (300 x 7.8 mm, 8 µm particle size, Phenomenex) and a Rezex ROA organic acid H+ (8%) guard column (50 x 7.8 mm). For determination of the glucose content, the oven temperature was set at 50 °C and 5 mM H<sub>2</sub>SO<sub>4</sub> was used as eluent, while 60 °C and 3 mM H<sub>2</sub>SO<sub>4</sub> were chosen for the analysis of acetate and acetol concentrations. In both cases, elution was performed isocratically at a flow rate of 0.5 mL/min. Glucose was detected with a refractive index detector, whereas a UV detector with wavelengths of 220 and 280 nm was used for detection of acetate and acetol, respectively. The actual quantification was performed via calibration curves in the range of 0.1-5 g/L.

### 2.5.3. Gas chromatographic (GC) analysis of inhibiting PAC components

While the untreated PAC as well as its composition after detoxification for the transcriptome experiments were analyzed in detail by GC/MS at the Thünen Institute for Wood Research (**Appendix 1**), only selected PAC components were quantified during the optimization of the pretreatment procedure. The change in the content of acetol, furfural, 2-cyclopenten-1-one, guaiacol and phenol in the PAC was determined using a GC system (Agilent 6850 series, Agilent, Germany) equipped with a DB WAX column (30 m × 0.25 mm ID × 0.25 µm film thickness) and an FID detector. A sample volume of 1 µL entered the system via a split–splitless injector, operated at a split ratio of 25:1 and 250 °C. Helium was used as carrier gas. The GC

oven program started with a temperature hold at 40 °C for 1 min, followed by three 5 °C/min ramps to 60 °C, 120°, 200 °C, respectively. The temperature at the end of every ramp was held for 2 min. The GC was operated at a constant pressure of 0.489 bar. The concentrations of acetol and 2-cyclopenten-1-one were quantified using calibration curves ranging from 0.005-5 g/L, whereas those for furfural, phenol, and guaiacol covered a range of 0.001-1 g/L.

#### **2.5.4. Folin-Ciocalteu (FC) analysis**

The concentration of the total phenolics in the laccase treated PAC was quantified via microscale Folin-Ciocalteu colorimetry according to Waterhouse [245], but the reaction volume was halved. Accordingly, 10 µL of sample were added to a mixture of 0.79 mL of ultrapure water and 50 µL FC reagent. After vortexing, the mixture was incubated for 5 min and 150 µL of 25 % (w/v) sodium carbonate were added into the cuvettes. The solution was again thoroughly mixed by vortexing and incubated for 1 h at room temperature. The actual measurement was performed at 765 nm using a spectrophotometer (Spectronic 200, Thermo Scientific) and the amount of total phenolics was determined as gallic acid equivalents (= GAE) via a calibration curve ranging from 0.05-1 g/L of gallic acid. Like the laccase samples, the calibration points were prepared as 1:10 dilutions using 10 % acetic acid to compensate for possible side reactions of the acetic acid with the FC reagent.

#### **2.5.5. Spectrometric quantification of ammonia**

Nitrogen source consumption in the *A. oryzae* shake flask pre-cultures containing 100 % PAC was analyzed using the Spectroquant® ammonium test kit (114752, Merck KGaA, Darmstadt, Germany). The measurement was performed following the procedure recommended by the manufacturer, except for adaptation to microtiter plate scale by reducing the volume to 200 µL.

#### **2.5.6. Quantification of acetate by enzyme assays**

The acetate content of PAC during optimization of the pretreatment procedure and in the 20 % PAC cultures was analyzed by enzyme assays (10148261035, R-Biopharm AG, Darmstadt, Germany). The final volume specified in the manual was reduced to either a quarter or a twentieth when cuvettes or microtiter plates were used for quantification. While in cuvette scale the measurement was performed according to the manufacturer's instructions, the concentration in microtiter plates was determined via an acetate calibration curve ranging from 0.03-0.15 g/L.

### 3. Variations in the fungal gene expression in response to growth on the pyrolytic aqueous condensate

This chapter is mainly based on the publication:

**RNA-seq based transcriptome analysis of *Aspergillus oryzae* DSM 1863 grown on glucose, acetate and an aqueous condensate from fast pyrolysis of wheat straw**

Christin Kubisch; Aline Kövilein; Habibu Aliyu and Katrin Ochsenreither

Institute of Process Engineering in Life Science 2: Technical Biology, Karlsruhe Institute of Technology, Karlsruhe, Germany

**Publication details:**

*Journal of Fungi*

Volume: 8, Article 765

Publication date: 23 July 2022

DOI: 10.3390/jof8080765

**Author's contribution:**

**Christin Kubisch** designed and performed the experiments, performed the laboratory and computational analysis of the data and drafted the manuscript.

**Aline Kövilein** designed and performed the experiments, performed the laboratory and computational analysis and revised the manuscript.

**Habibu Aliyu** contributed in the conceptualization of the study, performed and supervised the computational analysis and revised the manuscript.

**Katrin Ochsenreither** contributed in the conceptualization of the study, supervised the laboratory work and revised the manuscript.

### 3.1. Introduction

In this chapter, RNA-seq-based transcriptome analysis was performed to investigate the gene expression of *A. oryzae* DSM 1863 in response to using PAC as carbon source for growth in shake flask cultures and to compare it with the transcriptome during cultivations on glucose or pure acetate. Since the low resistance of the fungal wildtype strain towards the untreated condensate prevents its use as substrate in liquid cultures, the transcriptome analysis required pretreatment by a combination of overliming with  $\text{Ca}(\text{OH})_2$ , rotary evaporation, and activated carbon. This detoxification procedure allowed growth on 20 % PAC and the acetate content therein served as a reference value for the initial substrate concentration in the cultures with glucose and pure acetate. Despite the same substrate content, the fungus was expected to show a different growth behavior during cultivation on the individual C-sources. Therefore, the optimal time point for total RNA isolation from the cultures had to be determined first to ensure comparable experimental conditions for the transcriptome analysis.

The isolated RNA was then sequenced and the reads obtained for each substrate were aligned to the genome of the reference strain *A. oryzae* RIB40. The number of reads mapped to each gene was counted and the filtered and processed count data provided the basis for the actual differential gene expression analysis. Gene ontology and metabolic pathway analyses of the resulting significantly differentially expressed ( $\log_2\text{FC} > 2$  &  $\text{FDR} < 0.05$ ) genes were performed to gain insights into their cellular functions.

Comparison of the transcriptome during growth on acetate and PAC was intended to distinguish genes involved in metabolizing the major C-source contained in the condensate from those whose expression changed in response to the presence of the PAC inhibitors. Especially the latter are of great interest when it comes to increasing fungal PAC tolerance by genetic strain engineering.

## 3.2. Results and discussion

### 3.2.1. Characterization of fungal growth on the different carbon sources

To ensure the construction of comparable RNA libraries for all substrates, growth of *A. oryzae* on the different C-sources was first characterized in a preliminary shake flask experiment. As shown in **Figure 10**, substrate concentrations at the beginning of the cultivation ranged from  $6.99 \pm 0.03$  g/L to  $7.48 \pm 0.19$  g/L.

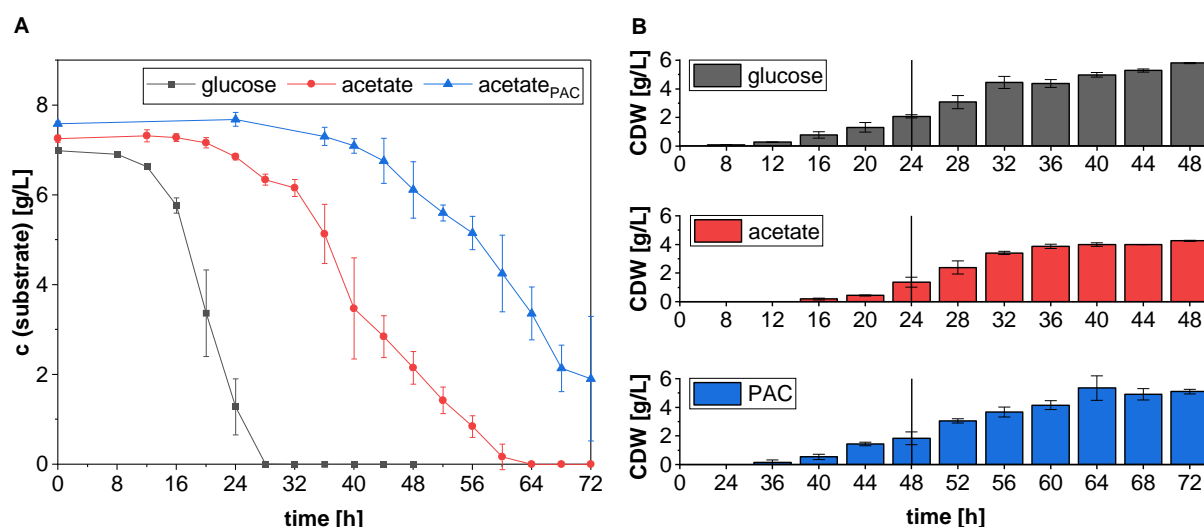


**Figure 10:** Substrate consumption (A) and biomass formation (B) in *A. oryzae* cultures containing glucose, acetate and 20 % detoxified PAC. The vertical lines indicate the time of sampling for RNA isolation. The data are means of three biological replicates and the error bars represent the standard deviation.

Besides these minor differences in the initial substrate concentration, the cultures differed primarily in the duration of their lag phase. While in the cultures with glucose the substrate conversion and biomass formation started already after 8-12 h, the lag phase in the two other cultures was considerably prolonged. For the flasks containing pure acetate, a formation of  $0.19 \pm 0.06$  g/L biomass was observed after 16 h, although no decrease in substrate concentration could be detected. This indicates that at that time the fungus was still consuming the reserves stored in the conidia as well as the remaining glycerol from the spore suspension. The fungal ability to metabolize the polyol has been reported by Ochsenreither et al. [33]. However, after these first 16 h, the acetate concentration began to decrease gradually. The longest lag phase was observed in the PAC cultures, as in these flasks an onset of acetate consumption and biomass formation became detectable only after 36 h of cultivation. This is most likely due to the presence of growth inhibitory components in the pyrolysis condensate.

According to Dörsam et al, among the compounds that were still present in the PAC after the detoxification procedure (**Appendix 1**), hydroxyacetone, 2-cyclopenten-1-one, and furfural were the most relevant growth inhibitors, whereas ethylene glycol and  $\gamma$ -butyrolactone were found to be rather harmless to *A. oryzae* [149]. Considering that 20 % PAC were used, only the concentration of 2-cyclopenten-1-one was still close to the growth limit of 0.00625 wt.-% determined by Dörsam et al. [149]. However, it can be assumed that some inhibition already occurs at concentrations below the growth limit.

By the time growth and acetate metabolization were just starting in the flasks with PAC, the substrate had already been completely consumed in the glucose-containing cultures. However, the depletion of glucose did not result in transition to the stationary phase. Rather, after a short stagnation between 32-36 h, the biomass concentration increased again and resulted in a final CDW of  $5.80 \pm 0.04$  g/L. This suggests that after glucose was consumed, other substrates were used for growth, which may possibly have been organic acids previously produced by the fungus itself. In the acetate cultures, the end of the exponential growth phase was reached after 36 h, and the biomass concentration increased only slightly from  $3.87 \pm 0.14$  g/L to  $4.26 \pm 0.04$  g/L during the last 12 h of cultivation. As **Figure 10** indicates, this retardation in cell growth cannot be attributed to substrate depletion, since at this time  $5.13 \pm 0.66$  g/L of acetate was still present in the medium. Furthermore, as there was also no reduction in acetate consumption, it can be assumed that the fungus was still metabolically active. This activity resulted in complete depletion of the substrate after 64 h. However, at this stage of cultivation no further determination of CDW was performed, since the main objective of the experiment was to characterize the exponential growth phase.

There was hardly any exponential phase observed during growth on PAC, as the increase in biomass in these cultures was rather linear. The maximum CDW of  $5.35 \pm 0.86$  g/L was reached after 64 h of cultivation and biomass formation largely stagnated afterwards. As already observed for the acetate cultures, no reduction in substrate consumption was detected. However, due to the later onset of acetate metabolization in the PAC cultures,  $1.26 \pm 0.38$  g/L substrate remained unused at the end of the experiment.

Interestingly, the maximum CDW achieved on PAC was only slightly lower than in the glucose cultures, while the lowest biomass concentration was obtained for pure acetate. This suggests that the fungus is able to utilize other PAC components in addition to acetate. Moreover, the fact that the fungus was able to grow normally on PAC after overcoming the initial lag phase may indicate that the inhibitors either exerted their negative influence mainly on the early developmental stages of the fungus or that the toxic substances can at least partially be

degraded. For example, it has been reported for some *Aspergillus* strains that they are capable of converting furanic compounds like HMF or furfural [246, 247].

In summary, this experiment demonstrated the necessity to first characterize growth on the different C-sources to ensure similar cultivation conditions by the time of RNA sampling. This is important because He et al. revealed that the growth phase has a major impact on gene expression in *A. oryzae*, with the greatest differences occurring during the transition from the adaptive to the exponential phase [248]. As indicated by the vertical line in **Figure 10**, the RNA sampling was therefore performed after 24 h in the flasks containing glucose and acetate, whereas the biomass of the PAC cultures was harvested after 48 h.

### 3.2.2. General characteristics of the RNA-seq data

After determination of the ideal sampling time the actual RNA isolation and sequencing was performed. We obtained  $184.30 \times 2$  million reads (mean read length: 75 bp), ranging between 18.72 and 22.87 million reads per sample (**Table 6**).

**Table 6:** Quality characteristics of the RNA-seq data obtained for *A. oryzae* cultivated on glucose, acetate and 20 % detoxified PAC

sample	read count		alignment ratio [%]	
	raw	clean	uniquely mapped	unaligned
Glc1	22,221,898	17,902,548	97	3
Glc2	20,409,071	16,336,686	96	3
Glc3	21,015,522	16,346,846	93	6
Ace1	19,792,462	15,781,442	95	4
Ace2	18,718,483	14,332,714	93	7
Ace3	20,242,931	15,735,543	93	7
PAC1	22,870,039	17,628,982	94	5
PAC2	19,884,644	15,059,444	96	4
PAC3	19,141,036	14,198,088	86	14

After removing the adaptor sequences as well as low-quality and ambiguous reads, the final RNA-seq data comprised 14.20-17.90 million clean reads per sample. These clean reads were aligned against the *A. oryzae* RIB 40 genome (ASM18445v3) [237] and could be uniquely mapped at an average rate of 94 %, confirming the high quality of our RNA-seq data. Only PAC sample 3 showed a slightly lower, but still acceptable alignment ratio of 86 %. Overall,

9,634 genes passed the set filter of 0.5 CPM in a minimum of one library and formed the basis of subsequent analyses. **Figure 11** displays the distribution and the principal component analysis (PCA) of the transformed and normalized gene counts.

The PCA showed a close clustering of the individual samples within a triplicate and a clear separation between the different C-sources, suggesting high repeatability of the RNA-seq data. Approximately 79 % of the transcriptome variation among the compared samples could be explained in PC1 (60 %) and PC2 (19 %), indicating clear variation in transcriptome profiles among the three treatment regimes.

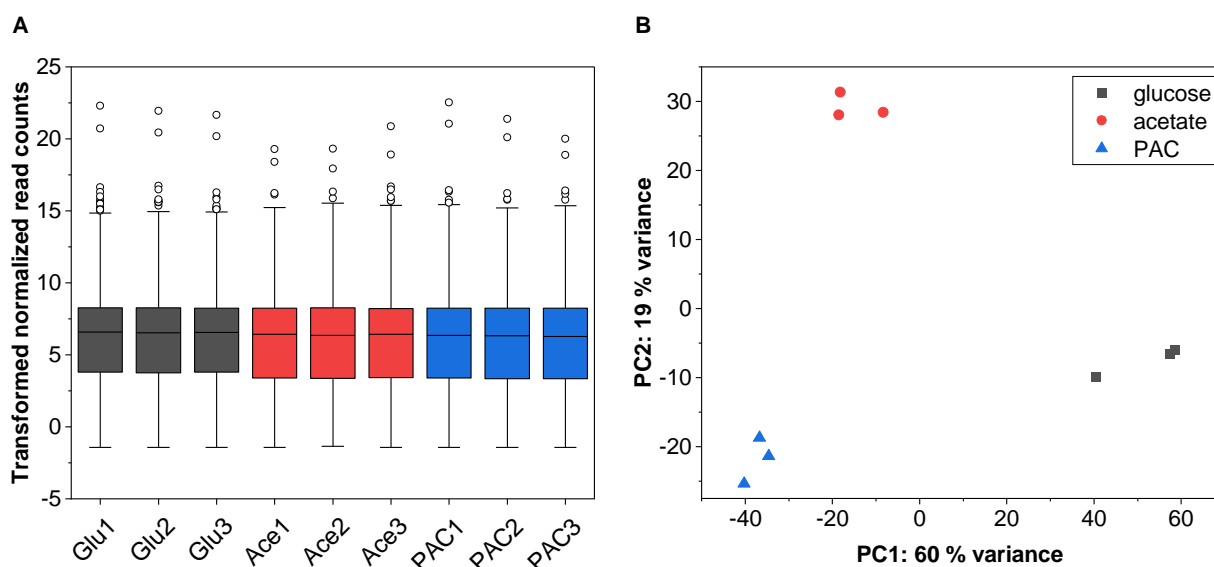


**Figure 11:** Box plot of the transformed and normalized read count data (A) and principal component analysis (PCA) showing the variance between the individual samples (B)

### 3.2.3. Differential gene expression during growth on the different carbon sources

DGE analysis revealed 3,463 significantly differentially expressed ( $FDR \leq 0.05$  and  $\log_2FC \geq 2$ ) genes, of which only 275 genes (7.94 %) showed differential expression in all three conditions (**Figure 12**). In comparison to glucose, growth on PAC and acetate led to significant expression changes in 2,902 and 1,986 genes, respectively. By contrast, when comparing the transcription profiles between acetate and PAC, only 901 genes showed significant differential expression. This value is considerably lower than for the other conditions, which is probably due to the fact that acetate is one of the main components of PAC (**Appendix 1**). Therefore, many of the changes in transcription induced by acetate are probably also found during growth on PAC. Conversely, this may also explain why the number of differentially expressed genes for the comparison between glucose and PAC was 32 % higher than for glucose and pure acetate as it

is very likely that the additional PAC components cause changes in fungal gene expression that are beyond those induced by the acetate.

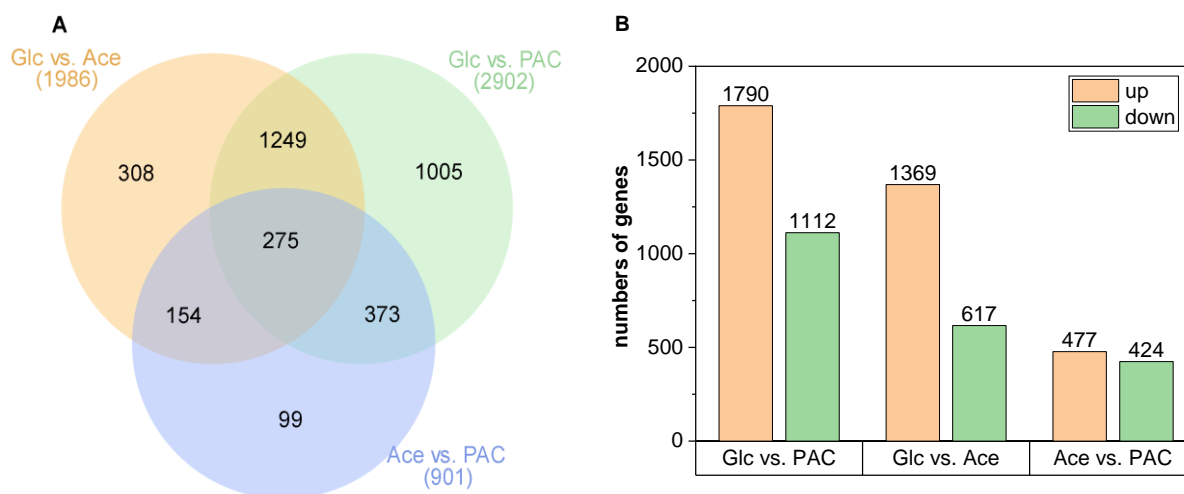


**Figure 12:** Differentially expressed genes of *A. oryzae* during cultivation with 20 % detoxified PAC, acetate or glucose. Venn diagram showing the distribution and overlap of DGE for the comparisons of the different substrates (A). Number of up and downregulated genes for the individual comparisons (B).

Among the 2,902 genes that were differentially expressed during growth on glucose and PAC, there was a set of 1,790 genes being upregulated, whereas 1,112 genes were downregulated. However, even more remarkable when comparing these two C-sources was the relatively large number of 1,005 genes that were uniquely differentially expressed between these two conditions. This corresponds to 29.02 % of the 3,463 genes for which a significant change in expression was detected during this RNA-seq experiment. By contrast, of the 1,369 and 617 genes that were up and downregulated between glucose and pure acetate, respectively, only 308 were found to be differentially expressed exclusively between these two C-sources. Instead, the majority of 1,294 genes, showed an identical transcriptional regulation as observed in the comparison of glucose and PAC. For the reason already stated above, the lowest number of only 477 upregulated and 424 downregulated genes was found for the comparison of acetate and PAC, of which only 99 were differentially expressed solely between these two C-sources. However, these genes are of particular interest for understanding which changes in transcriptional regulation are triggered by the other components of PAC rather than acetate.

### 3.2.4. Functional enrichment and pathway analyses

To gain insight into the functional categories associated with the differentially expressed genes, a gene ontology (GO) enrichment analysis was performed. According to this analysis, upregulated genes in the glucose cultures compared with both pure acetate and PAC were primarily enriched in membrane (GO:0016020) related activities and transmembrane transport (Figure 13 and Figure 14).

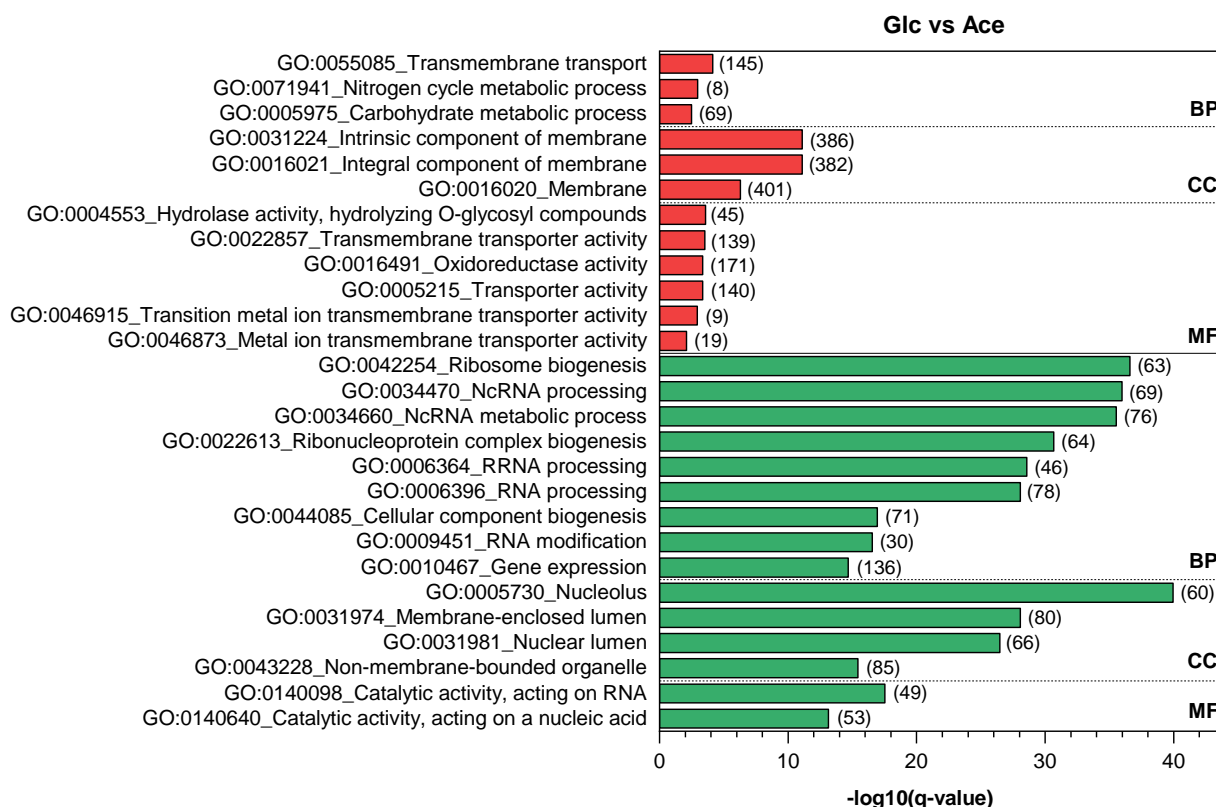


**Figure 13:** Functional enrichment analysis of genes being differentially expressed during cultivation of *A. oryzae* on glucose (Glc) compared to acetate (Ace). GO terms that were upregulated on glucose are shown in red, whereas those that were overrepresented in the acetate cultures are colored in green. The numbers in brackets indicate the set size of genes assigned to the corresponding GO term. BP = Biological process, CC = Cellular component and MF = Molecular function

Unsurprisingly, several of the genes assigned to the latter GO term (GO:0055085) were found to be putative sugar transporters of the major facilitator superfamily (MFS) (Appendix 2). The MFS is one of the largest transporter families in living organisms, whose members can transport a broad spectrum of substances. For instance, in addition to sugar transporters, MFS also includes the families of proton-dependent oligopeptide transporters (POT) and monocarboxylate transporters (MCT) [249], for which some upregulated genes were also found in the present transcriptome analysis. It was rather unexpected that the latter were upregulated

in the glucose cultures and not during growth on acetate or PAC, since a gene encoding an MCT in *Aspergillus* species was described to show increased expression when acetate was used as sole C-source [250]. However, in this study it has also been suggested that the transporter plays a role in the drug resistance of the fungus. Consistent with these findings, several genes belonging to the ATP-binding cassette (ABC) transporters superfamily and thus associated with multidrug resistance (MDR) were found to be upregulated in the glucose cultures. Initially, this also seemed contrary to our expectations, since involvement of an ABC transporter in acetate tolerance had been reported in *S. cerevisiae* [251]. Moreover, there was another study showing that growth of the same organism on a lignocellulosic hydrosylate led to an increased expression of MDR transporters [252].

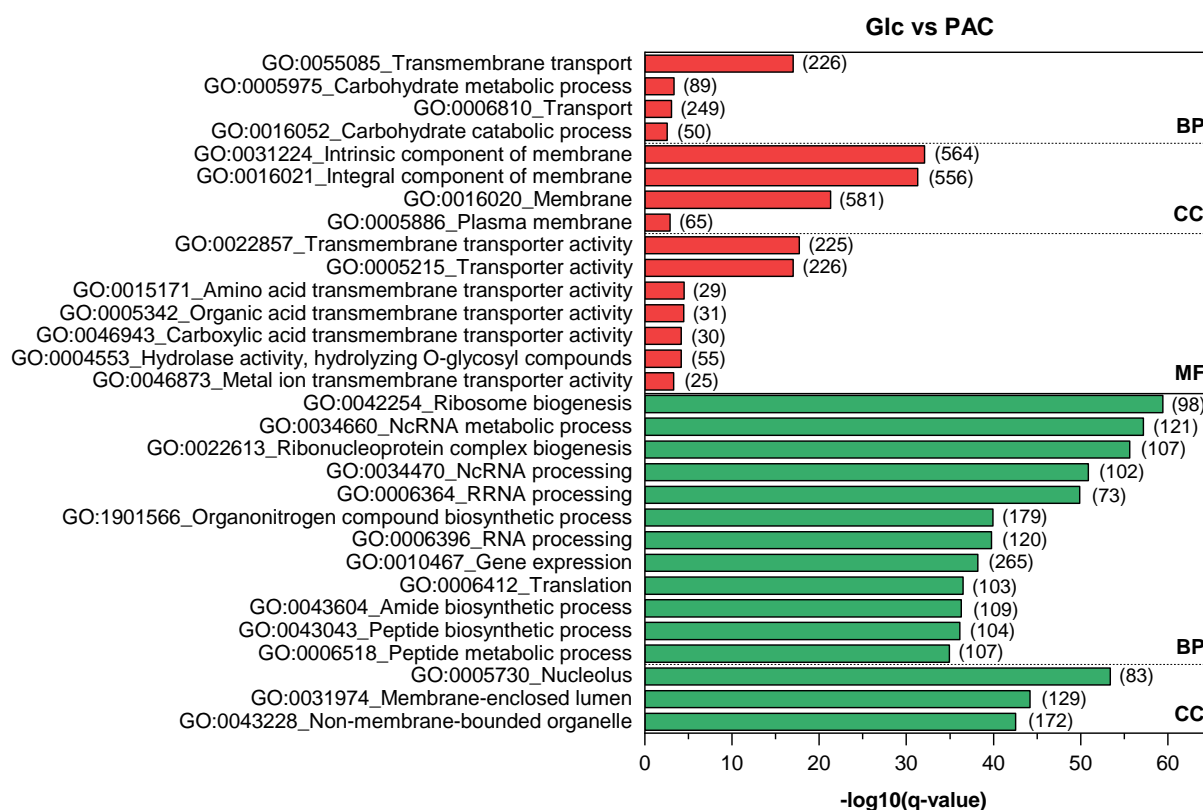


**Figure 14:** Functional enrichment analysis of genes being differentially expressed during cultivation of *A. oryzae* on glucose compared to PAC. GO terms that were upregulated on glucose are shown in red, whereas those that were overrepresented in the PAC cultures are colored in green. The numbers in brackets indicate the set size of genes assigned to the corresponding GO term. BP = Biological process, CC = Cellular component and MF = Molecular function

However, it has been hypothesized that ABC and MFS transporters may also be associated with the synthesis and secretion of secondary metabolites (SM) and mycotoxins [253, 254]. It is therefore assumed that the export of SM might be impaired in the acetate-containing cultures,

leading to the comparatively higher relative expression of transporters in the glucose controls. For example, the *wykF* gene was identified to be upregulated on glucose compared with PAC. This gene encodes an H<sup>+</sup>/oligopeptide symporter of the POT family involved in the secretion of *wyk-1*, a dipeptidyl peptidase IV inhibitor reported to be produced by the *A. oryzae* strain AO-1 [255]. In addition, genes of other MFS transporters including *cpaT* (AO090026000005), *hepF* (AO090011000413) *kojT* (AO090113000138) and a gene of the MCT family (AO090003001541), which are responsible for the export of the antimicrobial agents cyclopiazonic acid [256], heptelidic acid [257], kojic acid [258] and aspergillic acid [259], respectively, all showed increased expression in the glucose cultures. However, since even among the currently uncharacterized transporters in our data sets, most genes belong to the MFS or at least contain a corresponding domain, it seems conceivable that there are even more of these genes involved in SM secretion. The genes that did not belong to the MFS were primarily ion transporters for iron, calcium, potassium and sodium, but also ammonia and amino acid permeases. For the latter, it has been described in both bacteria and yeasts that they can be inhibited by weak organic acids such as acetic acid [260, 261], which could thus explain the downregulation of these genes in the acetate-containing cultures compared to glucose.

The fact that transmembrane transport also played a central role in the comparison of pure acetate and PAC, and that this GO term was downregulated in the cultures containing the pyrolysis condensate (**Figure 15**), suggests that the other PAC components exert an additional inhibitory effect on cellular transport processes. One example is the inhibition of amino acid transport by furfural, as demonstrated for *S. cerevisiae* [175]. Consistent with this study, ~ 20 % of the 68 genes associated with transmembrane transport were identified as amino acid transporters (**Appendix 2**).

However, despite these additional PAC components, the GO terms that were found to be upregulated in comparison to glucose were very similar for both acetate-containing cultures, as they were mainly related to ribosomes and non-coding RNA processing (**Figure 13** and **Figure 14**). It can therefore be assumed that the upregulation is primarily caused by acetate or the high salt concentration in these cultures resulting from the pH adjustment. This was consistent with a transcriptional analysis on the salt tolerance mechanism of the yeast *Zygosaccharomyces rouxii*, which appears to involve increased expression of genes associated with ribosome synthesis and RNA processing [262]. Similar results were obtained in a transcriptome analysis investigating the effects of a sugarcane biomass hydrolysate and its main inhibitors on *Pichia pastoris*. Among the GO terms that were overexpressed in response to

hydrolysate addition were primarily those related to processing of noncoding RNA, and based on the analysis of the individual inhibitors, this observation could be attributed to acetate [263].

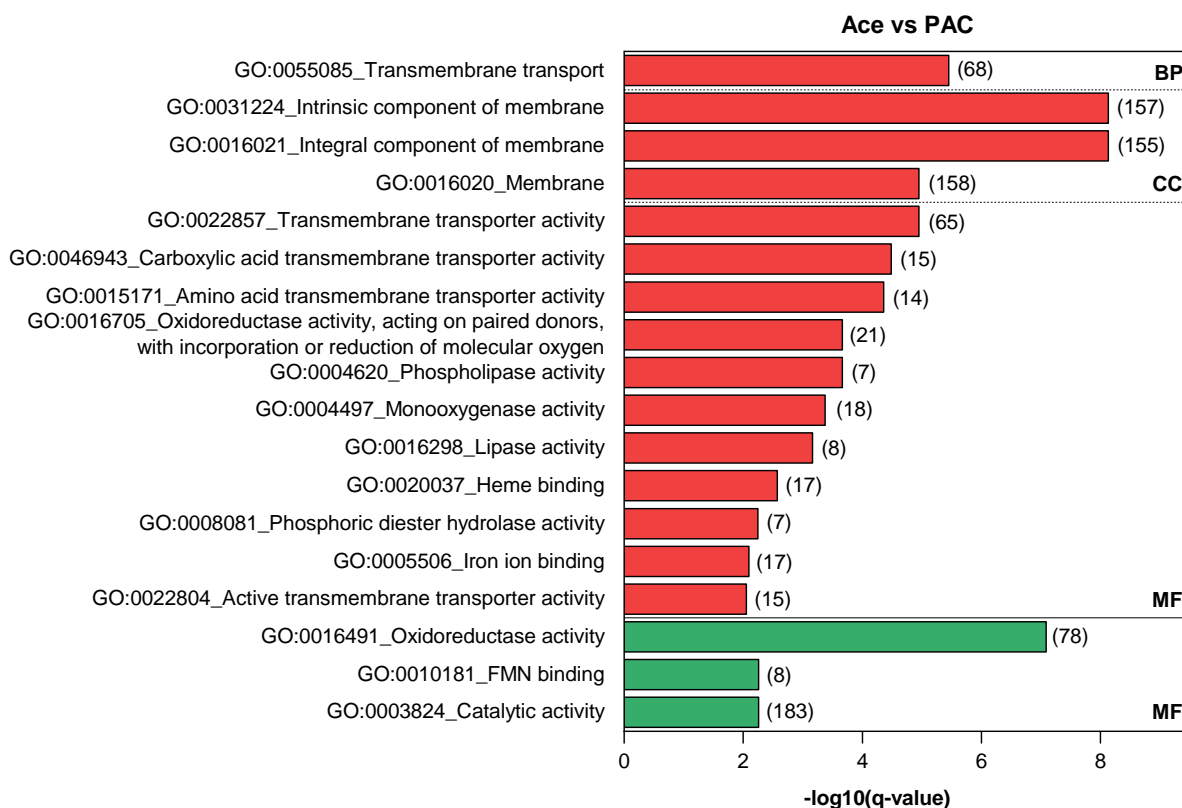


**Figure 15:** Functional enrichment analysis of genes being differentially expressed during cultivation of *A. oryzae* on acetate compared to PAC. GO terms that were upregulated on acetate are shown in red, whereas those that were overrepresented in the PAC cultures are colored in green. The numbers in brackets indicate the set size of genes assigned to the corresponding GO term. BP = Biological process, CC = Cellular component and MF = Molecular function

Since the functional enrichment analysis also included GO terms assigned to carbohydrate degradation process (GO:0016052) and carbohydrate metabolic process (GO:0005975), pathway analysis based on the Kyoto Encyclopedia of Genes and Genomes (KEGG) database was performed to further assess the function of the differentially expressed genes in the fungal metabolism. The analysis revealed that 18 metabolic pathways were differentially expressed between glucose and acetate, while 33 pathways showed an altered expression when the cultures containing glucose and PAC were compared (Table 7 and Table 8). This once again indicates that the additional components of the pyrolysis condensate exert an impact on the transcriptional regulation of the fungus.

**Table 7:** Differentially expressed pathways for the comparisons of glucose with PAC

condition	DGE	KEGG pathway ID	KEGG pathway name	set size	adjusted p-value	
Glc vs PAC	up	aor00500	Starch and sucrose metabolism	25	$1.50 \cdot 10^{-4}$	
		aor00520	Amino sugar and nucleotide sugar metabolism	19	$4.40 \cdot 10^{-3}$	
		aor00100	Steroid biosynthesis	13	0.01	
			aor02010	ABC transporters	10	0.09
			aor00564	Glycerophospholipid metabolism	16	0.17
	down		aor03008	Ribosome biogenesis in eukaryotes	40	$1.46 \cdot 10^{-15}$
			aor03010	Ribosome	39	$8.16 \cdot 10^{-14}$
			aor01230	Biosynthesis of amino acids	61	$1.03 \cdot 10^{-11}$
			aor01210	2-Oxocarboxylic acid metabolism	25	$5.34 \cdot 10^{-9}$
			aor03013	RNA transport	25	$6.75 \cdot 10^{-9}$
			aor01200	Carbon metabolism	51	$1.16 \cdot 10^{-7}$
			aor00270	Cysteine and methionine metabolism	19	$1.50 \cdot 10^{-6}$
			aor00970	Aminoacyl-tRNA biosynthesis	19	$2.78 \cdot 10^{-6}$
			aor03040	Spliceosome	16	$3.68 \cdot 10^{-6}$
			aor01110	Biosynthesis of secondary metabolites	182	$1.22 \cdot 10^{-5}$
			aor03020	RNA polymerase	12	$1.31 \cdot 10^{-5}$
			aor00190	Oxidative phosphorylation	16	$2.23 \cdot 10^{-5}$
			aor01100	Metabolic pathways	365	$2.98 \cdot 10^{-5}$
			aor03018	RNA degradation	18	$5.57 \cdot 10^{-5}$
			aor00020	Citrate cycle (TCA cycle)	16	$8.90 \cdot 10^{-5}$
			aor00290	Valine, leucin and isoleucine biosynthesis	11	$1.22 \cdot 10^{-3}$
			aor00630	Glyoxylate and dicarboxylate metabolism	20	$1.27 \cdot 10^{-3}$
			aor00680	Methane metabolism	11	$2.18 \cdot 10^{-3}$
			aor00250	Alanine, aspartate and glutamate metabolism	15	$8.81 \cdot 10^{-3}$
			aor00380	Tryptophan metabolism	20	$9.44 \cdot 10^{-3}$
			aor00620	Pyruvate metabolism	26	0.01
			aor00770	Pantothenate and CoA biosynthesis	15	0.02
			aor01212	Fatty acid metabolism	14	0.03
			aor00230	Purine metabolism	20	0.03
			aor00260	Glycine, serine and threonine metabolism	19	0.06
			aor04146	Peroxisome	20	0.11
			aor00330	Arginine and proline metabolism	16	0.11

**Table 8:** Differentially expressed pathways for the comparisons of glucose with pure acetate

condition	DGE	KEGG pathway ID	KEGG pathway name	set size	adjusted
Glc vs Ace	up	aor00500	Starch and sucrose metabolism	18	$4.12 \cdot 10^{-4}$
		aor00010	Glycolysis/ Gluconeogenesis	14	$2.61 \cdot 10^{-2}$
	down	aor03008	Ribosome biogenesis in eukaryotes	27	$7.72 \cdot 10^{-14}$
		aor01230	Biosynthesis of amino acids	39	$4.10 \cdot 10^{-8}$
		aor01210	2-Oxocarboxylic acid metabolism	12	$4.12 \cdot 10^{-4}$
		aor01200	Carbon metabolism	32	$4.12 \cdot 10^{-4}$
		aor01110	Biosynthesis of secondary metabolites	126	$4.76 \cdot 10^{-4}$
		aor00270	Cysteine and methionine metabolism	11	$5.20 \cdot 10^{-4}$
		aor01100	Metabolic pathways	253	$1.23 \cdot 10^{-3}$
		aor00380	Tryptophan metabolism	16	$4.14 \cdot 10^{-3}$
		aor00230	Purine metabolism	16	$9.92 \cdot 10^{-3}$
		aor00630	Glyoxylate and dicarboxylate metabolism	12	0.01
		aor00360	Phenylalanine metabolism	11	0.02
		aor00330	Arginine and proline metabolism	14	0.06
		aor01212	Fatty acid metabolism	13	0.10
		aor00071	Fatty acid degradation	12	0.17
		aor00250	Alanine, aspartate and glutamate metabolism	14	0.17
		aor00260	Glycine, serine and threonine metabolism	12	0.20

Most of the differentially expressed genes for both comparisons were assigned to "metabolic pathways" and the "synthesis of secondary metabolites". However, since "metabolic pathways" can be considered a generic term encompassing a whole range of cellular processes, the present study was also focused on the subordinated pathways that showed significant differences in expression. Among these, "biosynthesis of amino acids" and "carbon metabolism" showed the largest set size, regardless of whether glucose was compared with PAC or pure acetate. Thus, the following sections will provide a deeper insight into these two metabolic pathways and also highlight some relevant secondary metabolite clusters. When the transcriptional regulation during growth on pure acetate and PAC was compared, "pyruvate metabolism" was identified as the only significantly different pathway and will therefore also be discussed in further detail.

#### 3.2.4.1. Carbon metabolism

As expected, cultivation of *A. oryzae* on the different substrates had a significant impact on the transcriptional regulation of the fungal carbon metabolism. The “2-oxocarboxylic acid metabolism” and the “glyoxylate and dicarboxylate metabolism” were found to be the most significantly affected pathways of carbon utilization in the acetate-containing cultures (**Table 7** and **Table 8**). In addition, upregulation of the TCA cycle and the closely associated oxidative phosphorylation occurred during growth on PAC. It is furthermore not particularly surprising that the two pathways upregulated in glucose compared to acetate were “glycolysis/gluconeogenesis” and “starch and sucrose metabolism”, which are central pathways for the utilization of the monosaccharide and its polymers.

##### Starch and sucrose metabolism

Most of the genes involved in “starch and sucrose metabolism” were already included in the GO term “hydrolase activity, hydrolyzing O-glycosyl compounds” in the functional enrichment analysis and code for a variety of oligosaccharide degrading enzymes (**Table 9**).

There was a general upregulation of this pathway when glucose was compared with both acetate and PAC, although two genes showed a decreased expression in the latter comparison. These involved a glucan-1,3- $\beta$ -glucosidase (AO090038000279) and a beta-glucosidase gene (AO090701000841). The induction of fungal beta-glucosidases by lignocellulosic hydrolysates has already been shown in literature [264]. But in contrast to PAC, these hydrolysates contained sugars as degradation products of cellulose and hemicellulose, which might have induced the expression of the enzymes.

However, the majority of genes were upregulated in glucose, although it is well known that the expression of carbohydrate-degrading enzymes is usually suppressed via catabolite repression as long as glucose is present [265]. This regulatory system was extensively studied in *A. oryzae*, especially for starch-degrading enzymes such as alpha-amylases, for which we also observed high fold changes (**Table 9**). It was shown that the system allows some basal enzymatic activity despite the presence of glucose [266], whereas no activity was detected when acetate was used as sole substrate [267]. These results support our observations of a downregulated expression of these genes in the acetate and PAC cultures.

**Table 9:** Differentially expressed genes involved in the starch and sucrose metabolism

Enzyme	E.C.	Regulation	Gene ID	Fold change	
				Glc vs Ace	Glc vs PAC
β-fructofuranosidase	3.2.1.26	up	AO090020000640	1.71	2.71
			AO090701000038	1.51	1.50
α-glucosidase	3.2.1.20		AO090003001209	4.18	3.93
trehalose 6-phosphate (T6P) synthase	2.4.1.15		AO090102000159	3.83	3.39
	2.4.1.347				
T6P synthase/phosphatase subunit	2.4.1.15		AO090005001531	1.40	1.46
	3.1.3.12				
glucan endo-1,3-β-D-glucosidase	3.2.1.39		AO090009000117	1.24	1.13
glucan 1,3-β-glucosidase	3.2.1.58		AO090011000362	1.39	-
			AO090001000604	-	1.53
			AO090003000990	-	3.11
β-glucosidase	3.2.1.21		AO090001000544	1.42	1.80
			AO090038000425	2.37	-
			AO090003000497	-	1.97
			AO090001000266	-	3.66
			AO090701000274	-	1.12
endoglucanase	3.2.1.4		AO090011000715	2.34	2.54
			AO090003001342	-	3.70
arabinogalactan endo-1,4-β-galactosidase	3.2.1.89		AO090001000492	2.04	-
cellulose 1,4-β-cellobiosidase	3.2.1.91		AO090001000348	2.16	3.95
glycogen debranching enzyme	2.4.1.25		AO090005000884	1.43	1.79
	3.2.1.33				
α-amylase	3.2.1.1		AO090003001497	4.19	2.50
			AO090003001498	2.24	1.20
			AO090023000944	6.33	7.45
			AO090120000196	6.40	7.07
glucoamylase	3.2.1.3		AO090010000746	6.63	9.13
1,4-α-glucan branching enzyme	2.4.1.18		AO090010000483	1.02	1.66
1,3-β-glucan synthase	2.4.1.34		AO090009000174	-	1.11
glucan 1,3-β-glucosidase	3.2.1.58	down	AO090038000279	-	-1.04
β-glucosidase	3.2.1.21		AO090701000841	-	-3.24

In addition to enzymes catalyzing oligosaccharide degradation, the differentially expressed genes of this pathway also encoded several anabolic enzymes (**Table 9**). Among these were two enzymes involved in the formation of trehalose, a disaccharide consisting of two glucose units linked by an  $\alpha,\alpha$ -1,1-glycosidic bond. Trehalose plays a crucial role as a storage component in spores and during vegetative growth, but has also been reported to act as a protectant against a variety of stressors such as heat or oxidative and osmotic stress [268, 269]

by stabilizing membranes [270] and proteins [271]. Therefore, upregulation of these genes would have been more expected in the acetate-containing cultures. However, in addition to these functions, an involvement of the disaccharide and its biosynthetic genes in the regulation of glycolytic flux [272] and cell wall integrity [273] in filamentous fungi have previously been reported. The latter matches our observation of an upregulation of the "amino sugar and nucleotide sugar metabolism" in the glucose cultures, as this metabolic pathway involves genes associated with the synthesis and degradation of chitin, the major component of the fungal cell wall. Thammahong et al. studied the role of the regulatory subunits of trehalose synthesis, *tslA* and *tslB*, in *A. fumigatus* and showed that deletion of these genes resulted in increased sensitivity to cell wall-perturbing agents. Moreover, TslA in particular interacts with the chitin synthase CsmA and affects its activity and cellular localization [274]. In accordance with these findings, we found increased expression of an *A. oryzae* homolog to *tslB* (AO090005001531, 73% amino acid identity, **Table 9**) as well as the *csmA* gene (AO090026000321) in the glucose cultures. Furthermore, upregulation of 5 other genes encoding chitin synthases was observed (**Appendix 3**). However, this is in contrast to a study showing that osmotic stress induced by high sodium acetate concentrations results in increased expression of the chitin synthases *chsA-C* in *A. nidulans* [275].

In addition to the cell wall, the cellular membrane is also an important barrier against external stressors, with its composition varying greatly depending on the environmental conditions. For example, in *S. cerevisiae* increased incorporation of oleic acid (C<sub>18:1</sub>) into the cell membrane enabled the organism to overcome the toxic effects of ethanol [276]. Moreover, heterologous expression of oleate  $\Delta 12$  desaturases in the same organism improved its NaCl tolerance by increasing the fluidity of the membrane [277]. Accordingly, we observed an increased expression of two such  $\Delta 12$ -desaturase genes in our acetate-containing cultures, with one being exclusively upregulated in acetate (AO090001000224:  $\log_2FC = 1.04$ ) and the other showing an increased expression for both C-sources (AO090010000714;  $\log_2FC_{Acetate} = 3.07$  &  $\log_2FC_{PAC} = 3.12$ ). These enzymes are required for the production of linoleic acid, a di-unsaturated fatty acid (C<sub>18:2</sub>) whose intracellular content has been described to be significantly increased in *A. oryzae* under high salinity conditions [143].

### Glycolysis, glyoxylate and TCA cycle

Contrary to expectations, comparing the gene expression of glycolytic enzymes between glucose and the acetate-containing cultures revealed only a few differentially expressed genes (**Figure 16**). One possible reason for this observation could be that most glycolytic enzymes also catalyze the reverse reactions required for gluconeogenesis, and therefore increased flux through this pathway in the cultures with acetate could have resulted in the low number of differences. However, since some of the reactions are not reversible and are thus specific to glycolysis or gluconeogenesis, at least the genes encoding these enzymes should be differentially expressed. Indeed, the data showed a slight downregulation of a gene that codes for the gluconeogenesis enzyme pyruvate carboxylase in the glucose cultures, whereas expression of a gene encoding for 6-phosphofruktokinase (*pfk*), an enzyme exclusively involved in glycolysis, was increased. However, the *pfk* gene that was found to be upregulated in the glucose cultures (AO090010000444) encodes for *pfkB* and not *pfkA*. In *A. oryzae*, the expression of both *pfk* orthologues during growth on glucose has already been studied and it was reported that *pfkB*, unlike *pfkA*, is even slightly repressed by glucose [278], suggesting that it is not the primary enzyme of glycolysis.

Glyceraldehyde 3-phosphate dehydrogenase (*gpd*) is also encoded by multiple genes in *Aspergillus* species, with *gpdA* being certainly involved in glycolysis [279]. However, similar to *pfk*, we found that primarily the other two *gpd* genes (*gpdB* and *gpdC*) were upregulated on glucose when compared with the acetate-containing cultures. The highest fold change was found for *gpdC* (AO090020000265), a gene whose exact function is unknown and which has a low similarity to *gpdA* (only 44 % amino acid identity). In contrast, *gpdB* is known to be a part of the heptelic acid gene cluster and is therefore discussed in more detail in the "secondary metabolite" section of this article.

Of central importance in linking glycolysis and TCA cycle is the pyruvate dehydrogenase multi-enzyme complex, which catalyzes the conversion of pyruvate to acetyl-CoA with the release of CO<sub>2</sub> and is composed of 3 individual catalytic enzymes (E1-E3). Our data contained two differentially expressed genes encoding for the  $\alpha$  subunit of E1 as well as the dihydrolipoamide dehydrogenase gene (E3). However, their regulation was quite ambiguous, because one of the E1 genes was highly upregulated on glucose, whereas the other two genes were slightly downregulated when the monosaccharide and PAC were compared. But since E3 is also a part of the alpha-ketoglutarate dehydrogenase complex, which is a key enzyme in the TCA cycle, its downregulation cannot be clearly attributed to glycolysis.

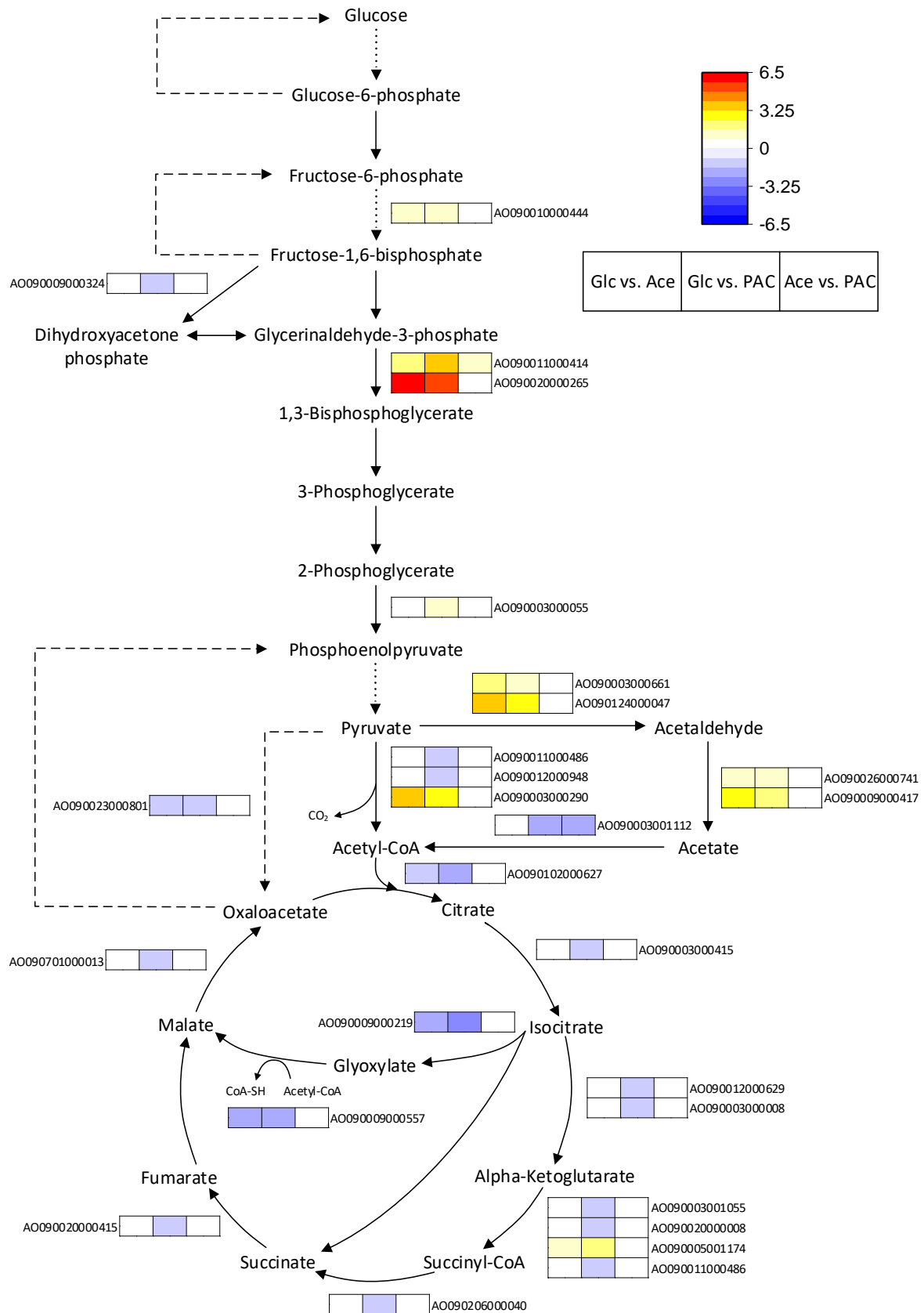


**Figure 16:** Differentially expressed genes of glycolysis, gluconeogenesis, and the TCA cycle during cultivation of *A. oryzae* on glucose, acetate and PAC. The dashed and dotted lines indicate gluconeogenesis- and glycolysis-specific genes, respectively.

Pyruvate decarboxylase is another enzyme that catalyzes the cleavage of CO<sub>2</sub> from pyruvate and for which two genes were found to be upregulated in the glucose cultures. The acetaldehyde formed in this reaction can be further converted either to ethanol by alcohol dehydrogenases (ADH) or to acetate by the action of aldehyde dehydrogenases. Whereas transcriptional regulation of ADHs was dependent on whether the enzyme was NADH- or NADPH-preferring (discussed in more detail in the pyruvate metabolism section), the latter showed clear upregulation during growth on glucose. However, this should rather be interpreted as a downregulation in the other two cultures, since they already contain acetate, which can directly enter the TCA cycle after reaction with coenzyme A. This is at least partly confirmed by the upregulation of acetyl-CoA synthetase although it is unclear why this gene only showed a higher expression for PAC and not in the cultures containing pure acetate.

Consistent with these findings, genes encoding carnitine O-acetyltransferases were also found to be upregulated only on PAC (AO090001000295, AO090026000404; **Appendix 3**). Since the outer mitochondrial membrane is impermeable to acetyl-CoA, these enzymes are required to convert acetyl-CoA formed by the cytosolic acetyl-CoA synthetase to O-acetylcarnitine, thus enabling entrance into the mitochondrion and the TCA cycle [280]. However, as previously described, and also confirmed by the strong upregulation of the isocitrate lyase and malate synthase genes in our data, acetate is metabolized mainly via the glyoxylate cycle [281]. Since this process does not take place in the mitochondrion, the results regarding the carnitine-mediated acetate transport seem plausible. The glyoxylate cycle genes were also upregulated during growth on the pyrolysis condensate, but in addition, the PAC cultures also showed increased expression of almost the entire TCA cycle. The fact that TCA cycle genes were exclusively upregulated during growth in PAC indicates that this is a transcriptional response caused by the additional components of the condensate. This assumption is confirmed, for example, by a transcriptome analysis of *Kluyveromyces marxianus*, which revealed an upregulation of most TCA cycle genes during growth of this yeast on an inhibitor mixture containing acetic acid, phenols, furfural, and HMF [282]. Moreover, a metabolic flux analysis in glucose-limited *S. cerevisiae* chemostats showed that feeding 2.25 g/L furfural increased the specific rates of TCA cycle and respiration by 50 % each, thus also providing an explanation for the observed upregulation of oxidative phosphorylation in the PAC cultures (**Table 7**) [283].

### 3.2.4.2. Secondary metabolites (SM)

Since functional enrichment analysis revealed that several transporters involved in SM secretion were upregulated in the glucose cultures (**Appendix 2**), the associated gene clusters will be investigated more intensively in the following section.

Probably the best-known SM produced by *A. oryzae* is kojic acid, whose synthesis gene cluster comprises only three genes: *kojA*, *kojR*, and *kojT* [284]. Among these genes, *kojR* was previously shown to serve as a transcription factor exerting an activating effect on the gene of FAD-dependent oxidoreductase (*kojA*), which is likely responsible for the actual kojic acid biosynthesis, and the MFS transporter (*kojT*) [258, 285]. As indicated in **Table 10**, all three genes were upregulated in the glucose cultures, although for *kojT* the increased expression was only observed in comparison with PAC.

**Table 10:** Selection of differentially expressed secondary metabolite clusters

Secondary metabolite	Gene name	Gene ID	Fold change		
			Glc vs Ace	Glc vs PAC	Ace vs PAC
heptelidic acid	<i>hepA</i>	AO090011000408	4.82	8.09	3.28
	<i>hepB</i> <sup>1</sup>	-	-	-	-
	<i>hepC</i>	AO090011000410	6.05	8.52	-
	<i>hepD</i>	AO090011000411	4.85	7.03	-
	<i>hepE</i>	AO090011000412	5.51	7.27	-
	<i>hepF</i>	AO090011000413	2.61	5.50	2.89
	<i>hepG (gpdB)</i>	AO090011000414	2.03	3.46	1.43
	<i>hepH</i>	AO090011000415	3.99	7.46	3.47
	<i>hepR</i>	AO090011000416	-	1.29	-
	<i>hepS</i>	AO090011000417	-	1.32	-
kojic acid	<i>kojA</i>	AO090113000136	1.67	2.11	-
	<i>kojR</i>	AO090113000137	2.13	2.95	-
	<i>kojT</i>	AO090113000138	-	2.05	-
cyclopiazonic acid	<i>cpaR</i> <sup>1</sup>	-	-	-	-
	<i>cpaA</i>	AO090026000001	-	5.67	5.42
	<i>cpaD</i>	AO090026000002	-	6.88	7.56
	<i>cpaO</i>	AO090026000003	-	7.37	7.83
	<i>cpaH</i>	AO090026000004	1.45	9.43	7.98
	<i>cpaM</i> <sup>2</sup> / <i>cpaT</i>	AO090026000005	-	6.00	5.34

<sup>1</sup> gene is not found in the genome annotation of *A. oryzae* RIB40

<sup>2</sup> according to [286] the coding region of *cpaM* is partially contained in AO090026000005

The upregulation of the kojic acid cluster during growth on glucose seems plausible, since it has been suggested that unlike other SM, this compound can be synthesized directly from glucose [284].

Heptelidic acid (HA) is another secondary metabolite produced by *A. oryzae* and has been reported to inhibit halotolerant lactic acid bacteria during the second stage of soy sauce fermentation [287]. HA acts by irreversibly inactivating the *gpd* enzyme of bacteria via covalent modification of a cysteine thiol in the active center of the protein [288, 289]. It was therefore suggested that the *gpdB* (or *hepG*) gene contained in the HA cluster is involved in fungal self-resistance to this SM [288]. In addition to *hepG* and the MFS transporter gene *hepF*, the HA gene cluster includes a sesquiterpene synthase (*hepA*), four cytochrome P450 genes (*hepC*, *hepD*, *hepE*, and *hepH*), a putative antibiotic biosynthesis monooxygenase (*hepB*) and two transcription factors (*hepR* and *hepS*) [257, 288]. **Table 10** shows that differential expression was found for all these genes except *hepB*, which is not predicted in the *A. oryzae* RIB40 genome. The two transcriptional regulator genes were upregulated only in the comparison of glucose and PAC, whereas the other genes also showed increased expression when the monosaccharide and acetate were compared. The fold changes were always lower for the latter comparison, indicating once again that the PAC components may cause additional inhibition. However, as far as the authors are aware, there are currently no studies addressing the effects of lignocellulosic inhibitors on fungal SM production.

Since the second stage of the soy sauce fermentation involves the addition of salt water and osmotolerant lactic acid bacteria and yeast to the koji (*Aspergillus*) culture [257], the high salinity in the acetate and PAC cultures would have been expected to induce the expression of the HA gene cluster. Instead, upregulation during growth on glucose was observed, suggesting that there may be other triggers of expression. For instance, it is conceivable that HA synthesis was induced by the low pH in the glucose cultures (**Appendix 4**), since the lactic acid fermentation occurring during the soy sauce production process also causes a pH drop [290]. However, the findings could also be related to the fact that the HA precursor farnesyl pyrophosphate is formed from acetyl-CoA via the mevalonate pathway. Since the overexpression of the TCA and glyoxylate cycle genes in the two acetate-containing cultures indicates an increased flux through these pathways, less acetyl-CoA may be available for HA synthesis. This assumption is supported by the downregulation of some mevalonate pathway genes observed particularly in the PAC cultures (**Appendix 3**).

Another SM cluster, which also relies on acetyl-CoA as a precursor and for whose upregulation in glucose cultures the same possible explanation could therefore apply, codes for the mycotoxin cyclopiazonic acid (CPA). The annotation of the corresponding synthesis cluster in *A. oryzae* RIB40 comprises only 6 genes since the *cpaR* gene encoding a C6 zinc finger transcription factor is absent [286]. Moreover, the polyketide synthase gene *cpaA* is severely truncated in this strain, which is probably the main reason for its non-toxicity [286].

Highly significant differential expression of *cpaA*, as well as of all other genes of the cluster annotated in *A. oryzae* RIB40 was observed (**Table 10**). However, due to the incompleteness of this cluster in our reference strain, it is difficult to assess whether the observed expression actually results in the formation of a functional SM. In contrast to HA, transcription of genes involved in CPA synthesis seemed to be inhibited mainly by PAC, as the comparison between glucose and pure acetate showed only one putative cytochrome P450 gene (*cpaH*) to be upregulated. Since CPA is a mycotoxin [291], it might be of interest to investigate which PAC components caused the inhibition in the gene expression and whether such inhibitors might make the handling of mycotoxin-producing strains easier and safer.

#### 3.2.4.3. Biosynthesis of amino acids

As it can be seen from **Table 7** and **Table 8** amino acids synthesis seems to be a key target in the regulation of the fungal gene expression during growth on the different C-sources. The pathway analysis revealed a significant downregulation of this pathway when glucose was compared to both acetate and PAC. Looking more closely at the individual amino acids, it becomes apparent that the "cysteine and methionine metabolism" showed the highest significance for both comparisons. The "tryptophan metabolism" was also significantly downregulated and moreover contained the highest number of genes among all differentially expressed amino acid pathways with a set size of 16 and 20 genes for acetate and PAC, respectively. Although not being significantly differentially expressed (p-value > 0.5), the "glycine, serine and threonine metabolism" as well as the "arginine and proline metabolism" were also chosen to be included in the analysis, as they might still contain genes relevant for the evaluation of the overall transcriptional regulation.

### Arginine and proline metabolism

Differentially expressed genes of the arginine synthesis identified in this work, showed a comparable transcriptional regulation to that previously described by He et al. for high salinity stress in *A. oryzae* [143]. In their work, salt concentrations of 5-15 g/L NaCl induced an upregulation of almost every gene involved in the formation of arginine from the citrate cycle intermediate alpha-ketoglutarate.

Due to pH adjustment of our medium containing pure acetate using NaOH, a high sodium ion concentration was present in these cultures. However, as indicated in the data in **Appendix 3**, even more genes of this pathway were upregulated on PAC and also the fold changes were slightly higher than when acetate was used as substrate. This can most likely be attributed to the increased salt ion concentration resulting from the overliming treatment of the pyrolysis condensate with Ca(OH)<sub>2</sub>. The upregulation of genes involved in arginine synthesis being also observed in the presence of calcium ions suggests that the observed transcriptional response may be triggered not only by NaCl but also by other osmotic stressors. This assumption is supported by the work of Ma et al. who reported intracellular accumulation of free arginine in the cytosol of *A. oryzae* in response to ethanol stress [292]. Moreover, in the yeast *Candida glabrata*, not only an upregulation of the arginine synthesis was observed, but also downregulation of genes involved in the degradation of this amino acid [293]. This is partially consistent with our results, as we observed a decreased expression of the arginase gene (AO090003000697) during growth on acetate compared to the glucose control ( $\log_2FC = -1.18$ , **Appendix 3**). The positive effect of this amino acid on the integrity of the cell wall and membrane [294], as well as its activity as a suppressor of protein aggregation [295], have been described in the literature and may provide a possible explanation for the increased arginine demand of cells during osmotic stress.

### Glycine, serine and threonine metabolism

The "glycine, serine, and threonine metabolism" is another pathway whose expression was not significant changed, but which nevertheless should not be neglected due to its close association to other relevant amino acid pathways like tryptophan and cysteine metabolism.

An interesting gene of this pathway, which was upregulated in PAC relative to glucose ( $\log_2FC = 1.09$ ), encodes the betaine-aldehyde dehydrogenase (AO090103000021). This enzyme catalyzes the second step of the synthesis of glycine-betaine, a trimethylated derivative of the amino acid glycine, which has been described as an osmoregulator, especially in plants [296] and bacteria [297]. Accordingly, the increased expression of the betaine-aldehyde

dehydrogenase gene in the PAC-containing cultures could possibly be a reaction to the high osmolarity of the medium. However, it is still unclear whether glycine-betaine also contributes to the regulation of osmotic stress in *Aspergillus* species. While Kelavkar et al. reported that external addition of this amino acid derivative led to an improved growth of *A. repens* under high NaCl conditions [298], Lambou et al. suggested glycine-betaine biosynthesis to rather be a salvage pathway for the utilization of unusual nitrogen or carbon sources under nutrient starvation conditions [299].

In addition to this glycine-related gene, DGE on acetate and PAC mainly involved genes for the synthesis of serine and its conversion to other amino acids and metabolites (**Appendix 3**). Serine formation occurs in three enzymatic steps with the glycolysis intermediate 3-phosphoglycerate serving as the starting substance (**Figure 17**). This pathway was identified to be entirely upregulated when the fungus was grown on PAC, whereas on pure acetate the gene for the final reaction step was excluded by our strict filter despite a slight upregulation ( $\log_2FC = 0.83$ ). The increased expression of this pathway might be related to the higher flux through the glyoxylate cycle during growth on acetate-containing media. For example, a metabolic flux analysis using *A. niger* revealed that overexpression of isocitrate lyase, the key enzyme of the glyoxylate shunt, resulted in an increased flux towards serine [300].

#### Cysteine and its role in antioxidant defense

The upregulation of genes involved in serine formation could also be explained by an increased demand for amino acids such as tryptophan or cysteine, which require serine for their synthesis. Indeed, both acetate-containing cultures showed increased expression of almost the entire cysteine synthesis pathway starting from homoserine (**Figure 17**).

In addition to this pathway, a cysteine synthase gene (AO090102000276) was found to be upregulated during growth on PAC ( $\log_2FC = 1.45$ ). This enzyme is part of a second cysteine synthesis route that originates from serine. In the reaction step catalyzed by this enzyme, O-acetyl-L-serine reacts with sulfide under simultaneous cleavage of acetate to form cysteine. However, since sulfate was the only source of sulfur in the media used for the present study, a multistep reduction to sulfide had to occur prior to cysteine synthesis [301]. Accordingly, some genes involved in sulfate reduction were differentially expressed in the acetate-containing cultures (**Figure 17**).

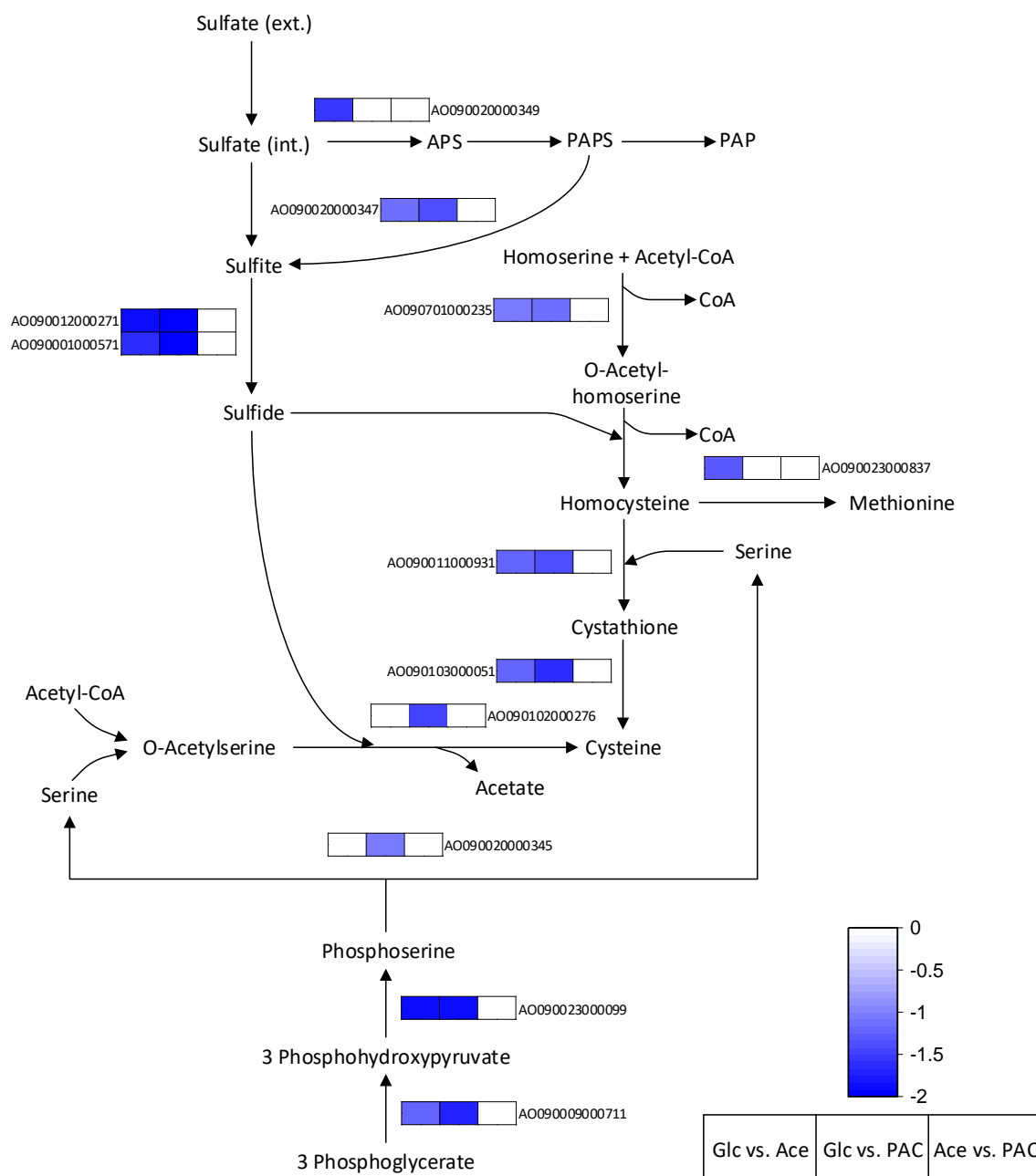


**Figure 17:** Differentially expressed genes of the cysteine and methionine metabolism as well as the closely related serine synthesis and sulfur metabolism. APS = Adenosine-5'-phosphosulfate, PAPS = 3'-phosphoadenosin-5'-phosphosulfate, PAP = 3'-phosphoadenosine 5-phosphate

Compared with glucose, more genes were upregulated on pure acetate than on PAC, since the latter did not show an altered expression of the sulfate adenylyltransferase gene, catalyzing the reaction of sulfate to adenosine-5'-phosphosulfate (APS). A possible explanation for this observation could be that the PAC component furfural inhibits sulfur metabolism prior to its assimilation into cysteines, as reported for *E. coli* [168]. Moreover, it was described in this study that the sulfur limitation caused by furfural lead to increased expression of genes involved

in methionine and cysteine biosynthesis [168], which is consistent with the slightly higher fold changes in the PAC cultures.

Both cysteine and methionine are considered as targets for oxidation by ROS in proteins [302]. And although most ROS are generated as an inevitable consequence of cellular metabolism during aerobic growth, additional oxidative stress can also be caused by external environmental factors. For example, it was shown for *S. cerevisiae* that the addition of acetate to the growth medium caused a significant increase in superoxide dismutase and catalase activity, two enzymes that are responsible for the direct elimination of ROS like hydrogen peroxide (H<sub>2</sub>O<sub>2</sub>) [251]. Our data, revealed a significant upregulation of genes encoding superoxide dismutase, but also cytochrome c peroxidases, for both PAC and acetate (**Table 11**). In contrast, the transcriptional regulation of catalases was not that clear, as one gene (AO090701000158) was also found to be upregulated on glucose. However, this gene encodes for catalase A, whose expression in *A. oryzae* has been shown not to be altered by exposure to H<sub>2</sub>O<sub>2</sub> [303]

**Table 11:** Transcriptional regulation of genes involved in the oxidative stress defense

Enzyme	EC	Gene ID	Fold change		
			Glc vs Ace	Glc vs PAC	Ace vs PAC
catalase	1.11.1.6	AO090701000158	2.38	2.76	-
		AO090120000068	-1.15	-	1.07
		AO090020000389	-	-6.43	-4.00
cytochrome c peroxidase	1.11.1.5	AO090023000654	-1.26	-1.48	-
		AO090103000329	-2.95	-2.67	-
superoxide dismutase	1.15.1.1	AO090005001580	-1.01	-1.60	-
		AO090020000521	-1.20	-1.30	-
glutathione synthase	6.3.2.3	AO090701000193	-	-1.07	-0.96
glutaredoxin 3	-	AO090009000473	-	-1.17	-0.95
monothiol glutaredoxin	-	AO090023001002	-	-1.47	-
thioredoxin		AO090026000065	-	-	-5.80
		AO090026000708	-	-1.28	-1.40
		AO090020000504	2.05	1.78	-
glutathione S-transferase	2.5.1.18	AO090005000973	-1.36	-1.16	-
		AO090003000631	-	-2.87	-3.31
		AO090103000485	-	-2.73	-2.37
		AO090012000378	2.34	-	-2.51
		AO090010000447	-	1.18	-
		AO090103000134	1.49	1.79	-
		AO090103000149	9.85	5.37	-4.50

Besides these enzymes of the primary antioxidant defense, there is also a non-enzymatic mechanism for the elimination of oxidative stress involving glutathione [304]. Addition of this compound to *C. glutamicum* shake flask cultures containing PAC from the bioliq® plant at KIT has already been reported to counteract the growth-inhibiting effect of the condensate [228]. Glutathione is a tripeptide composed of glutamate, glycine and cysteine. Thus, the higher expression of genes needed for the synthesis of the latter amino acid could also be due to an increased demand for glutathione during growth in the acetate-containing media. For example, it has been shown for *Candida utilis* that not only ROS but also osmotic stress caused by high NaCl concentrations leads to an increased glutathione synthesis [141]. Accordingly, we found upregulation of several genes related to the glutathione system in the cultures with PAC and acetate (**Table 11**).

In addition to glutathione synthase, these genes encode for enzymes such as glutathione S-transferases (GST), but also for several glutathione- and thioredoxins. While GSTs are involved in the detoxification of xenobiotics via conjugation of the foreign compounds with the sulfhydryl group of glutathione [305], the latter are mainly responsible for the repair of ROS-induced damage to cysteine residues in proteins [306, 307]. However, some (monothiol) glutaredoxins also appear to be involved in the maintenance of iron homeostasis as well as the synthesis of iron/sulfur clusters [308–310]. Since the respiratory chain includes numerous proteins containing such clusters and oxidative phosphorylation was upregulated in the PAC cultures, the increased expression of glutaredoxin 3 as well as a monothiol glutaredoxin during fungal growth on the pyrolysis condensate seems reasonable. A few thioredoxin genes were also identified to be differentially expressed during growth on the different C-sources. One of these genes appeared to be strongly downregulated exclusively between pure acetate and PAC (AO090026000065), whereas another (AO090026000708) additionally showed decreased expression when comparing glucose and the pyrolysis condensate. However, one gene was also found to be upregulated in glucose, suggesting that oxidative stress may also occur under normal aerobic growth conditions.

Transcriptional regulation of GST genes also proved to be quite ambiguous under the applied experimental conditions (**Table 11**). It was expected that inhibitory PAC components might induce an increased expression of these enzymes, as this has recently been observed in *S. cerevisiae* in response to the addition of furfural and HMF [311]. And indeed, two GST genes (AO090003000631 & AO090103000485) were found to be upregulated on PAC compared to glucose and pure acetate. However, there were also some genes that showed higher expression levels during growth on glucose. Of particular note is the gene AO090103000149, for which a

5-fold and almost 10-fold increased expression was observed when glucose was compared with PAC and acetate, respectively. This observation may possibly be explained by the fact that GSTs have been ascribed several additional functions in the metabolism of endogenous compounds [305]. For example, the GST that was strongly upregulated in the glucose cultures had 47 % similarity to URE2 in *S. cerevisiae*, a protein that was reported to function as a regulator in nitrogen metabolism [312]. Moreover, a possible involvement of GST in aflatoxin production of filamentous fungi has been suggested for *A. flavus* [313]. It would be conceivable that GSTs are also involved in the formation of other mycotoxins and that the upregulation of some GST genes during growth on glucose may therefore be associated with the increased expression of SM clusters in these cultures.

Despite the rather unclear transcriptional regulation of GSTs, the present results generally indicate that cultivation of the fungus in both acetate-containing media caused osmotic and oxidative stress, which led to an upregulation of genes responsible for their defense. Since the molecules involved in these defense mechanisms often rely on cysteines, this was probably the main reason for the increased expression of the cysteine synthesis pathway as well as the closely related sulfur metabolism.

#### Tryptophan metabolism

In addition to the significant upregulation of the "cysteine and methionine metabolism," an increased expression of the tryptophan metabolism was also observed in both acetate-containing cultures (**Table 7** and **Table 8**). These findings are consistent with previous reports in which *S. cerevisiae* showed an upregulation of the tryptophan metabolism after addition of acetate [314]. However, in our data, differential expression already started several reaction steps earlier, since genes of the shikimate pathway were found to be upregulated in the acetate-containing cultures (**Figure 18**).

This pathway represents the first common part in the synthesis of all three aromatic amino acids and starts with the reaction of phosphoenolpyruvate and erythrose-4-phosphate, to form 3-deoxy-D-arabino-heptulosonic acid 7-phosphate (DAHP). This first step is catalyzed by DAHP synthase, which is encoded by several genes in *A. oryzae*. Two of these genes (AO09000500086, AO09000500086) were found to be upregulated in both acetate and PAC when compared to growth on glucose. In the fungus, the majority of the subsequent reaction steps involved in the shikimate pathway require the participation of a common enzyme complex termed pentafunctional AROM polypeptide. The gene (AO090012000502) encoding for this enzyme was exclusively upregulated when PAC was compared with glucose ( $\log_2FC = 1.08$ ).

After the final reaction step catalyzed by this complex, 3-enolpyruvyl shikimate 5-phosphate is formed, which is then further converted to chorismate by chorismate synthase. Although the latter enzyme was not differentially expressed under any of the conditions tested, an increased requirement for chorismate, especially in the PAC-containing cultures, seems quite plausible, since the compound serves as a precursor for the synthesis of ubiquinone.

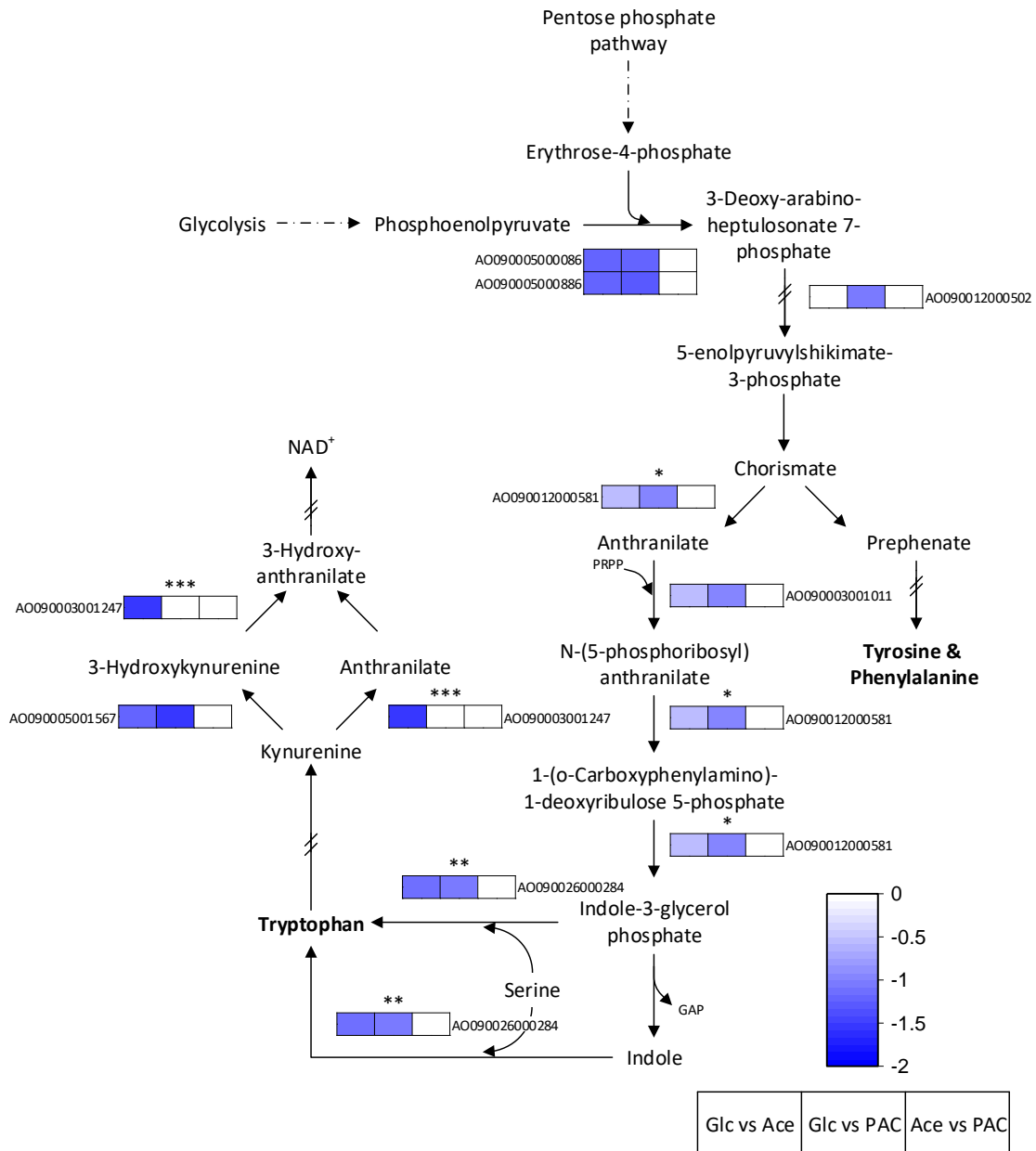


**Figure 18:** Differentially expressed genes of the tryptophan metabolism during cultivation of *A. oryzae* on glucose, acetate, and PAC. Genes marked with asterisks (\*) code for enzymes involved in multiple reactions

This molecule, in turn, represents a key electron carrier in oxidative phosphorylation, a pathway that was found to be upregulated during fungal growth on the pyrolysis condensate (**Table 7**). Indeed, several genes involved in ubiquinone synthesis showed an increased expression, especially in the PAC cultures (**Appendix 3**), reinforcing the hypothesis of an enhanced requirement for the electron carrier.

After the formation of chorismate, the synthesis pathway of the aromatic amino acids divides into prephenate, which is a precursor of phenylalanine and tyrosine, and anthranilate, from which tryptophan is formed in several further reaction steps. Three genes associated with tryptophan synthesis showed significant overrepresentation ( $FDR < 0.05$ ), with  $\log_2FC$  values ranging between 1.16 and 0.54, in cultures grown on acetate and PAC compared to the glucose control (**Appendix 3**). Of these, the gene encoding tryptophan synthase, which catalyzes the final reaction step of indole-3-glycerol phosphate and serine to tryptophan showed the highest increase ( $\log_2FC = 1.16$ ), thus providing a further explanation for the aforementioned enhanced demand of serine.

Although the underlying mechanism is still poorly understood, there are a number of studies showing that tryptophan plays a role in mitigating the effects of various types of stress such as DNA damage [315] and in particular cell membrane stress. For example, the presence of the wild-type phosphoribosylanthranilate isomerase gene TRP1 in *S. cerevisiae* strains counteracted growth defects caused by the cell membrane disrupting detergent SDS [316]. Ethanol is also known for its negative effects on the cell membrane of microorganisms, as it causes disorganization of membrane structures and increases its permeability [317]. Accordingly, in a phenotypic analysis of *S. cerevisiae* single gene deletion strains, especially those strains with knock-outs in the tryptophan metabolism revealed increased ethanol sensitivity [318]. Interestingly, Yoshikawa et al showed the occurrence of distinct phenotypes that were alcohol-specific and deletions that also resulted in growth deficits at high NaCl concentrations. It was revealed that knock-outs of genes involved in the synthesis of the precursor chorismate lead to increased sensitivity to both stressors, whereas the majority of tryptophan-specific genes only caused a reduced tolerance to ethanol stress. However, this is contrary to our observation that increased expression of the tryptophan synthase gene also occurred in the pure acetate cultures.

Our findings are further supported by the study of Bauer et al. in which tryptophan was shown to play a role in the response to stress caused by weak acids such as acetic acid. In this work, tryptophan auxotrophic *S. cerevisiae* strains exhibited hypersensitivity to this acid, which could be recovered by supplementation with external tryptophan [260]. Moreover, it was stated in this

study that weak acid stress inhibits uptake of aromatic amino acids from the medium. This appears to be consistent with the results of our functional enrichment analysis, where several amino acid transporters were found to be downregulated in both acetate-containing cultures. Among them was also the homologue (AO090005000114) with the highest amino acid similarity (52 % identity and 68 % positives) to TAT2 in *S. cerevisiae*. TAT2 encodes for a tryptophan permease whose overexpression has been reported to reduce the cellular sensitivity to several types of stresses [316, 319, 320]. This homologue was upregulated on glucose compared to pure acetate ( $\log_2FC = 2.71$ ) and PAC ( $\log_2FC = 5.38$ ). Moreover, the gene was also overexpressed in the comparison of acetate and PAC ( $\log_2FC = 2.67$ ) and might therefore be a potential candidate for a genetic modification of *A. oryzae* to further increase its PAC tolerance.

However, in addition to genes related to tryptophan synthesis and transport, some genes of the so-called kynurenine pathway were also differentially expressed. This pathway represents the central metabolic route of tryptophan degradation and is required for the *de novo* synthesis of NAD (**Figure 18**). The upregulation of such genes by acetate has been reported previously for *S. cerevisiae* [314] and may indicate a higher requirement for reduction equivalents in the acetate-containing cultures.

#### 3.2.4.4. Pyruvate metabolism as key pathway in the comparison of pure acetate and PAC

Pathway analysis for the comparison of acetate and the pyrolysis condensate revealed that "pyruvate metabolism" was the only pathway that showed significant differences in transcriptional regulation. The differentially expressed genes associated with this pathway mainly included those for the degradation of methylglyoxal (MG) (**Figure 19**) and several alcohol dehydrogenases. The former are of particular interest as MG is a reactive electrophile that is capable of causing damage to proteins and nucleotides [321].

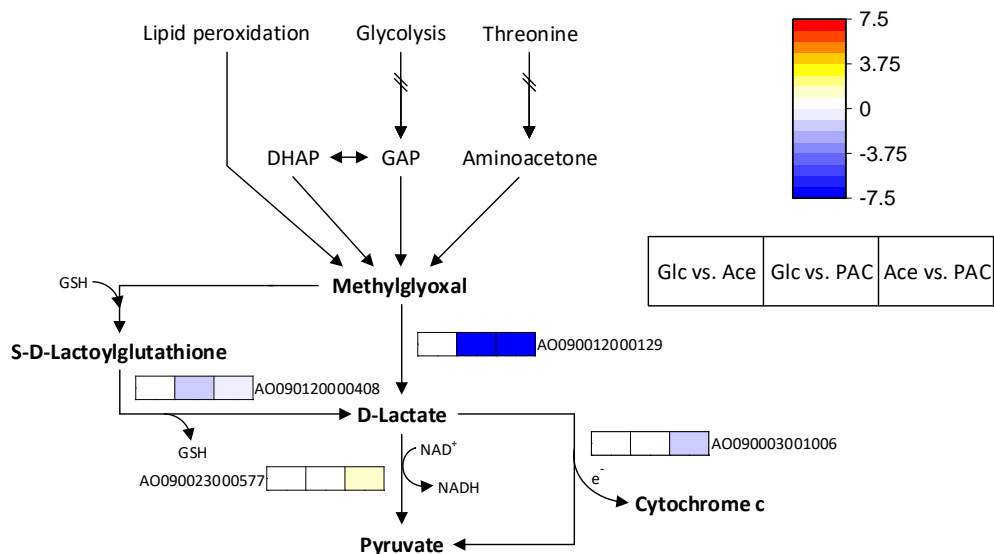


**Figure 19:** Differentially expressed genes of the pyruvate metabolism during cultivation of *A. oryzae* on glucose, acetate, and PAC. GAP = Glyceraldehyde-3-phosphate, DHAP = Dihydroxyacetone phosphate

In the cell, the oxoaldehyde is mainly formed from triose phosphate intermediates of glycolysis either by a non-enzymatic mechanism [322] or with the participation of the enzyme methylglyoxal synthase [127]. However, to the best of the authors' knowledge, the presence of this enzyme has not yet been described for *A. oryzae*. In fact, the only glycolysis gene that was found to be upregulated in the PAC cultures encoded for fructose-bisphosphate aldolase (AO090009000324,  $\log_2FC = 1.57$ ), an enzyme that catalyzes the synthesis of the triosephosphate DHAP (**Figure 16**). Thus, its increased expression might indicate enhanced MG formation from glycolysis intermediates in response to the presence of the pyrolysis condensate.

However, lipid peroxidation [323] and threonine degradation [324] have also been reported as possible pathways for the formation of the oxoaldehyde. Moreover, it is also conceivable that the MG in the PAC cultures was derived from acetol, since the ketone is the major PAC component (**Appendix 1**) and its potential to serve as substrate for microbial fermentation has already been reported for several yeasts [110]. However, the underlying pathway is still unclear as literature rather focused on the reverse reaction of the MG degradation to acetol or lactaldehyde. There are various enzymes capable of performing this conversion using NADH or NADPH as cofactors [133], but to date there are no studies reporting their reversibility.

Due to the high cytotoxicity of MG, there are further degradation mechanisms to prevent its accumulation and the resulting cellular damage. Probably the most well-known is the

glyoxalase system, which has also been partly described in *A. niger* [325]. This system consists of two enzymatic steps, with glyoxalase I first catalyzing the condensation reaction of MG and glutathione. Subsequently, the resulting S-D-lactoylglutathione is hydrolyzed to D-lactic acid by glyoxalase II, recovering the glutathione (**Figure 19**). Accordingly, this mechanism represents a link between MG degradation and the oxidative stress defense and its increased expression may provide an additional explanation for the upregulation of genes related to the glutathione system and cysteine synthesis.

Comparison of pure acetate and PAC revealed an upregulation of glyoxalase II ( $\log_2FC = 1.05$ ) in the cultures containing the pyrolysis condensate, whereas no significant difference was detected for glyoxalase I. The latter observation could possibly be explained by the fact that glyoxalase I was reported to be induced by osmotic stress [326], a condition that was present in both cultures. By contrast, the upregulation of glyoxalase II during growth on PAC may be related to the increased expression of oxidative phosphorylation genes in these cultures (**Table 7**). D-lactate formed by glyoxalase II can be converted to pyruvate by a mitochondrial D-lactate dehydrogenase (D-LDH). During this reaction, electrons are transferred to cytochrome c, thus coupling MG degradation and cellular respiration. Accordingly, oxidation of D-lactate under oxidative stress conditions can drive the respiratory chain without involving complex I, as this is considered one of the major sites of mitochondrial ROS production [327]. In the PAC cultures, we found a gene encoding cytochrome c-linked D-LDH to be upregulated compared to pure acetate (AO090003001006;  $\log_2FC = 1.75$ ), whereas a NADH-dependent D-LDH gene showed decreased expression (AO090023000577;  $\log_2FC = -1.11$ ) (**Appendix 3**).

However, an even more significant differential expression was observed for another MG degradation pathway that also leads to the formation of D-lactate. This pathway has already been described for yeasts [328, 329] and involves only a single glutathione-independent reaction catalyzed by another glyoxalase (**Figure 19**). For the gene encoding this enzyme (AO090012000129), a strong upregulation in the PAC-containing cultures compared with both pure acetate ( $\log_2FC = 7.49$ ) and glucose ( $\log_2FC = 6.63$ ) was observed, indicating that the glutathione-independent reaction appears to be the main MG degradation pathway during growth on PAC. This raised the question of whether cellular glutathione levels were insufficient to compensate for the amount of MG produced and whether a deficiency of this thiol compound may have occurred. In addition to the aforementioned upregulation of the glutathione synthase gene, this assumption might also be supported by the differential expression of alcohol dehydrogenases (ADH) in our cultures (**Table 12**).

**Table 12:** Differentially expressed NADH- (EC 1.1.1.1) and NADPH-dependent (EC 1.1.1.2) alcohol dehydrogenases

Condition	EC	Gene ID	Fold change
Glc vs. PAC	1.1.1.1	AO090005000125	1.68
		AO090038000108	2.85
		AO090026000555	3.43
	1.1.1.2	AO090005001358	-3.78
		AO090010000668	-6.14
Glc vs Ace	1.1.1.1	AO090009000634	1.47
		AO090038000108	4.19
	1.1.1.2	AO090038000575	-1.62
Ace vs PAC	1.1.1.1	AO090026000555	2.28
		AO090005001358	-3.63
	1.1.1.2	AO090023000460	-3.39
		AO090010000668	-8.02

For example, it has been observed that in glutathione-depleted *Candida albicans* strains ADH1 functions as methylglyoxal dehydrogenase and catalyzes the oxidation of MG to pyruvate [330]. Moreover, the reduction of the oxoaldehyde to acetol can also be performed by this enzyme [330, 331]. However, the ADHs involved in these reactions were NADH-dependent, whereas in our PAC-containing cultures we rather found an increased expression of ADHs that require NADPH as cofactor (**Table 12**). Among these, the genes AO090010000668 and AO090023000460 might be of particular interest. While the former showed remarkably high expression compared to both glucose ( $\log_2FC = 6.14$ ) and acetate ( $\log_2FC = 8.02$ ), the latter was differentially expressed exclusively between acetate and PAC and the altered gene expression can therefore probably be attributed to additional PAC components.

Furan compounds like HMF and furfural might represent such components, since their microbial conversion into less harmful alcohols has been reported to involve the action of ADHs in *S. cerevisiae* [170, 180]. In particular, the NADPH-preferring ADH6 was characterized by its high in vitro activity towards the two furans, but also the overexpression of the corresponding gene led to an increase in growth and HMF uptake rate in anaerobic batch cultivations [180]. Conversely, an inhibitory effect of furfural towards NADH-dependent ADH (EC 1.1.1.1) has been described by Modig et al. [166], which could partly explain the observed downregulation of these genes in the PAC-containing cultures. In addition, there is a study on *S. cerevisiae*

showing that carbon catabolite repression in microorganisms is not limited to glucose, but that growth on acetate can lead to a decreased expression of alcohol dehydrogenases like ADH2 [332].

Besides the NADPH-dependent ADHs, a gene encoding for an old yellow enzyme (OYE) also showed a strongly increased expression on PAC in comparison to acetate and glucose (AO090005001535;  $\log_2FC_{\text{Acetate}} = 7.81$ ,  $\log_2FC_{\text{Glucose}} = 4.81$ ). These oxidoreductases may be of particular interest for further improving the fungal PAC resistance, as they catalyze the NADPH-dependent reduction of  $\alpha$ ,  $\beta$ -carbon double bonds in a variety of substrates [333]. Since these potential substrates also include cyclic components, it is quite conceivable that the enzyme is capable of converting the highly toxic 2-cyclopenten-1-one into the less harmful alkane. However, the other genes encoding enzymes of MG degradation and NADPH-dependent ADHs described in this section may also be potential targets for a future strain engineering aimed at increasing fungal PAC tolerance.

## 4. Optimization of the pretreatment procedure for detoxification of the pyrolytic aqueous condensate

This chapter is mainly based on the publication:

**Detoxification of a pyrolytic aqueous condensate from wheat straw for utilization as substrate in *Aspergillus oryzae* DSM 1863 cultivations**

Christin Kubisch and Katrin Ochsenreither

Institute of Process Engineering in Life Science 2: Technical Biology, Karlsruhe Institute of Technology, Karlsruhe, Germany

### **Publication details:**

*Biotechnology for Biofuels and Bioproducts*

Volume 15, Article 18

Publication date: 17 February 2022

DOI: 10.1186/s13068-022-02115-z

**Author's contribution:**

**Christin Kubisch** designed and performed the experiments, analyzed the data and drafted the manuscript.

**Katrin Ochsenreither** contributed in the conceptualization of the study, supervised the laboratory work and revised the manuscript.

## 4.1. Introduction

Although the pretreatment procedure performed prior to the transcriptome analysis already resulted in a significant increase in fungal PAC tolerance from about 1-2 % to 20 %, the substrate concentration contained therein was not sufficient to allow utilization of the condensate for malic acid production with *A. oryzae*. The aim of the following chapter was therefore to further optimize the pretreatment of the PAC in such a way that the concentrations of inhibiting components are reduced to a minimum while the content of utilizable carbon sources in the pyrolysis condensate is largely maintained.

In addition to the methods already applied in the third chapter, enzymatic pretreatment of the PAC with laccase from the white rot fungus *Trametes versicolor* was investigated, particularly with respect to its ability to reduce the inhibitory effect of phenolic components. To enable the most effective detoxification of the PAC, the optimal conditions for a sole pretreatment with laccase, overliming, activated carbon and rotary evaporation were first identified. Subsequently, combinations of individual methods were performed under the previously determined optimum conditions. The detoxification efficiency was evaluated by growth tests on agar plates and quantification of selected model substances via GC analysis. At the end of this chapter, it was further evaluated in shake flask cultivations whether the optimized detoxification method is suitable to allow fungal growth on pure pyrolysis condensate.

## 4.2. Results

### 4.2.1. Single methods

#### 4.2.1.1. Enzymatic laccase treatment

In a first experiment, the optimum enzyme concentration and duration for the laccase treatment were determined. **Figure 20 A** shows that the initial total phenol concentration in the untreated PAC was  $7.96 \pm 0.04$  g(GAE)/L and only marginally decreased during the incubation period. The same behavior was observed for laccase concentrations of 1 and 2.5 U/mL. Only when 5 U/mL or more were applied a considerable decrease in the amount of total phenols became apparent. Even in the samples taken immediately after the addition of the enzyme, a slight decrease in phenol content was observed, indicating that the enzymatic reaction was quite fast. This assumption is supported by the almost linear decline in phenol concentration during the first hour of incubation. Afterwards, the curves progressively flattened and the concentrations of the total phenolics remained largely constant during the last 8 h of treatment. The final titers ranged from  $5.93 \pm 0.20$  g(GAE)/L for 5 U/mL to values of  $3.92 \pm 0.18$  g GAE/L and  $2.92 \pm 0.05$  g(GAE)/L when enzyme amounts of 10 and 25 U/mL were used. This corresponds to a percentage removal of 19.32 %, 46.67 % and 60.27 % and shows that even with the highest laccase concentration the phenolics were not completely eliminated. This observation was also confirmed by the GC analysis of the two phenolic model substances phenol and guaiacol (**Figure 20 B and C**). Whereas a complete removal of guaiacol was achieved after 24 h and 1 h when the PAC was treated with 10 U/mL and 25 U/mL laccase, respectively, the phenol concentration was only slightly affected by the enzyme addition. Only for the highest laccase concentration, a considerable removal of 17.8 % phenol was observed after 24 h. Thus, the results show that the elimination of phenolics does not only strongly depend on the enzyme concentration, but also on the phenolic substance.

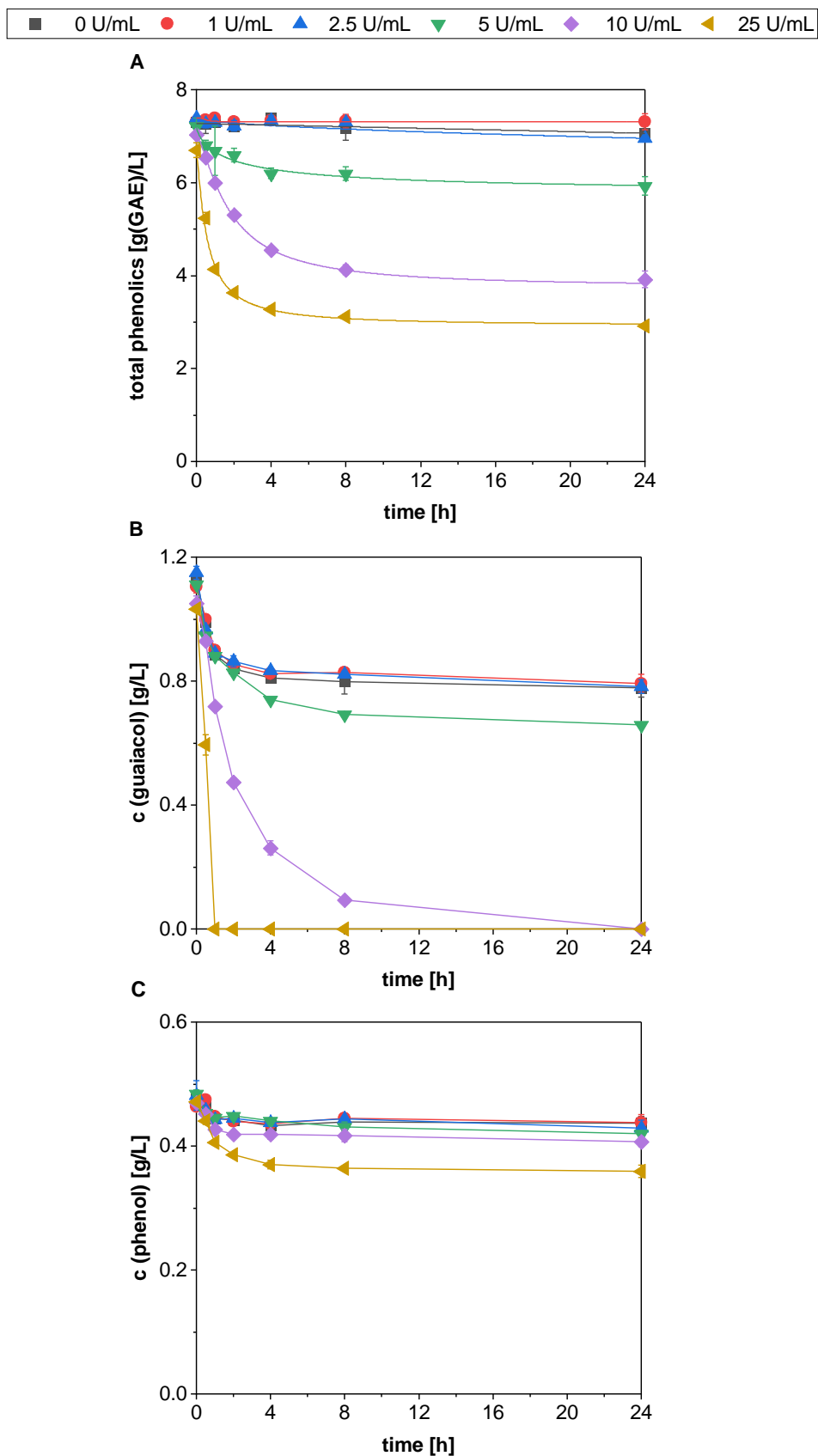


**Figure 20:** Removal of phenolic substances from PAC during 24 h treatment with different concentrations of *T. versicolor* laccase. The concentrations of total phenolics (A) were determined via FC analysis and expressed as g(GAE)/L. The phenolic model compounds phenol (B) and guaiacol (C) were analyzed via GC. The experiments were performed in duplicates and the graph shows the mean values and the standard deviations as error bars.

For the growth test, the highest enzyme concentration of 25 U/mL and the maximum incubation time of 24 h were chosen (**Figure 21**). The fungal colony diameters were larger on plates that contained laccase treated PAC than on those with untreated condensate. However, growth was still strongly inhibited compared to the control without PAC and the overall tolerance level did not exceed 1.25 %. Due to its ineffectiveness, laccase treatment was not included in the experiments on the combinations of different treatment methods.

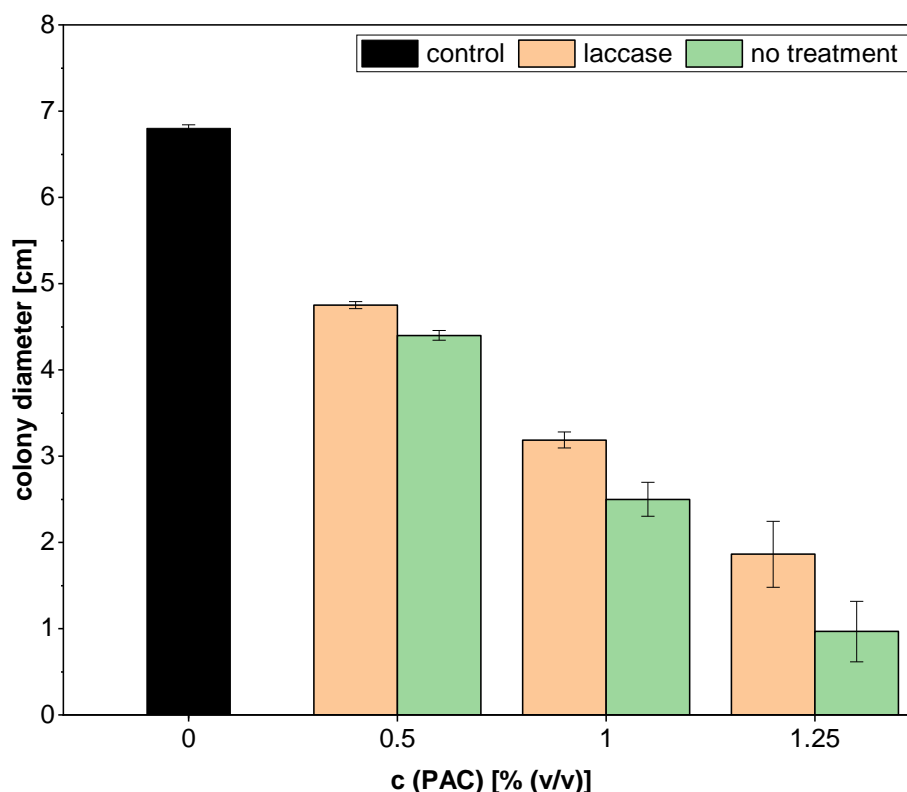


**Figure 21:** Colony diameters of *A. oryzae* after 5 days of growth on agar plates containing different contents of PAC treated with 25 U/mL *T. versicolor* laccase for 24 h. The experiment was performed in quadruplicates and the graph shows the mean values and the standard deviations as error bars.

#### 4.2.1.2. Activated carbon treatment

To determine the optimum concentration of activated carbon required for effective PAC detoxification, carbon loads of 0-10 % (w/v) were tested. As shown in **Figure 22** only 1.125 % PAC was tolerated when the condensate did not undergo any additional treatment besides a pH adjustment and subsequent filtration.

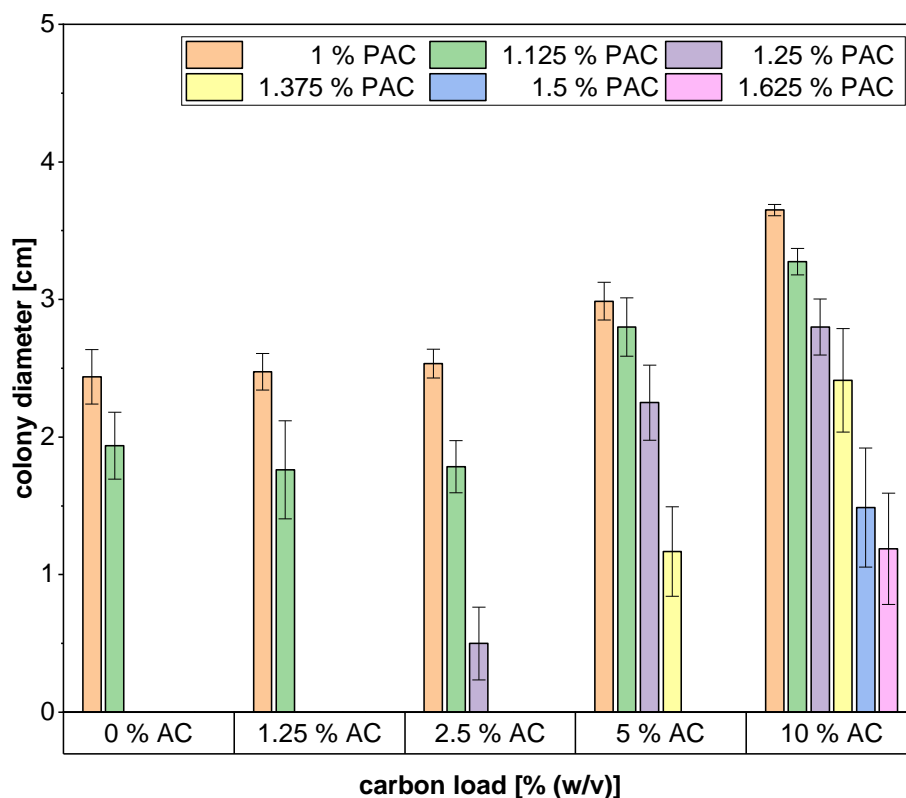


**Figure 22:** Colony diameters of *A. oryzae* after 5 days of growth on agar plates containing different volumetric contents of PAC, that was obtained after 1-h treatment with increasing activated carbon (AC) loads (0-10 % (w/v)). The experiment was performed in quadruplicates and the graph shows the mean values and the standard deviations as error bars.

Detoxification with 1.25 % activated carbon did also not lead to any growth on higher PAC concentrations. But with carbon loads  $\geq 2.5$  % an enhanced fungal PAC tolerance was detected. The growth limit of *A. oryzae* increased to 1.25 %, 1.375 % and 1.625 % when the PAC was treated with 2.5 %, 5 % and 10 % activated carbon, respectively. Furthermore, colony diameters increased for the same PAC content when applying higher activated carbon concentrations. Consequently, the best results were achieved using the highest amount of carbon leading to an improvement of 44.44 % compared to the untreated control. The GC analysis revealed that the treatment resulted in at least a partial removal of all inhibitory compounds (**Figure 23**).

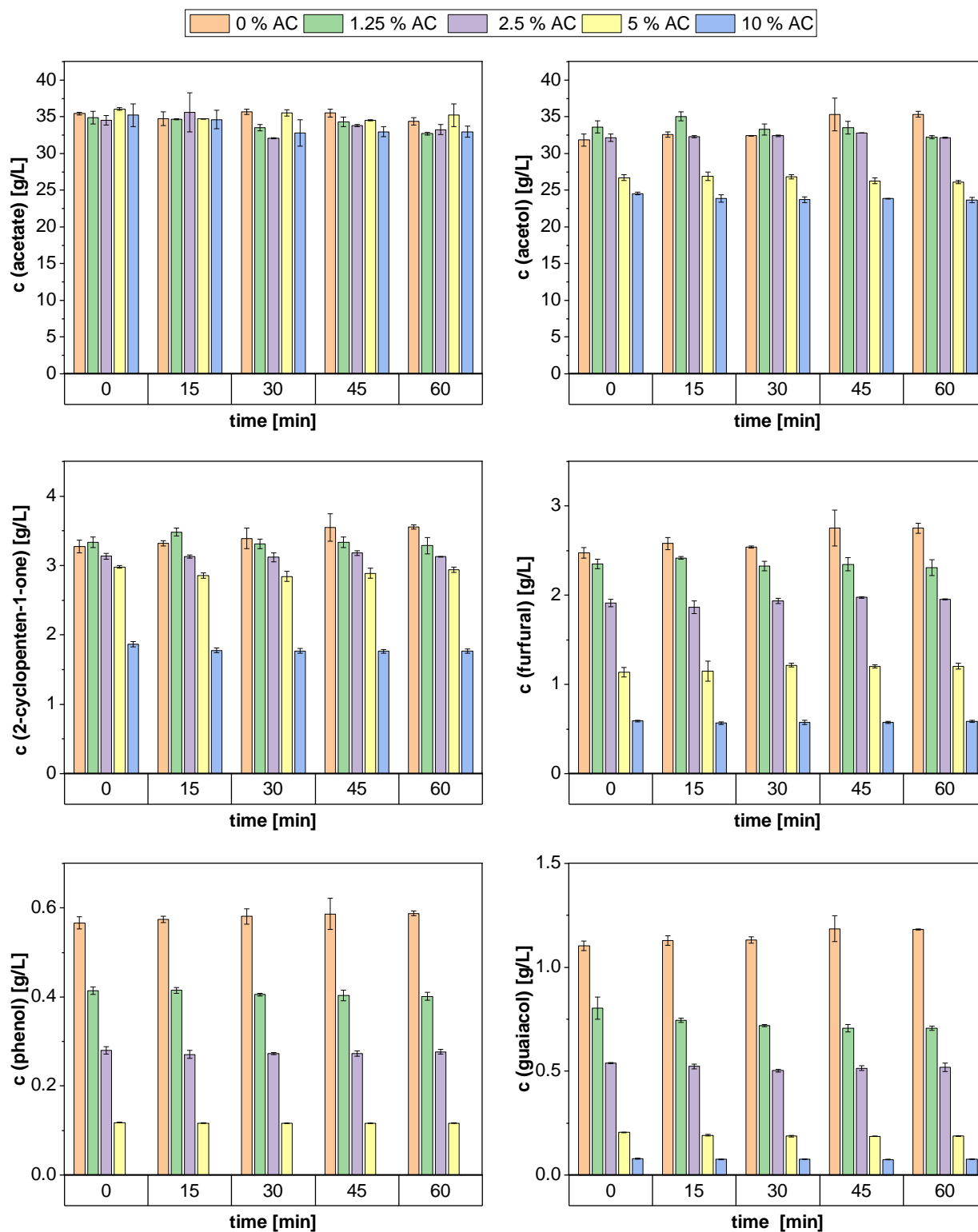


**Figure 23:** Temporal change in concentration of selected PAC compounds during treatment with increasing activated carbon loads (0-10 % (w/v)). The data represent mean values of two replicates and error bars indicate the standard deviation.

Interestingly, the lowest concentrations of inhibitors were already reached immediately after the addition of the carbon and longer incubation times did not lead to any further improvement, which indicates that the adsorption to the char particles is a rather fast process.

The effectiveness of the activated carbon treatment was highly dependent on the inhibitory PAC component. For acetol, 2-cyclopenten-1-one and furfural only slight changes in the concentration were detected after treatment with 1.25 % carbon, which is consistent with the results of the growth test. By contrast, a notable removal of the phenolic compounds already occurred at the lowest carbon load applied as their concentration was reduced by about 30 %. Moreover, **Figure 23** shows that the concentration of the inhibitory compounds was further decreased by using higher carbon contents. In the case of phenol, the use of 10 % carbon even resulted in a complete removal of the compound and also the concentration of guaiacol was decreased by 93.4 %. Although the concentration of the ketones and aldehydes was not reduced to such a high extent, a carbon load of 10 % was still the most effective condition for the removal of these compounds as the concentration of acetol, 2-cyclopenten-1-one and furfural decreased by 29.5 %; 48.3 % and 77.7 %, respectively. In contrast, the amount of acetic acid remained relatively constant at an average concentration of  $34.44 \pm 1.40$  g/L throughout the whole incubation period regardless of the carbon loads applied.

Accordingly, since the treatment with 10 % carbon showed the best removal efficiency without causing any substrate loss, it was chosen for further combination experiments and the incubation time was shortened to 10 min.

#### *4.2.1.3. Overliming treatment at different temperatures*

Growth tests revealed a general positive relation between the temperature applied for the overliming treatment and the fungal tolerance towards the pretreated PAC (**Figure 24 A**). However, the temperature dependence appeared to be different for the two hydroxides. For NaOH the tolerance level improved from 2 % at room temperature to 2.5 % and 2.75 % when the incubation temperature was doubled to 40 °C and 80 °C, respectively. Thus, a clear correlation between the temperature and the detoxification efficiency was observed. Contrarily, the overliming treatment with Ca(OH)<sub>2</sub> seemed to be already quite effective at low temperatures as even with a treatment performed at 20 °C the fungus could tolerate PAC concentrations of 3 %. This represents a 50 % increased growth limit compared to NaOH overliming under the same conditions and was still 8.33 % better than NaOH treatment at 80 °C.

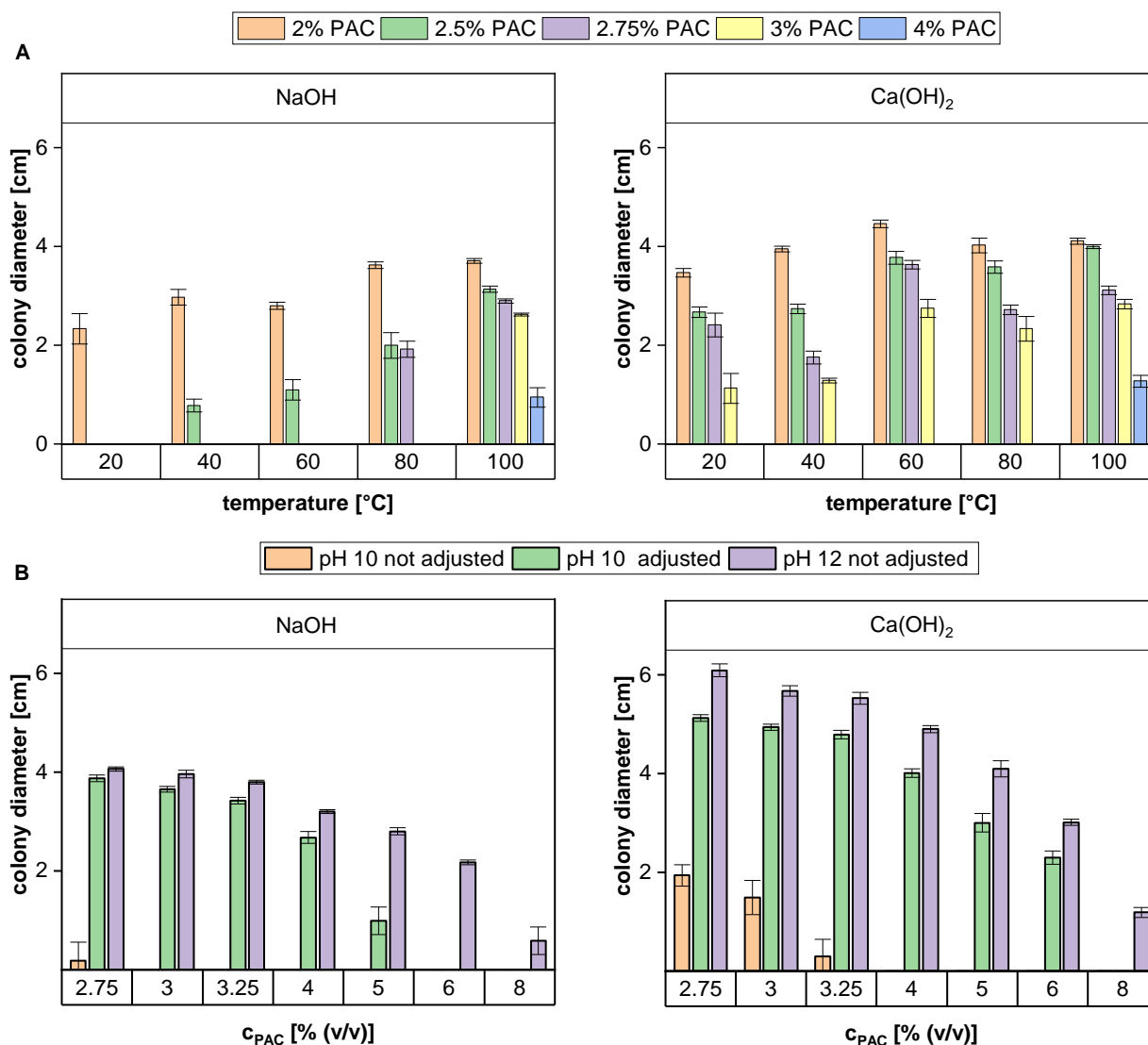


**Figure 24:** Colony diameters of *A. oryzae* after 5 days of growth on agar plates containing different amounts of PAC treated with overliming at various temperatures for 4 h (A) and two different pH values for 90 min (B). In the latter experiment, two different initial pH values (pH 10 and 12) as well as manual adjustment to pH 10 throughout the process were tested for a fixed temperature of 80 °C. The experiment was performed in quadruplicates and the graph shows the mean values and the standard deviations as error bars.

However, the growth limit did not increase for higher temperatures up to 80 °C. Only when a temperature of 100 °C was used for the overliming treatment with Ca(OH)<sub>2</sub> the fungal tolerance was further improved to 4 %. The same tolerance level was also achieved for NaOH at that temperature, thus leading to the assumption that the influence of the metal ion that became apparent at low temperatures was compensated at 100 °C. This assumption is also confirmed by GC analysis of the PAC compounds after 4 h of treatment at 100 °C as it revealed comparable concentrations for both hydroxides (**Table 13**). Only two inhibitory compounds, guaiacol and 2-cyclopenten-1-one, differed notably in their final concentrations. For guaiacol, a slightly higher concentration of  $0.67 \pm 0.01$  g/L was observed in the NaOH treated PAC, but for both

hydroxides its content was below the growth limit of 1 % that was determined by Dörsam et al. [149]. Regarding 2-cyclopenten-1-one, the concentration of  $1.22 \pm 0.01$  g/L was 9 % higher in the Ca(OH)<sub>2</sub> treated PAC than when sodium was used. Although the treatment already resulted in a reduction of the 2-cyclopenten-1-one content to about one third of the concentration in the original PAC, the fungal growth limit of 0.0625 g/L was still significantly exceeded in both cases, which was also reflected in the results of the growth test. While the concentration of all inhibitory substances decreased during the overliming treatment, acetic acid concentrations were found to be increased (**Table 13**), partly due to evaporation effects.

**Table 13:** GC analysis of PAC treated by overliming at different conditions

substance	<i>A. oryzae</i> growth limit [g/L] <sup>1</sup>	c in original PAC [g/L] <sup>2</sup>	c [g/L] in PAC after treatment at 100 °C and the following conditions...			
			duration	4	4	1.5
			initial pH	10	10	12
			hydroxide	Ca(OH) <sub>2</sub>	NaOH	NaOH
acetate	>70	35.40 <sup>3</sup>		$40.51 \pm 0.19$	$38.35 \pm 0.33$	$41.24 \pm 1.87$
acetol	15	51.46		$9.99 \pm 0.91$	$11.50 \pm 0.75$	$6.31 \pm 0.42$
guaiacol	1	1.80		$0.55 \pm 0.01$	$0.67 \pm 0.01$	$0.48 \pm 0.00$
furfural	0.3	2.94		$0.22 \pm 0.03$	$0.31 \pm 0.06$	$0.12 \pm 0.00$
phenol	0.7	0.64		$0.44 \pm 0.00$	$0.46 \pm 0.01$	$0.4 \pm 0.00$
2-cyclo-penten-1-one	0.0625	3.40		$1.22 \pm 0.01$	$1.11 \pm 0.03$	$0.45 \pm 0.00$

<sup>1</sup>determined by Dörsam et al. [149] as % (w/w). The concentration was converted into g/L assuming the density of water [77]. The only exception was acetate, for which, according to Kövilein et al. [104], no growth limit was determined so far.

<sup>2</sup>GC/MS analysis performed by Thünen Institute of Wood Research in Hamburg for PAC that was neither pH adjusted nor filtered

<sup>3</sup>quantified by an enzymatic acetate assay

In general, the results show that a temperature of 100 °C serves best for PAC detoxification. Hence, this temperature was chosen for the overliming treatments performed in the combination experiments. However, a PAC tolerance of 4 % is still far too low to enable its utilization as sole substrate for fungal growth and a further optimization of the treatment procedure is therefore required.

#### 4.2.1.4. Overliming treatment using different pH strategies

As it can be seen from the pH curve of the temperature experiment (**Appendix 5**), the pH drops back into the neutral range very quickly, especially when high temperatures are applied. Consequently, it was assumed that the hydroxide ions were depleted and that a higher supply could further enhance detoxification. Therefore, two different ways to increase the hydroxide concentration were evaluated: raising the initial pH to 12 or manually adjusting the pH to a value of 10 throughout the incubation period. **Figure 24 B** shows, that both strategies led to a remarkable increase in the PAC tolerance of *A. oryzae* as for NaOH the maximum tolerated concentration could be enhanced to 5 % for the pH adjusted PAC and even to 8 % when the treatment is performed at an initial pH of 12. This corresponds to a 0.8-fold and 1.9-fold improvement compared to the standard procedure performed at an initial pH of 10.

The results obtained for  $\text{Ca}(\text{OH})_2$  were again slightly better than for NaOH as for the pH adjusted PAC the maximum concentration tolerated by the fungus was 6 %. However, for the pH strategy that was most effective (initial pH of 12), the impact of the hydroxide again appeared to be negligible, as both hydroxide treatments resulted in the same PAC tolerance of 8%. Therefore, this pH strategy was chosen for the subsequent combination experiments and NaOH was selected as the favored hydroxide in order to reduce the risk of precipitation of medium components. Due to the upper temperature limit of the pH probe used, the pH experiment had to be performed at 80 °C even though a temperature of 100 °C was previously identified to be ideal. A combination of the optimum conditions for temperature and pH resulted in an even higher tolerated PAC concentration of 12.5 % (data not shown) and the GC results shown in **Table 13**. The results underline, that the pH is of particular importance for an efficient overliming treatment, since the concentration of all inhibitory compound measured was further reduced by the pH optimization in an even shorter reaction time. Especially, the amount of acetol, furfural and 2-cyclopenten-1-one was considerably reduced by 45.1 %, 61.3 % and 59.5 %, respectively, compared to the overliming treatment with an initial pH of 10. In contrast, only minor decreases in guaiacol and phenol were observed, leading to the conclusion that overliming is not the preferred method for the removal of phenolic substances.

### Rotary evaporation

In this experiment different pressures were selected for a 4-h rotary evaporation at 80 °C. As **Figure 25** shows the maximum concentration that was still tolerated by *A. oryzae* was enhanced to 5 %, 15 % and even 30 % when the condensate was treated at 400 mbar, 300 mbar and 200 mbar, respectively. These results indicate a clear dependence of the detoxification efficiency on the pressure applied for the evaporation.

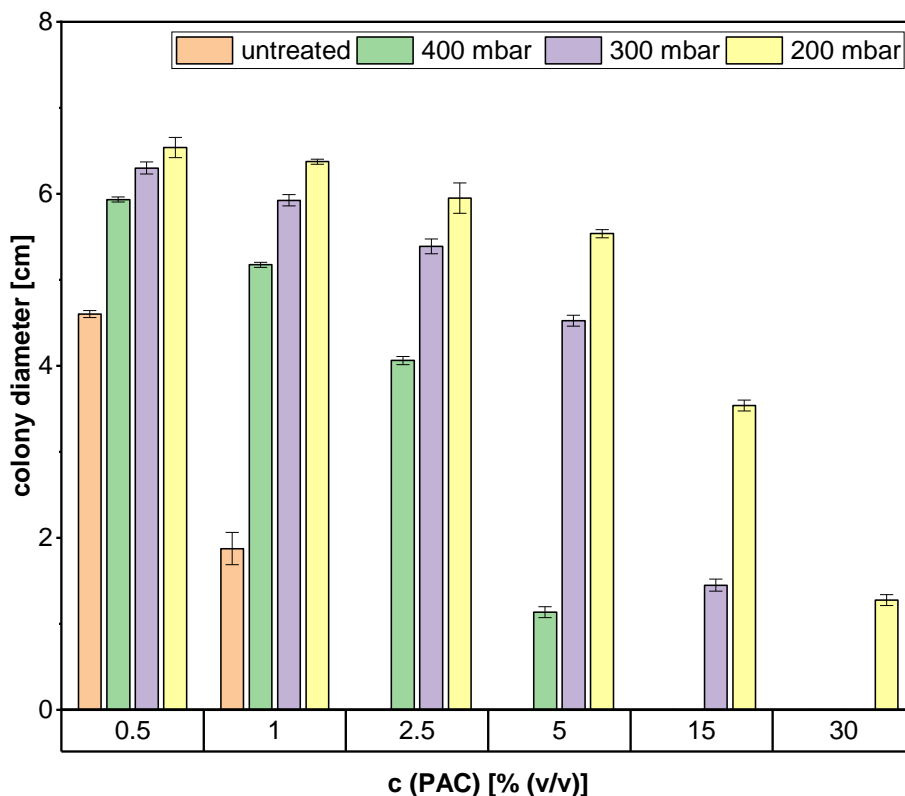


**Figure 25:** Colony diameters of *A. oryzae* after 5 days of growth on agar plates containing different volumetric contents of PAC treated with 4-h rotary evaporation at different pressures and 80 °C. The data represent mean values of quadruplicates and the error bars indicate the standard deviation.

The growth results are supported by the GC analysis since the concentration of every measured inhibitory PAC compound decreased remarkably. Even at 400 mbar the removal of the toxic compounds ranged from 23.6 % for acetol to a maximum of 79.4 % for furfural compared to the untreated control (**Figure 26**).

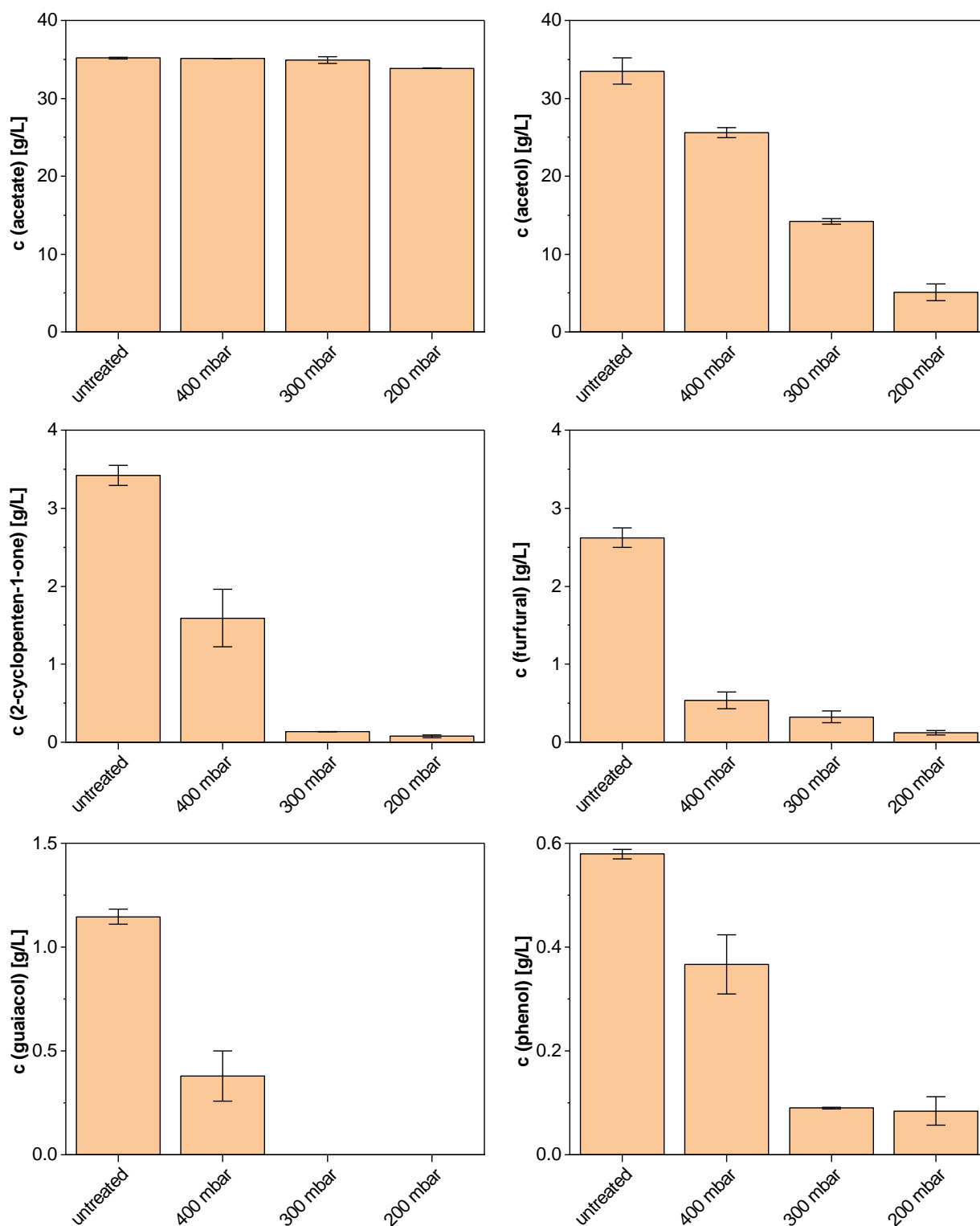


**Figure 26:** Concentration of selected PAC compounds after 4h treatment with rotary evaporation at different pressures and 80 °C. The data represent mean values of two replicates and error bars indicate the standard deviation.

The detoxification results were further improved when lower pressures were applied for the evaporation procedure. A reduction of the pressure to 300 mbar resulted in the complete removal of the phenolic compound guaiacol and also the concentration of 2-cyclopenten-1-one

was decreased remarkably to 0.14 g/L. However, the content of the latter and the  $0.32 \pm 0.08$  g/L of furfural remaining still exceeded the growth limit of *A. oryzae* (**Table 13**). By further decreasing the pressure to 200 mbar, it was possible to obtain an additional removal of almost every substance, except for phenol. The concentrations of furfural and 2-cyclopenten-1-one were now determined to be  $0.12 \pm 0.03$  g/L and  $0.08 \pm 0.02$  g/L, which were below or at least close to the growth limit of the fungus. Similar to the previous experiments, it was found that the acetic acid content remained largely unchanged during the evaporation treatment with an average concentration of  $35.07 \pm 0.45$  g/L. Only when a pressure of 200 mbar was applied, a slight decrease to a concentration of  $33.86 \pm 0.04$  g/L was observed. However, due to the fact that the best detoxification results were obtained for this condition, it was chosen for the following combination experiment.

#### 4.2.2. Combinations of methods

The previous sections showed that the application of single methods was not sufficient to enable fungal growth on the pure condensate. Therefore, it was evaluated whether combinations of activated carbon (AC), overliming (OL) and rotary evaporation (RE) treatments further improve the fungal PAC tolerance (**Figure 27**).

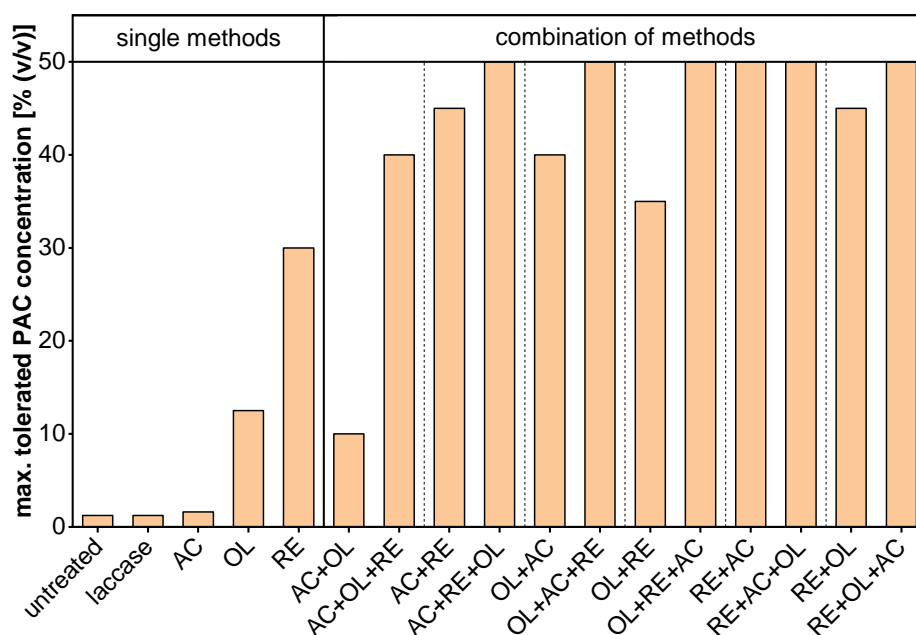


**Figure 27:** Maximum tolerance of *A. oryzae* on agar plates containing PAC obtained after single treatment with laccase, activated carbon (AC), overliming (OL) or rotary evaporation (RE) as well as combinations of the latter three detoxification methods.

Every possible combination of two and three methods was performed and all of them except the combination of AC+OL resulted in a higher tolerance than achieved for the single methods. Unsurprisingly, the data also show that the improved growth achieved after combining two methods was further enhanced by a subsequent third treatment. Except for AC+OL+RE, all combinations of three methods allowed fungal growth on 50 % PAC, which was the maximum concentration that could be tested on agar plates. Therefore, these data were not suitable for assessing how the order in which the detoxification methods are performed affects detoxification.

However, the results obtained for the combinations of two methods show that the order seems to be of crucial importance. For instance, the combination AC+OL led to a tolerance of only 10 %, whereas performing the combination in the reverse order resulted in a fungal growth on up to 40 % PAC. A similar observation was made for the combinations of AC+RE and RE+AC, which leads to the assumption that the activated carbon treatment should be conducted at the end of the detoxification procedure. Conversely, the latter example also indicates that it has a positive effect on the PAC detoxification to perform the rotary evaporation in the beginning. This hypothesis is further supported by the comparison of the combinations OL+RE and RE+OL, since the tolerated PAC concentration was 10 % higher for the latter combination. Accordingly, performing RE in the beginning and AC in the end (RE+AC) gave the best results among all combinations of two methods as a growth on the maximum concentration of 50 % PAC was observed. This raised the question of whether an additional OL treatment is even needed to enable the utilization of the pure condensate as substrate for fungal growth. Therefore, RE+AC and the two best performing combinations of three methods according to their colony diameter and morphological appearance were selected for a shake flask cultivation using 100 % PAC (data not shown). It was found that *A. oryzae* could only grow in cultures containing PAC treated with the combination of RE+OL+AC. Therefore, this combination was henceforth considered as the optimum detoxification procedure.

To gain insight into how a combination of methods affects the inhibitors present in the PAC, samples were taken after each individual treatment step and analyzed by GC (**Table 14**). The data obtained after the first step of each combination are largely in agreement with the findings of the single method experiments performed in the previous sections. It was again confirmed that, in contrast to overliming, activated carbon treatment is particularly suitable for removing phenolic compounds. In addition, the concentration of acetic acid remained largely unchanged after AC and RE treatments, while it even increased for OL. This demonstrates that the treatment results are quite reproducible despite the complex composition of the PAC.

**Table 14:** GC analysis of PAC treated with different combinations of detoxification methods

Combination	c (PAC compound) [g/L]					
	acetate	acetol	2-cyclopenten-1-one	furfural	guaiacol	phenol
<b>Untreated</b>	35.17 ± 0.13	33.58 ± 1.86	3.42 ± 0.13	2.63 ± 0.15	1.15 ± 0.04	0.58 ± 0.01
<b>Growth limit<sup>1</sup></b>	>70	15	0.0625	0.3	1	0.7
<b>RE</b>	36.06	6.89	0.09	0.21	0.16	0.06
<b>RE+OL</b>	39.97	3.95	0.08	0.00	0.16	0.06
<b>RE+OL+AC</b>	39.02	2.96	0.00	0.00	0.14	0.00
<b>RE</b>	35.17	6.34	0.09	0.20	0.15	0.06
<b>RE+AC</b>	35.40	5.06	0.00	0.00	0.14	0.00
<b>RE+AC+OL</b>	40.07	3.54	0.00	0.00	0.00	0.00
<b>OL</b>	42.56	6.61	0.44	0.12	0.48	0.41
<b>OL+RE</b>	42.83	2.76	0.11	0.23	0.22	0.09
<b>OL+RE+AC</b>	43.49	2.10	0.07	0.15	0.14	0.11
<b>OL</b>	39.92	6.01	0.45	0.12	0.48	0.41
<b>OL+AC</b>	42.40	5.79	0.30	0.04	0.21	0.06
<b>OL+AC+RE</b>	42.41	1.96	0.08	0.00	0.15	0.00
<b>AC</b>	35.81	21.64	1.62	0.40	0.16	0.00
<b>AC+RE</b>	34.59	5.69	0.24	0.10	0.14	0.00
<b>AC+RE+OL</b>	44.43	3.58	0.16	0.00	0.13	0.00
<b>AC</b>	35.43	21.93	1.64	0.40	0.14	0.00
<b>AC+OL</b>	41.84	14.15	0.61	0.05	0.14	0.00
<b>AC+OL+RE</b>	41.22	6.18	0.12	0.00	0.00	0.00

<sup>1</sup> determined by Dörsam et al. [149] as % (w/w). The concentration was converted into g/L assuming the density of water [77]. The only exception was acetate, for which, according to the results of Kövilein et al. [104], no growth limit was determined so far.

Regarding the combination of two methods, the lowest fungal tolerance was observed for AC+OL. The GC results show that after the initial AC treatment, phenol was completely removed. However, 0.40 g/L furfural and 1.62 g/L 2-cyclopenten-1-one were still present in the PAC. Although the subsequent OL procedure led to a further removal of the analyzed inhibitors, the concentrations of 2-cyclopenten-1-one and acetol were still even higher than when OL was performed as sole treatment. This leads to the assumption that OL is impaired by the preceding carbon adsorption and confirms that the AC treatment should better be conducted at the end of the detoxification procedure. In contrast, performing RE in the beginning resulted in very low concentrations of every inhibitory compound and for the best performing combination of two methods (RE+AC), even a complete removal of furfural and 2-cyclopenten-1-one was observed. The same observations were made for both of the combinations of three methods that started with a RE treatment. One of these detoxification procedures, namely RE+OL+AC, was the only one that enabled *A. oryzae* to grow on 100 % PAC. However, the GC analysis of only six PAC compounds cannot fully explain why RE+AC and RE+AC+OL combinations were less effective, since also for these combinations the concentrations of all the inhibitors measured was below the growth limit of *A. oryzae*.

#### 4.2.3. *Aspergillus oryzae* pre-culture cultivation on detoxified PAC

The PAC obtained after treatment with the optimized detoxification procedure was now utilized for the evaluation of the growth and substrate consumption of *A. oryzae* cultivated in shake flasks containing 100 % PAC (**Figure 28**).

The initial acetate concentration in the cultures was  $42.00 \pm 0.07$  g/L and remained largely unchanged during the first 24 h of cultivation. The same observation was made for the pH and the ammonium concentration. However, **Figure 28** shows that a CDW of  $0.95 \pm 0.03$  g/L was already obtained at this stage of fermentation, indicating that either additional substrates are present in the PAC or that the fungus consumed the nutrient reserves that were still contained in the spores and the glycerol stock solution. After the first lag phase, the pH increased considerably due to the incipient acetate consumption. The concentration of the C-source decreased by 4.91 g/L and also the amount of ammonium was reduced to  $0.62 \pm 0.03$  g/L during the exponential growth phase (24-48 h). The high substrate consumption led to a sharp increase in biomass formation, as a tripling of the CDW to  $3.00 \pm 0.21$  g/L was detected. Although this was followed by an flattening of the substrate and pH curves, the biomass continued to increase and the maximum CDW of  $5.21 \pm 0.46$  g/L was reached after 72 h.

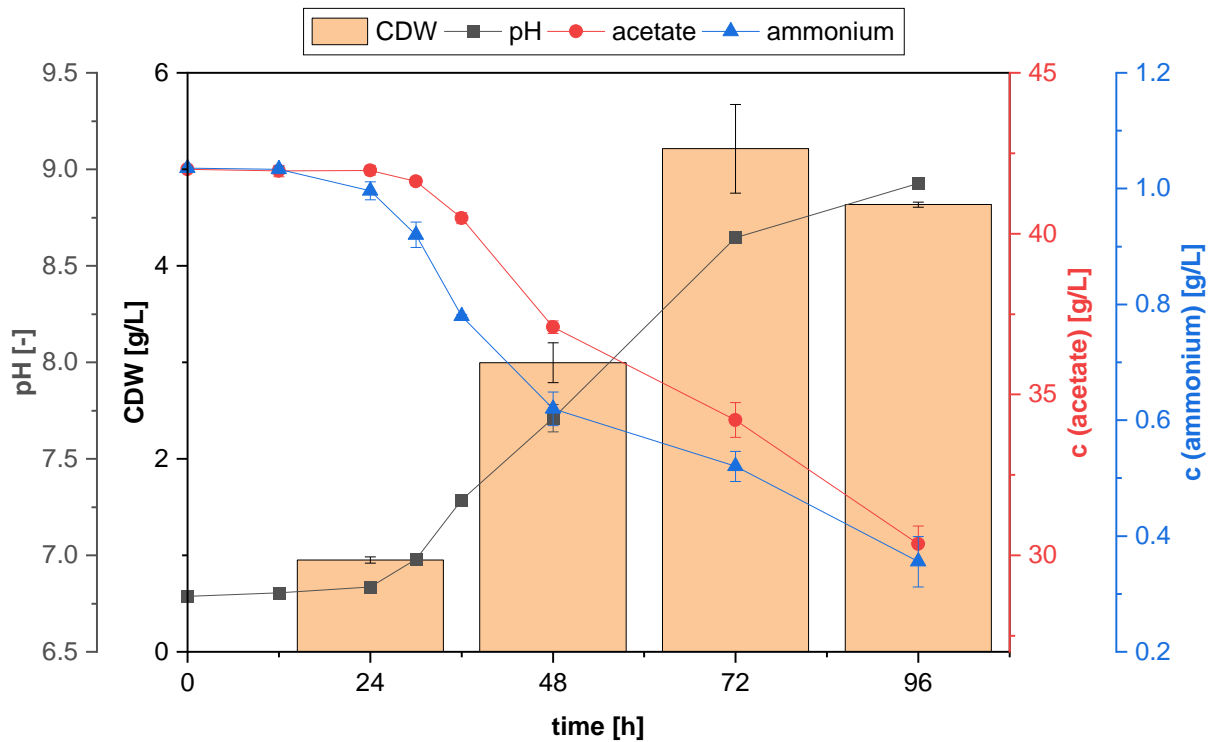


**Figure 28:** Shake flask cultivations of *A. oryzae* in pre-culture medium containing 100 % PAC detoxified by a combination of rotary evaporation, overliming and activated carbon. The data represent mean values of triplicates and the error bars show the standard deviation.

Only in the last 24 h of cultivation a slight decrease in the biomass concentration to  $4.63 \pm 0.03$  g/L was observed. Thus, the fungus gradually entered the stationary growth phase, even though  $30.35 \pm 0.57$  g/L acetate and  $0.36 \pm 0.04$  g/L ammonium were still present at the end of the cultivation. Nevertheless, the results of the shake flask experiment show that with the choice of an appropriate detoxification procedure, it is possible to use 100 % PAC as the sole substrate for the growth of *A. oryzae*.

## 4.3. Discussion

### 4.3.1. Single methods

#### 4.3.1.1. Laccase treatment

In contrast to the other tested methods, laccase treatment did not improve fungal PAC tolerance, even though at least a partial removal of phenolics was detected via FC assay and GC. The mechanism of removal is based on the oxidation of phenolic compounds which is catalyzed by the copper-containing enzyme and is accompanied by the simultaneous reduction of oxygen to water. This oxidation is a one-electron reaction that leads to the formation of a free phenoxy radical, which can undergo further non-enzymatic reactions, including polymerization with other phenolic molecules [334]. Since these polymers are insoluble in aqueous solutions, they form reddish to dark brown precipitates as it was also observed in the current study (data not shown). This observation confirms that the enzyme was active under the selected conditions as previously reported by Kurniawati et al. [235]. However, since they used defined solutions with only 500  $\mu\text{M}$  pure phenol for their experiments, it is rather difficult to compare their results with the complex PAC, which contains a large variety and high concentrations of phenolic substances. In contrast, the study by Jönsson et al. was carried out under much more comparable conditions, as they used ligninolytic enzymes from *T. versicolor* for detoxification of wood hydrolysates and also did not observe a complete removal of all phenolic substances [335]. Furthermore, they found the concentration of guaiacol to be decreased by 97 %, whereas 34 % of phenol was still left in the hydrolysate. This observation is consistent with the results obtained in the present work and is further supported by Kolb et al., who classified phenolic compounds into three different laccase reaction groups and identified guaiacol to be among the molecules that are eliminated relatively fast [336]. The occurrence of different reaction groups can be explained by the fact that the effectiveness of laccase appears to be dependent on the chemical structure of the phenolic substrates. For example, Jarosz-Wilkolazka et al. revealed that the enzymatic conversion of guaiacol by laccase originating from *Cerrena unicolor* appeared to be faster than for phenol due to its methoxy substituent in ortho-position [337].

Additionally, enzymatic removal of phenolic compounds might be inhibited by non-phenolic PAC components as it was already shown in literature that laccase activity can be impaired by carboxylic acids like acetic and propionic acid [338, 339]. However, Kreuter et al. stated that inhibition was only observed for the acid and not for its salt form. Since the enzymatic treatment of the PAC was performed at pH 6.5 it can be assumed that most of the carboxylic acids were in a dissociated state making an inhibition rather unlikely. Not only the enzyme, but also the FC assay can be negatively affected by acetate and other interfering substances [340, 341] which might explain why some differences in the FC and the GC results occurred. While according to the FC assay the total phenolics content was only marginally decreased in the negative control, a considerable decline was observed for the GC measurements, especially for guaiacol. Such discrepancy between the FC measurement and the analysis of individual phenols was already noted earlier by Kolb et al., however, no explanation was given [336].

According to the FC analysis, the phenolics could not be removed completely even when 25 U/mL of enzyme was used. Presumably, higher laccase concentrations could further improve the elimination of phenolic substances, but an enzymatic treatment of the PAC is comparatively expensive. Furthermore, considering the growth limits of *A. oryzae* for single PAC components (**Table 3**), it can be assumed that even a complete removal of phenolics would most likely not lead to a substantial improvement of the fungal PAC tolerance, as even the content of phenolics in untreated PAC is already close to the growth limit. In their work, the strongest inhibition of the fungal growth was caused by cyclic aldehydes and ketones like furfural and especially 2-cyclopenten-1-one. Therefore, a biological detoxification that aims at a valorization of the PAC using *A. oryzae* should primarily target these molecules. For instance, there have been several approaches for the biological removal of furfural and other furanic compounds from lignocellulose degradation products using fungi [190, 210, 342, 343], but also bacterial strains [194, 207, 344].

#### 4.3.1.2. Activated carbon

The application of activated carbon especially for the effective removal of phenolic substances from contaminated wastewater has been described extensively in literature [345–348] and could thus represent a more cost-effective alternative to laccase.

Indeed, the treatment of PAC with 10 % (w/v) activated carbon reduced the concentration of guaiacol by 96 % and even a complete removal of phenol was observed. However, this also indicates that the adsorption of phenolics on the carbon surface depends at least partly on their chemical structure. Mattson et al. suggested that phenolic substances adsorb on activated carbon

via the formation of a “donor–acceptor complex” between carbonyl oxygen groups on the carbon surface acting as electron donor, and the aromatic ring of the adsorbate acting as acceptor [349]. In contrast to phenol, guaiacol contains an additional methoxy group increasing the electron density in the aromatic ring. This might lead to a weaker binding of the guaiacol and give a potential explanation for its uncomplete removal. Moreover, the PAC does not only contain the two phenolic species measured, but rather a complex mixture of phenolic components (**Appendix 1**) that can impair each other in their adsorption behavior [350].

In contrast to detoxification with laccase, treatment with activated carbon is less specific and also removes other non-phenolic PAC components that were identified to be more harmful to the fungus [149]. For example, furfural content was decreased by 78 % after 1 h of treatment with 10 % carbon. Several other studies have evaluated the potential of activated carbon for removal of furfural as a well-known antimicrobial agent [351–354]. However, these studies were based on diluted furfural solutions, which makes it difficult to compare the results with those obtained for the PAC, since its components can influence each other in their adsorption behavior. For example, it is known that a competitive adsorption of furfural and phenolic compounds exists with the latter having a higher potential to bind to the carbon surface and even to displace the weakly bound furfural [355].

Therefore, the adsorption of inhibitory compounds on activated carbon has to be evaluated in authentic liquid lignocellulose degradation products. Lee et al. performed a treatment of wood hydrolysate with carbon loads of 1-10 % (w/v), which is a comparable range to the one tested in the this work. They analyzed the impact of the carbon content on the elimination of sugars, carboxylic acids and the furans HMF and furfural observing an improved removal with increasing carbon loads [356]. This is in accordance to the results obtained in the present study and can most likely be attributed to the increase in the carbon surface area and the higher number in adsorption sites. In contrast to our study, an almost complete removal of both furans was detected for concentrations  $\geq 2.5$  % activated carbon that might potentially be explained by the applied elevated temperature of 50 °C. However, previous findings on the effect of the temperature on furfural removal were contradictory. While in some studies an improvement in detoxification with increasing temperature was reported due to a higher molecular motion [357], others claimed that the adsorption of furfural is an exothermic process that is impaired by increasing temperatures [351, 354]. Another explanation for the discrepancy could be that hydrolysates often contain less inhibitory substances than pyrolytic condensates due to milder reaction conditions, and therefore fewer compounds may interfere with the adsorption of furans.

Liang et al. performed their activated carbon experiments with an acid-rich fraction of the fast pyrolysis of mixed softwood and provided a comprehensive insight into the adsorption of various inhibitors [221]. Especially the results obtained for the adsorption behavior of acetol are of great importance for PAC valorization with *Aspergillus oryzae*, since the ketone is the main component of the condensate, but has been reported to completely inhibit fungal growth already at concentrations of  $\geq 1.5\%$  [149]. In addition, acetol may be seen as a model compound for the adsorption of other ketones contained in the PAC. Liang et al. did not observe a complete removal of acetol, even though they used high activated carbon loads of up to 2 g/mL. This is in accordance with our work, where adsorption of ketones like acetol and 2-cyclopenten-1-one was the weakest with a removal of only 29.5 % and 48.3 %, respectively.

In their study, Liang et al. also evaluated the impact of the pH on the adsorption of the model compounds and found that the binding of carboxylic acids in particular was strongly dependent on the pH of the solution. While they observed significant removal of acetic acid and formic acid at low pH values, almost no decrease in concentration was detected at  $\text{pH} > 6$ . This is confirmed by the present results since the experiments were performed at pH 6.5 and the acetic acid concentration remained largely constant at  $34.44 \pm 1.40$  g/L. The pH dependence can most likely be explained by the functional groups that are attached to the surface of the carbon. These groups can be acidic, neutral, or alkaline and impart an amphoteric character to the carbon surface, making its properties dependent on the pH of the surrounding solution. When the pH of the PAC is higher than the  $\text{pK}_a$  of acetic acid ( $\text{pK}_a = 4.75$ ), the acid becomes dissociated and its adsorption is dependent on the charge of the carbon surface [358]. However, a rise in pH also results in an increasing number of negatively charged functional groups on the carbon surface and causes an electrostatic repulsion between the carboxylate and the surface groups [358, 359].

Despite the partial removal of all analyzed inhibitors, the fungal tolerance to the PAC was only slightly increased from 1.125 % to 1.625 % after 1 h of treatment with 10 % carbon. As it was shown in this work, prolonging the contact time between carbon and PAC did not result in an improved inhibitor removal. In contrast, chemical treatment of the activated carbon could be a potential strategy to improve detoxification, as it increases the number of functional groups on the carbon surface and its microporosity [360]. Additionally, the utilization of even higher carbon loads seems to be a possible way to improve detoxification, as our results show a clear correlation between the amount of activated carbon used and the removal of toxins. However, an increase in the carbon content also results in a higher viscosity of the suspension, making it increasingly difficult to ensure sufficient mixing. Moreover, it results in greater losses of PAC

and a larger amount of saturated carbon that needs to be disposed after the treatment. For this reason, various studies have already been published on the regeneration and repeated use of activated carbon in order to reduce the amount of waste produced (for example reviewed in [361]). However, re-use of carbon can only be considered as an alternative for discarding if the regeneration costs do not greatly exceed the disposal costs and if no additional waste streams such as solvents are generated during the process. Alternatively, the char fraction that is produced during the pyrolysis process could be used for activated carbon production. For the bioliq® process, the feasibility of this alternative char utilization was already assessed, but primarily with the objective of selling the activated carbon to cover the process costs [362]. In contrast, in the work of del Campo et al. the carbon obtained was used directly for the detoxification of the water-soluble fraction of the pyrolysis oil aiming at its fermentative valorization [363].

#### 4.3.1.3. Overliming

The overliming treatments performed in this work resulted in a partial removal of all inhibitors analyzed, but appeared to have varying efficacy depending on the PAC component. For example, even a treatment at pH 12 and 100 °C reduced the concentration of phenol by only about 38 %. Similarly, Millati et al. tested the effects of different pH values, temperatures and treatment durations on the overliming of a dilute-acid hydrolysate and found the phenol concentration to be only marginally effected by the conditions applied [364]. By contrast, they detected a strong decrease in furfural and HMF concentration and also a positive correlation between pH and the removal of furans. In our work, the concentration of furfural was also considerably reduced by 90 % compared to the original PAC when an initial pH of 10 was applied and was even further reduced to 4 % of the initial concentration when a starting pH of 12 was chosen. The drastic reduction in furfural concentration is not particularly surprising, since the presence of an aldehyde group and the heterocyclic structure of the furfural molecule enable a variety of chemical reactions [365]. Some of these reactions have already been shown to occur under strongly alkaline conditions, among them the resinification, in which furfural molecules polymerize to form a black insoluble residue [366]. The formation of dark precipitates was also observed during the overliming experiments performed in our study. However, resinification may not only occur between furfural molecules, but has also been observed between the aldehyde and phenol [367–369], which could provide a possible explanation for the 38 % decrease in phenol concentration. In addition to reacting with phenol, Hronec et al. found that furfural may undergo aldol condensation reactions with cyclic ketones

such as cyclopentanone, in which the components polymerize to form C15-C17 molecules and also oily insoluble intermediates were observed [370]. However, the reaction is also possible for the highly inhibitory unsaturated ketone 2-cyclopenten-1-one, for which a remarkable removal of up to 87 % was observed.

Some of the chemical reactions induced by the presence of hydroxide species can cause the formation of acids, which could potentially explain the pH drop observed during overliming (**Appendix 5**). One possible example could be the intermolecular Cannizzaro reaction, in which two furfural molecules react to form furfuryl alcohol and furoic acid [371]. A conversion of acetol to lactic acid and pyruvic acid has also been reported under alkaline conditions [372] and could therefore explain the reduction in the acetol concentration by up to 88 %. However, the decline in pH may also be due to the observed increase in acetic acid, which was the only PAC component measured whose concentration was not reduced by the overliming. Although the unsuitability of this detoxification procedure to remove acetic acid has repeatedly been described [222, 223, 364], only one study mentions an increase, but attributes it to the degradation of sugar molecules [283]. Since the pyrolysis condensate used in the current work does not contain any sugars, this explanation does not apply here. Alternatively, the treatment temperature of 100 °C might have resulted in an increased evaporation and a partial escape of the hot vapors. But since the increase in concentration at this temperature was even higher when the initial pH was raised from 10 to 12, a chemical reaction can be assumed as the main cause of this observation. For example, Machell et al. studied the effect of aqueous calcium and sodium hydroxide solutions on diacetyl, a compound present in untreated PAC at a concentration of 2.40 g/L (**Appendix 1**), and found acetate formation with no apparent dependence on the type of hydroxide [373].

The GC analysis in the present study also showed hardly any differences between the use of NaOH and Ca(OH)<sub>2</sub> for the overliming treatment at 100 °C, which is consistent with the growth results for *A. oryzae* at this temperature. Only for lower temperatures an enhanced growth was detected, when overliming was performed with Ca(OH)<sub>2</sub>. An improved detoxification with Ca(OH)<sub>2</sub> has already been reported several times in literature [216, 220, 374] with Zhao et al. suggesting, that calcium ions may react with certain inhibitory compounds to form insoluble precipitants such as the calcium half-salt PhO-Ca-OH [222].

Although the concentration of inhibitors was noticeably decreased by the overliming treatment, the fungus was still unable to grow at a PAC concentration above 12.5 %. This could possibly be explained by the fact that the 2-cyclopenten-1-one content was still significantly higher than the maximum concentration of 0.0625 g/L tolerated by the fungus (**Table 13**). Moreover, the

PAC also contains numerous other substances that were not analyzed and whose toxic effects on the fungus are still unknown. Due to the diversity of PAC constituents, the high energy input by heating and the high reactivity of the hydroxides, it can be assumed that many more reactions occur than those mentioned here. It is therefore also conceivable that these reactions may even produce additional toxic compounds that prevent further increases in fungal tolerance.

#### 4.3.1.4. Rotary evaporation

Among all the single methods tested, the rotary evaporation at 200 mbar was the most effective, as it reduced the concentration of all inhibitors to a level below or at least close to the growth limit of *A. oryzae*. For example, the concentration of the most toxic components furfural and 2-cyclopenten-1-one could be reduced by up to 95.4 % and 97.7 %, respectively, when the treatment was carried out at 200 mbar. The suitability of rotary evaporation as a method to remove furfural from lignocellulosic degradation products has already been demonstrated by Wilson et al. when they rotoevaporated an aspen wood hydrolysate at 55 °C to near dryness and demonstrated complete removal of furfural [375]. The same observation was made by Larsson et al. after they reduced the volume of a spruce hydrolysate by 90 % via rotary evaporation [216].

In addition to the furfural removal, both groups observed at least a partial decrease in the acetic acid content after their treatments. This is not consistent with the findings of the present evaporation experiments, where the concentration of acid remained largely constant. The differences in the results obtained can probably be attributed to the pH value. Since none of these studies mention an adjustment of the pH prior to evaporation, it can be assumed that it was carried out in the acidic range. Rodrigues et al. described the pH dependence of the evaporation of acetic acid and found that the acid can only be removed in its undissociated, but not in its dissociated form [230]. Since the experiments in the present study were conducted at pH 6.5 most of the acid was dissociated to acetate and thus remained unaffected.

In contrast, the treatment at 200 mbar caused a considerable decrease in acetol concentration by up to 84.5 %. This compound was also part of the studies by Lange et al. who performed evaporation of the volatiles present in PAC from the bioliq® plant by heat treatment at 80 °C in open jars. They observed a decline in the acetol content by up to 77.7 % compared to untreated PAC after 1.5 h of treatment [228]. The slightly improved removal that was obtained in the present work can be attributed to the reduction in pressure, which promotes evaporation. Even harsher conditions were applied in the work of Lian et al. since they performed their evaporation at the same temperature of 80 °C, but gradually decreased the pressure to values of

up to 20 Torr ( $\approx 27$  mbar). They stated to remove light volatile aldehydes and ketones like acetol, hydroxyacetaldehyde and furfural with this procedure, but unfortunately did not provide any analysis of their concentrations [110].

The GC results showed that at least under the harshest evaporation conditions, the content of toxic components was below or close to the growth limit of *A. oryzae*. Accordingly, growth on pure PAC should have been possible, but the fungal tolerance did not exceed 30 %. This again suggests that the PAC contains other substances that are toxic to fungal growth, or that the inhibitory components reinforce each other's toxic effects. Since rotary evaporation was the most effective single method, but is quite time and energy consuming, it might be an alternative to use the existing knowledge about the evaporation behavior of the individual PAC components for a selective separation of the vapors already during the pyrolysis process. Such fractional condensations have already been described in the literature [376, 377] and could possibly provide fractions that can be utilized by the fungus without extensive treatment.

#### **4.3.2. Combination of detoxification methods and *A. oryzae* cultivation**

The present study showed that a combination of treatments further increased fungal tolerance and allowed growth on pure PAC. Various approaches to combine detoxification methods have been described in literature. For example, Hodge et al. used a combination of activated carbon and a subsequent overliming treatment with  $\text{Ca}(\text{OH})_2$  for the detoxification of softwood hydrolysates. They found that the effective removal of phenolic compounds, which they obtained by treatment with 2.5-5 % activated carbon, was not considerably enhanced by additional overliming [231]. This is consistent with our findings, as the reduction in the concentration of guaiacol achieved by the AC treatment could not be improved by the subsequent overliming treatment, but remained constant at 0.14 g/L. In contrast, the combination of AC+OL performed by Hodge et al. resulted in complete removal of the furan HMF in almost all hydrolysates studied. We could confirm this observation as we also noted a decrease in the concentration of furfural (the furan model compound used in our work) from 0.4 g/L after single AC treatment to 0.05 g/L when combined with OL.

Xu et al. performed combined AC and OL treatments in both possible orders and examined their influence on the concentrations of lignin, furfural and xylose sugars in the pre-hydrolysis liquor from pulping process [378]. They determined activated carbon treatment following initial overliming to be the more effective order, which is in accordance with our results. Even though PAC contained neither residual lignin nor sugar molecules, it was tolerated to levels up to 40 %

after OL+AC treatment, whereas the reverse order only resulted in a fungal tolerance of 10 %. Based on the GC data, this observation can be mainly attributed to an enhanced removal of ketones. It was found that the concentrations of acetol and 2-cyclopenten-1-one were reduced by only 57.9 % and 82.2 %, respectively, after detoxification with AC+OL, whereas treatment with OL+AC resulted in 82.8 % and 91.2 % removal. This is confirmed by the study of Zhang et al. in which they give a comprehensive insight into the composition of a poplar prehydrolysate before and after detoxification with overliming and activated carbon via GC/MS analysis and observed that the sequential treatment resulted in an elimination of ketones [218]. A possible explanation for the improved detoxification with OL+AC was given by Randtke et al. as they reported the capacity of activated carbon to be improved by calcium, magnesium and sodium [379]. Since a large amount of NaOH is needed for overliming, this could have had a positive effect on the subsequent activated carbon treatment. However, also for the combination of activated carbon and rotary evaporation, it was advantageous to perform the carbon treatment at the end of the detoxification procedure. This was most likely due to the complete removal of 2-cyclopenten-1-one, that could be achieved after RE+AC treatment whereas the concentration of this toxic compound was still 0.24 g/L when the detoxification was conducted in the reverse order. Lian et al. also performed rotary evaporation combined with a subsequent activated carbon treatment to detoxify an aqueous phase formed during the pyrolysis of pelletized wood [110]. With their treatment, growth of *C. curvatus* on pure condensate was enabled. In the present work, this could only be achieved by combining rotary evaporation, overliming and activated carbon treatment yielding a PAC that contained 2.96 g/L acetol and 0.14 g/L guaiacol as the only measurable inhibitors. However, the concentrations of both components were below the growth limits determined by Dörsam et al. [149] and it can therefore be assumed that these compounds did no longer cause any inhibition

It even seems conceivable that some of the substances remaining in the PAC may serve as additional C-sources for fungal growth. This assumption results from the comparison of acetate consumption and CDW formation observed in the present study with the data of Kövilein et al. [104]. They performed a cultivation of *A. oryzae* on different acetate concentrations ranging from 5-70 g/L and determined a CDW of 1.14 g/L after 48 h in medium containing 40 g/L acetate, which is comparable to the content in PAC. In our work, a CDW of 3.0 g/L was formed in the same cultivation time, with the fungus consuming only 2.2 g/L acetate. The resulting high yield of 1.36 g/g indicates the utilization of alternative C-sources. Further studies are therefore needed to investigate whether the fungus is able to metabolize other PAC components such as acetol.

## 5. Malic acid production from the pyrolytic aqueous condensate and its main components

This chapter is mainly based on the publication:

**Valorization of a pyrolytic aqueous condensate and its main components for L-malic acid production with *Aspergillus oryzae* DSM 1863**

Christin Kubisch and Katrin Ochsenreither

Institute of Process Engineering in Life Science 2: Technical Biology, Karlsruhe Institute of Technology, Karlsruhe, Germany

### **Publication details:**

*Fermentations*

Volume 8, Article 107

Publication date: 28 February 2022

DOI: 10.3390/fermentation8030107

**Author's contribution:**

**Christin Kubisch** designed and performed the experiments, analyzed the data and drafted the manuscript.

**Katrin Ochsenreither** contributed in the conceptualization of the study, supervised the laboratory work and revised the manuscript.

## 5.1. Introduction

Having shown that establishing a suitable detoxification procedure allows the utilization of 100 % PAC as substrate for the growth of *Aspergillus oryzae*, the following chapter aimed to investigate whether the pretreated condensate can also serve as C-source for fungal malic acid production in main cultures.

The high acetate-based biomass yield obtained in the pre-culture with 100 % PAC as well as the results of the transcriptome analysis indicate that the fungus might be able to utilize other PAC carbons in addition to acetate. The hydroxyketone acetol seems to be the most likely candidate for such a co-metabolization, as it has already been reported to be a suitable carbon source for growth of several yeasts. Since acetol is the main organic component of the pyrolysis condensate ( $\approx 5$  wt.%), the fungal ability to metabolize this ketone would significantly increase the amount of usable substrates contained in the PAC. Therefore, it was assessed whether *A. oryzae* is capable of utilizing acetol as a substrate for fungal growth and acid production both as a sole C-source and in simple PAC model mixtures with acetate.

## 5.2. Results

### 5.2.1. Utilization of acetol as substrate for biomass formation of *A. oryzae*

In this experiment the ability of *A. oryzae* to metabolize acetol concentrations in the range of 3-50 g/L as carbon source for biomass formation was evaluated (**Figure 29**). No growth or substrate consumption were observed in the cultures containing 50 g/L acetol, so the corresponding data is not included. However, even at lower concentrations, the ketone already appears to exert an inhibiting effect on the fungus.

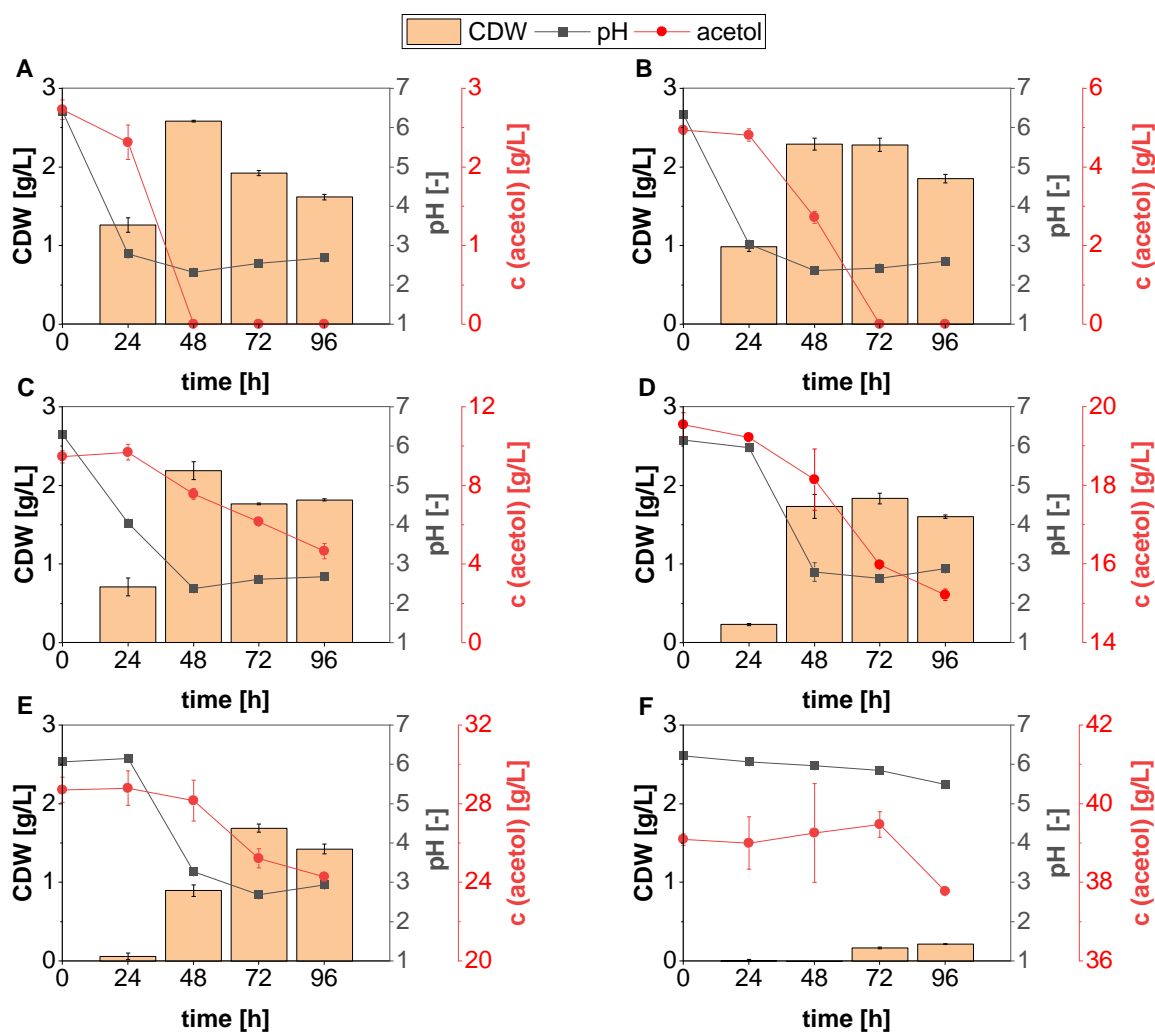


**Figure 29:** Substrate consumption and biomass formation of *A. oryzae* in shake flask pre-cultures containing acetol concentrations of 3 g/L (A); 5 g/L (B); 10 g/L (C); 20 g/L (D); 30 g/L (E) and 40 g/L (F) as carbon source. The data represent mean values of three replicates and error bars indicate the standard deviation.

While in the flasks containing 3 g/L and 5 g/L of acetol complete consumption of the substrate was observed, with 10-40 g/L acetol only 50.7 %, 22.1 %, 15.4 % and 3.4 % of the ketone were metabolized within 96 h of cultivation. The initial lag phase also lengthened with increasing acetol content. In the flasks with the lowest substrate concentration, metabolization of the ketone was already observed after 24 h and thus no lag phase could be detected. In contrast, it took at least 48 h for substrate consumption to start in the cultures containing 5-20 g/L acetol. At an initial concentration of 30 g/L acetol, the onset of metabolization was delayed by another 24 h. The longest lag phase was observed in the flasks containing 40 g/L acetol, as a decrease in substrate concentration was not detected until the last day of cultivation. The delayed and reduced metabolization of the substrate also affected the biomass formation. While the highest CDW of  $2.59 \pm 0.01$  g/L was reached in flasks containing 3 g/L acetol, the maximum biomass concentration was gradually reduced to  $2.29 \pm 0.08$  g/L,  $2.19 \pm 0.11$  g/L,  $1.83 \pm 0.07$  g/L,  $1.69 \pm 0.05$  g/L and  $0.22 \pm 0.01$  g/L with increasing acetol concentration. Moreover, the time point of reaching the maximum CDW and the subsequent transition to the death phase was increasingly postponed. For substrate concentrations  $\leq 10$  g/L the highest CDW was detected after 48 h of cultivation and a decrease in biomass was observed in the following samples. By contrast, for 20-30 g/L acetol a transition to the death phase occurred only after 72 h, and for the flasks containing 40 g/L acetol a decrease in the CDW has not been detected until the end of the cultivation. In the cultures with 3 and 5 g/L acetol, the transition to the death phase coincided with the complete consumption of the C-source. However, even for the flasks with 10-30 g/L, a decrease in CDW was observed at the end of cultivation, although acetol was still present. This suggests that at least one other nutrient in the medium was depleted. It is also noticeable that in the first 24 h of cultivation biomass formation as well as a drop in pH was already detected, even in the flasks in which no acetol had been consumed at that time. This might indicate that *A. oryzae* uses additional substrates for its initial growth. The most likely candidates for alternative C-sources are the glycerol contained in the spore solution and substances that probably result from Maillard reactions occurring during autoclaving. The latter could also explain why the initial acetol concentration in the cultures was always lower than expected. Nevertheless, it was successfully demonstrated that the main component of the PAC is a suitable substrate for fungal growth, whereas malate production could not be achieved in any of the cultures containing acetol as sole C-source (data not shown).

### 5.2.2. Acetate-acetol mixtures as substrates for fungal growth

Since it is already known that acetate concentrations as high as the 40 g/L contained in the PAC can be utilized by *A. oryzae*, artificial PAC model mixtures containing 40 g/L acetate and different concentrations of 0-40 g/L acetol were tested for their suitability as substrates for fungal growth (**Figure 30**). However, since no biomass formation was observed for the flasks containing 30 and 40 g/L of the ketone, data for these cultures are not included.

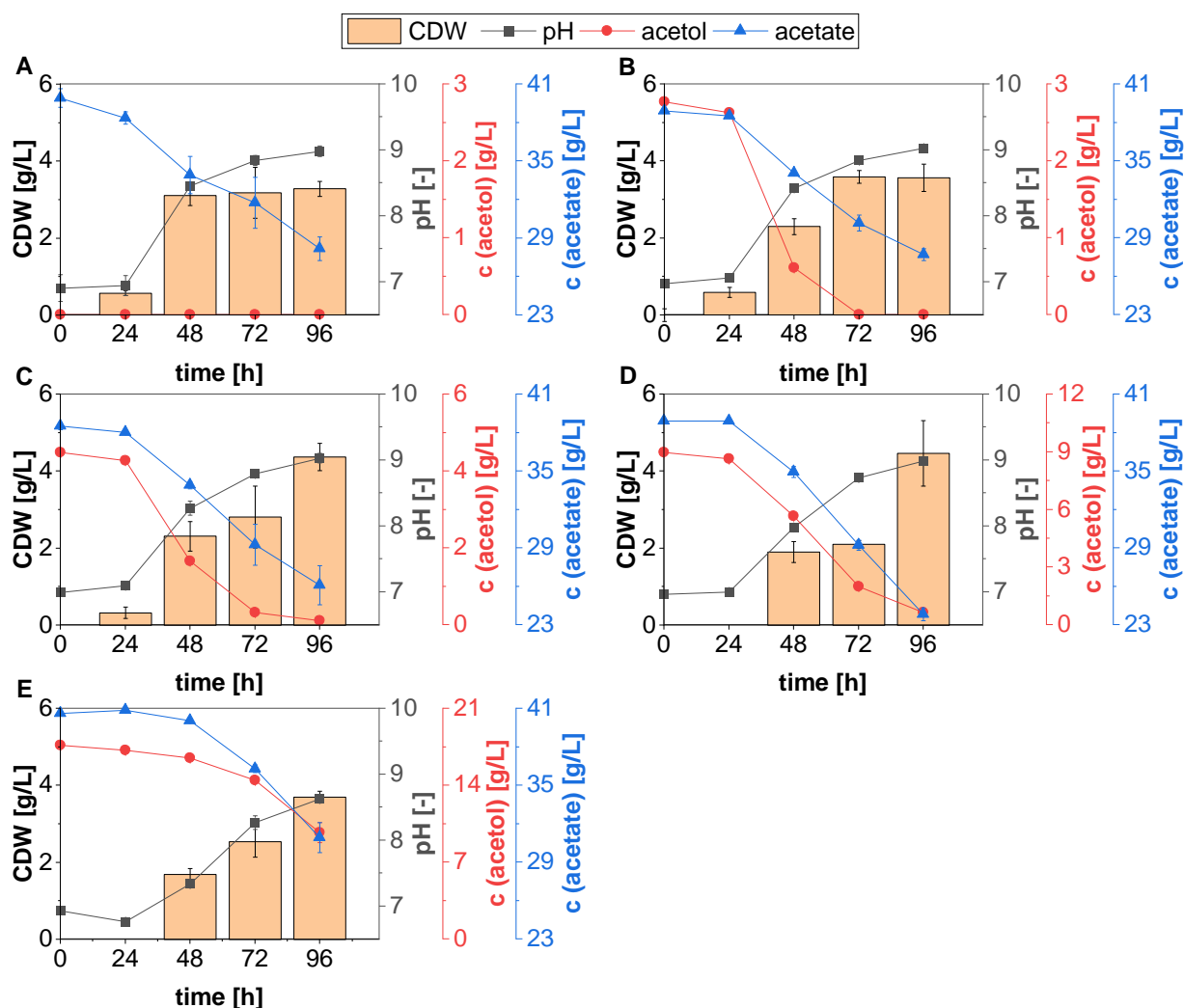


**Figure 30:** Substrate consumption and biomass formation of *A. oryzae* in shake flask pre-cultures containing 40 g/L of acetate as sole carbon source (A) as well as mixtures of acetate and acetol concentrations of 3 g/L (B); 5 g/L (C); 10 g/L (D); 20 g/L (E). The data represent mean values of three replicates and error bars indicate the standard deviation.

As displayed in **Figure 30**, the acetate control did not show any lag phase, since metabolization of the initially contained  $39.91 \pm 0.73$  g/L acetate started immediately and a CDW of  $0.56 \pm 0.06$  g/L was already detected after 24 h. The largest decrease in the acetate concentration was observed between 24-48 h and was measured to be 4.43 g/L. The high

substrate consumption at this stage of cultivation resulted in almost a six-fold increase in fungal biomass to  $3.13 \pm 0.25$  g/L. Subsequently, the biomass formation curve flattened as only a negligible increase to  $3.29 \pm 0.21$  g/L was observed after 96 h leading to the conclusion that the fungus entered the stationary growth phase after only 48 h in these cultures.

In contrast, biomass formation in the flasks containing acetol was slowed down with increasing ketone concentration. While the cultures containing 3 and 5 g/L acetol still behaved comparably to the control and biomass formation started after 24 h, it was delayed by another 24 h in the flasks with 10 and 20 g/L acetol. As already observed in the first experiment, the delayed onset of biomass formation also shifted the time point at which the maximum CDW was reached. In the 3 g/L acetol cultures, the highest biomass concentration of  $3.58 \pm 0.17$  g/L was obtained after 72 h, and the fungus entered the stationary growth phase 24 h later than in the acetate control. In contrast, for acetol concentrations  $\geq 5$  g/L, an increase in biomass was detected until the end of cultivation. Accordingly, no stationary phase was observed and it cannot be assessed whether the maximum CDW has already been reached. Despite the increasing lag phase in the acetol containing cultures, no reduction in the final CDW was observed compared to the control (**Table 15**).

**Table 15:** Substrate consumption and growth parameters after 96 h cultivation of *A. oryzae* in media containing 40 g/L of acetate and different concentrations of acetol (0-20 g/L)

c acetol [g/L]	consumed acetate [g/L]	consumed acetol [g/L]	consumed substrate [g/L]	final CDW [g/L]	final yield $Y_{x/s}^1$ [g/g]
0	$11.74 \pm 1.18$	$0.00 \pm 0.00$	$11.74 \pm 1.18$	$3.29 \pm 0.21$	$0.28 \pm 0.03$
3	$11.21 \pm 0.49$	$2.77 \pm 0.00$	$13.97 \pm 0.49$	$3.57 \pm 0.35$	$0.26 \pm 0.03$
5	$12.42 \pm 1.57$	$4.38 \pm 0.01$	$16.80 \pm 1.57$	$4.37 \pm 0.36$	$0.26 \pm 0.03$
10	$15.09 \pm 0.51$	$8.35 \pm 0.13$	$23.44 \pm 0.53$	$4.46 \pm 0.64$	$0.19 \pm 0.03$
20	$9.71 \pm 1.17$	$7.96 \pm 0.92$	$17.66 \pm 1.49$	$3.47 \pm 0.40$	$0.21 \pm 0.02$

<sup>1</sup> The biomass yield  $Y_{x/s}$  was calculated as g (biomass) / g (substrate)

Rather, acetol contents of up to 10 g/L even seemed to have a slightly positive effect on fungal growth, as biomass concentration appeared to increase with increasing amount of ketone resulting in the highest CDW of  $4.46 \pm 0.64$  g/L obtained in the 10 g/L acetol cultures. However, due to the large standard deviation, this cannot be assumed to be significant. Only when the acetol content was raised to 20 g/L, the biomass formation decreased considerably to a maximum CDW of  $3.47 \pm 0.40$  g/L, which was still comparable to the acetate control. The

increase in biomass concentration in the cultures with 3-10 g/L acetol can be attributed to the metabolization of the ketone as an additional C-source, since acetate consumption in the flasks behaved largely similar. In the flasks with 3 g/L, a complete conversion of acetol was observed after 72 h, and also the cultures with 5 g/L and 10 g/L contained only  $0.10 \pm 0.00$  g/L and  $0.63 \pm 0.13$  g/L of the ketone at the end of cultivation. Accordingly, the overall concentration of carbon metabolized by the fungus increased (**Figure 30**). In contrast, in the flasks with an acetol content of 20 g/L, only 37.5 % of the acetol was metabolized. The consumption of acetate was also lowest and slowest in these flasks, as  $30.92 \pm 1.16$  g/L of the substrate remained unused.

Despite the reduced substrate utilization in the cultures with the highest ketone concentration, it was nevertheless demonstrated that combinations of 40 g/L acetate and up to 20 g/L acetol were suitable C-sources for *A. oryzae* and resulted in biomass titers comparable to those in the control. However, **Table 15** shows that increasing acetol concentrations reduced the biomass yield from  $0.28 \pm 0.03$  g/g for the control to  $0.19 \pm 0.03$  g/g and  $0.21 \pm 0.02$  g/g for the flasks containing 10 and 20 g/L acetol. This indicates an increasing inhibitory effect of the ketone, as it was already observed in the first experiment. The inhibition appeared to be even enhanced in the presence of acetate, since no fungal growth could be observed for concentrations >20 g/L acetol, whereas up to 40 g/L were tolerated when the ketone was the sole C-source.

### 5.2.3. L-malic acid production with acetate-acetol mixtures

Having demonstrated that model mixtures of 40 g/L acetate and acetol in concentrations up to 20 g/L are suitable for fungal growth, it was investigated how these mixtures affect the L-malic acid production of *A. oryzae*. **Figure 31** shows that for acetol concentrations  $\leq 10$  g/L, no considerable differences were observed in both acetate consumption and malate production compared with the acetate control.

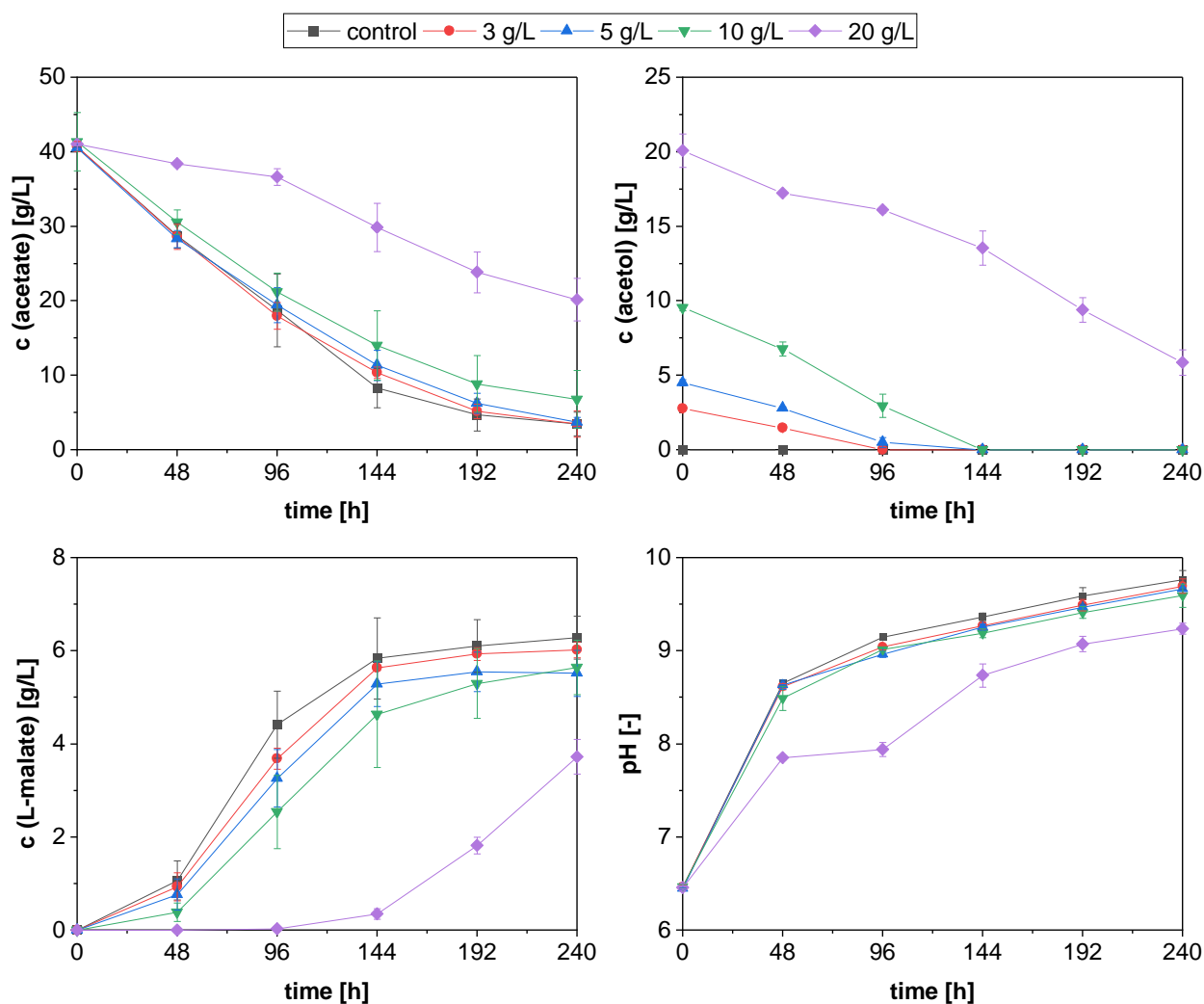


**Figure 31:** Malic acid production, substrate consumption, and pH values in *A. oryzae* shake flask main cultures containing mixtures of 40 g/L acetate and different concentrations of acetol (0-20 g/L). The data represent mean values of four replicates and error bars indicate the standard deviation.

In these flasks, a strong reduction in acetate concentration was already detected after the first 48 h. The decrease in concentration continued throughout the cultivation and at the end, the final concentration of acetate was about 3.48-3.68 g/L in the flasks containing 0-5 g/L acetol and  $6.78 \pm 3.91$  g/L in the 10 g/L cultures. The comparatively high final concentration in the latter might indicate an incipient inhibition of the fungal acetate utilization induced by the

ketone, but due to the high standard deviation it cannot be considered significant. At an acetol concentration of 20 g/L, however, the inhibitory effect became clearly evident. In these flasks the acetate consumption was considerably reduced resulting in a final concentration of  $20.17 \pm 2.84$  g/L. In addition to acetate, all acetol containing cultures simultaneously metabolized the ketone. In the flasks with an acetol content of 3 g/L, a complete conversion was detected after only 96 h, whereas in the cultures containing 5 and 10 g/L, it took 144 h for the acetol to be depleted. Similar to acetate, reduced consumption of the ketone was observed in the flasks containing 20 g/L acetol, with a concentration of  $5.86 \pm 0.85$  g/L remaining unused at the end of the cultivation. The metabolization of the substrates, especially acetate, also had an impact on the culture pH (**Figure 31**). Although the first increase in pH after 48 h can be largely attributed to the outgassing of CO<sub>2</sub> from the carbonate buffer, the flasks with acetol concentrations of 0-10 g/L already showed a higher pH at this time than the cultures with 20 g/L due to acetate consumption. However, as cultivation progressed, the pH curve flattened considerably for the flasks containing low acetol contents  $\leq 10$  g/L since malic acid production in these cultures started after 48 h and counteracted the pH increase. Nevertheless, both pH and malate concentration in these flasks continued to rise until the end of cultivation, with the greatest increase in product titer being observed between 48 and 144 h.

Consequently, these cultures reached their maximum yield and productivity at this stage of fermentation (**Table 16**). In the cultures containing 20 g/L acetol, only a slight change in pH was observed after the initial CO<sub>2</sub>-induced sharp increase, because little acetate was metabolized and no malate was formed during the first 96 h of cultivation. However, after 144 h a clear pH increase and the onset of malic acid production were detected, showing that product formation was clearly delayed compared to the flasks with 0-10 g/L acetol. This was followed by an exponential increase in malate concentration until the end of cultivation reaching a final titer of  $3.72 \pm 0.37$  g/L malate. In comparison to the product concentrations achieved in the other cultures, the titer was considerably reduced, and also the lowest values for yield and productivity were obtained (**Table 16**). In general, the values for these parameters tended to decrease with increasing acetol concentrations and it can therefore be assumed that the presence of the ketone does not have any beneficial effect on the fungal malate production.

**Table 16:** Substrate consumption and L-malate production in *A. oryzae* main cultures containing 40 g/L acetate and different concentrations of acetol (0-20 g/L) as sole carbon sources

<b>c acetol</b> <b>[g/L]</b>	<b>consumed</b> <b>acetate [g/L]</b>	<b>consumed</b> <b>acetol [g/L]</b>	<b>consumed</b> <b>carbon [g/L]</b>	<b>final malate</b> <b>titer [g/L]</b>	<b>maximum yield</b> <b><math>Y_{P/S, \text{carbon}}^1</math> [g/g]</b>	<b>max. productivity</b> <b><math>P_{\text{max}}^1</math> [g/(L·h)]</b>	<b>P overall<sup>2</sup></b> <b>[g/(L·h)]</b>
0	37.16 ± 1.58	0.00 ± 0.00	15.12 ± 0.64	6.29 ± 0.46	0.18 ± 0.05 (96 h)	0.046 ± 0.008 (96 h)	0.026 ± 0.002
3	37.23 ± 1.89	2.73 ± 0.12	16.47 ± 0.77	6.02 ± 0.17	0.15 ± 0.00 (144 h)	0.039 ± 0.000 (144 h)	0.025 ± 0.001
5	36.81 ± 0.68	4.51 ± 0.20	17.17 ± 0.29	5.71 ± 0.38	0.14 ± 0.01 (144 h)	0.037 ± 0.003 (144 h)	0.024 ± 0.002
10	34.57 ± 5.53	9.54 ± 0.21	18.71 ± 2.25	5.64 ± 0.59	0.11 ± 0.02 (240 h)	0.032 ± 0.008 (144 h)	0.024 ± 0.002
20	20.86 ± 2.85	14.23 ± 1.41	15.41 ± 1.35	3.72 ± 0.37	0.09 ± 0.01 (240 h)	0.016 ± 0.002 (240 h)	0.016 ± 0.002

<sup>1</sup>The time at which the maximum value was reached is indicated in brackets

<sup>2</sup>Overall productivity P was calculated as final malate titer divided by the cultivation time of 240 h.

#### 5.2.4. PAC as sole substrate for L-malic acid formation

As shown in the previous experiment, the acetol contained in the PAC does not favor malic acid production with *A. oryzae* and should therefore be removed. After the optimized detoxification procedure, the acetol content in the PAC was  $< 3$  g/L. Hence, the focus in the following experiments was on acetate as the main substrate for malate production. In a first shake flask cultivation, it was assessed whether *A. oryzae* is in principle able to use the acetate contained in 100 % PAC for acid formation. Subsequently, pH optimization was performed by lowering the initial medium pH and the optimized process was finally transferred to 500 mL bioreactors.

##### 5.2.4.1. General suitability of PAC for fungal acid formation

In the first shake flask main culture experiment with 100 % detoxified PAC the fungus immediately started to convert the initially contained  $40.15 \pm 1.87$  g/L of acetate to malic acid without any apparent lag phase (**Figure 32**).

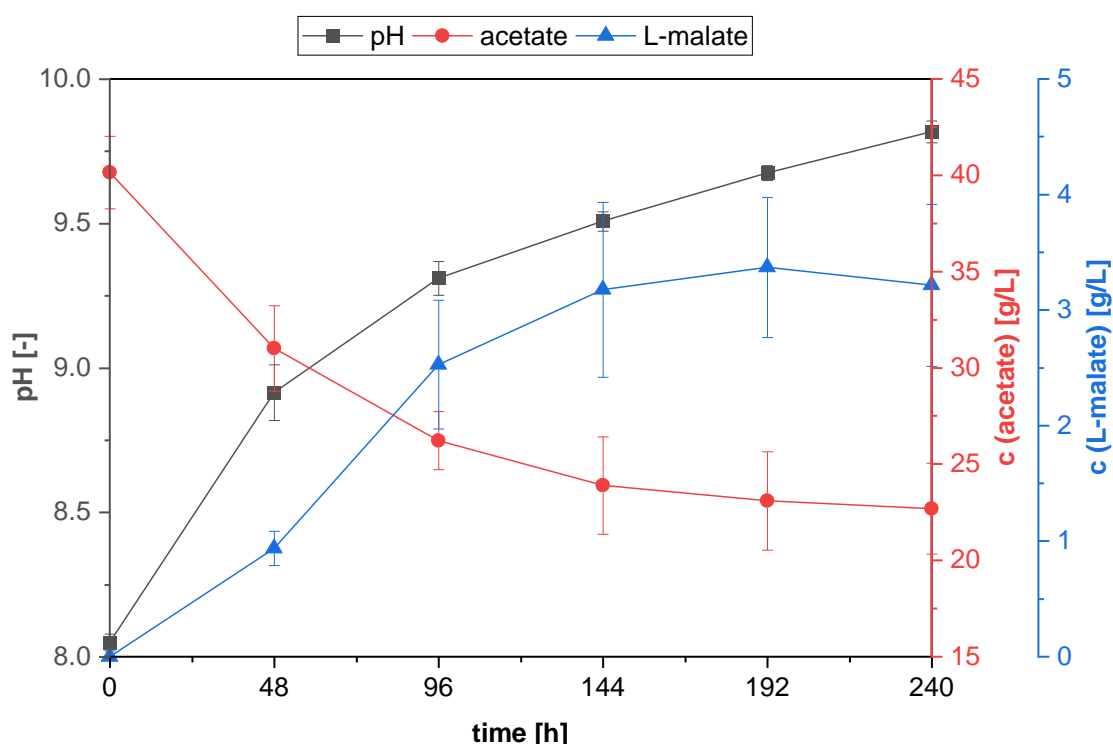


**Figure 32:** Malic acid production of *A. oryzae* in shake flask main cultures containing 100 % PAC detoxified by rotary evaporation, overliming and a subsequent activated carbon treatment. The data represent mean values of four replicates and error bars indicate the standard deviation

The substrate concentration continued to decrease as the cultivation progressed and resulted in the formation of a maximum malate titer of  $3.37 \pm 0.61$  g/L and a maximum yield of  $0.20 \pm 0.05$  g/g after 192 h (**Table 17**). However, in the last 2 days of fermentation, both the acetate consumption and the malic acid production curves flattened, leading to a final malate concentration of  $3.22 \pm 0.70$  g/L and  $22.70 \pm 2.36$  g/L of substrate remaining unused. The decrease in metabolic activity can most likely be attributed due to the sharp pH increase from an initial value of  $8.05 \pm 0.03$  to  $9.82 \pm 0.04$  at the end of cultivation and raised the question of whether a lower initial pH could improve malic acid production.

**Table 17:** Summary of substrate consumption and malic acid production in *A. oryzae* cultivations with PAC

<b>cultivation</b>	<b>condition</b>	<b>consumed acetate [g/L]</b>	<b>maximum malate titer<sup>1</sup> [g/L]</b>	<b>maximum yield Yp/s<sup>1</sup> [g/g]</b>	<b>maximum yield Yp/s, carbon<sup>1</sup> [g/g]</b>	<b>maximum productivity Pmax<sup>1</sup> [g/(L·h)]</b>	<b>overall productivity P<sup>2</sup> [g/(L·h)]</b>
first shake flask cultivation	pH not adjusted	17.45 ± 3.01	3.37 ± 0.61 (192 h)	0.20 ± 0.05 (192 h)	0.18 ± 0.05 (192 h)	0.026 ± 0.006 (96 h)	0.013 ± 0.003
pH optimization	pH not adjusted	22.07 ± 4.69	3.96 ± 1.46 (240 h)	0.18 ± 0.08 (240 h)	0.16 ± 0.07 (240 h)	0.026 ± 0.007 (96 h)	0.016 ± 0.006
in shake flasks	pH adjusted with H <sub>2</sub> SO <sub>4</sub>	38.19 ± 0.75	8.29 ± 0.26 (240 h)	0.22 ± 0.01 (192 h)	0.19 ± 0.01 (192 h)	0.054 ± 0.001 (144 h)	0.035 ± 0.001
	pH adjusted with CH <sub>3</sub> COOH	42.82 ± 2.36	9.77 ± 0.55 (240 h)	0.23 ± 0.03 (144 h)	0.21 ± 0.02 (144 h)	0.061 ± 0.002 (144 h)	0.041 ± 0.002
bioreactor cultivations	acetate control	29.71 ± 2.30	2.73 ± 0.47 (144 h)	0.09 ± 0.02 (144 h)	0.08 ± 0.02 (144 h)	0.032 ± 0.008 (72 h)	0.019 ± 0.003
	PAC	40.82 ± 0.37	7.30 ± 0.29 (144 h)	0.18 ± 0.01 (144 h)	0.16 ± 0.01 (144 h)	0.054 ± 0.010 (120 h)	0.051 ± 0.002

<sup>1</sup>The time at which the maximum value was reached is indicated in brackets.

<sup>2</sup>The overall productivity was calculated as final malate titer divided by the cultivation time and differed for the shake flask experiments (240 h) and the reactor cultivations (144 h).

#### 5.2.4.2. Influence of the initial medium pH on L-malic acid production from PAC

To evaluate the role of the initial pH of the PAC on malate production with *A. oryzae*, two different acids (100 % acetic acid and 96 % sulfuric acid) were used to lower the pH-value of the medium to 5.5 prior to sterile filtration. Due to the presence of CaCO<sub>3</sub> in the flasks, the initial pH increased to about 6.5 in the pH adjusted cultures while, as in the previous experiment, a slightly alkaline pH of 8.20 ± 0.03 was measured for the flasks containing non-adjusted PAC (**Figure 33**). Despite the different initial values, all cultures had a similar pH of 9.7-9.8 at the end of cultivation, mainly due to the strong pH increase, that was observed in the adjusted flasks during the first 48 h. Since there was no visible difference in acetate consumption or malic acid production at that time compared to the non-adjusted control, this first increase is most likely due to an outgassing of CO<sub>2</sub> from the carbonate buffer. However, the stronger pH increase was maintained during the further course of cultivation, which can be attributed to improved substrate utilization.

While in the control flasks acetate consumption flattened sharply after 48 h of cultivation, leaving 16.40 ± 4.69 g/L of the substrate unused, the utilization was considerably improved by the pH adjustment. Apart from the difference in initial concentrations, the substrate was metabolized equally in both pH-adjusted cultures, resulting in a parallel progression of the two curves over 144 h of cultivation. In the last four days of fermentation, however, the substrate consumption began to flatten increasingly, especially in the H<sub>2</sub>SO<sub>4</sub> adjusted cultures, leading to comparably low final concentrations.

The improved metabolization of the substrate in the pH-optimized cultures also had a positive effect on the malic acid production. Although small amounts of the acid were already detected in all cultures after only 48 h, the curve of the control was again noticeably flatter in the further course of cultivation and a final malate titer of only 3.96 ± 1.46 g/L was obtained. In contrast, a steep increase in malic acid concentration was observed in the pH adjusted cultures, resulting in considerably higher malate concentrations than in the controls after only 96 h. At this time, very similar titers of 5.56 ± 0.88 g/L and 5.11 ± 0.40 g/L were measured in the flasks adjusted with H<sub>2</sub>SO<sub>4</sub> and acetic acid, respectively. However, as already observed for acetate consumption, malate production gradually leveled off, especially in the flasks adjusted with H<sub>2</sub>SO<sub>4</sub>, resulting in an increasing difference in malate titer between the two cultures. Despite the gradual flattening of the curves, the maximum malate concentrations were reached at the end of cultivation and were found to be 8.30 ± 0.26 g/L and 9.77 ± 0.55 g/L, corresponding to increases of 2.1- and 2.5-fold, respectively, compared with the unadjusted control.

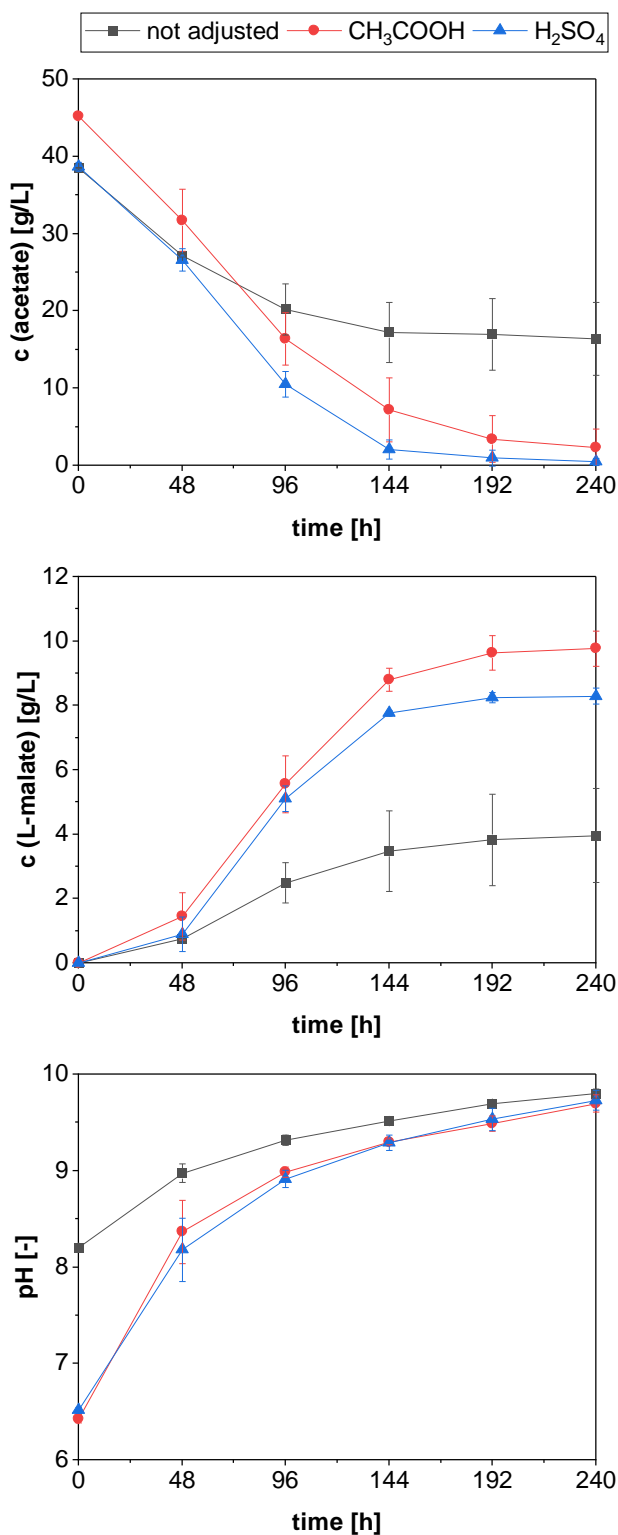


**Figure 33:** Optimization of the initial medium pH in *A. oryzae* shake flasks main cultures containing 100 % detoxified PAC (original pH = 6.5). The pH of the PAC was either not adjusted or set to 5.5 prior to sterile filtration using 96 % sulfuric acid (H<sub>2</sub>SO<sub>4</sub>) or 100 % acetic acid (CH<sub>3</sub>COOH). The data represent mean values of quadruplicates and error bars indicate the standard deviation.

As indicated in **Table 17**, the yield and productivity values calculated for the control are comparable to those of the first shake flask cultivation, thus the process appears reproducible despite the complexity of the substrate. Although a significantly higher malate titer was measured in the flasks, whose pH was lowered with acetate, comparable yields were obtained in both pH-adjusted cultures. Therefore, H<sub>2</sub>SO<sub>4</sub> was chosen for pH adjustment in the subsequent reactor culture, since the main objective of this work was to use PAC as the sole substrate for fungal malate production.

#### 5.2.4.3. Malic acid production in bioreactor cultivations

In the following experiment, it was investigated whether the process of fungal malic acid production on PAC can be transferred from shake flasks to 500 mL bioreactor scale. For comparison, a control fermentation was performed with a defined medium containing 40 g/L acetate (**Figure 34**).

Although the pH of the media in this experiment was also adjusted to 5.5 with H<sub>2</sub>SO<sub>4</sub> prior to sterilization, the initial pH values in the reactors of about 6.7 were slightly higher than in the previous shake flask experiments. The main reason for this observation, as well as for the rapid pH increase within the first 3-4 h of cultivation, is the enhanced outgassing of CO<sub>2</sub> due to aeration and stirring. The pH subsequently stabilized to values of 7.7-7.9 until there was a further increase in the pH of the controls after a fermentation time of about 12 h, indicating the onset of acetate metabolization. Since this occurred before the first sampling, no lag phase in substrate consumption could be observed in these reactors. According to the pH values, acetate utilization started later in the reactors with PAC and the time point also differed greatly within the duplicate. While the increase in pH in the first reactor coincided with the 24 h sampling, it did not start in the second reactor until 13 h later. Moreover, the increase was lower than in the controls. After 72 h of cultivation, a pH of 9.0-9.1 was measured in the PAC-containing reactors, whereas it had already reached values of 9.7-9.8 in the acetate controls by this time. Since the previous experiment showed that pH plays an important role in malate production, it was decided to manually adjust the pH to values < 7.5 with 72 % H<sub>2</sub>SO<sub>4</sub> after each sampling to prevent a further increase. However, by the time the next sample was taken, the pH had already returned to nearly the original value in all reactors, primarily due to outgassing of CO<sub>2</sub>.

Consistent with the pH curve, substrate utilization at the beginning of the cultivation was slower in the reactors with PAC than in the controls. While in the latter 52.1 % of the initial acetate concentration had already been metabolized after 48 h, only 23.7 % were consumed in the PAC reactors. However, in the controls, substrate conversion decreased considerably as cultivation

progressed, leaving a final concentration of  $11.62 \pm 2.29$  g/L acetate unused. In contrast, a sharp decrease in substrate concentration was observed in the reactors with PAC after the initial lag phase, leading to almost a complete conversion of acetate by the end of the cultivation.

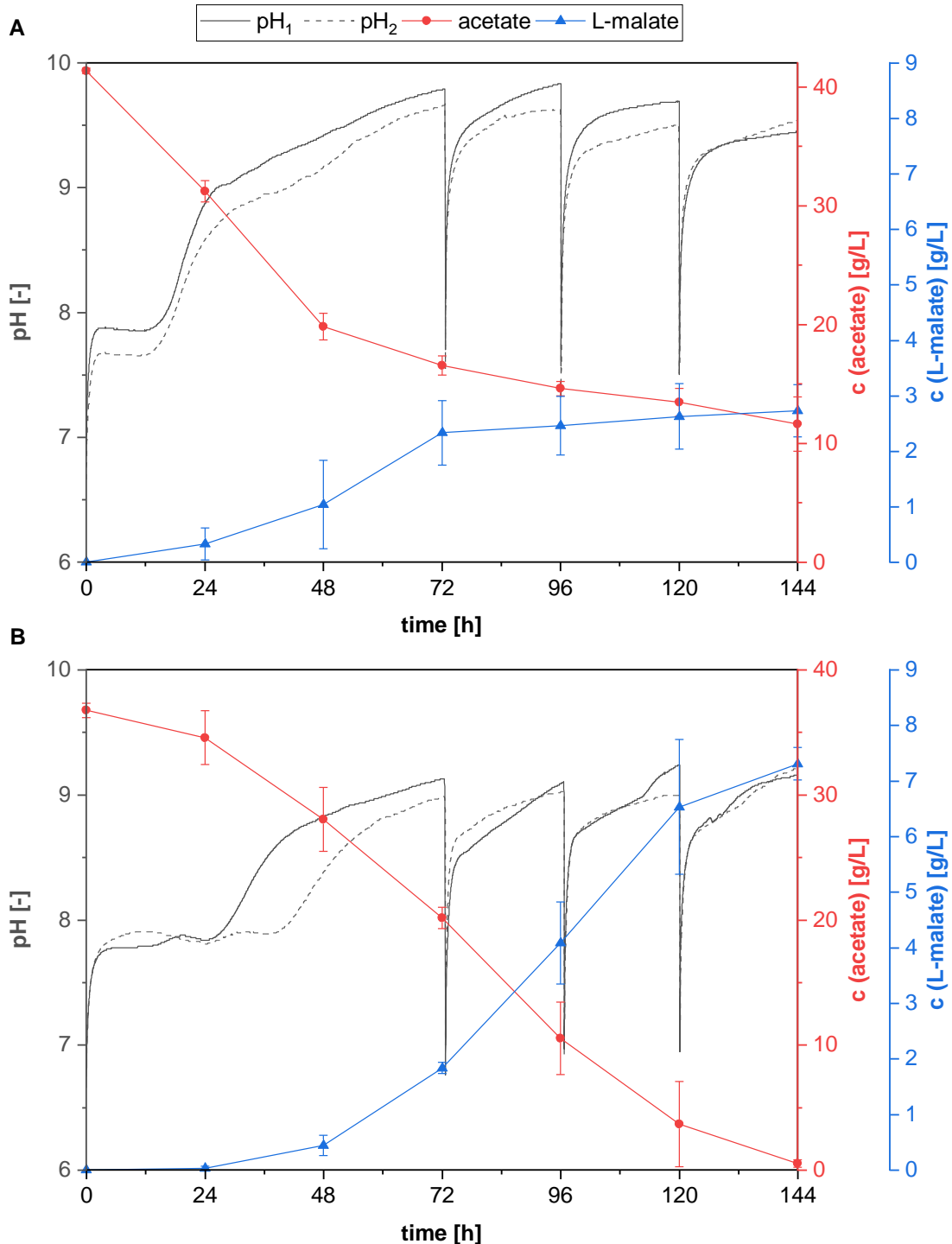


**Figure 34:** Bioreactor cultivations of *A. oryzae* in main culture medium containing 40 g/L acetate (A) or 100 % detoxified PAC (B). The initial medium pH was set to 5.5 using 96 % H<sub>2</sub>SO<sub>4</sub> prior to CaCO<sub>3</sub> addition and a daily manual pH adjustment with 72 % H<sub>2</sub>SO<sub>4</sub> to values < 7.5 was performed starting after 72 h of fermentation. The data represent mean values of duplicates and error bars indicate the standard deviation.

The reduced substrate consumption observed in the control cultures also affected their product formation. Although in the controls first malate titers were already measured in the 24 h samples due to the earlier onset of acetate consumption, comparably high titers were obtained after only 72 h of fermentation. As cultivation progressed, malate production in the controls flattened noticeably and a final titer of only  $2.73 \pm 0.47$  g/L was reached. In contrast, the malate concentration continued to increase strongly in the reactors with PAC and the production only weakened slightly in the last 24 h of fermentation. A maximum malate titer of  $7.31 \pm 0.29$  g/L was obtained in these reactors, which was 2.7 times higher than in the controls. Thus, it was successfully demonstrated that the process of fungal malate production from detoxified PAC can be transferred to the reactor scale.

### 5.3. Discussion

#### 5.3.1. Acetol utilization in *A. oryzae* pre-culture

In this work, it was successfully demonstrated that *Aspergillus oryzae* is able to use acetol as a C-source for biomass formation at concentrations up to 40 g/L, although growth inhibition was observed with increasing ketone concentration. While several studies have been conducted on how pretreatments can effectively remove inhibitory compounds such as acetol from liquid pyrolysis products [110, 221–223], there is little information on acetol as a single substance. Lian et al. investigated the inhibitory effect of various components of an aqueous pyrolysis sugar solution on *S. cerevisiae* strain ATCC 200062 and determined its growth and ethanol production to be inhibited by 80.07 % and 99.08 %, respectively, when the medium contained 2.16 wt.% acetol [148]. For *Aspergillus oryzae*, tolerance towards the ketone was also already studied previously on glucose-containing agar plates, and it was found that the fungus ceased growth at concentrations greater than 1.5 wt.% acetol [149]. The tolerated acetol concentration was thus significantly lower than the 40 g/L achieved in the current work although the medium contained glucose as an additional easily metabolizable C-source. Thus, as far as the authors are aware, acetol has not yet been reported to serve as sole substrate for growth of filamentous fungi, nor is there any knowledge on its metabolization in these organisms. In contrast, for bacteria such as *Thermoanaerobacterium thermosaccharolyticum* [135, 380] and *Clostridium sphenoides* [134], it is well known that acetol occurs as an intermediate in the production of 1,2-propanediol from dihydroxyacetone phosphate. In the first step of the process, an enzyme called methylglyoxal synthase catalyzes the conversion of the triose phosphate to methylglyoxal by cleavage of an inorganic phosphate. This is followed by a stepwise reduction

of the methylglyoxal to 1,2-propanediol, which proceeds with the formation of lactaldehyde or acetol as an intermediate and requires different reduction equivalents (NADH, NAD(P)H) depending on the oxidoreductase involved [133]. Although 1,2-propanediol formation has been observed predominantly in bacteria, there is evidence that at least parts of this pathway are also present in yeasts and fungi. For example, two methylglyoxal oxidoreductases have already been identified for *A. niger* [381] and it has been shown in the same species as well as in *A. nidulans* that these two fungi possess glycerol dehydrogenases that have an activity of 18 % towards methylglyoxal and thus can potentially catalyze its conversion to acetol or lactaldehyde [382]. Moreover, it was reported by Walti et al. that *A. niger* is able to convert 1,2-propanediol back to acetol, suggesting that the reaction steps involved in this metabolic pathway are at least partially reversible [383]. Although the enzymes of the methylglyoxal pathway have also been identified in the yeast *S. cerevisiae* [384, 385], the production of 1,2-propanediol by the yeast has so far mostly required genetic engineering [136, 137, 386, 387], or was carried out as yeast-mediated bioconversion of acetol using ethanol or acetate as the primary energy source [138, 139, 388, 389]. This raises the question of whether *A. oryzae* actually utilized acetol as sole substrate for its growth in the pre-culture experiments or whether residual glycerol from the spore solution or Maillard products formed during autoclaving may have been used for this purpose. It is already known that the fungus is able to use glycerol as a C-source for growth [33] and that the formation of pyrazines can occur as products of the Maillard reaction between acetol and ammonia [121]. The decreased acetol concentration at the beginning of the cultivation indicates the formation of Maillard products. However, the reduction in initial acetol content was only 1.2-9.0 %, and the concentration of Maillard products formed was therefore probably too low to meet the fungal energy requirements. Moreover, at least for the cultures with 3 and 5 g/L acetol, there was a significant decrease in biomass concentration after the complete depletion of the ketone and thus a clear coupling of growth and acetol consumption. This is also supported by the work of Lian et al. who investigated the suitability of acetol, acetate as well as the mixture of both carbon sources for biomass formation and lipid production of the yeasts *Cryptococcus curvatus*, *Rhodotorula glutinis* and *Lipomyces starkeyi* and showed that all strains tested were capable of metabolizing the ketone as the sole substrate at a concentration of 1 wt.% [110]. Assuming the density of water for the medium, these results are comparable to the cultures with 10 g/L acetol in our experiment, which still showed normal growth with a maximum CDW of  $2.19 \pm 0.11$  g/L. Furthermore, for two of the three yeasts studied, slightly increased CDWs were obtained on mixtures of 1 wt.% acetol and 1 wt.% acetate compared with the use of only one C-source. This is consistent with the current

findings, as the presence of an additional 10 g/L acetol also resulted in slightly elevated titers compared with the pure acetate control. Despite the improved titers observed at low acetol concentrations in the mixtures with acetate, overall tolerance to the ketone was decreased in this experiment. Whereas 40 g/L of the ketone could still be tolerated when acetol was the only C-source, fungal growth was no longer observed at concentrations >20 g/L acetol when an additional 40 g/L acetate was present in the medium. As demonstrated by the transcriptome analysis in chapter 3, this can be attributed to the fact, that the acetate generates additional osmotic and oxidative stress for the fungus.

Although the pre-culture experiment with mixtures of acetol and acetate ( $pK_a = 4.76$ ) in this work were performed at an initial pH of 7 and thus most of the acetic acid was deprotonated, the small fraction of protonated uncharged acid molecules can enter the cell and lower its internal pH [90]. Using the Henderson-Hasselbalch equation, the concentration of protonated acetic acid in the medium was determined to be 0.23 g/L (0.004 mol/L) for our cultivation conditions. However, according to Alcano et al. only concentrations above 0.018-0.022 mol/L were found to completely inhibit spore germination of *A. carbonarius*, *A. flavus*, and *A. parasiticus* [390], so the concentration of protonated acetic acid in our medium was most likely not the main reason for the decreased acetol tolerance. As previously discussed by Kövilein et al. another possible osmotic stress factor results from the large amount of sodium ions that accumulates during media preparation when the 40 g/L of acetic acid is neutralized to a pH of 7 using NaOH pellets [104]. However, the pH adjustment resulted in a sodium ion concentration of only about 0.7 mol/L in the medium, which did not exceed the tolerance limits already determined for other *Aspergillus* species [391, 392]. Accordingly, none of the individual stressors (acetol, protonated acetic acid, sodium ions) can explain the reduced acetol tolerance of *A. oryzae* in acetate-acetol mixtures. Nevertheless, it can be assumed that the inhibitory effects of the individual stressors add up or possibly even reinforce each other and probably cause the increased sensitivity to the ketone.

### **5.3.2. Malic acid production on artificial and authentic PAC**

Similar to the pre-cultures experiment, the main cultures with acetate-acetol mixtures also revealed a clear inhibitory effect of ketone concentrations  $\geq 20$  g/L on fungal malate production. Whereas the product titers obtained at low acetol concentrations of 3-10 g/L ( $5.64 \pm 0.59$  g/L- $6.02 \pm 0.17$  g/L) were still comparable with the acetate control ( $6.29 \pm 0.46$  g/L), the final malate concentration was reduced by 40.9 % in the cultures containing 20 g/L acetol, and no more

product formation was detected when the medium contained  $\geq 30$  g/L of the ketone (data not shown). Yield and productivity also decreased with increasing acetol content in the cultures. This is consistent with the results of Dörsam et al. who also observed a considerable reduction in malate yield when increasing acetol concentrations were added to glucose containing *A. oryzae* main cultures [149]. They identified the maximum ketone concentration suitable for malate production to be 2.5 wt-%. And even though this was not a concentration that was studied in the present work, it was nevertheless exactly between the acetol content at which we observed a first inhibition and the one for which malate formation could no longer be detected. The fact that similar results were obtained in acetol mixtures with both acetate and glucose suggests that inhibition in the main cultures was quite independent of the primary C-source used. Consequently, the proportion of protonated acid or the concentration of sodium ions in our acetate cultures appeared to be of minor importance. The assumption that acetol is the main contributor to the reduced malate production is also confirmed by the fact that although concentrations up to 40 g/L acetol seem to be utilizable for fungal growth, we did not succeed in using acetol as the sole C-source for acid production (data not shown).

Dörsam also investigated malate production in shake flask cultures with artificial PAC consisting of acetol, acetate, and three other main PAC components (propionic acid, ethylene glycol, and methanol) and compared them with a 45 g/L acetate control. Consistent with the results in the glucose containing cultures, as well as those from our experiment, a level of 3.5 wt.% of acetol was found to be completely inhibitory to malate production, while a reduction to 1.75 wt.% still yielded comparable titers to the control [393]. Complete omission of the ketone from the model PACs even resulted in a significant increase in malate concentration to more than threefold, indicating that additional PAC components can be used as C-sources for acid formation.

After detoxification of the PAC by rotary evaporation, overliming, and a subsequent activated carbon treatment, the acetol content was significantly reduced to  $< 3$  g/L and it was shown for the first time that the condensate is indeed a suitable substrate for fungal malate production. However, the final malate titer of  $3.22 \pm 0.70$  g/L obtained after 240 h was significantly lower than for the 40 g/L acetate control in the experiment with acetate-acetol mixtures ( $6.29 \pm 0.46$  g/L). The main reason for this observation is probably the high pH of the PAC medium, as it was already 8.05 at the beginning of the experiment and even increased to 9.81 as cultivation progressed. The inhibitory effect of alkaline medium pH has already been shown for other *Aspergillus* species. For example, Pinchai et al. found that the growth of *A. fumigatus* was significantly inhibited at a pH of 9 compared to the acidic range [394], and

*Aspergillus nidulans* even showed inhibition at a pH of 8, especially in the presence of high sodium concentrations (1 mol/L) [395]. In our PAC main culture experiments, we reached similarly high values (about 0.9 mol/L) due to the neutralization of the condensate to a pH of 6.5 and the overliming with NaOH. However, since the two mentioned pH inhibition studies were growth experiments on agar plates, they were performed under completely different cultivation conditions and are therefore difficult to compare with the current experiment on product formation in shake flasks.

In contrast, the study by Kövilein et al. seems more suitable for comparison, as they investigated the influence of the initial pH on malic acid production with *A. oryzae* in acetate-containing main cultures. They found that for optimal malate production, the pH should ideally be adjusted to 5.5 before CaCO<sub>3</sub> addition, as both lower and higher values result in decreased malate titers [104]. Therefore, in a follow-up experiment, two different pH adjusting agents, 96 % H<sub>2</sub>SO<sub>4</sub> and 100 % acetic acid, were tested to lower the initial pH of the culture medium. The adaptation indeed resulted in an increase in the final malate titers to 8.30 ± 0.26 g/L and 9.77 ± 0.55 g/L, thus confirming that the high pH was the main cause of the reduced malate production. Although the use of acetic acid for pH adjustment increased the initial substrate concentration to 45 g/L, both adjusted cultures showed nearly identical maximum yield of 0.23 ± 0.03 g/g (acetic acid) and 0.22 ± 0.01 g/g (H<sub>2</sub>SO<sub>4</sub>). This is in accordance with the results of Kövilein et al. who performed main cultures containing acetate concentrations of 10-55 g/L and also obtained identical yields for the cultures with 40 g/L and 45 g/L acetate, respectively [104]. In their work, the yield was calculated to be 0.19 g/g, which was comparable to the values obtained in our experiment.

Since the main objective of the present work was to use PAC as the sole C-source for fungal acid production, H<sub>2</sub>SO<sub>4</sub> was chosen as the pH adjusting agent in the subsequent bioreactor cultivation. For both the acetate control (2.73 ± 0.47 g/L) and the bioreactors containing PAC (7.30 ± 0.29 g/L), noticeably reduced titers were measured compared to the shake flask cultivations (acetate: 6.29 ± 0.46 g/L, PAC: 8.29 ± 0.26 g/L), but due to the shorter fermentation time of 144 h, yield and productivity should rather be used for comparison. In the bioreactors with PAC, the yield was similar to the value obtained in the shake flask experiments, and even the highest overall productivity of all cultivations (0.051 ± 0.002 g/(L·h)) was achieved, indicating that upscaling into the bioreactor was successful. In contrast, the acetate control showed a significant deterioration, since the yield was halved and the maximum and overall productivity were also reduced by 30.4 % and 26.9 %, respectively. One possible reason for the lower values could be the increased shear stress caused by stirring in the bioreactor.

Furthermore, since filamentous growth was observed in both the PAC and acetate pre-cultures, it is conceivable that some of the biomass became attached to the reactor internals after transfer to the bioreactor, where it was exposed to different conditions than the properly suspended cells. Another difference between cultivation in shake flasks and bioreactors was aeration, which, according to Halliwell et al., could affect acetate metabolism and production of certain organic acids [396], and therefore may have shifted the product spectrum. Aeration also resulted in increased outgassing of CO<sub>2</sub>, which in turn led to significantly higher pH values ( $\approx 7.6-7.9$ ) than in shake flask experiments already at the beginning of the fermentation. Especially in the control reactors, this was followed by a further sharp pH increase to values of 9.8 after 72 hours of cultivation due to acetate metabolization. Accordingly, inhibition of the acid production by the alkaline medium pH is most likely to explain the reduction in yield and productivity in the control reactors. Although attempts were made to counteract the inhibition by manually readjusting the pH once a day, the acetate controls showed a considerable drop in metabolic activity as cultivation progressed, indicating that the cells in these reactors had already been irreversibly damaged. Moreover, the effect of the pH correction did not last long, since outgassing of CO<sub>2</sub> probably caused the pH to rise again quickly to almost the original value. Therefore, the authors consider the implementation of an automatic pH control particularly promising to allow further improvements in fungal acid production. However, in the reactors containing PAC, the acetate was almost completely depleted at the end of cultivation, so more substrate is needed in addition to pH control to increase acid production. One way to combine pH regulation and substrate supply is to use acetic acid or PAC as pH adjusting agents, although the latter is of limited suitability due to its relatively high pH of 6.5 after the pretreatment procedure. An alternative to feeding acetic acid that is more compatible with the objective of using PAC as the sole substrate might be the utilization of genetically modified strains whose carbon flux has been redirected toward an increased formation of malic acid. Several approaches to genetically modify the malic acid production in *Aspergillus* species have already been described in the literature [397, 398]. In these studies, significant improvement was achieved by targeted overexpression of genes directly involved in malate production and/or by deletion of metabolic pathways leading to the formation of by-products. The introduction and heterologous expression of genes from other organisms has also been carried out to enhance fungal acid production [399, 400] and ultimately even offers the possibility of completely reconstructing metabolic pathways. Such an approach could potentially be pursued to allow malate production from acetol, which would both eliminate the need to remove the ketone by pretreatment and allow more carbon in the condensate to be used for malate formation.

## 6. Summary and conclusions

By using the pyrolytic aqueous condensate (PAC) as substrate, this work aimed to establish a process for sustainable L-malic acid production with *Aspergillus oryzae* on the basis of a lignocellulosic waste material. To achieve this objective, a detoxification process was established that allowed inhibitory substances to be removed from the condensate while keeping the concentration of useful substrates like acetate as high as possible.

When detoxifying such waste streams, the efficacy and expense of treatment must be carefully balanced to maintain the advantage of low substrate cost over using glucose as substrate for microbial fermentations. Since laccase treatment is comparatively expensive, it is thus not necessarily a negative result that this detoxification method proved unsuitable for increasing the fungal PAC tolerance despite the removal of phenols. These findings indicate that the fungus is naturally characterized by a sufficiently high tolerance to phenolic substances, and therefore the pretreatment procedure does not need to be directed toward the elimination of these compounds. Instead, biological detoxification of PAC should be aimed at reducing the concentration of substances like 2-cyclopenten-1-one or furfural, which have a strong inhibitory effect on *A. oryzae*. For cost reasons, it is furthermore advisable to use whole cells or crude cell extracts rather than purified enzymes.

If the PAC or other lignocellulosic degradation products are intended to be used as a substrate for less phenol-resistant microorganisms, activated carbon treatment might be a more cost-effective alternative to detoxification with laccase. An additional reduction of the costs might be achieved by using the char fraction from the pyrolysis process as feedstock for the production of the activated carbon. But since the pyrolysis char is part of the final “biosyncrude” formed in the bioliq® process at KIT careful consideration must be given to whether an alternative use is economically viable. Similar to laccase, this method proved to be very effective for the elimination of phenolic components, as at the highest carbon loading of 10 % (w/v) the concentration of guaiacol was reduced by 93.4 % and phenol could even be completely removed. However, activated carbon was found to be less specific than the enzymatic treatment, which resulted in partial removal of non-phenolic substances and consequently an increase in the fungal growth limit. Nevertheless, this method offers potential for further optimization, as even the use of 10 % carbon only led to an improvement from 1.25 % to 1.625 % PAC. Since further increases of the carbon load are not advisable due to the resulting high viscosity of the suspension and the accumulation of large quantities of spent carbon, reactivation and repeated use could be a promising alternative.

Regarding the overliming treatment, it had been shown that high reaction temperatures and pH-values were beneficial for detoxification, while the influence of the type of hydroxide used seemed to become irrelevant with increasing temperature. This method is considered promising as it drastically reduced the concentration of the inhibitory PAC components furfural and 2-cyclopenten-1-one by up to 96 % and 87 %, respectively, and additionally caused an increase in the acetate content. Besides evaporation effects, the latter observation could also be attributed to chemical reactions between the individual PAC constituents. Although this work provided some hypotheses about possible reactions that may occur during the overliming treatment, it is difficult to draw conclusions based on a few selected PAC components. Therefore, more detailed analyses are needed in the future to gain a better understanding of the mechanism underlying this detoxification method and to enable its further improvement.

Rotary evaporation could potentially also be used to increase the substrate concentration in the PAC, but the potential risk of an accumulation of non-volatile toxic compounds needs to be considered. However, all inhibitors studied in this work appeared to be volatile when subjected to rotary evaporation at 200 mbar, as their concentrations were reduced to levels below or at least close to the growth limit of *A. oryzae*. Although rotary evaporation was thus the most effective among all the single detoxification methods, only 30 % PAC tolerance was achieved. This indicates the presence of additional growth inhibitors or the occurrence of synergistic effects between the toxic compounds. While the former once again points to the need for more extensive analysis of the PAC composition, the latter should also be studied in more detail in the future to use this information for a further improvement of the detoxification procedure.

The combination of pretreatment methods also appeared to be a suitable approach to increase the fungal PAC tolerance. Moreover, it was revealed that the order in which the methods are performed is of crucial importance for an effective detoxification, suggesting that they might influence each other. This influence was particularly evident with the activated carbon treatment, as it hardly improved the PAC tolerance as a single method, whereas its effectiveness increased significantly when combined with other methods.

Therefore, the carbon treatment was also included in the final detoxification procedure and was carried out after the rotary evaporation and overliming. This procedure allowed the fungus to use 100 % PAC as a substrate for growth and malate production, which is the best possible result in terms of the fungal PAC tolerance. However, it required all three detoxification methods and thus a high pretreatment effort. Moreover, based on the few substrates analyzed, it was not possible to clearly conclude why this procedure was the only one that allowed growth on 100 % PAC, as other combinations resulted in comparably low inhibitor concentrations.

After some of these treatments, only acetate and very low amounts of other components remained in the condensate. This raises the question of whether it might be more advantageous to use a method that allows direct separation of acetate from the pyrolysis condensate. For example, membrane filtration and liquid-liquid extraction have already been proven effective for this purpose and might therefore be investigated for their applicability to PAC.

In addition to the optimization of the pretreatment procedure, the process of PAC-based malate production also offered potential for further improvement. For example, 56.5 % of the acetate contained in the pyrolysis condensate remained unused at the end of the first shake flask cultivation, presumably due to a pH inhibition of the fungus. Subsequent reduction of the initial medium pH and manual pH regulation enabled almost complete conversion of acetate in 500 mL bioreactor fermentations and resulted in a 3.9-fold higher overall malate productivity compared to the shake flask cultures. While on the one hand these results have successfully demonstrated that the process can be transferred to the bioreactor scale, the depletion of the substrate also shows the need for the implementation of an appropriate feeding strategy. Coupling feeding with an automated pH control using PAC or pure acetic acid as pH adjusting agent is considered to be particularly promising for this purpose, since the pH is of crucial importance for the formation of organic acids from acetate-containing media.

In comparison to the control fermentations with pure acetate, the PAC containing reactors showed a 2.7-fold higher malate titer, indicating that *A. oryzae* might be able to metabolize other PAC components in addition to acetate. Indeed, this study revealed for the first time that concentrations of up to 40 g/L acetol, the second major PAC component, can be converted into fungal biomass. This is a promising result with regard to a more efficient utilization of the pyrolysis condensate, as it expands the spectrum of usable carbons contained therein. Since high C:N ratios in the medium are known to be required for organic acid production with *A. oryzae*, this broadening of the substrate spectrum might represent an important step in further enhancing fungal malate formation from the pyrolysis condensate. However, a conversion of acetol to malic acid could not be achieved with the *A. oryzae* wild-type strain used in this work, highlighting the need for a more detailed examination of the acetol metabolism in this fungus. Although the current transcriptome analysis provided indications that the increased degradation of methylglyoxal in the PAC-containing cultures might be related to the metabolization of acetol, a different experimental setup will be required in the future to verify this assumption. Comprehensive knowledge of the metabolic routes involved in the conversion of this ketone might allow targeted genetic modification of the fungus with regard to directing intracellular carbon flux from acetol to malate formation. Moreover, the transcriptome analysis has revealed

potential targets for enhancing the fungal tolerance to PAC inhibitors, which might possibly result in a reduction of the pretreatment effort. This reduction is desirable, since especially the highly effective overliming and rotary evaporation treatments were quite energy and time consuming elements of the PAC detoxification process developed in this work. However, it is unclear whether altered expression of the identified genes will significantly improve the fungal resistance to the pyrolysis condensate. These genetic modifications may probably only attenuate the inhibitory effects of some individual PAC components, whereas the results of this work indicate the presence of previously unknown inhibitors and additional synergistic effects. Furthermore, the genetic modification of filamentous fungi also involves considerable laboratory effort. However, since gene constructs in fungi are usually stably integrated into the genome, this effort is likely to be required only once, whereas detoxification of the condensate needs to be performed prior to each application as a substrate.

In summary, it is necessary to carefully consider which approach should be followed in the future to realize fungal malate production based on the pyrolysis condensate. This work has provided a good basis for both approaches by gaining comprehensive knowledge about potential substrates and inhibitors present in PAC and their effects on *A. oryzae*. Ideally, this knowledge might already be used in the pyrolysis process to generate a PAC that is even more suitable as a substrate for microbial fermentations.

# List of references

1. Wyman, H., Palmer, J.K.: Organic acids in the ripening banana fruit. *Plant Physiol.* **39**(4), 630 (1964)
2. Eisele, T.A., Drake, S.R.: The partial compositional characteristics of apple juice from 175 apple varieties. *J. Food Compos. Anal.* **18**(2-3), 213–221 (2005)
3. Wang, H.C., Huang, H.B., Huang, X.M., Hu, Z.Q.: Sugar and acid compositions in the arils of Litchi chinensis Sonn.: cultivar differences and evidence for the absence of succinic acid. *The Journal of Horticultural Science and Biotechnology* **81**(1), 57–62 (2006)
4. Hale, C.R.: Synthesis of organic acids in the fruit of the grape. *Nature* **195**(4844), 917–918 (1962)
5. Kubo, H., Kato, Y.: Soft candy and soft candy production method. Google Patents (2012)
6. Aldrich, D., Vink, W., Deptula, R.W., Muskus, D.J., Fronczkowski, P.R., Chrusch, M.: Sugarless candies. Google Patents (1981)
7. Grignard, R.: New quaternary ammonium salts of malic acid and their application in cosmetics Patent 3,954,846
8. Gore, V., Gadkar, M., Pokharkar, K.: Novel process to prepare almotriptan Patent US 2010/0292290 A1
9. Stallcup, O.T.: Use of malic acid as a ruminant feed additive. Google Patents (1979)
10. Geng, H., Wang, F., Yan, C., Tian, Z., Chen, H., Zhou, B., Yuan, R., Yao, J.: Leaching behavior of metals from iron tailings under varying pH and low-molecular-weight organic acids. *Journal of Hazardous Materials* **383**, 121136 (2020)
11. Nishiwaki, Y., Takahashi, T., Takahashi, K.: Cleaning agent for semiconductor device and method for producing semiconductor device using the cleaning agent. Google Patents (2010)
12. Werpy, T., Petersen, G.: Top Value Added Chemicals from Biomass: Volume I -- Results of Screening for Potential Candidates from Sugars and Synthesis Gas. National Renewable Energy Lab., Golden, CO (US) (2004)
13. Lenz, R.W., Vert, M.: Malic acid polymers. Google Patents (1981)
14. Hutchings, G.J., Higgins, R.: Production of maleic anhydride. Google Patents (1981)
15. Nesty, G.A.: Malic acid and process of making the same. Google Patents (1970)
16. Giorno, L., Drioli, E., Carvoli, G., Cassano, A., Donato, L.: Study of an enzyme membrane reactor with immobilized fumarase for production of L-malic acid. *Biotechnol. Bioeng.* **72**(1), 77–84 (2001)

17. Presečki, A.V., Zelić, B., Vasić-Rački, Đ.: Comparison of the L-malic acid production by isolated fumarase and fumarase in permeabilized baker's yeast cells. *Enzyme Microb. Technol.* **41**(5), 605–612 (2007)
18. Wang, X., Gong, C.S., T Tsao, G.: Production of L-malic acid via biocatalysis employing wild-type and respiratory-deficient yeasts. *Applied Biochemistry and Biotechnology* **70**(1), 845–852 (1998)
19. Pandurić, N., Šalić, A., Zelić, B.: Fully integrated biotransformation of fumaric acid by permeabilized baker's yeast cells with in situ separation of L-malic acid using ultrafiltration, acidification and electro dialysis. *Biochem. Eng. J.* **125**, 221–229 (2017)
20. Stojković, G., Žnidaršič-Plazl, P.: Continuous synthesis of L-malic acid using whole-cell microreactor. *Process Biochemistry* **47**(7), 1102–1107 (2012)
21. Oliveira, E.A., Costa, A.A.R., Figueiredo, Z., Carvalho, L.B.: L-malic acid production by entrapped *Saccharomyces cerevisiae* into polyacrylamide gel beads. *Applied Biochemistry and Biotechnology* **47**(1), 65–72 (1994)
22. Bressler, E., Pines, O., Goldberg, I., Braun, S.: Conversion of fumaric acid to L-malic by sol-gel immobilized *Saccharomyces cerevisiae* in a supported liquid membrane bioreactor. *Biotechnol. Progr.* **18**(3), 445–450 (2002)
23. Roa Engel, C.A., Straathof, A.J.J., Zijlmans, T.W., van Gulik, W.M., van der Wielen, L. am: Fumaric acid production by fermentation. *Appl. Microbiol. Biotechnol.* **78**(3), 379–389 (2008)
24. Zelle, R.M., Hulster, E. de, van Winden, W.A., Waard, P. de, Dijkema, C., Winkler, A.A., Geertman, J.-M.A., van Dijken, J.P., Pronk, J.T., van Maris, A.J.A.: Malic acid production by *Saccharomyces cerevisiae*: engineering of pyruvate carboxylation, oxaloacetate reduction, and malate export. *Appl. Environ. Microbiol.* **74**(9), 2766–2777 (2008)
25. Ma, H., Kubicek, C.P., Röhr, M.: Malate dehydrogenase isoenzymes in *Aspergillus niger*. *FEMS Microbiol. Lett.* **12**(2), 147–151 (1981)
26. Walker, M.E., Val, D.L., Rohde, M., Devenish, R.J., Wallace, J.C.: Yeast pyruvate carboxylase: identification of two genes encoding isoenzymes. *Biochem. Biophys. Res. Commun.* **176**(3), 1210–1217 (1991)
27. Shigeo, A., Akira, F., Ichiro, T.K.: Method of producing L-malic acid by fermentation. Google Patents (1962)
28. Battat, E., Peleg, Y., Bercovitz, A., Rokem, J.S., Goldberg, I.: Optimization of L-malic acid production by *Aspergillus flavus* in a stirred fermentor. *Biotechnol. Bioeng.* **37**(11), 1108–1116 (1991)

29. Nesbitt, B.F., O'Kelly, J., Sargeant, K., Sheridan, A.N.: Toxic metabolites of *Aspergillus flavus*. Nature, London **195**(4846) (1962)
30. Barbesgaard, P., Heldt-Hansen, H.P., Diderichsen, B.: On the safety of *Aspergillus oryzae*: a review. Appl. Microbiol. Biotechnol. **36**(5), 569–572 (1992)
31. Payne, G.A., Nierman, W.C., Wortman, JR, Pritchard, B.L., Brown, D., Dean, R.A., Bhatnagar, D., Cleveland, T.E., Machida, M., Yu, J.: Whole genome comparison of *Aspergillus flavus* and *A. oryzae*. Med. Mycol. **44**(Supplement\_1), S9-S11 (2006)
32. Knuf, C., Nookaew, I., Brown, S.H., McCulloch, M., Berry, A., Nielsen, J.: Investigation of malic acid production in *Aspergillus oryzae* under nitrogen starvation conditions. Appl. Environ. Microbiol. **79**(19), 6050–6058 (2013)
33. Ochsenreither, K., Fischer, C., Neumann, A., Syltatk, C.: Process characterization and influence of alternative carbon sources and carbon-to-nitrogen ratio on organic acid production by *Aspergillus oryzae* DSM1863. Appl. Microbiol. Biotechnol. **98**(12), 5449–5460 (2014)
34. Zambanini, T., Kleineberg, W., Sarikaya, E., Buescher, J.M., Meurer, G., Wierckx, N., Blank, L.M.: Enhanced malic acid production from glycerol with high-cell density *Ustilago trichophora* TZ1 cultivations. Biotechnol. Biofuels **9**(1), 1–10 (2016)
35. Li, X., Liu, Y., Yang, Y., Zhang, H., Wang, H., Wu, Y., Zhang, M., Sun, T., Cheng, J., Wu, X.: High levels of malic acid production by the bioconversion of corn straw hydrolyte using an isolated *Rhizopus delemar* strain. Biotechnol. Bioprocess Eng. **19**(3), 478–492 (2014)
36. Kövilein, A., Kubisch, C., Cai, L., Ochsenreither, K.: Malic acid production from renewables: a review. J. Chem. Technol. Biotechnol. **95**(3), 513–526 (2020)
37. West, T.P.: Fungal biotransformation of crude glycerol into malic acid. Zeitschrift für Naturforschung C **70**(5-6), 165–167 (2015)
38. West, T.P.: Microbial production of malic acid from biofuel-related coproducts and biomass. Fermentation **3**(2), 14 (2017)
39. Iyyappan, J., Baskar, G., Bharathiraja, B., Saravanathamizhan, R.: Malic acid production from biodiesel derived crude glycerol using morphologically controlled *Aspergillus niger* in batch fermentation. Bioresource technology **269**, 393–399 (2018)
40. West, T.P.: Malic acid production from thin stillage by *Aspergillus* species. Biotechnol. Lett **33**(12), 2463–2467 (2011)

41. Dörsam, S., Fessler, J., Gorte, O., Hahn, T., Zibek, S., Syldatk, C., Ochsenreither, K.: Sustainable carbon sources for microbial organic acid production with filamentous fungi. *Biotechnol. Biofuels* **10**(1), 1–12 (2017)
42. Kosamia, N.M., Samavi, M., Uprety, B.K., Rakshit, S.K.: Valorization of biodiesel byproduct crude glycerol for the production of bioenergy and biochemicals. *Catalysts* **10**(6), 609 (2020)
43. Yang, F., Hanna, M.A., Sun, R.: Value-added uses for crude glycerol—a byproduct of biodiesel production. *Biotechnology for biofuels* **5**(1), 1–10 (2012)
44. Morrison, L.R.: Glycerol. *Kirk-Othmer encyclopedia of chemical technology* (2000)
45. Samul, D., Leja, K., Grajek, W.: Impurities of crude glycerol and their effect on metabolite production. *Ann. Microbiol.* **64**(3), 891–898 (2014)
46. Iyyappan, J., Bharathiraja, B., Baskar, G., Jayamuthunagai, J., Barathkumar, S.: Malic acid production by chemically induced *Aspergillus niger* MTCC 281 mutant from crude glycerol. *Bioresource technology* **251**, 264–267 (2018)
47. Kim, Y., Mosier, N.S., Hendrickson, R., Ezeji, T., Blaschek, H., Dien, B., Cotta, M., Dale, B., Ladisch, M.R.: Composition of corn dry-grind ethanol by-products: DDGS, wet cake, and thin stillage. *Bioresource technology* **99**(12), 5165–5176 (2008)
48. Menon, V., Rao, M.: Trends in bioconversion of lignocellulose: biofuels, platform chemicals & biorefinery concept. *Progress in Energy and Combustion Science* **38**(4), 522–550 (2012)
49. Nanda, S., Mohammad, J., Reddy, S.N., Kozinski, J.A., Dalai, A.K.: Pathways of lignocellulosic biomass conversion to renewable fuels. *Biomass Convers. Biorefin.* **4**(2), 157–191 (2014)
50. Zhao, X., Zhang, L., Liu, D.: Biomass recalcitrance. Part I: the chemical compositions and physical structures affecting the enzymatic hydrolysis of lignocellulose. *Biofuels, Bioprod. Biorefin.* **6**(4), 465–482 (2012)
51. Saha, B.C.: Hemicellulose bioconversion. *J. Ind. Microbiol. Biotechnol.* **30**(5), 279–291 (2003)
52. Zhao, H., Kwak, J.H., Wang, Y., Franz, J.A., White, J.M., Holladay, J.E.: Effects of crystallinity on dilute acid hydrolysis of cellulose by cellulose ball-milling study. *Energy & Fuels* **20**(2), 807–811 (2006)
53. Ghaemi, F., Abdullah, L.C., Ariffin, H.: Lignocellulose structure and the effect on nanocellulose production. In: *Lignocellulose for Future Bioeconomy*, pp. 17–30. Elsevier (2019)

54. Harmsen, P.F., Lips, S.J., Bakker, R.R.: Pretreatment of lignocellulose for biotechnological production of lactic acid, 1384, public version. Wageningen UR FBR (2013)
55. Agbor, V.B., Cicek, N., Sparling, R., Berlin, A., Levin, D.B.: Biomass pretreatment: fundamentals toward application. *Biotechnol. Adv.* **29**(6), 675–685 (2011)
56. Sharma, H.K., Xu, C., Qin, W.: Biological pretreatment of lignocellulosic biomass for biofuels and bioproducts: an overview. *Waste Biomass Valorization* **10**(2), 235–251 (2019)
57. Guragain, Y.N., Vadlani, P.V.: Renewable biomass utilization: a way forward to establish sustainable chemical and processing industries. *Clean Technologies* **3**(1), 243–259 (2021)
58. Bridgwater, A.: Thermal biomass conversion and utilization: biomass information system. Office for Official Publications of the European Communities (1996)
59. Bhattacharya, A.S., Bhattacharya, A., Pletschke, B.I.: Synergism of fungal and bacterial cellulases and hemicellulases: a novel perspective for enhanced bio-ethanol production. *Biotechnol. Lett* **37**(6), 1117–1129 (2015)
60. Shallom, D., Shoham, Y.: Microbial hemicellulases. *Curr. Opin. Microbiol.* **6**(3), 219–228 (2003)
61. Chen, H., Fu, X.: Industrial technologies for bioethanol production from lignocellulosic biomass. *Renewable and Sustainable Energy Reviews* **57**, 468–478 (2016)
62. Lai, Z., Zhu, M., Yang, X., Wang, J., Li, S.: Optimization of key factors affecting hydrogen production from sugarcane bagasse by a thermophilic anaerobic pure culture. *Biotechnology for biofuels* **7**(1), 1–11 (2014)
63. Lo, Y.-C., Lu, W.-C., Chen, C.-Y., Chang, J.-S.: Dark fermentative hydrogen production from enzymatic hydrolysate of xylan and pretreated rice straw by *Clostridium butyricum* CGS5. *Bioresource technology* **101**(15), 5885–5891 (2010)
64. Huang, C., Xiong, L., Guo, H.-J., Li, H.-L., Wang, C., Chen, X.-F., Zhao, C., Chen, X.-D.: Anaerobic digestion of elephant grass hydrolysate: biogas production, substrate metabolism and outlet effluent treatment. *Bioresource technology* **283**, 191–197 (2019)
65. Sulbarán-Rangel, B., Alarcón Aguirre, J.S., Breton-Deval, L., Del Real-Olvera, J., Gurubel Tun, K.J.: Improvement of anaerobic digestion of hydrolysed corncob waste by organosolv pretreatment for biogas production. *Applied Sciences* **10**(8), 2785 (2020)
66. Magalhães, B.L., Grassi, M.C.B., Pereira, Gonçalo AG, Brocchi, M.: Improved n-butanol production from lignocellulosic hydrolysate by *Clostridium* strain screening and culture-medium optimization. *Biomass and Bioenergy* **108**, 157–166 (2018)

67. Survase, S.A., van Heiningen, A., Granström, T.: Continuous bio-catalytic conversion of sugar mixture to acetone–butanol–ethanol by immobilized *Clostridium acetobutylicum* DSM 792. *Appl. Microbiol. Biotechnol.* **93**(6), 2309–2316 (2012)
68. Ruan, Z., Zanotti, M., Wang, X., Ducey, C., Liu, Y.: Evaluation of lipid accumulation from lignocellulosic sugars by *Mortierella isabellina* for biodiesel production. *Bioresource technology* **110**, 198–205 (2012)
69. Fei, Q., O’Brien, M., Nelson, R., Chen, X., Lowell, A., Dowe, N.: Enhanced lipid production by *Rhodospiridium toruloides* using different fed-batch feeding strategies with lignocellulosic hydrolysate as the sole carbon source. *Biotechnology for biofuels* **9**(1), 1–12 (2016)
70. Wang, G., Di Huang, Li, Y., Wen, J., Jia, X.: A metabolic-based approach to improve xylose utilization for fumaric acid production from acid pretreated wheat bran by *Rhizopus oryzae*. *Bioresource technology* **180**, 119–127 (2015)
71. Patra, T.K., Sheth, P.N.: Techno-economic Assessment of Thermochemical Biomass Conversion Technologies. In: *Recent Advancements in Biofuels and Bioenergy Utilization*, pp. 339–361. Springer (2018)
72. Luque, R., Speight, J.: *Gasification for synthetic fuel production: fundamentals, processes and applications*. Elsevier (2014)
73. Molino, A., Chianese, S., Musmarra, D.: Biomass gasification technology: The state of the art overview. *J. Energy Chem.* **25**(1), 10–25 (2016)
74. Demirbas, A., Arin, G.: An overview of biomass pyrolysis. *Energy Sources* **24**(5), 471–482 (2002)
75. Czernik, S., Bridgwater, A.V.: Overview of applications of biomass fast pyrolysis oil. *Energy & Fuels* **18**(2), 590–598 (2004)
76. Bridgwater, A.V.: Review of fast pyrolysis of biomass and product upgrading. *Biomass and Bioenergy* **38**, 68–94 (2012)
77. Pfitzer, C., Dahmen, N., Troger, N., Weirich, F., Sauer, J., Gunther, A., Muller-Hagedorn, M.: Fast pyrolysis of wheat straw in the bioliq pilot plant. *Energy Fuels* **30**(10), 8047–8054 (2016)
78. Kubisch, C., Ochsenreither, K.: Detoxification of a pyrolytic aqueous condensate from wheat straw for utilization as substrate in *Aspergillus oryzae* DSM 1863 cultivations. *Biotechnol Biofuels* **15**(1), 18 (2022)

79. Vassilev, S.V., Vassileva, C.G., Song, Y.-C., Li, W.-Y., Feng, J.: Ash contents and ash-forming elements of biomass and their significance for solid biofuel combustion. *Fuel* **208**, 377–409 (2017)
80. Nicoleit, T., Dahmen, N., Sauer, J.: Production and storage of gasifiable slurries based on flash-pyrolyzed straw. *Energy Technol.* **4**(1), 221–229 (2016)
81. Auersvald, M., Macek, T., Schulzke, T., Staš, M., Šimáček, P.: Influence of biomass type on the composition of bio-oils from ablative fast pyrolysis. *J. Anal. Appl. Pyrolysis* **150**, 104838 (2020)
82. Dahmen, N., Dinjus, E., Kolb, T., Arnold, U., Leibold, H., Stahl, R.: State of the art of the bioliq® process for synthetic biofuels production. *Environ. Prog. Sustainable Energy* **31**(2), 176–181 (2012)
83. Niebel, A., Funke, A., Pfitzer, C., Dahmen, N., Weih, N., Richter, D., Zimmerlin, B.: Fast Pyrolysis of Wheat Straw—Improvements of Operational Stability in 10 Years of Bioliq Pilot Plant Operation. *Energy & Fuels* **35**(14), 11333–11345 (2021)
84. Henrich, E., Dahmen, N., Weirich, F., Reimert, R., Kornmayer, C.: Fast pyrolysis of lignocellulosics in a twin screw mixer reactor. *Fuel Process. Technol.* **143**, 151–161 (2016)
85. Krutof, A., Hawboldt, K.: Blends of pyrolysis oil, petroleum, and other bio-based fuels: a review. *Renewable and Sustainable Energy Reviews* **59**, 406–419 (2016)
86. Dahmen, N., Henrich, E., Dinjus, E., Weirich, F.: The bioliq® bioslurry gasification process for the production of biosynfuels, organic chemicals, and energy. *Energy Sustainability Soc.* **2**(1), 1–44 (2012)
87. Emde, F.: Vinegar. In: *Ullmann's Encyclopedia of Industrial Chemistry*, pp. 1–24. Wiley-VCH Verlag GmbH & Co. KGaA, Weinheim, Germany (2000)
88. Le Berre, C., Serp, P., Kalck, P., Torrence, G.P.: Acetic Acid. *Ullmann's Encyclopedia of Industrial Chemistry*, 1–34 (2000)
89. Cramer, F.B.: Preparation of polyethylene terephthalate Patent 3,024,220
90. Kiefer, D., Merkel, M., Lilge, L., Henkel, M., Hausmann, R.: From acetate to bio-based products: underexploited potential for industrial biotechnology. *Trends Biotechnol.* **39**(4), 397–411 (2021)
91. Lim, H.G., Lee, J.H., Noh, M.H., Jung, G.Y.: Rediscovering acetate metabolism: its potential sources and utilization for biobased transformation into value-added chemicals. *Journal of agricultural and food chemistry* **66**(16), 3998–4006 (2018)
92. Haynes, A.: Catalytic methanol carbonylation. In: *Advances in catalysis*, vol. 53, pp. 1–45. Elsevier (2010)

93. BASF Ludwigshafen: Verfahren zur Darstellung von Kohlenwasserstoffen und deren Derivaten Patent 295202
94. Kim, J.-S., Choi, G.-G.: Pyrolysis of lignocellulosic biomass for biochemical production. In: Waste Biorefinery, pp. 323–348. Elsevier (2018)
95. Islam, Z.U., Zhisheng, Y., Hassan, E.B., Dongdong, C., Hongxun, Z.: Microbial conversion of pyrolytic products to biofuels: a novel and sustainable approach toward second-generation biofuels. *J. Ind. Microbiol. Biotechnol.* **42**(12), 1557–1579 (2015)
96. Robellet, X., Flippi, M., Pégot, S., MacCabe, A.P., Vélot, C.: AcpA, a member of the GPR1/FUN34/YaaH membrane protein family, is essential for acetate permease activity in the hyphal fungus *Aspergillus nidulans*. *Biochem. J* **412**(3), 485–493 (2008)
97. Jolkver, E., Emer, D., Ballan, S., Krämer, R., Eikmanns, B.J., Marin, K.: Identification and characterization of a bacterial transport system for the uptake of pyruvate, propionate, and acetate in *Corynebacterium glutamicum*. *J. Bacteriol.* **191**(3), 940–948 (2009)
98. Paiva, S., Devaux, F., Barbosa, S., Jacq, C., Casal, M.: Ady2p is essential for the acetate permease activity in the yeast *Saccharomyces cerevisiae*. *Yeast* **21**(3), 201–210 (2004)
99. Kornberg, H.L., Madsen, N.B.: The metabolism of C<sub>2</sub> compounds in micro-organisms. 3. Synthesis of malate from acetate via the glyoxylate cycle. *Biochem. J* **68**(3), 549 (1958)
100. Arnold, S., Tews, T., Kiefer, M., Henkel, M., Hausmann, R.: Evaluation of small organic acids present in fast pyrolysis bio-oil from lignocellulose as feedstocks for bacterial bioconversion. *GCB Bioenergy* **11**(10), 1159–1172 (2019)
101. Noh, M.H., Lim, H.G., Woo, S.H., Song, J., Jung, G.Y.: Production of itaconic acid from acetate by engineering acid-tolerant *Escherichia coli* W. *Biotechnol. Bioeng.* **115**(3), 729–738 (2018)
102. Uwineza, C., Sar, T., Mahboubi, A., Taherzadeh, M.J.: Evaluation of the cultivation of *Aspergillus oryzae* on organic waste-derived vfa effluents and its potential application as alternative sustainable nutrient source for animal feed. *Sustainability* **13**(22), 12489 (2021)
103. Uwineza, C., Mahboubi, A., Atmowidjojo, A., Ramadhani, A., Wainaina, S., Millati, R., Wikandari, R., Niklasson, C., Taherzadeh, M.J.: Cultivation of edible filamentous fungus *Aspergillus oryzae* on volatile fatty acids derived from anaerobic digestion of food waste and cow manure. *Bioresource technology* **337**, 125410 (2021)
104. Kövilein, A., Umpfenbach, J., Ochsenreither, K.: Acetate as substrate for l-malic acid production with *Aspergillus oryzae* DSM 1863. *Biotechnol. Biofuels* **14**(1), 1–15 (2021)

105. Oswald, F., Dörsam, S., Veith, N., Zwick, M., Neumann, A., Ochsenreither, K., Syldatk, C.: Sequential mixed cultures: from syngas to malic acid. *Frontiers in microbiology* **7**, 891 (2016)
106. Hu, P., Chakraborty, S., Kumar, A., Woolston, B., Liu, H., Emerson, D., Stephanopoulos, G.: Integrated bioprocess for conversion of gaseous substrates to liquids. *Proceedings of the National Academy of Sciences* **113**(14), 3773–3778 (2016)
107. Huang, X.-F., Liu, J.-N., Lu, L.-J., Peng, K.-M., Yang, G.-X., Liu, J.: Culture strategies for lipid production using acetic acid as sole carbon source by *Rhodospiridium toruloides*. *Bioresour. Technol.* **206**, 141–149 (2016)
108. Fei, Q., Chang, H.N., Shang, L., Kim, N., Kang, J.: The effect of volatile fatty acids as a sole carbon source on lipid accumulation by *Cryptococcus albidus* for biodiesel production. *Bioresource technology* **102**(3), 2695–2701 (2011)
109. Huang, X., Chen, R., Yuan, M., Liu, J.: Efficient bioconversion of high-content volatile fatty acids into microbial lipids by *Cryptococcus curvatus* ATCC 20509. *Bioresource technology* **239**, 394–401 (2017)
110. Lian, J., Garcia-Perez, M., Coates, R., Wu, H., Chen, S.: Yeast fermentation of carboxylic acids obtained from pyrolytic aqueous phases for lipid production. *Bioresour. Technol.* **118**, 177–186 (2012)
111. Shen, D.K., Gu, S.: The mechanism for thermal decomposition of cellulose and its main products. *Bioresour. Technol.* **100**(24), 6496–6504 (2009)
112. Hu, B., Lu, Q., Jiang, X., Liu, J., Cui, M., Dong, C., Yang, Y.: Formation mechanism of hydroxyacetone in glucose pyrolysis: A combined experimental and theoretical study. *Proc. Combust. Inst.* **37**(3), 2741–2748 (2019)
113. Paine III, J.B., Pithawalla, Y.B., Naworal, J.D.: Carbohydrate pyrolysis mechanisms from isotopic labeling: Part 3. The Pyrolysis of D-glucose: Formation of C3 and C4 carbonyl compounds and a cyclopentenedione isomer by electrocyclic fragmentation mechanisms. *Journal of Analytical and Applied Pyrolysis* **82**(1), 42–69 (2008)
114. Stefanidis, S.D., Kalogiannis, K.G., Iliopoulou, E.F., Michailof, C.M., Pilavachi, P.A., Lappas, A.A.: A study of lignocellulosic biomass pyrolysis via the pyrolysis of cellulose, hemicellulose and lignin. *Journal of Analytical and Applied Pyrolysis* **105**, 143–150 (2014)
115. Patwardhan, P.R., Brown, R.C., Shanks, B.H.: Product distribution from the fast pyrolysis of hemicellulose. *ChemSusChem* **4**(5), 636–643 (2011)
116. Levene, P.A., Walti, A.: Acetol: 2-Propanone, 1-hydroxy-. *Org. Synth.* **10**, 1 (1930)

117. Basu, S., Sen, A.K.: A review on catalytic dehydration of glycerol to acetol. *ChemBioEng Rev.* **8**(6), 633–653 (2021)
118. Dasari, M.A., Kiatsimkul, P.-P., Sutterlin, W.R., Suppes, G.J.: Low-pressure hydrogenolysis of glycerol to propylene glycol. *Appl. Catal., A* **281**(1-2), 225–231 (2005)
119. Saxena, R.K., Anand, P., Saran, S., Isar, J., Agarwal, L.: Microbial production and applications of 1, 2-propanediol. *Indian Journal of Microbiology* **50**(1), 2–11 (2010)
120. Li, G., Li, N., Li, S., Wang, A., Cong, Y., Wang, X., Zhang, T.: Synthesis of renewable diesel with hydroxyacetone and 2-methyl-furan. *Chem. Commun.* **49**(51), 5727–5729 (2013)
121. Yu, A.-N., Tan, Z.-W., Wang, F.-S.: Mechanistic studies on the formation of pyrazines by Maillard reaction between L-ascorbic acid and L-glutamic acid. *LWT Food Sci. Technol.* **50**(1), 64–71 (2013)
122. Yaylayan, V.A., Keyhani, A.: Origin of carbohydrate degradation products in L-alanine/D-[13C] glucose model systems. *Journal of agricultural and food chemistry* **48**(6), 2415–2419 (2000)
123. Taylor, D.G., Trudgill, P.W., Cripps, R.E., Harris, P.R.: The microbial metabolism of acetone. *Microbiology* **118**(1), 159–170 (1980)
124. Ashraf, W., Mihdhir, A., Colin Murrell, J.: Bacterial oxidation of propane. *FEMS Microbiol. Lett.* **122**(1-2), 1–6 (1994)
125. Kotani, T., Yurimoto, H., Kato, N., Sakai, Y.: Novel acetone metabolism in a propane-utilizing bacterium, *Gordonia* sp. strain TY-5. *J. Bacteriol.* **189**(3), 886–893 (2007)
126. Hartmans, S., Bont, J. am de: Acetol monooxygenase from *Mycobacterium* Pyl cleaves acetol into acetate and formaldehyde. *FEMS Microbiol. Lett.* **36**(2-3), 155–158 (1986)
127. Cooper, R.A.: Metabolism of methylglyoxal in microorganisms. *Annual Reviews in Microbiology* **38**(1), 49–68 (1984)
128. Inoue, Y., Kimura, A.: Methylglyoxal and regulation of its metabolism in microorganisms. *Advances in microbial physiology* **37**, 177–227 (1995)
129. Willetts, A.J., Turner, J.M.: Threonine metabolism in a strain of *Bacillus subtilis*: enzymes acting on methylglyoxal. *Biochimica et Biophysica Acta (BBA)-General Subjects* **222**(3), 668–670 (1970)
130. Higgins, I.J., Turner, J.M.: Enzymes of methylglyoxal metabolism in a Pseudomand which rapidly metabolizes aminoacetone. *Biochimica et Biophysica Acta (BBA)-General Subjects* **184**(2), 464–467 (1969)

131. Rhee, H.-I., Watanabe, K., Murata, K., Kimura, A.: Metabolism of 2-ketoaldehydes in bacteria: oxidative conversion of methylglyoxal to pyruvate by an enzyme from *Pseudomonas putida*. *Agricultural and biological chemistry* **51**(4), 1059–1066 (1987)
132. Simon, E.S., Plante, R., Whitesides, G.M.: D-lactate dehydrogenase. *Applied Biochemistry and Biotechnology* **22**(2), 169–179 (1989)
133. Bennett, G.N., San, K.-Y.: Microbial formation, biotechnological production and applications of 1, 2-propanediol. *Appl. Microbiol. Biotechnol.* **55**(1), 1–9 (2001)
134. Tran-Din, K., Gottschalk, G.: Formation of D (-)-1, 2-propanediol and D (-)-lactate from glucose by *Clostridium sphenoides* under phosphate limitation. *Arch. Microbiol.* **142**(1), 87–92 (1985)
135. Cameron, D.C., Cooney, C.L.: A novel fermentation: the production of R (-)-1, 2-propanediol and acetol by *Clostridium thermosaccharolyticum*. *Bio/technology* **4**(7), 651–654 (1986)
136. Jeon, E., Lee, S., Kim, D., Yoon, H., Oh, M., Park, C., Lee, J.: Development of a *Saccharomyces cerevisiae* strain for the production of 1, 2-propanediol by gene manipulation. *Enzyme Microb. Technol.* **45**(1), 42–47 (2009)
137. Lee, W., DaSilva, N.A.: Application of sequential integration for metabolic engineering of 1, 2-propanediol production in yeast. *Metab. Eng.* **8**(1), 58–65 (2006)
138. Kometani, T., Kitatsuji, E., Matsuno, R.: Bioreduction of ketones mediated by baker's yeast with acetate as ultimate reducing agent. *Agric. Biol. Chem.* **55**(3), 867–868 (1991)
139. Kometani, T., Kitatsuji, E., Matsuno, R.: Baker's yeast mediated bioreduction: practical procedure using EtOH as energy source. *J. Ferment. Bioeng.* **71**(3), 197–199 (1991)
140. Levine, A.S., Fellers, C.R.: Action of acetic acid on food spoilage microorganisms. *J. Bacteriol.* **39**(5), 499–515 (1940)
141. Liang, G., Du, G., Chen, J.: Salt-induced osmotic stress for glutathione overproduction in *Candida utilis*. *Enzyme and microbial technology* **45**(4), 324–329 (2009)
142. Oliveira, M.V.V. de, Intorne, A.C., Vespoli, L.d.S., Madureira, H.C., Leandro, M.R., Pereira, T.N.S., Olivares, F.L., Berbert-Molina, M.A., Souza Filho, G.A. de: Differential effects of salinity and osmotic stress on the plant growth-promoting bacterium *Gluconacetobacter diazotrophicus* PAL5. *Arch. Microbiol.* **198**(3), 287–294 (2016)
143. He, B., Ma, L., Hu, Z., Li, H., Ai, M., Long, C., Zeng, B.: Deep sequencing analysis of transcriptomes in *Aspergillus oryzae* in response to salinity stress. *Appl. Microbiol. Biotechnol.* **102**(2), 897–906 (2018)

144. Legiša, M., Golič Grdadolnik, S.: Influence of dissolved oxygen concentration on intracellular pH and consequently on growth rate of *Aspergillus niger*. *Food Technology and Biotechnology* **40**(1), 27–32 (2002)
145. Stratford, M., Nebe-von-Caron, G., Steels, H., Novodvorska, M., Ueckert, J., Archer, D.B.: Weak-acid preservatives: pH and proton movements in the yeast *Saccharomyces cerevisiae*. *Int. J. Food Microbiol.* **161**(3), 164–171 (2013)
146. Roe, A.J., McLaggan, D., Davidson, I., O’Byrne, C., Booth, I.R.: Perturbation of anion balance during inhibition of growth of *Escherichia coli* by weak acids. *J. Bacteriol.* **180**(4), 767–772 (1998)
147. Roe, A.J., O’Byrne, C., McLaggan, D., Booth, I.R.: Inhibition of *Escherichia coli* growth by acetic acid: a problem with methionine biosynthesis and homocysteine toxicity. *Microbiology* **148**(7), 2215–2222 (2002)
148. Lian, J., Chen, S., Zhou, S., Wang, Z., O’Fallon, J., Li, C.-Z., Garcia-Perez, M.: Separation, hydrolysis and fermentation of pyrolytic sugars to produce ethanol and lipids. *Bioresour. Technol.* **101**(24), 9688–9699 (2010)
149. Dörsam, S., Kirchoff, J., Bigalke, M., Dahmen, N., Syldatk, C., Ochsenreither, K.: Evaluation of Pyrolysis Oil as Carbon Source for Fungal Fermentation. *Front. Microbiol.* **7**, 2059 (2016)
150. Lourencon, T.V., Mattos, B.D., Cademartori, P.H.G., Le Magalhães, W.: Bio-oil from a fast pyrolysis pilot plant as antifungal and hydrophobic agent for wood preservation. *Journal of Analytical and Applied Pyrolysis* **122**, 1–6 (2016)
151. Mohan, D., Shi, J., Nicholas, D.D., Pittman Jr, C.U., Steele, P.H., Cooper, J.E.: Fungicidal values of bio-oils and their lignin-rich fractions obtained from wood/bark fast pyrolysis. *Chemosphere* **71**(3), 456–465 (2008)
152. Firouzbehi, F., Efhamisizi, D., Hamzeh, Y., Tarmian, A., Oladi, R.: Pyrolysis acid as sustainable wood preservative against rot fungi. *Biofuels, Bioprod. Biorefin.* **15**(1), 74–84 (2021)
153. Gao, Z., Li, N., Chen, M., Yi, W.: Comparative study on the pyrolysis of cellulose and its model compounds. *Fuel Processing Technology* **193**, 131–140 (2019)
154. Lee, K.-H., Furukawa, H., Huang, E.-S.: Antitumor agents. 3. Synthesis and cytotoxic activity of helenalin amine adducts and related derivatives. *J. Med. Chem.* **15**(6), 609–611 (1972)
155. Lee, K., Ibuka, T., Wu, R.: Beta unsubstituted cyclopentenone, a structural requirement for antimicrobial and cytotoxic activities. *Chem. Pharm. Bull.* **22**(9), 2206–2208 (1974)

156. Dong, C., Zhang, Z., Lu, Q., Yang, Y.: Characteristics and mechanism study of analytical fast pyrolysis of poplar wood. *Energy Conversion and Management* **57**, 49–59 (2012)
157. Kabbour, M., Luque, R.: Furfural as a platform chemical: From production to applications. *Biomass, Biofuels, Biochemicals*, 283–297 (2020)
158. Rosatella, A.A., Simeonov, S.P., Frade, R.F.M., Afonso, C. am: 5-Hydroxymethylfurfural (HMF) as a building block platform: Biological properties, synthesis and synthetic applications. *Green Chem.* **13**(4), 754–793 (2011)
159. Mariscal, R., Maireles-Torres, P., Ojeda, M., Sádaba, I., Granados, M.L.: Furfural: a renewable and versatile platform molecule for the synthesis of chemicals and fuels. *Energy Environ. Sci.* **9**(4), 1144–1189 (2016)
160. Bozell, J.J., Petersen, G.R.: Technology development for the production of biobased products from biorefinery carbohydrates—the US Department of Energy’s “Top 10” revisited. *Green Chem.* **12**(4), 539–554 (2010)
161. Li, Y., Hu, B., Naqvi, S.R., Zhang, Z., Li, K., Lu, Q.: Selective preparation of 5-hydroxymethylfurfural by catalytic fast pyrolysis of cellulose over zirconium-tin mixed metal oxides. *Journal of Analytical and Applied Pyrolysis* **155**, 105103 (2021)
162. Lu, Q., Dong, C., Zhang, X., Tian, H., Yang, Y., Zhu, X.: Selective fast pyrolysis of biomass impregnated with ZnCl<sub>2</sub> to produce furfural: Analytical Py-GC/MS study. *Journal of Analytical and Applied Pyrolysis* **90**(2), 204–212 (2011)
163. Zdzienicka, M., Tudek, B., Zieleńska, M., Szymczyk, T.: Mutagenic activity of furfural in *Salmonella typhimurium* TA100. *Mutation Research/Genetic Toxicology* **58**(2-3), 205–209 (1978)
164. Khan, Q.A., Hadi, S.M.: Effect of furfural on plasmid DNA. *Biochem. Mol. Biol. Int.* **29**(6), 1153–1160 (1993)
165. Allen, S.A., Clark, W., McCaffery, J.M., Cai, Z., Lanctot, A., Slininger, P.J., Liu, Z.L., Gorsich, S.W.: Furfural induces reactive oxygen species accumulation and cellular damage in *Saccharomyces cerevisiae*. *Biotechnology for biofuels* **3**(1), 1–10 (2010)
166. Modig, T., Liden, G., Taherzadeh, M.J.: Inhibition effects of furfural on alcohol dehydrogenase, aldehyde dehydrogenase and pyruvate dehydrogenase. *Biochem. J* **363**(3), 769–776 (2002)
167. Banerjee, N., Bhatnagar, R., Viswanathan, L.: Inhibition of glycolysis by furfural in *Saccharomyces cerevisiae*. *Eur. J. Appl. Microbiol. Biotechnol.* **11**(4), 226–228 (1981)
168. Miller, E.N., Jarboe, L.R., Turner, P.C., Pharkya, P., Yomano, L.P., York, S.W., Nunn, D., Shanmugam, K.T., Ingram, L.O.: Furfural inhibits growth by limiting sulfur assimilation

- in ethanologenic *Escherichia coli* strain LY180. *Appl. Environ. Microbiol.* **75**(19), 6132–6141 (2009)
169. Miller, E.N., Jarboe, L.R., Yomano, L.P., York, S.W., Shanmugam, K.T., Lo Ingram: Silencing of NADPH-dependent oxidoreductase genes (*yqhD* and *dkgA*) in furfural-resistant ethanologenic *Escherichia coli*. *Appl. Environ. Microbiol.* **75**(13), 4315–4323 (2009)
170. Petersson, A., Almeida, J.R.M., Modig, T., Karhumaa, K., Hahn-Hägerdal, B., Gorwa-Grauslund, M.F., Lidén, G.: A 5-hydroxymethyl furfural reducing enzyme encoded by the *Saccharomyces cerevisiae ADH6* gene conveys HMF tolerance. *Yeast* **23**(6), 455–464 (2006)
171. Heer, D., Heine, D., Sauer, U.: Resistance of *Saccharomyces cerevisiae* to high concentrations of furfural is based on NADPH-dependent reduction by at least two oxidoreductases. *Appl. Environ. Microbiol.* **75**(24), 7631–7638 (2009)
172. Zhao, X., Tang, J., Wang, X., Yang, R., Zhang, X., Gu, Y., Li, X., Ma, M.: YNL134C from *Saccharomyces cerevisiae* encodes a novel protein with aldehyde reductase activity for detoxification of furfural derived from lignocellulosic biomass. *Yeast* **32**(5), 409–422 (2015)
173. Divate, N.R., Huang, P.-J., Chen, G.-H., Chung, Y.-C.: Construction of Recombinant *Saccharomyces cerevisiae* with Ethanol and Aldehydes Tolerance via Overexpression of Aldehyde Reductase. *Microorganisms* **10**(5), 850 (2022)
174. Lewis Liu, Z., Moon, J., Andersh, B.J., Slininger, P.J., Weber, S.: Multiple gene-mediated NAD (P) H-dependent aldehyde reduction is a mechanism of in situ detoxification of furfural and 5-hydroxymethylfurfural by *Saccharomyces cerevisiae*. *Appl. Microbiol. Biotechnol.* **81**(4), 743–753 (2008)
175. Ask, M., Bettiga, M., Mapelli, V., Olsson, L.: The influence of HMF and furfural on redox-balance and energy-state of xylose-utilizing *Saccharomyces cerevisiae*. *Biotechnology for biofuels* **6**(1), 1–13 (2013)
176. Singh, R., Mailloux, R.J., Puiseux-Dao, S., Appanna, V.D.: Oxidative stress evokes a metabolic adaptation that favors increased NADPH synthesis and decreased NADH production in *Pseudomonas fluorescens*. *J. Bacteriol.* **189**(18), 6665–6675 (2007)
177. Wang, X., Miller, E.N., Yomano, L.P., Zhang, X., Shanmugam, K.T., Lo Ingram: Increased furfural tolerance due to overexpression of NADH-dependent oxidoreductase FucO in *Escherichia coli* strains engineered for the production of ethanol and lactate. *Appl. Environ. Microbiol.* **77**(15), 5132–5140 (2011)

178. Jilani, S.B., Prasad, R., Yazdani, S.S.: Overexpression of Oxidoreductase YghA Confers Tolerance of Furfural in Ethanologenic *Escherichia coli* Strain SSK42. *Appl. Environ. Microbiol.* **87**(23), e01855-21 (2021)
179. Sauer, U., Canonaco, F., Heri, S., Perrenoud, A., Fischer, E.: The soluble and membrane-bound transhydrogenases UdhA and PntAB have divergent functions in NADPH metabolism of *Escherichia coli*. *J. Biol. Chem.* **279**(8), 6613–6619 (2004)
180. Almeida, J.R.M., Röder, A., Modig, T., Laadan, B., Lidén, G., Gorwa-Grauslund, M.-F.: NADH-vs NADPH-coupled reduction of 5-hydroxymethyl furfural (HMF) and its implications on product distribution in *Saccharomyces cerevisiae*. *Appl. Microbiol. Biotechnol.* **78**(6), 939–945 (2008)
181. Wang, X., Gao, Q., Bao, J.: Enhancement of furan aldehydes conversion in *Zymomonas mobilis* by elevating dehydrogenase activity and cofactor regeneration. *Biotechnology for biofuels* **10**(1), 1–9 (2017)
182. Liu, Z.L., Moon, J.: A novel NADPH-dependent aldehyde reductase gene from *Saccharomyces cerevisiae* NRRL Y-12632 involved in the detoxification of aldehyde inhibitors derived from lignocellulosic biomass conversion. *Gene* **446**(1), 1–10 (2009)
183. Liu, C.-G., Li, K., Li, K.-Y., Sakdaronnarong, C., Mehmood, M.A., Zhao, X.-Q., Bai, F.-W.: Intracellular redox perturbation in *Saccharomyces cerevisiae* improved furfural tolerance and enhanced cellulosic bioethanol production. *Front. Bioeng. Biotechnol.* **8**, 615 (2020)
184. Chen, D., Cang, R., Zhang, Z.-D., Huang, H., Zhang, Z.-G., Ji, X.-J.: Efficient reduction of 5-hydroxymethylfurfural to 2, 5-bis (hydroxymethyl) furan by a fungal whole-cell biocatalyst. *Mol. Catal.* **500**, 111341 (2021)
185. Feldman, D., Kowbel, D.J., Glass, N.L., Yarden, O., Hadar, Y.: Detoxification of 5-hydroxymethylfurfural by the *Pleurotus ostreatus* lignolytic enzymes aryl alcohol oxidase and dehydrogenase. *Biotechnology for biofuels* **8**(1), 1–11 (2015)
186. Troiano, D., Orsat, V., Meyer, F., Dumont, M.-J.: Recyclable immobilized *Trichoderma reesei* whole-cells for the catalytic oxidation of 5-hydroxymethylfurfural. *Biomass and Bioenergy* **160**, 106442 (2022)
187. Zheng, Y., Yu, X., Zeng, J., Chen, S.: Feasibility of filamentous fungi for biofuel production using hydrolysate from dilute sulfuric acid pretreatment of wheat straw. *Biotechnology for biofuels* **5**(1), 1–10 (2012)

188. Nichols, N.N., Sharma, L.N., Mowery, R.A., Chambliss, C.K., van Walsum, G.P., Dien, B.S., Iten, L.B.: Fungal metabolism of fermentation inhibitors present in corn stover dilute acid hydrolysate. *Enzyme Microb. Technol.* **42**(7), 624–630 (2008)
189. Ran, H., Zhang, J., Gao, Q., Lin, Z., Bao, J.: Analysis of biodegradation performance of furfural and 5-hydroxymethylfurfural by *Amorphotheca resinae* ZN1. *Biotechnology for biofuels* **7**(1), 1–12 (2014)
190. López, M.J., Nichols, N.N., Dien, B.S., Moreno, J., Bothast, R.J.: Isolation of microorganisms for biological detoxification of lignocellulosic hydrolysates. *Applied microbiology and biotechnology* **64**(1), 125–131 (2004)
191. Wierckx, N., Koopman, F., Bandounas, L., Winde, J.H. de, Ruijsenaars, H.J.: Isolation and characterization of *Cupriavidus basilensis* HMF14 for biological removal of inhibitors from lignocellulosic hydrolysate. *Microb. Biotechnol.* **3**(3), 336–343 (2010)
192. Trudgill, P.W.: The metabolism of 2-furoic acid by *Pseudomonas* F2. *Biochem. J* **113**(4), 577–587 (1969)
193. Wierckx, N., Koopman, F., Ruijsenaars, H.J., Winde, J.H. de: Microbial degradation of furanic compounds: biochemistry, genetics, and impact. *Appl. Microbiol. Biotechnol.* **92**(6), 1095–1105 (2011)
194. Koopman, F., Wierckx, N., Winde, J.H. de, Ruijsenaars, H.J.: Identification and characterization of the furfural and 5-(hydroxymethyl) furfural degradation pathways of *Cupriavidus basilensis* HMF14. *Proc. Natl. Acad. Sci. U.S.A.* **107**(11), 4919–4924 (2010)
195. Henson, W.R., Meyers, A.W., Jayakody, L.N., DeCapite, A., Black, B.A., Michener, W.E., Johnson, C.W., Beckham, G.T.: Biological upgrading of pyrolysis-derived wastewater: Engineering *Pseudomonas putida* for alkylphenol, furfural, and acetone catabolism and (methyl) muconic acid production. *Metab. Eng.* **68**, 14–25 (2021)
196. Hsu, C.-T., Kuo, Y.-C., Liu, Y.-C., Tsai, S.-L.: Green conversion of 5-hydroxymethylfurfural to furan-2, 5-dicarboxylic acid by heterogeneous expression of 5-hydroxymethylfurfural oxidase in *Pseudomonas putida* S12. *Microbial biotechnology* **13**(4), 1094–1102 (2020)
197. Evans, R.J., Milne, T.A.: Molecular characterization of the pyrolysis of biomass. *Energy & Fuels* **1**(2), 123–137 (1987)
198. Zhang, L., Larsson, A., Moldin, A., Edlund, U.: Comparison of lignin distribution, structure, and morphology in wheat straw and wood. *Ind. Crops Prod.* **187**, 115432 (2022)
199. Isikgor, F.H., Becer, C.R.: Lignocellulosic biomass: a sustainable platform for the production of bio-based chemicals and polymers. *Polym. Chem.* **6**(25), 4497–4559 (2015)

200. Larsson, S., Quintana-Sáinz, A., Reimann, A., Nilvebrant, N.-O., Jönsson, L.J.: Influence of lignocellulose-derived aromatic compounds on oxygen-limited growth and ethanolic fermentation by *Saccharomyces cerevisiae*. *Appl. Biochem. Biotechnol.* **84–86**, 617–632 (2000)
201. Sierra-Alvarez, R., Lettinga, G.: The effect of aromatic structure on the inhibition of acetoclastic methanogenesis in granular sludge. *Appl. Microbiol. Biotechnol.* **34**(4), 544–550 (1991)
202. Keweloh, H., Weyrauch, G., Rehm, H.-J.: Phenol-induced membrane changes in free and immobilized *Escherichia coli*. *Appl. Microbiol. Biotechnol.* **33**(1), 66–71 (1990)
203. Heipieper, H.-J., Keweloh, H., Rehm, H.-J.: Influence of phenols on growth and membrane permeability of free and immobilized *Escherichia coli*. *Appl. Environ. Microbiol.* **57**(4), 1213–1217 (1991)
204. Zaldivar, J., Martinez, A., Ingram, L.O.: Effect of selected aldehydes on the growth and fermentation of ethanologenic *Escherichia coli*. *Biotechnol. Bioeng.* **65**(1), 24–33 (1999)
205. Palmqvist, E., Grage, H., Meinander, N.Q., Hahn-Hägerdal, B.: Main and interaction effects of acetic acid, furfural, and p-hydroxybenzoic acid on growth and ethanol productivity of yeasts. *Biotechnol. Bioeng.* **63**(1), 46–55 (1999)
206. Mussatto, S.I., Roberto, I.C.: Alternatives for detoxification of diluted-acid lignocellulosic hydrolyzates for use in fermentative processes: a review. *Bioresource technology* **93**(1), 1–10 (2004)
207. Okuda, N., Soneura, M., Ninomiya, K., Katakura, Y., Shioya, S.: Biological detoxification of waste house wood hydrolysate using *Ureibacillus thermosphaericus* for bioethanol production. *J. Biosci. Bioeng.* **106**(2), 128–133 (2008)
208. Schneider, H.: Selective removal of acetic acid from hardwood-spent sulfite liquor using a mutant yeast. *Enzyme and microbial technology* **19**(2), 94–98 (1996)
209. Fonseca, B.G., Moutta, R.d.O., Ferraz, F.d.O., Vieira, E.R., Nogueira, A.S., Baratella, B.F., Rodrigues, L.C., Hou-Rui, Z., Da Silva, S.S.: Biological detoxification of different hemicellulosic hydrolysates using *Issatchenkia occidentalis* CCTCC M 206097 yeast. *J. Ind. Microbiol. Biotechnol.* **38**(1), 199–207 (2011)
210. Nichols, N.N., Hector, R.E., Frazer, S.E. (eds.): Bioabatement to remove inhibitors from biomass-derived sugar hydrolysates. *Twenty-Sixth Symposium on Biotechnology for Fuels and Chemicals*. Springer (2005)

211. Palmqvist, E., Hahn-Hägerdal, B., Szengyel, Z., Zacchi, G., Réczey, K.: Simultaneous detoxification and enzyme production of hemicellulose hydrolysates obtained after steam pretreatment. *Enzyme and microbial technology* **20**(4), 286–293 (1997)
212. Yu, Y., Feng, Y., Xu, C., Liu, J., Li, D.: Onsite bio-detoxification of steam-exploded corn stover for cellulosic ethanol production. *Bioresource technology* **102**(8), 5123–5128 (2011)
213. Moreno, A.D., Ibarra, D., Alvira, P., Tomás-Pejó, E., Ballesteros, M.: A review of biological delignification and detoxification methods for lignocellulosic bioethanol production. *Crit. Rev. Biotechnol.* **35**(3), 342–354 (2015)
214. Zhu, J., Yong, Q., Xu, Y., Yu, S.: Detoxification of corn stover prehydrolyzate by trialkylamine extraction to improve the ethanol production with *Pichia stipitis* CBS 5776. *Bioresource technology* **102**(2), 1663–1668 (2011)
215. Persson, P., Larsson, S., Jönsson, L.J., Nilvebrant, N.-O., Sivik, B., Munteanu, F., Thörneby, L., Lo Gorton: Supercritical fluid extraction of a lignocellulosic hydrolysate of spruce for detoxification and to facilitate analysis of inhibitors. *Biotechnol. Bioeng.* **79**(6), 694–700 (2002)
216. Larsson, S., Reimann, A., Nilvebrant, N.-O., Jönsson, L.J.: Comparison of different methods for the detoxification of lignocellulose hydrolyzates of spruce. *Appl. Biochem. Biotechnol.* **77**(1), 91–103 (1999)
217. Nilvebrant, N.-O., Reimann, A., Larsson, S., Jönsson, L.J.: Detoxification of lignocellulose hydrolysates with ion-exchange resins. *Applied Biochemistry and Biotechnology* **91**(1), 35–49 (2001)
218. Zhang, Y., Xia, C., Lu, M., Tu, M.: Effect of overliming and activated carbon detoxification on inhibitors removal and butanol fermentation of poplar prehydrolysates. *Biotechnol. Biofuels* **11**(1), 1–14 (2018)
219. Chi, Z., Rover, M., Jun, E., Deaton, M., Johnston, P., Brown, R.C., Wen, Z., Jarboe, L.R.: Overliming detoxification of pyrolytic sugar syrup for direct fermentation of levoglucosan to ethanol. *Bioresour. Technol.* **150**, 220–227 (2013)
220. Alriksson, B., Horváth, I.S., Sjöde, A., Nilvebrant, N.-O., Jönsson, L.J.: Ammonium hydroxide detoxification of spruce acid hydrolysates. *Appl. Biochem. Biotechnol.* **124**(1), 911–922 (2005)
221. Liang, Y., Zhao, X., Chi, Z., Rover, M., Johnston, P., Brown, R., Jarboe, L., Wen, Z.: Utilization of acetic acid-rich pyrolytic bio-oil by microalga *Chlamydomonas reinhardtii*:

- reducing bio-oil toxicity and enhancing algal toxicity tolerance. *Bioresour. Technol.* **133**, 500–506 (2013)
222. Zhao, X., Davis, K., Brown, R., Jarboe, L., Wen, Z.: Alkaline treatment for detoxification of acetic acid-rich pyrolytic bio-oil for microalgae fermentation: Effects of alkaline species and the detoxification mechanisms. *Biomass Bioenergy* **80**, 203–212 (2015)
223. Zhao, X., Chi, Z., Rover, M., Brown, R., Jarboe, L., Wen, Z.: Microalgae fermentation of acetic acid-rich pyrolytic bio-oil: Reducing bio-oil toxicity by alkali treatment. *Environ. Prog. Sustainable Energy* **32**(4), 955–961 (2013)
224. Nguyen, N., Fargues, C., Guiga, W., Lameloise, M.-L.: Assessing nanofiltration and reverse osmosis for the detoxification of lignocellulosic hydrolysates. *Journal of Membrane Science* **487**, 40–50 (2015)
225. Weng, Y.-H., Wei, H.-J., Tsai, T.-Y., Lin, T.-H., Wei, T.-Y., Guo, G.-L., Huang, C.-P.: Separation of furans and carboxylic acids from sugars in dilute acid rice straw hydrolysates by nanofiltration. *Bioresource technology* **101**(13), 4889–4894 (2010)
226. Pan, L., He, M., Wu, B., Wang, Y., Hu, G., Ma, K.: Simultaneous concentration and detoxification of lignocellulosic hydrolysates by novel membrane filtration system for bioethanol production. *J. Cleaner Prod.* **227**, 1185–1194 (2019)
227. Converti, A., Domínguez, J.M., Perego, P., Da Silva, S.S., Zilli, M.: Wood hydrolysis and hydrolyzate detoxification for subsequent xylitol production. *Chemical Engineering & Technology* **23**(11), 1013–1020 (2000)
228. Lange, J., Müller, F., Bernecker, K., Dahmen, N., Takors, R., Blombach, B.: Valorization of pyrolysis water: a biorefinery side stream, for 1, 2-propanediol production with engineered *Corynebacterium glutamicum*. *Biotechnol. Biofuels* **10**(1), 1–13 (2017)
229. Parajó, J.C., Dominguez, H., Domínguez, J.M.: Improved xylitol production with *Debaryomyces hansenii* Y-7426 from raw or detoxified wood hydrolysates. *Enzyme and microbial technology* **21**(1), 18–24 (1997)
230. Rodrigues, R., Felipe, M.G., Silva, J.B., Vitolo, M., Gómez, P.V.: The influence of pH, temperature and hydrolyzate concentration on the removal of volatile and nonvolatile compounds from sugarcane bagasse hemicellulosic hydrolyzate treated with activated charcoal before or after vacuum evaporation. *Braz. J. Chem. Eng.* **18**, 299–311 (2001)
231. Hodge, D.B., Andersson, C., Berglund, K.A., Rova, U.: Detoxification requirements for bioconversion of softwood dilute acid hydrolysates to succinic acid. *Enzyme Microb. Technol.* **44**(5), 309–316 (2009)

232. Parajó, J.C., Domínguez, H., Domínguez, J.M.: Xylitol production from Eucalyptus wood hydrolysates extracted with organic solvents. *Process Biochemistry* **32**(7), 599–604 (1997)
233. Barratt, R.W., Johnson, G.B., Ogata, W.N.: Wild-type and mutant stocks of *Aspergillus nidulans*. *Genetics* **52**(1), 233 (1965)
234. Hill, T.W., Kafer, E.: Improved protocols for *Aspergillus* minimal medium: trace element and minimal medium salt stock solutions. *Fungal Genet. Rep.* **48**(1), 20–21 (2001)
235. Kurniawati, S., Nicell, J.A.: Characterization of *Trametes versicolor* laccase for the transformation of aqueous phenol. *Bioresource technology* **99**(16), 7825–7834 (2008)
236. Bioinformatics, B.: *FastQC: a quality control tool for high throughput sequence data*. Cambridge, UK: Babraham Institute (2011)
237. Machida, M., Asai, K., Sano, M., Tanaka, T., Kumagai, T., Terai, G., Kusumoto, K.-I., Arima, T., Akita, O., Kashiwagi, Y.: Genome sequencing and analysis of *Aspergillus oryzae*. *Nature* **438**(7071), 1157–1161 (2005)
238. Dobin, A., Gingeras, T.R.: Mapping RNA-seq reads with STAR. *Current protocols in bioinformatics* **51**(1), 11.14. 1-11.14. 19 (2015)
239. Li, B., Dewey, C.N.: RSEM: accurate transcript quantification from RNA-Seq data with or without a reference genome. *BMC Bioinf.* **12**(1), 1–16 (2011)
240. Ge, S.X., Son, E.W., Yao, R.: iDEP: an integrated web application for differential expression and pathway analysis of RNA-Seq data. *BMC Bioinf.* **19**(1), 1–24 (2018)
241. Love, M.I., Huber, W., Anders, S.: Moderated estimation of fold change and dispersion for RNA-seq data with DESeq2. *Genome Biol.* **15**(12), 1–21 (2014)
242. Luo, W., Pant, G., Bhavnasi, Y.K., Blanchard Jr, S.G., Brouwer, C.: Pathview Web: user friendly pathway visualization and data integration. *Nucleic Acids Res.* **45**(W1), W501-W508 (2017)
243. Huerta-Cepas, J., Szklarczyk, D., Heller, D., Hernández-Plaza, A., Forslund, S.K., Cook, H., Mende, D.R., Letunic, I., Rattei, T., Jensen, L.J.: eggNOG 5.0: a hierarchical, functionally and phylogenetically annotated orthology resource based on 5090 organisms and 2502 viruses. *Nucleic Acids Res.* **47**(D1), D309-D314 (2019)
244. UniProt Consortium: UniProt: a worldwide hub of protein knowledge. *Nucleic Acids Res.* **47**(D1), D506-D515 (2019)
245. Waterhouse, A.L.: Determination of total phenolics. *Curr. Protoc. Food Anal. Chem.* **6**(1), II. 1.1-II. 1.8 (2002)
246. Zhang, X., Zhang, Y., Qi, W., Yuan, Z., Wang, Z.: Comparative metabolomic analysis of furfural stress response in *Aspergillus terreus*. *Cellulose* **26**(15), 8227–8236 (2019)

247. Rajesh, R.O., Godan, T.K., Rai, A.K., Sahoo, D., Pandey, A., Binod, P.: Biosynthesis of 2, 5-furan dicarboxylic acid by *Aspergillus flavus* APLS-1: process optimization and intermediate product analysis. *Bioresource technology* **284**, 155–160 (2019)
248. He, B., Hu, Z., Ma, L., Li, H., Ai, M., Han, J., Zeng, B.: Transcriptome analysis of different growth stages of *Aspergillus oryzae* reveals dynamic changes of distinct classes of genes during growth. *BMC Microbiol.* **18**(1), 1–11 (2018)
249. Drew, D., North, R.A., Nagarathinam, K., Tanabe, M.: Structures and general transport mechanisms by the major facilitator superfamily (MFS). *Chem. Rev.* **121**(9), 5289–5335 (2021)
250. Semighini, C.P., Goldman, M.H.S., Goldman, G.H.: Multi-copy suppression of an *Aspergillus nidulans* mutant sensitive to camptothecin by a putative monocarboxylate transporter. *Curr. Microbiol.* **49**(4), 229–233 (2004)
251. Semchyshyn, H.M., Abrat, O.B., Miedzobrodzki, J., Inoue, Y., Lushchak, V.I.: Acetate but not propionate induces oxidative stress in bakers' yeast *Saccharomyces cerevisiae*. *Redox Rep.* **16**(1), 15–23 (2011)
252. Bajwa, P.K., Ho, C.-Y., Chan, C.-K., Martin, V.J.J., Trevors, J.T., Lee, H.: Transcriptional profiling of *Saccharomyces cerevisiae* T2 cells upon exposure to hardwood spent sulphite liquor: comparison to acetic acid, furfural and hydroxymethylfurfural. *Antonie van Leeuwenhoek* **103**(6), 1281–1295 (2013)
253. Döhren, H. von: A survey of nonribosomal peptide synthetase (NRPS) genes in *Aspergillus nidulans*. *Fungal Genetics and Biology* **46**(1), S45-S52 (2009)
254. Stergiopoulos, I., Zwiers, L.-H., Waard, M.A. de: Secretion of natural and synthetic toxic compounds from filamentous fungi by membrane transporters of the ATP-binding cassette and major facilitator superfamily. *Eur. J. Plant Pathol.* **108**(7), 719–734 (2002)
255. Imamura, K., Tsuyama, Y., Hirata, T., Shiraishi, S., Sakamoto, K., Yamada, O., Akita, O., Shimoi, H.: Identification of a gene involved in the synthesis of a dipeptidyl peptidase IV inhibitor in *Aspergillus oryzae*. *Appl. Environ. Microbiol.* **78**(19), 6996–7002 (2012)
256. Shinohara, Y., Tokuoka, M., Koyama, Y.: Functional analysis of the cyclopiazonic acid biosynthesis gene cluster in *Aspergillus oryzae* RIB 40. *Biosci. Biotechnol., Biochem.* **74**, 2249–2252 (2011)
257. Shinohara, Y., Nishimura, I., Koyama, Y.: Identification of a gene cluster for biosynthesis of the sesquiterpene antibiotic, heptelidic acid, in *Aspergillus oryzae*. *Biosci. Biotechnol., Biochem.* **83**(8), 1506–1513 (2019)

258. Marui, J., Yamane, N., Ohashi-Kunihiro, S., Ando, T., Terabayashi, Y., Sano, M., Ohashi, S., Ohshima, E., Tachibana, K., Higa, Y.: Kojic acid biosynthesis in *Aspergillus oryzae* is regulated by a Zn (II) 2Cys6 transcriptional activator and induced by kojic acid at the transcriptional level. *Journal of bioscience and bioengineering* **112**(1), 40–43 (2011)
259. Lebar, M.D., Cary, J.W., Majumdar, R., Carter-Wientjes, C.H., Mack, B.M., Wei, Q., Uka, V., Saeger, S. de, Di Mavungu, J.D.: Identification and functional analysis of the aspergillic acid gene cluster in *Aspergillus flavus*. *Fungal Genetics and Biology* **116**, 14–23 (2018)
260. Bauer, B.E., Rossington, D., Mollapour, M., Mamnun, Y., Kuchler, K., Piper, P.W.: Weak organic acid stress inhibits aromatic amino acid uptake by yeast, causing a strong influence of amino acid auxotrophies on the phenotypes of membrane transporter mutants. *Eur. J. Biochem.* **270**(15), 3189–3195 (2003)
261. Sheu, C.W., Konings, W.N., Freese, E.: Effects of acetate and other short-chain fatty acids on sugar and amino acid uptake of *Bacillus subtilis*. *J. Bacteriol.* **111**(2), 525–530 (1972)
262. Wang, D., Hao, Z., Zhao, J., Jin, Y., Huang, J., Zhou, R., Wu, C.: Comparative physiological and transcriptomic analyses reveal salt tolerance mechanisms of *Zygosaccharomyces rouxii*. *Process Biochemistry* **82**, 59–67 (2019)
263. Paes, B.G., Steindorff, A.S., Formighieri, E.F., Pereira, I.S., Almeida, J.R.M.: Physiological characterization and transcriptome analysis of *Pichia pastoris* reveals its response to lignocellulose-derived inhibitors. *AMB Express* **11**(1), 1–15 (2021)
264. Reczey, K., Brumbauer, A., Bollok, M., Szengyel, Z.S., Zacchi, G.: Use of hemicellulose hydrolysate for  $\beta$ -glucosidase fermentation. *Applied Biochemistry and Biotechnology* **70**(1), 225–235 (1998)
265. Tanaka, M., Gomi, K.: Induction and repression of hydrolase genes in *Aspergillus oryzae*. *Frontiers in microbiology* **12**, 1237 (2021)
266. Ichinose, S., Tanaka, M., Shintani, T., Gomi, K.: Improved  $\alpha$ -amylase production by *Aspergillus oryzae* after a double deletion of genes involved in carbon catabolite repression. *Appl. Microbiol. Biotechnol.* **98**(1), 335–343 (2014)
267. Carlsen, M., Nielsen, J.: Influence of carbon source on  $\alpha$ -amylase production by *Aspergillus oryzae*. *Appl. Microbiol. Biotechnol.* **57**(3), 346–349 (2001)
268. Fillinger, S., Chaverroche, M.-K., van Dijck, P., Vries, R. de, Ruijter, G., Thevelein, J., d'Enfert, C.: Trehalose is required for the acquisition of tolerance to a variety of stresses in the filamentous fungus *Aspergillus nidulans*. The GenBank accession number for the sequence reported in this paper is AF043230. *Microbiology* **147**(7), 1851–1862 (2001)

269. Rodríguez-Pupo, E.C., Pérez-Llano, Y., Tinoco-Valencia, J.R., Sánchez, N.S., Padilla-Garfias, F., Calahorra, M., Del Sánchez, N.C., Sánchez-Reyes, A., Del Rodríguez-Hernández, M.R., Peña, A.: Osmolyte Signatures for the Protection of *Aspergillus sydowii* Cells under Halophilic Conditions and Osmotic Shock. *J. Fungi* **7**(6), 414 (2021)
270. Crowe, L.M., Mouradian, R., Crowe, J.H., Jackson, S.A., Womersley, C.: Effects of carbohydrates on membrane stability at low water activities. *Biochimica et Biophysica Acta (BBA)-Biomembranes* **769**(1), 141–150 (1984)
271. Jain, N.K., Roy, I.: Effect of trehalose on protein structure. *Protein Sci.* **18**(1), 24–36 (2009)
272. Panneman, H., Ruijter, G.J.G., van den Broeck, H.C., Visser, J.: Cloning and biochemical characterisation of *Aspergillus niger* hexokinase: The enzyme is strongly inhibited by physiological concentrations of trehalose 6-phosphate. *Eur. J. Biochem.* **258**(1), 223–232 (1998)
273. Puttikamonkul, S., Willger, S.D., Grahl, N., Perfect, J.R., Movahed, N., Bothner, B., Park, S., Paderu, P., Perlin, D.S., Cramer Jr, R.A.: Trehalose 6-phosphate phosphatase is required for cell wall integrity and fungal virulence but not trehalose biosynthesis in the human fungal pathogen *Aspergillus fumigatus*. *Mol. Microbiol.* **77**(4), 891–911 (2010)
274. Thammahong, A., Caffrey-Card, A.K., Dhingra, S., Obar, J.J., Cramer, R.A.: *Aspergillus fumigatus* trehalose-regulatory subunit homolog moonlights to mediate cell wall homeostasis through modulation of chitin synthase activity. *MBio* **8**(2), e00056-17 (2017)
275. Im Lee, J., Choi, J.H., Park, B.C., Park, Y.H., Lee, M.Y., Park, H.-M., Maeng, P.J.: Differential expression of the chitin synthase genes of *Aspergillus nidulans*, *chsA*, *chsB*, and *chsC*, in response to developmental status and environmental factors. *Fungal Genetics and Biology* **41**(6), 635–646 (2004)
276. You, K.M., Rosenfield, C.-L., Knipple, D.C.: Ethanol tolerance in the yeast *Saccharomyces cerevisiae* is dependent on cellular oleic acid content. *Appl. Environ. Microbiol.* **69**(3), 1499–1503 (2003)
277. Rodríguez-Vargas, S., Sánchez-García, A., Martínez-Rivas, J.M., Prieto, J.A., Rande-Gil, F.: Fluidization of membrane lipids enhances the tolerance of *Saccharomyces cerevisiae* to freezing and salt stress. *Appl. Environ. Microbiol.* **73**(1), 110–116 (2007)
278. Nakajima, K., Kunihiro, S., Sano, M., Zhang, Y., Eto, S., Chang, Y.-C., Suzuki, T., Jigami, Y., Machida, M.: Comprehensive cloning and expression analysis of glycolytic genes from the filamentous fungus, *Aspergillus oryzae*. *Current genetics* **37**(5), 322–327 (2000)

279. Flippi, M., Sun, J., Robellet, X., Karaffa, L., Fekete, E., Zeng, A.-P., Kubicek, C.P.: Biodiversity and evolution of primary carbon metabolism in *Aspergillus nidulans* and other *Aspergillus* spp. *Fungal Genetics and Biology* **46**(1), S19-S44 (2009)
280. Stemple, C.J., Davis, M.A., Hynes, M.J.: The *facC* gene of *Aspergillus nidulans* encodes an acetate-inducible carnitine acetyltransferase. *J. Bacteriol.* **180**(23), 6242–6251 (1998)
281. Armitt, S., Roberts, C.F., Kornberg, H.L.: The role of isocitrate lyase in *Aspergillus nidulans*. *FEBS Lett.* **7**(3), 231–234 (1970)
282. Wang, D., Wu, D., Yang, X., Hong, J.: Transcriptomic analysis of thermotolerant yeast *Kluyveromyces marxianus* in multiple inhibitors tolerance. *RSC Adv.* **8**(26), 14177–14192 (2018)
283. Horváth, I.S., Sjöde, A., Alriksson, B., Jönsson, L.J., Nilvebrant, N.-O.: Critical Conditions for Improved Fermentability During Overliming of Acid Hydrolysates from Spruce. In: Davison BH, Evans BR, Finkelstein M, McMillan JD (ed.) Twenty-Sixth Symposium on Biotechnology for Biofuels and Chemicals. ABAB Symposium, pp. 1031–1044. Humana Press (2005)
284. Terabayashi, Y., Sano, M., Yamane, N., Marui, J., Tamano, K., Sagara, J., Dohmoto, M., Oda, K., Ohshima, E., Tachibana, K.: Identification and characterization of genes responsible for biosynthesis of kojic acid, an industrially important compound from *Aspergillus oryzae*. *Fungal Genetics and Biology* **47**(12), 953–961 (2010)
285. Tamano, K., Kuninaga, M., Kojima, N., Umemura, M., Machida, M., Koike, H.: Use of the *kojA* promoter, involved in kojic acid biosynthesis, for polyketide production in *Aspergillus oryzae*: implications for long-term production. *BMC Biotech.* **19**(1), 1–10 (2019)
286. Kato, N., Tokuoka, M., Shinohara, Y., Kawatani, M., Uramoto, M., Seshime, Y., Fujii, I., Kitamoto, K., Takahashi, T., Takahashi, S.: Genetic safeguard against mycotoxin cyclopiazonic acid production in *Aspergillus oryzae*. *ChemBioChem* **12**(9), 1376–1382 (2011)
287. Nishimura, I., Shinohara, Y., Oguma, T., Koyama, Y.: Survival strategy of the salt-tolerant lactic acid bacterium, *Tetragenococcus halophilus*, to counteract koji mold, *Aspergillus oryzae*, in soy sauce brewing. *Bioscience, biotechnology, and biochemistry* **82**(8), 1437–1443 (2018)
288. Yan, Y., Zang, X., Jamieson, C.S., Lin, H.-C., Houk, K.N., Zhou, J., Tang, Y.: Biosynthesis of the fungal glyceraldehyde-3-phosphate dehydrogenase inhibitor heptelidic acid and mechanism of self-resistance. *Chem. Sci.* **11**(35), 9554–9562 (2020)

289. Kato, M., Sakai, K., Endo, A.: Koningic acid (heptelidic acid) inhibition of glyceraldehyde-3-phosphate dehydrogenases from various sources. *Biochimica Et Biophysica Acta (BBA)-Protein Structure and Molecular Enzymology* **1120**(1), 113–116 (1992)
290. Sugiyama, S.: Selection of micro-organisms for use in the fermentation of soy sauce. *Food Microbiol.* **1**(4), 339–347 (1984)
291. Chang, P.-K., Ehrlich, K.C., Fujii, I.: Cyclopiazonic acid biosynthesis of *Aspergillus flavus* and *Aspergillus oryzae*. *Toxins* **1**(2), 74–99 (2009)
292. Ma, L., Fu, L., Hu, Z., Li, Y., Zheng, X., Zhang, Z., Jiang, C., Zeng, B.: Modulation of fatty acid composition of *Aspergillus oryzae* in response to ethanol stress. *Microorganisms* **7**(6), 158 (2019)
293. Xu, S., Zhou, J., Liu, L., Chen, J.: Arginine: A novel compatible solute to protect *Candida glabrata* against hyperosmotic stress. *Process Biochemistry* **46**(6), 1230–1235 (2011)
294. Cheng, Y., Du, Z., Zhu, H., Guo, X., He, X.: Protective effects of arginine on *Saccharomyces cerevisiae* against ethanol stress. *Sci. Rep.* **6**(1), 1–12 (2016)
295. Baynes, B.M., Wang, D.I.C., Trout, B.L.: Role of arginine in the stabilization of proteins against aggregation. *Biochemistry* **44**(12), 4919–4925 (2005)
296. Annunziata, M.G., Ciarmiello, L.F., Woodrow, P., Dell’Aversana, E., Carillo, P.: Spatial and temporal profile of glycine betaine accumulation in plants under abiotic stresses. *Frontiers in plant science* **10**, 230 (2019)
297. Boch, J., Kempf, B., Bremer, E.: Osmoregulation in *Bacillus subtilis*: synthesis of the osmoprotectant glycine betaine from exogenously provided choline. *J. Bacteriol.* **176**(17), 5364–5371 (1994)
298. Kelavkar, U.P., Chhatpar, H.S.: Polyol concentrations in *Aspergillus repens* grown under salt stress. *World Journal of Microbiology and Biotechnology* **9**(5), 579–582 (1993)
299. Lambou, K., Pennati, A., Valsecchi, I., Tada, R., Sherman, S., Sato, H., Beau, R., Gadda, G., Latgé, J.-P.: Pathway of glycine betaine biosynthesis in *Aspergillus fumigatus*. *Eukaryotic Cell* **12**(6), 853–863 (2013)
300. Meijer, S., Otero, J., Olivares, R., Andersen, M.R., Olsson, L., Nielsen, J.: Overexpression of isocitrate lyase—glyoxylate bypass influence on metabolism in *Aspergillus niger*. *Metab. Eng.* **11**(2), 107–116 (2009)
301. Borges-Walmsley, M.I., Turner, G., Bailey, A.M., Brown, J., Lehmbeck, J., Clausen, I.G.: Isolation and characterisation of genes for sulphate activation and reduction in *Aspergillus*

- nidulans*: implications for evolution of an allosteric control region by gene duplication. *Molecular and General Genetics MGG* **247**(4), 423–429 (1995)
302. Costa, V., Quintanilha, A., Moradas-Ferreira, P.: Protein oxidation, repair mechanisms and proteolysis in *Saccharomyces cerevisiae*. *IUBMB Life* **59**(4-5), 293–298 (2007)
303. Hisada, H., Hata, Y., Kawato, A., Abe, Y., Akita, O.: Cloning and expression analysis of two catalase genes from *Aspergillus oryzae*. *Journal of bioscience and bioengineering* **99**(6), 562–568 (2005)
304. Meister, A., Anderson, M.E.: Glutathione. *Annu. Rev. Biochem.* **52**(1), 711–760 (1983)
305. Hayes, J.D., Flanagan, J.U., Jowsey, I.R.: Glutathione transferases. *Annu. Rev. Pharmacol. Toxicol.* **45**, 51–88 (2005)
306. Sato, I., Shimizu, M., Hoshino, T., Takaya, N.: The glutathione system of *Aspergillus nidulans* involves a fungus-specific glutathione S-transferase. *J. Biol. Chem.* **284**(12), 8042–8053 (2009)
307. Thön, M., Al-Abdallah, Q., Hortschansky, P., Brakhage, A.A.: The thioredoxin system of the filamentous fungus *Aspergillus nidulans*: impact on development and oxidative stress response. *J. Biol. Chem.* **282**(37), 27259–27269 (2007)
308. Misslinger, M., Scheven, M.T., Hortschansky, P., López-Berges, M.S., Heiss, K., Beckmann, N., Heigl, T., Hermann, M., Krüger, T., Kniemeyer, O.: The monothiol glutaredoxin GrxD is essential for sensing iron starvation in *Aspergillus fumigatus*. *PLoS Genet.* **15**(9), e1008379 (2019)
309. Zhang, D., Dong, Y., Yu, Q., Kai, Z., Zhang, M., Jia, C., Xiao, C., Zhang, B., Zhang, B., Li, M.: Function of glutaredoxin 3 (Grx3) in oxidative stress response caused by iron homeostasis disorder in *Candida albicans*. *Future Microbiology* **12**(15), 1397–1412 (2017)
310. Rodríguez-Manzanares, M.T., Tamarit, J., Bellí, G., Ros, J., Herrero, E.: Grx5 is a mitochondrial glutaredoxin required for the activity of iron/sulfur enzymes. *Mol. Biol. Cell* **13**(4), 1109–1121 (2002)
311. Liu, Z.L., Ma, M.: Pathway-based signature transcriptional profiles as tolerance phenotypes for the adapted industrial yeast *Saccharomyces cerevisiae* resistant to furfural and HMF. *Appl. Microbiol. Biotechnol.* **104**(8), 3473–3492 (2020)
312. Coschigano, P.W., Magasanik, B.: The URE2 gene product of *Saccharomyces cerevisiae* plays an important role in the cellular response to the nitrogen source and has homology to glutathione S-transferases. *Mol. Cell. Biol.* **11**(2), 822–832 (1991)

313. Saxena, M., Allameh, A., Mukerji, KG, Raj, H.G.: Studies on glutathione S-transferases of *Aspergillus flavus* group in relation to aflatoxin production. *Journal of Toxicology: Toxin Reviews* **8**(1-2), 319–328 (1989)
314. Li, B.-Z., Yuan, Y.-J.: Transcriptome shifts in response to furfural and acetic acid in *Saccharomyces cerevisiae*. *Appl. Microbiol. Biotechnol.* **86**(6), 1915–1924 (2010)
315. Godin, S.K., Lee, A.G., Baird, J.M., Herken, B.W., Bernstein, K.A.: Tryptophan biosynthesis is important for resistance to replicative stress in *Saccharomyces cerevisiae*. *Yeast* **33**(5), 183–189 (2016)
316. Schroeder, L., Ikui, A.E.: Tryptophan confers resistance to SDS-associated cell membrane stress in *Saccharomyces cerevisiae*. *PLoS One* **14**(3), e0199484 (2019)
317. Jones, R.P., Greenfield, P.F.: Ethanol and the fluidity of the yeast plasma membrane. *Yeast* **3**(4), 223–232 (1987)
318. Yoshikawa, K., Tanaka, T., Furusawa, C., Nagahisa, K., Hirasawa, T., Shimizu, H.: Comprehensive phenotypic analysis for identification of genes affecting growth under ethanol stress in *Saccharomyces cerevisiae*. *FEMS Yeast Res.* **9**(1), 32–44 (2009)
319. Hirasawa, T., Yoshikawa, K., Nakakura, Y., Nagahisa, K., Furusawa, C., Katakura, Y., Shimizu, H., Shioya, S.: Identification of target genes conferring ethanol stress tolerance to *Saccharomyces cerevisiae* based on DNA microarray data analysis. *J. Biotechnol.* **131**(1), 34–44 (2007)
320. Abe, F., Horikoshi, K.: Tryptophan permease gene TAT2 confers high-pressure growth in *Saccharomyces cerevisiae*. *Mol. Cell. Biol.* **20**(21), 8093–8102 (2000)
321. Lee, C., Park, C.: Bacterial responses to glyoxal and methylglyoxal: reactive electrophilic species. *Int. J. Mol. Sci.* **18**(1), 169 (2017)
322. Richard, J.P.: Mechanism for the formation of methylglyoxal from triosephosphates. *Biochem. Soc. Trans.* **21**(2), 549–553 (1993)
323. Shibamoto, T.: Analytical methods for trace levels of reactive carbonyl compounds formed in lipid peroxidation systems. *J. Pharm. Biomed. Anal.* **41**(1), 12–25 (2006)
324. Murata, K., Saikusa, T., Fukuda, Y., Watanabe, K., Inoue, Y., Shimosaka, M., Kimura, A.: Metabolism of 2-oxoaldehydes in yeasts: Possible role of glycolytic bypath as a detoxification system in l-threonine catabolism by *Saccharomyces cerevisiae*. *Eur. J. Biochem.* **157**(2), 297–301 (1986)
325. Inoue, Y., Rhee, H.-I., Watanabe, K., Murata, K., Kimura, A.: Metabolism of 2-ketoaldehydes in mold: purification and characterization of glyoxalase I from *Aspergillus niger*. *The Journal of Biochemistry* **102**(3), 583–589 (1987)

326. Inoue, Y., Tsujimoto, Y., Kimura, A.: Expression of the glyoxalase I gene of *Saccharomyces cerevisiae* is regulated by high osmolarity glycerol mitogen-activated protein kinase pathway in osmotic stress response. *J. Biol. Chem.* **273**(5), 2977–2983 (1998)
327. Adam-Vizi, V., Chinopoulos, C.: Bioenergetics and the formation of mitochondrial reactive oxygen species. *Trends Pharmacol. Sci.* **27**(12), 639–645 (2006)
328. Bankapalli, K., Saladi, S., Awadia, S.S., Goswami, A.V., Samaddar, M., D'Silva, P.: Robust glyoxalase activity of Hsp31, a ThiJ/DJ-1/PfpI family member protein, is critical for oxidative stress resistance in *Saccharomyces cerevisiae*. *J. Biol. Chem.* **290**(44), 26491–26507 (2015)
329. Hasim, S., Hussin, N.A., Alomar, F., Bidasee, K.R., Nickerson, K.W., Wilson, M.A.: A glutathione-independent glyoxalase of the DJ-1 superfamily plays an important role in managing metabolically generated methylglyoxal in *Candida albicans*. *J. Biol. Chem.* **289**(3), 1662–1674 (2014)
330. Kwak, M.-K., Ku, M., Kang, S.-O.: NAD<sup>+</sup>-linked alcohol dehydrogenase 1 regulates methylglyoxal concentration in *Candida albicans*. *FEBS Lett.* **588**(7), 1144–1153 (2014)
331. Misra, K., Banerjee, A.B., Ray, S., Ray, M.: Reduction of methylglyoxal in *Escherichia coli* K12 by an aldehyde reductase and alcohol dehydrogenase. *Mol. Cell. Biochem.* **156**(2), 117–124 (1996)
332. Simpson-Lavy, K., Kupiec, M.: Carbon catabolite repression in yeast is not limited to glucose. *Sci. Rep.* **9**(1), 1–10 (2019)
333. Shi, Q., Wang, H., Liu, J., Li, S., Guo, J., Li, H., Jia, X., Huo, H., Zheng, Z., You, S.: Old yellow enzymes: structures and structure-guided engineering for stereocomplementary bioreduction. *Appl. Microbiol. Biotechnol.* **104**(19), 8155–8170 (2020)
334. Thurston, C.F.: The structure and function of fungal laccases. *Microbiology* **140**(1), 19–26 (1994)
335. Jönsson, L.J., Palmqvist, E., Nilvebrant, N.-O., Hahn-Hägerdal, B.: Detoxification of wood hydrolysates with laccase and peroxidase from the white-rot fungus *Trametes versicolor*. *Applied microbiology and biotechnology* **49**(6), 691–697 (1998)
336. Kolb, M., Sieber, V., Amann, M., Faulstich, M., Schieder, D.: Removal of monomer delignification products by laccase from *Trametes versicolor*. *Bioresour. Technol.* **104**, 298–304 (2012)

337. Jarosz-Wilkolażka, A., Ruzgas, T., Lo Gorton: Amperometric detection of mono- and diphenols at *Cerrena unicolor* laccase-modified graphite electrode: correlation between sensitivity and substrate structure. *Talanta* **66**(5), 1219–1224 (2005)
338. Ters, T., Kuncinger, T., Srebotnik, E.: Carboxylic acids used in common buffer systems inhibit the activity of fungal laccases. *J. Mol. Catal. B: Enzym.* **61**(3-4), 261–267 (2009)
339. Kreuter, T., Steudel, A., Pickert, H.: On the inhibition of laccase by lower fatty acids. *Acta Biotechnol.* **11**(1), 81–83 (1991)
340. Bastola, K.P., Guragain, Y.N., Bhadriraju, V., Vadlani, P.V.: Evaluation of standards and interfering compounds in the determination of phenolics by Folin-Ciocalteu assay method for effective bioprocessing of biomass. *Am. J. Analyt. Chem.* **8**(06), 416 (2017)
341. Sánchez-Rangel, J.C., Benavides, J., Heredia, J.B., Cisneros-Zevallos, L., Jacobo-Velázquez, D.A.: The Folin–Ciocalteu assay revisited: improvement of its specificity for total phenolic content determination. *Anal. Methods* **5**(21), 5990–5999 (2013)
342. Nichols, N.N., Dien, B.S., Cotta, M.A.: Fermentation of bioenergy crops into ethanol using biological abatement for removal of inhibitors. *Bioresour. Technol.* **101**(19), 7545–7550 (2010)
343. Zhang, J., Zhu, Z., Wang, X., Wang, N., Wang, W., Bao, J.: Biodetoxification of toxins generated from lignocellulose pretreatment using a newly isolated fungus, *Amorphotheca resiniae* ZN1, and the consequent ethanol fermentation. *Biotechnol. Biofuels* **3**(1), 1–15 (2010)
344. Zhang, D., Ong, Y.L., Li, Z., Wu, J.C.: Biological detoxification of furfural and 5-hydroxyl methyl furfural in hydrolysate of oil palm empty fruit bunch by *Enterobacter* sp. FDS8. *Biochem. Eng. J.* **72**, 77–82 (2013)
345. El-Naas, M.H., Al-Zuhair, S., Alhaija, M.A.: Removal of phenol from petroleum refinery wastewater through adsorption on date-pit activated carbon. *Chem. Eng. J.* **162**(3), 997–1005 (2010)
346. Garcia-Araya, J.F., Beltran, F.J., Alvarez, P., Masa, F.J.: Activated carbon adsorption of some phenolic compounds present in agroindustrial wastewater. *Adsorption* **9**(2), 107–115 (2003)
347. Rengaraj, S., Moon, S.-H., Sivabalan, R., Arabindoo, B., Murugesan, V.: Agricultural solid waste for the removal of organics: adsorption of phenol from water and wastewater by palm seed coat activated carbon. *Waste Manage.* **22**(5), 543–548 (2002)

348. Rengaraj, S., Moon, S.-H., Sivabalan, R., Arabindoo, B., Murugesan, V.: Removal of phenol from aqueous solution and resin manufacturing industry wastewater using an agricultural waste: rubber seed coat. *J. Hazard. Mater.* **89**(2-3), 185–196 (2002)
349. Mattson, J.A., Mark Jr, H.B., Malbin, M.D., Weber Jr, W.J., Crittenden, J.C.: Surface chemistry of active carbon: specific adsorption of phenols. *J. Colloid Interface Sci.* **31**(1), 116–130 (1969)
350. Wang, W., Pan, S., Xu, R., Zhang, J., Wang, S., Shen, J.: Competitive adsorption behaviors, characteristics, and dynamics of phenol, cresols, and dihydric phenols onto granular activated carbon. *Desalin. Water Treat.* **56**(3), 770–778 (2015)
351. Sahu, A.K., Srivastava, V.C., Mall, I.D., Lataye, D.H.: Adsorption of furfural from aqueous solution onto activated carbon: Kinetic, equilibrium and thermodynamic study. *Sep. Sci. Technol.* **43**(5), 1239–1259 (2008)
352. Zhang, K., Agrawal, M., Harper, J., Chen, R., Koros, W.J.: Removal of the fermentation inhibitor, furfural, using activated carbon in cellulosic-ethanol production. *Ind. Eng. Chem. Res.* **50**(24), 14055–14060 (2011)
353. Singh, S., Srivastava, V.C., Mall, I.D.: Fixed-bed study for adsorptive removal of furfural by activated carbon. *Colloids Surf., A* **332**(1), 50–56 (2009)
354. Cuevas, M., Quero, S.M., Hodaifa, G., López, A.J.M., Sánchez, S.: Furfural removal from liquid effluents by adsorption onto commercial activated carbon in a batch heterogeneous reactor. *Ecol. Eng.* **68**, 241–250 (2014)
355. Sulaymon, A.H., Ahmed, K.W.: Competitive adsorption of furfural and phenolic compounds onto activated carbon in fixed bed column. *Environ. Sci. Technol.* **42**(2), 392–397 (2008)
356. Lee, J.M., Venditti, R.A., Jameel, H., Kenealy, W.R.: Detoxification of woody hydrolyzates with activated carbon for bioconversion to ethanol by the thermophilic anaerobic bacterium *Thermoanaerobacterium saccharolyticum*. *Biomass Bioenergy* **35**(1), 626–636 (2011)
357. Li, Y., Shao, J., Wang, X., Yang, H., Chen, Y., Deng, Y., Zhang, S., Chen, H.: Upgrading of bio-oil: removal of the fermentation inhibitor (furfural) from the model compounds of bio-oil using pyrolytic char. *Energy & Fuels* **27**(10), 5975–5981 (2013)
358. Dąbrowski, A., Podkościelny, P., Hubicki, Z., Barczak, M.: Adsorption of phenolic compounds by activated carbon—a critical review. *Chemosphere* **58**(8), 1049–1070 (2005)

359. Beker, U., Ganbold, B., Dertli, H., Gülbayir, D.D.: Adsorption of phenol by activated carbon: Influence of activation methods and solution pH. *Energy Convers. Manage.* **51**(2), 235–240 (2010)
360. Fang, K., Yang, R.: A comparison on the efficiency of raw activated carbon, oxidized, and sulfurized adsorbents for furfural adsorption. *Alexandria Eng. J.* **60**(1), 1241–1248 (2021)
361. Zanella, O., Tessaro, I.C., Féris, L.A.: Desorption-and decomposition-based techniques for the regeneration of activated carbon. *Chem. Eng. Technol.* **37**(9), 1447–1459 (2014)
362. Funke, A., Niebel, A., Richter, D., Abbas, M.M., Müller, A.-K., Radloff, S., Paneru, M., Maier, J., Dahmen, N., Sauer, J.: Fast pyrolysis char—Assessment of alternative uses within the bioliq® concept. *Bioresour. Technol.* **200**, 905–913 (2016)
363. del Campo, B.G.: Production of activated carbon from fast pyrolysis biochar and the detoxification of pyrolytic sugars for ethanol fermentation, Iowa State University (2015)
364. Millati, R., Niklasson, C., Taherzadeh, M.J.: Effect of pH, time and temperature of overliming on detoxification of dilute-acid hydrolyzates for fermentation by *Saccharomyces cerevisiae*. *Process Biochem.* **38**(4), 515–522 (2002)
365. Mazumdar, N.J., Kataki, R., Pant, K.K.: Furfural and Chemical Routes for Its Transformation into Various Products. In: Pant, K.K., Gupta, S.K., Ahmad, E. (eds.) *Catalysis for Clean Energy and Environmental Sustainability. Biomass Conversion and Green Chemistry - Volume 1*, 1st edn., pp. 705–719. Springer, Cham (2021)
366. Gandini, A., Belgacem, M.N.: Furans in polymer chemistry. *Prog. Polym. Sci.* **22**(6), 1203–1379 (1997)
367. Ahuja, S., Singh, D.: A kinetic model of alkali catalyzed phenol-furfural novalac resinification. *Polym. Polym. Compos.* **19**(7), 581–586 (2011)
368. Brown, R.C.: Thermochemical processing of biomass. Conversion into fuels, chemicals and power, 2nd edn. John Wiley & Sons, Hoboken (2019)
369. Norton, A.J.: Furan resins. *Ind Eng Chem* **40**(2), 236–238 (1948)
370. Hronec, M., Fulajtárova, K., Liptaj, T., Štolcová, M., Prónayová, N., Soták, T.: Cyclopentanone: A raw material for production of C15 and C17 fuel precursors. *Biomass Bioenergy* **63**, 291–299 (2014)
371. Hurd, C.D., Garrett, J.W., Osborne, E.N.: Furan reactions. IV. Furoic acid from furfural. *J. Am. Chem. Soc.* **55**(3), 1082–1084 (1933)
372. Albuquerque, E.M., Borges, L.E.P., Fraga, M.A.: Lactic acid production from aqueous-phase selective oxidation of hydroxyacetone. *J. Mol. Catal. A: Chem.* **400**, 64–70 (2015)
373. Machell, G.: 142. The action of alkali on diacetyl. *J. Chem. Soc.*, 683–687 (1960)

374. Persson, P., Andersson, J., Lo Gorton, Larsson, S., Nilvebrant, N.-O., Jönsson, L.J.: Effect of different forms of alkali treatment on specific fermentation inhibitors and on the fermentability of lignocellulose hydrolysates for production of fuel ethanol. *J. Agric. Food. Chem.* **50**(19), 5318–5325 (2002)
375. Wilson, J.J., Deschatelets, L., Nishikawa, N.K.: Comparative fermentability of enzymatic and acid hydrolysates of steam-pretreated aspenwood hemicellulose by *Pichia stipitis* CBS 5776. *Applied microbiology and biotechnology* **31**(5), 592–596 (1989)
376. Westerhof, R.J.M., Brilman, D.W.F., Garcia-Perez, M., Wang, Z., Oudenhoven, S.R.G., van Swaaij, W.P.M., Kersten, S.R.A.: Fractional condensation of biomass pyrolysis vapors. *Energy & Fuels* **25**(4), 1817–1829 (2011)
377. Pollard, A.S., Rover, M.R., Brown, R.C.: Characterization of bio-oil recovered as stage fractions with unique chemical and physical properties. *J. Anal. Appl. Pyrolysis* **93**, 129–138 (2012)
378. Xu, F., Chen, J., Yang, G., Ji, X., Wang, Q., Liu, S., Ni, Y.: Combined treatments consisting of calcium hydroxide and activate carbon for purification of xylo-oligosaccharides of pre-hydrolysis liquor. *Polymers* **11**(10), 1558 (2019)
379. Randtke, S.J., Jepsen, C.P.: Effects of salts on activated carbon adsorption of fulvic acids. *J. Am. Water Works Assn.* **74**(2), 84–93 (1982)
380. Altaras, N.E., Etzel, M.R., Cameron, D.C.: Conversion of Sugars to 1, 2-Propanediol by *Thermoanaerobacterium thermosaccharolyticum* HG-8. *Biotechnol. Progr.* **17**(1), 52–56 (2001)
381. Inoue, Y., RHEE, H., Watanabe, K., Murata, K., Kimura, A.: Metabolism of 2-oxoaldehyde in mold: Purification and characterization of two methylglyoxal reductases from *Aspergillus niger*. *Eur. J. Biochem.* **171**(1-2), 213–218 (1988)
382. Schuurink, R., Busink, R., Hondmann, D.H., Wltteveen, C.F., Vlsser, J.: Purification and properties of NADP<sup>+</sup>-dependent glycerol dehydrogenases from *Aspergillus nidulans* and *A. niger*. *Microbiology* **136**(6), 1043–1050 (1990)
383. Walti, A.: Action of *Aspergillus niger* on normal 1, 2-diols. *J. Am. Chem. Soc.* **56**(12), 2723–2726 (1934)
384. Murata, K., Fukuda, Y., Watanabe, K., Saikusa, T., Shimosaka, M., Kimura, A.: Characterization of methylglyoxal synthase in *Saccharomyces cerevisiae*. *Biochem. Biophys. Res. Commun.* **131**(1), 190–198 (1985)

385. Nakamura, K., Kondo, S., Kawai, Y., Nakajima, N., Ohno, A.: Amino acid sequence and characterization of aldo-keto reductase from bakers' yeast. *Biosci. Biotechnol. Biochem.* **61**(2), 375–377 (1997)
386. Jung, J.-Y., Choi, E.-S., Oh, M.-K.: Enhanced production of 1, 2-propanediol by *tpil* deletion in *Saccharomyces cerevisiae*. *J. Microbiol. Biotechnol.* **18**(11), 1797–1802 (2008)
387. Jung, J.-Y., Yun, H.-S., Lee, J.-W., Oh, M.-K.: Production of 1, 2-propanediol from glycerol in *Saccharomyces cerevisiae*. *J. Microbiol. Biotechnol.* **21**(8), 846–853 (2011)
388. Kometani, T., Kitasuji, E., Matsuno, R.: Baker's yeast mediated bioreduction. A new procedure using ethanol as an energy source. *Chem. Lett.*(8), 1465–1466 (1989)
389. Kometani, T., Yoshii, H., Takeuchi, Y., Matsuno, R.: Large-scale preparation of (R)-1, 2-propanediol through baker's yeast-mediated bioreduction. *J. Ferment. Bioeng.* **76**(5), 414–415 (1993)
390. Alcano, M.d.J., Jahn, R.C., Scherer, C.D., Wigmann, É.F., Moraes, V.M., Garcia, M.V., Mallmann, C.A., Copetti, M.V.: Susceptibility of *Aspergillus* spp. to acetic and sorbic acids based on pH and effect of sub-inhibitory doses of sorbic acid on ochratoxin A production. *Food Res. Int.* **81**, 25–30 (2016)
391. O'Mahony, R.J., Burns, A.T.H., Millam, S., Hooley, P., Fincham, D.A.: Isotropic growth of spores and salt tolerance in *Aspergillus nidulans*. *Mycol. Res.* **106**(12), 1480–1486 (2002)
392. Wang, Y., Yan, H., Neng, J., Gao, J., Yang, B., Liu, Y.: The Influence of NaCl and Glucose content on Growth and Ochratoxin A production by *Aspergillus ochraceus*, *Aspergillus carbonarius* and *Penicillium nordicum*. *Toxins* **12**(8), 515 (2020)
393. Dörsam, S.: Evaluation of renewable resources as carbon sources for organic acid production with filamentous fungi. Dissertation, Karlsruhe Institute of Technology. <https://d-nb.info/115547435x/34> (2018)
394. Pinchai, N., Juvvadi, P.R., Fortwendel, J.R., Perfect, B.Z., Rogg, L.E., Asfaw, Y.G., Steinbach, W.J.: The *Aspergillus fumigatus* P-type Golgi apparatus  $\text{Ca}^{2+}/\text{Mn}^{2+}$  ATPase PmrA is involved in cation homeostasis and cell wall integrity but is not essential for pathogenesis. *Eukaryot. Cell* **9**(3), 472–476 (2010)
395. Markina-Iñárraigui, A., Spielvogel, A., Etxebeste, O., Ugalde, U., Espeso, E.A.: Tolerance to alkaline ambient pH in *Aspergillus nidulans* depends on the activity of ENA proteins. *Sci. Rep.* **10**(1), 1–16 (2020)
396. Halliwell, G.: The Effect of Aeration on the Metabolism of Acetate by *Aspergillus niger*. *J. Exp. Bot.*, 369–376 (1953)

397. Brown, S.H., Bashkirova, L., Berka, R., Chandler, T., Doty, T., McCall, K., McCulloch, M., McFarland, S., Thompson, S., Yaver, D.: Metabolic engineering of *Aspergillus oryzae* NRRL 3488 for increased production of L-malic acid. *Appl. Microbiol. Biotechnol.* **97**(20), 8903–8912 (2013)
398. Xu, Y., Zhou, Y., Cao, W., Liu, H.: Improved production of malic acid in *Aspergillus niger* by abolishing citric acid accumulation and enhancing glycolytic flux. *ACS Synth. Biol.* **9**(6), 1418–1425 (2020)
399. Liu, J., Li, J., Liu, Y., Shin, H., Ledesma-Amaro, R., Du, G., Chen, J., Liu, L.: Synergistic rewiring of carbon metabolism and redox metabolism in cytoplasm and mitochondria of *Aspergillus oryzae* for increased L-malate production. *ACS Synth. Biol.* **7**(9), 2139–2147 (2018)
400. Liu, J., Xie, Z., Shin, H., Li, J., Du, G., Chen, J., Liu, L.: Rewiring the reductive tricarboxylic acid pathway and L-malate transport pathway of *Aspergillus oryzae* for overproduction of L-malate. *J. Biotechnol.* **253**, 1–9 (2017)

# List of figures

<b>Figure 1:</b> Overview of the different malic acid production routes.....	3
<b>Figure 2:</b> The three key pathways of L-malic acid production in microorganisms.....	5
<b>Figure 3:</b> Composition of lignocellulosic biomass.....	9
<b>Figure 4:</b> The two key routes for the conversion of lignocellulosic biomass. ....	11
<b>Figure 5:</b> Process diagram of fast pyrolysis as a central part of the bioliq® process performed at KIT. ....	13
<b>Figure 6:</b> Potential applications of synthesis gas (syngas).....	14
<b>Figure 7:</b> Main routes for the formation of selected PAC components .....	16
<b>Figure 8:</b> Possible pathways for the microbial formation of acetol and its conversion into other metabolites .....	18
<b>Figure 9:</b> Oxidative and reductive furan conversion routes. ....	23
<b>Figure 10:</b> Substrate consumption (A) and biomass formation (B) in <i>A. oryzae</i> cultures containing glucose, acetate and 20 % detoxified PAC.....	42
<b>Figure 11:</b> Box plot of the transformed and normalized read count data (A) and principal component analysis (PCA) showing the variance between the individual samples (B) .....	45
<b>Figure 12:</b> Differentially expressed genes of <i>A. oryzae</i> during cultivation with 20 % detoxified PAC, acetate or glucose. ....	46
<b>Figure 13:</b> Functional enrichment analysis of genes being differentially expressed during cultivation of <i>A. oryzae</i> on glucose (Glc) compared to acetate (Ace).....	47
<b>Figure 14:</b> Functional enrichment analysis of genes being differentially expressed during cultivation of <i>A. oryzae</i> on glucose compared to PAC. ....	48
<b>Figure 15:</b> Functional enrichment analysis of genes being differentially expressed during cultivation of <i>A. oryzae</i> on acetate compared to PAC.....	50
<b>Figure 16:</b> Differentially expressed genes of glycolysis, gluconeogenesis, and the TCA cycle during cultivation of <i>A. oryzae</i> on glucose, acetate and PAC.....	57
<b>Figure 17:</b> Differentially expressed genes of the cysteine and methionine metabolism as well as the closely related serine synthesis and sulfur metabolism. ....	64
<b>Figure 18:</b> Differentially expressed genes of the tryptophan metabolism during cultivation of <i>A. oryzae</i> on glucose, acetate, and PAC. ....	68
<b>Figure 19:</b> Differentially expressed genes of the pyruvate metabolism during cultivation of <i>A. oryzae</i> on glucose, acetate, and PAC.....	71

<b>Figure 20:</b> Removal of phenolic substances from PAC during 24 h treatment with different concentrations of <i>T. versicolor</i> laccase. ....	79
<b>Figure 21:</b> Colony diameters of <i>A. oryzae</i> after 5 days of growth on agar plates containing different contents of PAC treated with 25 U/mL <i>T. versicolor</i> laccase for 24 h.....	80
<b>Figure 22:</b> Colony diameters of <i>A. oryzae</i> after 5 days of growth on agar plates containing different volumetric contents of PAC, that was obtained after 1-h treatment with increasing activated carbon (AC) loads (0-10 % (w/v)). ....	81
<b>Figure 23:</b> Temporal change in concentration of selected PAC compounds during treatment with increasing activated carbon loads (0-10 % (w/v)).....	82
<b>Figure 24:</b> Colony diameters of <i>A. oryzae</i> after 5 days of growth on agar plates containing different amounts of PAC treated with overliming at various temperatures for 4 h (A) and two different pH values for 90 min (B).....	84
<b>Figure 25:</b> Colony diameters of <i>A. oryzae</i> after 5 days of growth on agar plates containing different volumetric contents of PAC treated with 4-h rotary evaporation at different pressures and 80 °C.....	87
<b>Figure 26:</b> Concentration of selected PAC compounds after 4h treatment with rotary evaporation at different pressures and 80 °C. ....	88
<b>Figure 27:</b> Maximum tolerance of <i>A. oryzae</i> on agar plates containing PAC obtained after single treatment with laccase, activated carbon (AC), overliming (OL) or rotary evaporation (RE) as well as combinations of the latter three detoxification methods. ....	89
<b>Figure 28:</b> Shake flask cultivations of <i>A. oryzae</i> in pre-culture medium containing 100 % PAC detoxified by a combination of rotary evaporation, overliming and activated carbon....	93
<b>Figure 29:</b> Substrate consumption and biomass formation of <i>A. oryzae</i> in shake flask pre-cultures containing acetol concentrations of 3 g/L (A); 5 g/L (B);10 g/L (C);20 g/L (D);30 g/L (E) and 40 g/L (F) as carbon source.....	106
<b>Figure 30:</b> Substrate consumption and biomass formation of <i>A. oryzae</i> in shake flask pre-cultures containing 40 g/L of acetate as sole carbon source (A) as well as mixtures of acetate and acetol concentrations of 3 g/L(B); 5 g/L (C); 10 g/L (D); 20 g/L (E).....	108
<b>Figure 31:</b> Malic acid production, substrate consumption, and pH values in <i>A. oryzae</i> shake flask main cultures containing mixtures of 40 g/L acetate and different concentrations of acetol (0-20 g/L).....	111
<b>Figure 32:</b> Malic acid production of <i>A. oryzae</i> in shake flask main cultures containing 100 % PAC detoxified by rotary evaporation, overliming and a subsequent activated carbon treatment.....	114

<b>Figure 33:</b> Optimization of the initial medium pH in <i>A. oryzae</i> shake flasks main cultures containing 100 % detoxified PAC.....	118
<b>Figure 34:</b> Bioreactor cultivations of <i>A. oryzae</i> in main culture medium containing 40 g/L acetate (A) or 100 % detoxified PAC (B). .....	120

# List of tables

<b>Table 1:</b> Comparison of L-malic acid production from various renewable substrates .....	7
<b>Table 2:</b> Properties of the PAC formed during the bioliq® Campaign in 2018.....	14
<b>Table 3:</b> Maximum concentration of selected inhibitors from pyrolysis condensates that can be tolerated by <i>A. oryzae</i> .....	20
<b>Table 4:</b> Toxicity tests on agar plates containing glucose as main carbon source and different concentrations of cyclic ketones present in PAC .....	22
<b>Table 5:</b> Summary of the experiments for optimization of the pretreatment procedure .....	34
<b>Table 6:</b> Quality characteristics of the RNA-seq data obtained for <i>A. oryzae</i> cultivated on glucose, acetate and 20 % detoxified PAC.....	44
<b>Table 7:</b> Differentially expressed pathways for the comparisons of glucose with PAC.....	51
<b>Table 8:</b> Differentially expressed pathways for the comparisons of glucose with pure acetate .....	52
<b>Table 9:</b> Differentially expressed genes involved in the starch and sucrose metabolism .....	54
<b>Table 10:</b> Selection of differentially expressed secondary metabolite clusters.....	59
<b>Table 11:</b> Transcriptional regulation of genes involved in the oxidative stress defense.....	65
<b>Table 12:</b> Differentially expressed NADH- (EC 1.1.1.1) and NADPH-dependent (EC 1.1.1.2) alcohol dehydrogenases.....	73
<b>Table 13:</b> GC analysis of PAC treated by overliming at different conditions.....	85
<b>Table 14:</b> GC analysis of PAC treated with different combinations of detoxification methods .....	91
<b>Table 15:</b> Substrate consumption and growth parameters after 96 h cultivation of <i>A. oryzae</i> in media containing 40 g/L of acetate and different concentrations of acetol (0-20 g/L) .....	109
<b>Table 16:</b> Substrate consumption and L-malate production in <i>A. oryzae</i> main cultures containing 40 g/L acetate and different concentrations of acetol (0-20 g/L) as sole carbon sources .....	114
<b>Table 17:</b> Summary of substrate consumption and malic acid production in <i>A. oryzae</i> cultivations with PAC .....	116

# Appendix

**Appendix 1:** Composition of the PAC before and after the treatment procedure performed prior to transcriptome analysis. Quantification was carried out by the Thünen Institute for Wood Research in Hamburg using GC/MS analysis

component	concentration [g/L]	
	before detoxification	after detoxification
acetic acid	35.40 <sup>1</sup>	40.05
propionic acid	10.42	0
poss. propanoic acid, ethenyl ester <sup>2</sup>	0.18	0
ethylene glycol	3.27	7.63
hydroxy-acetaldehyde	1.90	0
3-hydroxy propionaldehyde	0.28	0
2-butenal	0.58	0
butandial (or propanal)	0.34	0
acetol (hydroxypropanone)	51.46	38.42
2-butanone	1.98	0.38
1-hydroxy-2-butanone	6.71	3.86
2,3- butandione (diacetyl)	2.40	0.37
3-hydroxy-2-butanone(acetoin)	1.42	1.54
1-acetyloxy-propan-2-one	1.07	0
cyclopentanone	1.12	0
2-cyclopenten-1-one	3.35	0.33
2,3-dimethyl-2-cyclopenten-1-one	0.22	0
2-methyl-2-cyclopenten-1-one	1.35	0
3-methyl-2-cyclopenten-1-one	0.68	0
2-cyclohexen-1-one	0.11	0
poss: 3-methyl-2-butanone <sup>2</sup>	0.09	0
poss: 3-methyl-3-buten-2-one <sup>2</sup>	0.16	0
2-pentanone	0.51	0
2,3-pentanedione	0.63	0.17
3-penten-2-one	0.44	0
isomere of 3-methyl-2-cyclopenten-1-one	0.28	0
poss: 2-ethyl-butanal <sup>2</sup>	0.31	0
poss: 3,4-dimethyl-2-cyclopenten-1-one <sup>2</sup>	0.27	0
isomere of 2,3-dimethyl-2-cyclopenten-1-one	0.42	0
3-methyl-1,2-cyclopentanedione	1.50	0
2,3,4-trimethyl-2-cyclopenten-1-one	0.17	0
2(5H)-furanone	0.64	0
2-furaldehyde	2.84	0.16
5-methyl-2-furaldehyde	0.13	0
1-(2-furanyl)-ethanone	0.30	0
3-methyl-, (5H)-furan-2-one	0.04	0
$\gamma$ -butyrolactone	0.71	0.71
1-methoxy-4-methyl-benzene	0.06	0
indene	0.08	0
phenol	0.63	0
<i>o</i> -cresol	0.46	0
<i>p</i> -cresol	0.17	0
<i>m</i> -cresol	0.21	0
2,5-dimethyl-phenol	0.19	0
2,4-dimethyl-phenol	0.08	0

<b>component</b>	<b>concentration [g/L]</b>	
	<b>before detoxification</b>	<b>after detoxification</b>
2,6-dimethyl-phenol	0.06	0
4-ethyl-phenol	0.14	0
guaiacol	1.80	0
3-methyl-guaiacol	0.16	0
4-methyl-guaiacol	0.36	0
4-ethyl-guaiacol	0.27	0
4-vinyl-guaiacol	0.24	0
syringol	0.17	0
D-limonene or isomere	0.14	0
2-acetyl-5-norbornene	0.06	0
2-methyl-1,3-dioxolane	0.12	0
poss: 2,3-dihydro-1,4-dioxin <sup>2</sup>	0.09	0

<sup>1</sup> quantified by an enzymatic acetate assay

<sup>2</sup> poss = possibly

**Appendix 2:** Differentially expressed genes assigned to “transmembrane transport” (GO:0055085)

Gene ID	Description	Fold change		
		Glc vs Ace	Glc vs PAC	Ace vs PAC
AO090001000215	MFS allantoate transporter	2.28	2.61	-
AO090001000232	Belongs to the MFS. Proton-dependent oligopeptide transporter (POT/PTR) family (TC 2.A.17)	5.12	4.75	-
AO090001000305	Belongs to the MFS. Proton-dependent oligopeptide transporter (POT/PTR) family (TC 2.A.17)	3.90	3.29	-
AO090001000313	Multidrug resistance-associated protein	4.59	6.22	-
AO090001000360	Major Facilitator Superfamily	1.87	1.58	-
AO090001000404	MFS transporter	2.41	3.84	-
AO090001000692	Predicted transporter	1.23	1.49	-
AO090001000707	Ammonium transporter	1.65	2.15	-
AO090003000044	MFS transporter	1.68	2.46	-
AO090003000227	Fungal potassium channel	1.55	1.93	-
AO090003000268	Belongs to the purine-cytosine permease family (2.A.39)	3.84	3.27	-
AO090003000529	Vacuolar iron transporter Ccc1	2.06	-	-
AO090003000614	Calcium-transporting ATPase	1.85	-1.92	-3.77
AO090003000854	Urea transporter; belongs to the sodium solute symporter (SSF) family (TC 2.A.21)	2.71	5.25	-
AO090003000971	MFS transporter	1.21	1.78	-
AO090003001015	Belongs to the major facilitator superfamily. Sugar transporter family (TC 2.A.1.1)	2.35	3.23	-
AO090003001191	Mitochondrial calcium uniporter	2.34	1.72	-
AO090003001260	MFS transporter	4.26	6.13	-
AO090003001277	Belongs to the major facilitator superfamily. Sugar transporter family (TC 2.A.1.1)	1.37	-	-
AO090003001296	Belongs to the ZIP transporter family (TC 2.A.5)	3.27	8.48	5.22
AO090003001428	Efflux pump antibiotic resistance protein	4.75	7.98	3.23
AO090003001436	amino acid transporter	2.57	4.03	-
AO090003001482	Small oligopeptide transporter, OPT family	10.53	8.79	-

Gene ID	Description	Fold change		
		Glc vs Ace	Glc vs PAC	Ace vs PAC
AO090003001549	Belongs to the MFS. Proton-dependent oligopeptide transporter (POT/PTR) family (TC 2.A.17)	3.76	6.23	2.47
AO090005000060	amino acid transporter	1.66	6.68	5.03
AO090005000114	Amino acid permease (Gap1)	2.71	5.38	2.67
AO090005000166	Putative siderochrome-iron transporter	1.77	1.90	-
AO090005000295	Major Facilitator Superfamily	1.02	2.18	1.16
AO090005000420	Sugar transporter family protein	4.41	5.06	-
AO090005000455	purine permease	1.72	2.22	-
AO090005000535	Major Facilitator Superfamily	9.01	7.68	-
AO090005000536	K <sup>+</sup> /H <sup>+</sup> -antiporter	1.33	1.21	-
AO090005000633	MFS transporter	1.24	1.01	-
AO090005000649	Amino acid permease	2.16	1.50	-
AO090005000863	Putative MFS transporter	1.19	2.15	-
AO090005001095	Auxin Efflux Carrier superfamily	1.20	1.27	-
AO090005001212	Predicted amino acid transporter	1.81	2.02	-
AO090005001328	Fungal trichothecene efflux pump (TRI12)	3.34	5.95	-
AO090005001343	Peptide transporter MTD1	1.96	4.50	2.54
AO090009000008	Sugar (and other) transporter	2.70	1.46	-
AO090009000479	Integral membrane protein	1.03	1.12	-
AO090009000565	Multidrug resistance-associated protein mitoxantrone resistance protein	3.76	-	-
AO090009000584	Major Facilitator Superfamily	2.47	2.50	-
AO090009000635	amino acid transporter	1.58	2.07	-
AO090009000651	multidrug/pheromone exporter, ABC superfamily	1.35	1.35	-
AO090010000024	Belongs to the MIP aquaporin family (TC 1.A.8)	3.05	2.10	-
AO090010000062	amino acid transporter	1.68	1.57	-
AO090010000119	AAT family amino acid transporter	2.17	3.36	-
AO090010000135	Iron-regulated transporter	6.76	4.89	-
AO090010000142	MFS transporter	2.18	-	-2.14
AO090010000195	Belongs to the MFS. Sugar transporter family (TC 2.A.1.1)	2.03	-	-
AO090010000219	ABC multidrug transporter atrA	1.40	2.20	-
AO090010000221	Bacteriorhodopsin-like protein	3.96	5.09	-
AO090010000222	Belongs to the MFS	2.47	3.49	-

Gene ID	Description	Fold change		
		Glc vs Ace	Glc vs PAC	Ace vs PAC
AO090010000345	Permease for cytosine/purines, uracil, thiamine, allantoin	3.92	9.42	5.51
AO090010000639	Belongs to the MFS	4.66	-8.74	-13.40
AO090010000652	MFS transporter	1.79	2.68	-
AO090010000674	Permease of the MFS	1.47	2.40	-
AO090010000705	Belongs to the MIP aquaporin family (TC 1.A.8)	1.67	1.59	-
AO090010000723	Belongs to the MFS	2.31	6.99	4.68
AO090010000733	Sugar (and other) transporter	3.20	3.19	-
AO090011000151	Belongs to the MFS	5.14	-	-
AO090011000212	Low affinity iron transporter	7.08	6.13	-
AO090011000335	MFS drug transporter	5.83	5.25	-
AO090011000363	Cation diffusion facilitator 1	1.23	1.48	-
AO090011000378	ABC multidrug transporter atrG	1.59	1.07	-
AO090011000413	MFS-type transporter hepF	2.61	5.50	2.89
AO090011000587	MFS transporter	1.85	2.03	-
AO090011000649	Belongs to the purine-cytosine permease family (2.A.39)	2.53	3.10	-
AO090011000734	Belongs to the TrkH potassium transport family	2.29	-	-
AO090011000744	Carboxylic acid transport protein	3.37	-	-
AO090012000284	Belongs to the MFS. Sugar transporter family (TC 2.A.1.1)	2.13	1.13	-
AO090012000288	Belongs to the MFS	1.55	1.66	-
AO090012000289	Vacuole effluxer Atg22 like	1.06	-	-1.03
AO090012000315	Small oligopeptide transporter, OPT family	5.09	11.48	6.39
AO090012000494	Putative MFS transporter	1.15	1.08	-
AO090012000565	Uridine permease	3.29	5.56	-
AO090012000623	Nitrate transporter of the MFS	7.14	6.56	-
AO090012000710	Belongs to the MFS	3.99	3.63	-
AO090012000732	Belongs to the MFS. Sugar transporter family (TC 2.A.1.1)	1.51	2.08	-
AO090012000758	Belongs to the MFS	1.86	-	-
AO090020000209	Belongs to the MFS. Sugar transporter family (TC 2.A.1.1)	2.10	1.38	-
AO090020000236	Sugar (and other) transporter	5.69	6.07	-
AO090020000259	Belongs to the MFS. Sugar transporter family (TC 2.A.1.1)	1.53	2.05	-

Gene ID	Description	Fold change		
		Glc vs Ace	Glc vs PAC	Ace vs PAC
AO090010000229	MFS peptide transporter Ptr2	-	1.05	1.12
AO090020000280	Predicted allantoate permease	1.26	1.43	-
AO090020000524	Belongs to the MFS. Proton-dependent oligopeptide transporter (POT/PTR) family (TC 2.A.17)	1.68	2.36	-
AO090020000533	Predicted protein	5.20	7.80	-
AO090020000639	Belongs to the MFS. Sugar transporter family (TC 2.A.1.1)	4.25	6.51	-
AO090020000668	Belongs to the MFS. Sugar transporter family (TC 2.A.1.1)	2.93	3.70	-
AO090020000694	Belongs to the MFS. Proton-dependent oligopeptide transporter (POT/PTR) family (TC 2.A.17)	3.06	3.29	-
AO090023000039	MFS toxin efflux pump (AflT)	2.93	1.84	-
AO090023000318	C4-dicarboxylate transporter malic acid transport protein	2.18	4.44	2.26
AO090023000411	Ammonium transporter	3.70	-	-
AO090023000430	Ctr copper transporter family	5.25	7.56	-
AO090023000482	MFS transporter	2.21	2.09	-
AO090023000488	Belongs to the MFS. Sugar transporter family (TC 2.A.1.1)	1.87	1.22	-
AO090023000585	MFS multidrug transporter	2.07	3.09	-
AO090026000101	amino acid transporter	2.48	1.87	-
AO090026000207	MFS transporter	3.38	2.78	-
AO090026000224	Belongs to the MFS	6.10	5.52	-
AO090026000255	K <sup>+</sup> potassium transporter	6.17	4.21	-1.96
AO090026000437	mitochondrial phosphate carrier protein	2.82	2.69	-
AO090026000494	Belongs to the MFS. Sugar transporter family (TC 2.A.1.1)	2.73	3.35	-
AO090026000749	Ammonium transporter	1.32	-	-
AO090026000760	monocarboxylate transporter	3.08	2.84	-
AO090026000778	Predicted transporter of the MFS	2.11	2.56	-
AO090038000297	Calcium channel subunit Cch1	1.30	2.02	-
AO090038000314	Ammonium transporter	8.88	10.10	-
AO090038000391	Putative MFS multidrug transporter	1.17	1.06	-
AO090038000535	MFS transporter Fmp42	1.31	1.61	-
AO090038000551	sugar transporter	1.61	2.70	-
AO090038000553	C4-dicarboxylate transporter malic acid transport protein	2.51	-	-1.93

Gene ID	Description	Fold change		
		Glc vs Ace	Glc vs PAC	Ace vs PAC
AO090102000073	Monocarboxylate transporter	3.60	-	-
AO090102000135	Putative MFS multidrug transporter	3.22	2.34	-
AO090102000255	Belongs to the MFS. Sugar transporter family (TC 2.A.1.1)	1.99	2.49	-
AO090102000282	Cation efflux protein of the cation diffusion facilitator superfamily	5.98	7.39	-
AO090102000351	Auxin Efflux Carrier superfamily	2.98	2.80	-
AO090102000476	amino acid transporter	1.34	2.15	-
AO090103000075	Belongs to the MFS	4.15	5.45	-
AO090103000099	Belongs to the MFS	1.44	-1.02	-2.45
AO090103000165	Putative MFS siderophore transporter	2.71	7.38	4.67
AO090103000166	ABC multidrug transporter	2.52	4.61	2.10
AO090103000396	Putative MFS multidrug transporter	5.99	8.28	-
AO090120000001	Belongs to the MFS. Proton-dependent oligopeptide transporter (POT/PTR) family (TC 2.A.17)	5.76	7.36	-
AO090120000175	Ctr copper transporter	3.07	3.92	-
AO090120000214	Ctr copper transporter family protein	5.21	6.72	1.50
AO090120000414	Iron-regulated transporter	1.22	1.31	-
AO090120000417	Belongs to the MFS. Sugar transporter family (TC 2.A.1.1)	1.53	1.34	-
AO090120000429	Low affinity iron transport protein	4.07	13.13	9.06
AO090124000012	MFS monocarboxylate transporter	1.79	-	-
AO090124000037	High-affinity iron transporter	3.32	3.82	-
AO090124000050	Ca <sup>2+</sup> :H <sup>+</sup> antiporter	4.32	10.42	6.10
AO090124000051	Ca <sup>2+</sup> :H <sup>+</sup> antiporter	4.29	7.12	2.83
AO090124000052	Ca <sup>2+</sup> :H <sup>+</sup> antiporter	5.19	11.76	6.57
AO090124000066	MFS transporter	1.40	2.75	1.35
AO090166000026	Amino acid permease	2.69	-	-
AO090701000037	Belongs to the MFS. Sugar transporter family (TC 2.A.1.1)	2.27	1.43	-
AO090701000347	MFS transporter	6.32	5.74	-
AO090701000423	Amino acid transporter	2.38	2.50	-
AO090701000437	MFS domain-containing protein	6.37	5.79	-
AO090701000480	C4-dicarboxylate transporter malic acid transport protein	2.90	2.66	-
AO090701000533	amino acid transporter	1.59	9.12	7.53
AO090701000689	Belongs to the SLC35F solute transporter family	1.12	1.71	-

Gene ID	Description	Fold change		
		Glc vs Ace	Glc vs PAC	Ace vs PAC
AO090701000839	Putative transporter of the ABC superfamily	2.15	5.10	2.96
AO090020000267	Permease of the MFS	5.06	4.68	-
AO090001000016	Oligopeptide transporter wykF	-	1.11	-
AO090001000146	Putative MFS transporter	-	6.06	6.58
AO090001000204	MFS domain-containing protein	-	3.87	3.84
AO090001000298	Amino acid transporter	-	1.61	-
AO090001000385	MFS transporter	-	2.09	-
AO090001000510	Belongs to the MIP aquaporin family (TC 1.A.8)	-	2.42	-
AO090003000051	Calcium-transporting ATPase	-	1.11	-
AO090003000167	Putative MFS phospholipid transporter (Git1)	-	1.09	1.21
AO090003000443	H <sup>+</sup> /nucleoside cotransporter	-	1.36	-
AO090003000575	Putative MFS monocarboxylate transporter (MCT)	-	2.12	1.61
AO090003000737	MFS transporter	-	5.31	5.96
AO090003000813	MFS monocarboxylate transporter	-	1.63	-
AO090003001081	Cell surface receptor MFS transporter (FLVCR)	-	1.22	-
AO090003001237	Putative transporter of the ABC superfamily	-	2.87	2.03
AO090003001378	Plasma membrane zinc ion transporter	-	1.46	-
AO090003001519	Amino acid permease	-	1.38	-
AO090003001541	Monocarboxylate transporter, MCT family, aspergillic acid transporter	-	5.00	-
AO090005000509	amino acid transporter	-	1.18	1.98
AO090005000693	MFS pantothenate transporter	-	4.33	-
AO090005000769	Belongs to the MFS. Sugar transporter family (TC 2.A.1.1)	-	4.37	-
AO090005000882	ATP-dependent Clp protease	-	1.22	-
AO090005000968	Belongs to the MFS	-	1.27	1.83
AO090005001027	MFS domain-containing protein	-	2.36	-
AO090005001086	Belongs to the MFS. Sugar transporter family (TC 2.A.1.1)	-	1.66	1.44
AO090005001194	Belongs to the MFS	-	4.57	-
AO090005001495	MFS Transporter	-	4.79	4.95
AO090005001596	Belongs to the MFS	-	1.48	-
AO090009000049	MFS transporter	-	1.83	-

Gene ID	Description	Fold change		
		Glc vs Ace	Glc vs PAC	Ace vs PAC
AO090009000061	MFS domain-containing protein	-	1.40	1.19
AO090009000270	MFS transporter	-	1.93	1.58
AO090009000552	Amino acid transporter	-	1.60	1.07
AO090010000101	MFS transporter	-	5.42	-
AO090010000351	amino acid transporter	-2.77	1.26	4.03
AO090010000406	Mitochondrial thiamine pyrophosphate carrier	-	3.03	-
AO090010000470	Belongs to the MFS. Sugar transporter family (TC 2.A.1.1)	-	1.90	-
AO090010000592	Voltage-gated potassium channel	-	2.85	2.11
AO090010000594	Putative MFS transporter	-	4.56	-
AO090010000689	ABC multidrug transporter	-	2.01	-
AO090010000699	Amino acid permease	-	3.61	3.02
AO090011000110	Putative MFS monocarboxylate transporter	-	4.97	-
AO090011000114	Putative multidrug resistance protein, ABC superfamily	-	3.77	3.19
AO090011000116	Amino acid permease	-	3.72	3.03
AO090011000204	Amino acid permease	-	1.27	1.79
AO090011000231	amino acid transporter	-	1.49	-
AO090011000474	MFS transporter	-	3.55	-
AO090011000706	Putative mechanosensitive ion channel	-	2.11	1.14
AO090011000817	Belongs to the NiCoT transporter family (TC 2.A.52)	-	2.56	1.87
AO090011000881	Putative MFS transporter	-	2.17	-
AO090011000912	Magnesium transporter NIPA-domain-containing protein	-	1.03	-
AO090012000048	Belongs to the MFS. Proton-dependent oligopeptide transporter (POT/PTR) family (TC 2.A.17)	-	5.29	-
AO090012000252	MFS transporter	-	1.56	-
AO090012000312	ABC transmembrane type-1 domain-containing protein	-	5.82	-
AO090012000469	Belongs to the MFS	-	1.82	-
AO090012000784	Predicted protein	-	1.29	-
AO090020000354	MFS domain-containing protein	-	2.77	3.27
AO090020000655	Belongs to the MFS. Sugar transporter family (TC 2.A.1.1)	-	2.36	-

Gene ID	Description	Fold change		
		Glc vs Ace	Glc vs PAC	Ace vs PAC
AO090023000092	Belongs to the oligopeptide OPT transporter family.	2.26	-	-
AO090023000988	Belongs to the MFS. Sugar transporter family (TC 2.A.1.1)	1.08	-	-
AO090026000005	MFS transporter cpaT	-	6.00	5.34
AO090026000008	Major facilitator superfamily transporter	6.19	5.13	-
AO090026000057	Sugar (and other) transporter	2.36	-	-
AO090026000071	Putative choline transport protein	-	5.48	-
AO090026000078	amino acid transporter	-	8.04	9.37
AO090026000144	MFS domain-containing protein	-	7.36	5.41
AO090026000365	MFS domain-containing protein	-	1.72	-
AO090026000396	MFS multidrug transporter	-	4.54	4.42
AO090026000485	Putative efflux pump, antibiotic resistance protein	-	4.83	-
AO090026000506	MFS domain-containing protein	-	2.01	-
AO090026000775	Belongs to the MFS. Sugar transporter family (TC 2.A.1.1)	-	2.75	-
AO090038000090	Belongs to the MFS. Sugar transporter family (TC 2.A.1.1)	-	2.01	-
AO090038000162	ABC transporter transmembrane region	-	1.84	1.94
AO090038000303	Belongs to the ABC transporter superfamily. ABCG family. PDR subfamily (TC 3.A.1.205)	-	1.55	-
AO090038000490	amino acid transporter	-2.78	3.28	6.05
AO090102000026	MFS monocarboxylate transporter	-	2.36	1.89
AO090102000036	Belongs to the MFS	-	5.62	4.87
AO090102000043	Amino acid permease/ SLC12A domain-containing protein	-	1.54	1.66
AO090102000094	Amino acid permease	-	2.73	-
AO090102000343	Belongs to the TrkH potassium transport family	-	1.86	-
AO090102000401	UNC93-like protein	-	4.39	-
AO090103000310	Belongs to the MFS. Sugar transporter family (TC 2.A.1.1)	-	2.86	-
AO090103000479	Belongs to the oligopeptide OPT transporter family	-	2.76	3.46
AO090103000481	Belongs to the MFS. Sugar transporter family (TC 2.A.1.1)	-	6.16	-
AO090113000038	Major facilitator superfamily transporter	-	2.64	-

Gene ID	Description	Fold change		
		Glc vs Ace	Glc vs PAC	Ace vs PAC
AO090113000138	Synaptic vesicle transporter SVOP and related transporters	-	2.05	-
AO090113000139	Belongs to the MFS. Sugar transporter family (TC 2.A.1.1)	-	2.51	-
AO090120000025	MFS domain-containing protein	-	4.98	-
AO090120000093	Magnesium transporter NIPA	-	1.03	-
AO090120000463	Putative MFS monocarboxylic acid transporter	-	1.20	-
AO090138000118	Synaptic vesicle transporter SVOP and related transporters	-	2.23	-
AO090166000046	oligopeptide transporter	-	3.73	3.46
AO090166000089	MFS sugar transporter	-	2.33	-
AO090701000182	MFS domain-containing protein	-	4.74	4.46
AO090701000190	Putative MFS multidrug transporter	-	1.50	-
AO090701000292	Putative magnesium transporter of the NIPA family	-	1.87	-
AO090701000329	MFS domain-containing protein	-	2.77	-
AO090701000616	ABC transmembrane type-1 domain-containing protein	-	4.24	-
AO090701000617	ABC transmembrane type-1 domain-containing protein	-	5.56	4.92
AO090701000621	Amino acid permease	-	7.67	6.47
AO090701000872	Belongs to the ABC transporter superfamily. ABCG family. PDR subfamily (TC 3.A.1.205)	-	2.54	-
AO090003000798	Sulfate permease	-	-	1.13
AO090005001081	Amino acid permease	-1.70	-	2.21
AO090009000115	Sodium/hydrogen exchanger family-domain-containing protein	-3.58	-	5.03
AO090009000400	UDP-Glc Gal endoplasmic reticulum nucleotide sugar transporter	-	-	1.03
AO090010000743	Belongs to the MFS. Proton-dependent oligopeptide transporter (POT/PTR) family (TC 2.A.17)	-6.91	-2.38	4.53
AO090012000602	ABC fatty acid transporter	-	-	1.52
AO090012000689	MFS transporter	-	-	6.13
AO090012000719	Putative multidrug resistance protein, ABC superfamily	-	-	1.27

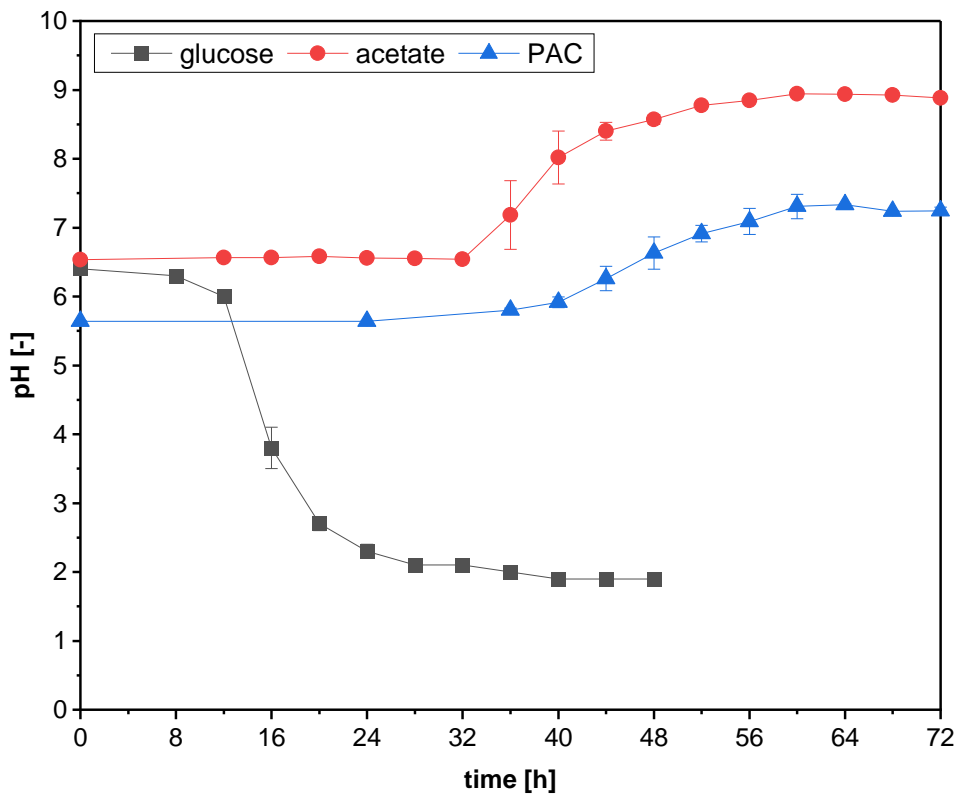
**Appendix 3: Summary on differentially expressed genes included in the transcriptome analysis**

Enzyme	EC	Gene ID	Fold change		
			Glc vs Ace	Glc vs PAC	Ace vs PAC
<b>Amino sugar and nucleotide sugar metabolism</b>					
glucosamine-phosphate N-acetyltransferase	2.3.1.4	AO090120000132	2.11	1.20	-
glucosamine-6-phosphate deaminase	3.5.99.6	AO090103000020	-1.39	2.06	3.45
chitin synthase	2.4.1.16	AO090026000212	4.56	5.68	-
		AO090026000321	1.42	1.52	-
		AO090026000323	1.36	1.37	-
		AO090005000579	1.27	1.36	-
		AO090011000449	1.26	1.30	-
AO090012000084	1.56	1.19	-		
glutamine-fructose-6-phosphate transaminase	2.6.1.16	AO090003001475	2.88	1.65	-
chitinase	3.2.1.14	AO090102000586	-	3.16	2.17
		AO090003000680	2.13	2.22	-
		AO090103000218	-5.36	-	6.20
$\alpha$ -L-arabinofuranosidase	3.2.1.55	AO090012000298	-	3.93	3.06
UDP-glucose 4-epimerase	5.1.3.2	AO090005001490	-	2.48	2.24
		AO090010000463	-	1.08	-
mannose-6-phosphate isomerase	5.3.1.8	AO090023000719	3.60	4.00	-
<b>fatty acid desaturases</b>					
bifunctional $\Delta$ -12/ $\omega$ -3 fatty acid desaturase	1.14.19.6	AO090010000714	-3.07	-3.12	-
$\omega$ -6 fatty acid / acyl-lipid $\omega$ -6 desaturase ( $\Delta$ -12 desaturase)	1.14.19.6/	AO090001000224	-1.04	-	-
	1.14.19.22				
<b>Glycolysis</b>					
6-phosphofructokinase	2.7.1.11	AO090010000444	1.18	1.26	-
fructose-bisphosphate aldolase	4.1.2.13	AO090009000324	-	-1.57	-
glyceraldehyde 3-phosphate dehydrogenase	1.2.1.12	AO090020000265	6.29	5.66	-
		AO090011000414	2.03	3.46	1.43
enolase	4.2.1.11	AO090003000055	-	1.00	-
pyruvate dehydrogenase E1 component $\alpha$ subunit	1.2.4.1	AO090003000290	3.45	3.07	-
		AO090012000948	-	-1.07	-

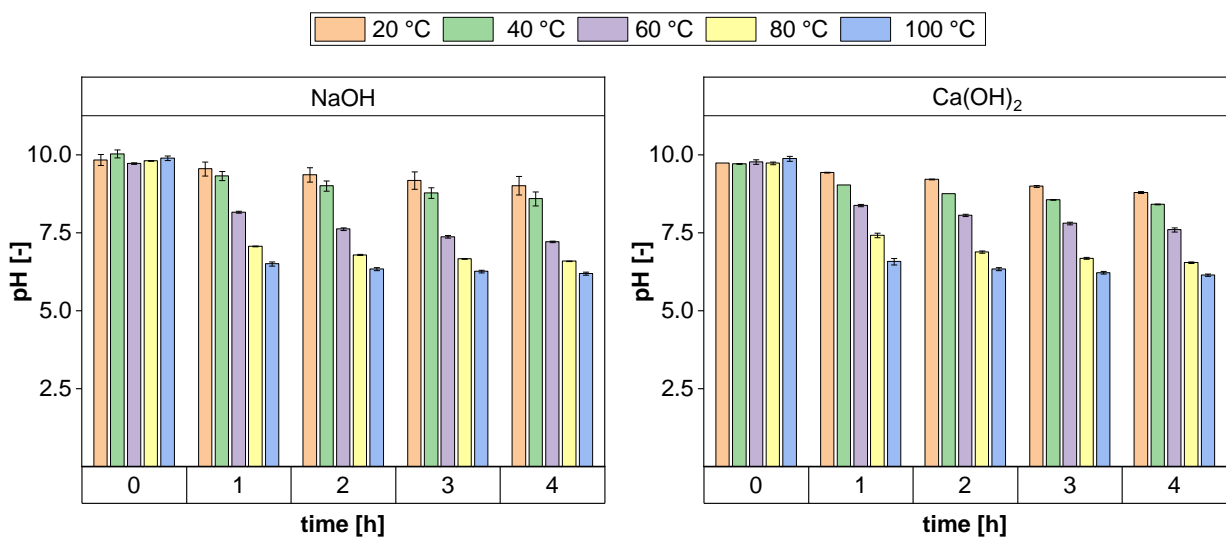
dihydrolipoamide dehydrogenase	1.8.1.4	AO090011000486	-	-1.25	-
pyruvate decarboxylase	4.1.1.1	AO090124000047	3.26	2.64	-
		AO090003000661	1.73	1.07	-
aldehyde dehydrogenase (NAD <sup>+</sup> )	1.2.1.3	AO090009000417	2.55	2.17	-
		AO090026000741	1.32	1.56	-
acetyl-CoA synthetase	6.2.1.1	AO090003001112	-	-1.89	-1.63
carnitine O-acetyltransferase	2.3.1.7	AO090001000295	-	-1.32	-1.54
		AO090026000404	-	-1.15	-
<b>Glyoxylate and TCA cycle</b>					
citrate synthase	2.3.3.1	AO090102000627	-1.36	-1.87	-
aconitase	4.2.1.3	AO090003000415	-	-1.03	-
isocitrate dehydrogenase (NAD <sup>+</sup> )	1.1.1.41	AO090012000629	-	-1.37	-
α subunit					
isocitrate dehydrogenase (NAD <sup>+</sup> )		AO090003000008	-	-1.31	-
γ subunit					
isocitrate dehydrogenase (NADP <sup>+</sup> )	1.1.1.42	AO090005001404	-	-1.07	-
α-ketoglutarate dehydrogenase	1.2.4.2	AO090003001055	-	-1.22	-
E1 component					
α-ketoglutarate dehydrogenase	2.3.1.61	AO090020000008	-	-1.34	-
E2 component		AO090005001174	1.06	1.95	-
succinyl-CoA synthetase β subunit	6.2.1.4	AO090206000040	-	-1.01	-
	6.2.1.5				
succinate dehydrogenase	1.3.5.1	AO090020000415	-	-1.10	-
(ubiquinone) flavoprotein subunit					
malate dehydrogenase	1.1.1.37	AO090701000013	-1.28	-1.33	-
isocitrate lyase	4.1.3.1	AO090009000219	-2.29	-2.95	-
malate synthase	2.3.3.9	AO090009000557	-1.64	-1.73	-
<b>Arginine and proline metabolism</b>					
aspartate aminotransferase	2.6.1.1	AO090120000135	-	-1.36	-
alanine transaminase	2.6.1.2	AO090003000164	-1.39	-1.62	-
glutamate N-acetyltransferase/ amino-acid N-acetyltransferase	2.3.1.35/ 2.3.1.1	AO090701000729	-1.12	-1.39	-
acetylornithine aminotransferase	2.6.1.11	AO090026000394	-	-1.46	-
ornithine carbamoyltransferase	2.1.3.3	AO090023000856	-1.18	-1.98	-
argininosuccinate synthase	6.3.4.5	AO090023000395	-1.59	-1.48	-
argininosuccinate lyase	4.3.2.1	AO090020000418	-1.03	-1.02	-
arginase	3.5.3.1	AO090003000697	1.18	-	-

<b>Glycine, serine and threonine metabolism</b>					
betaine-aldehyde dehydrogenase	1.2.1.8	AO090103000021	-	-1.09	-
D-3-phosphoglycerate dehydrogenase/	1.1.1.95/ 1.1.1.399	AO090009000711	-1.20	-1.74	-
2-oxoglutarate reductase					
phosphoserine aminotransferase	2.6.1.52	AO090023000099	-1.88	-1.89	-
phosphoserine phosphatase	3.1.3.3	AO090020000345	-	-1.08	-
<b>Sulfur metabolism</b>					
sulfate adenylyltransferase	2.7.7.4	AO090020000349	-1.55	-	-
phosphoadenosine phosphosulfate reductase	1.8.4.8 1.8.4.10	AO090020000347	-1.13	-1.39	-
sulfite reductase (NADPH) flavoprotein $\alpha$ -component	1.8.1.2	AO090001000571	-1.62	-1.99	-
sulfite reductase (NADPH) hemoprotein $\beta$ -component	1.8.1.2	AO090012000271	-1.85	-1.94	-
<b>Cysteine and methionine metabolism</b>					
homoserine acetyltransferase/ O-succinyltransferase	2.3.1.3/ 2.3.1.46	AO090701000235	-1.06	-1.15	-
cystathionine $\beta$ -synthase	4.2.1.22	AO090011000931	-1.17	-1.35	-
cystathionine $\gamma$ -lyase	4.4.1.1	AO090103000051	-1.25	-1.63	-
cysteine synthase	2.5.1.47	AO090102000276	-	-1.45	-
5-methyltetrahydropteroyl-triglutamate-homocysteine methyltransferase	2.1.1.14	AO090023000837	-1.33	-	-
<b>Shikimate pathway</b>					
3-deoxy-D-arabino-heptulosonic acid 7-phosphate synthase	2.5.1.54	AO090005000086	-1.20	-1.20	-
		AO090005000886	-1.27	-1.21	-
pentafunctional AROM polypeptide	4.2.3.4 4.2.1.10 1.1.1.25 2.7.1.71 2.5.1.19	AO090012000502	-	-1.08	-
<b>Tryptophan synthesis and degradation</b>					
anthranilate synthase component I	4.1.3.27	AO090003000371	-0.54	-0.66	-
anthranilate phosphoribosyltransferase	2.4.2.18	AO090003001011	-0.54	-0.95	-

anthranilate synthase	4.1.3.27	AO090012000581	-0.54	-0.93	-
indole-3-glycerol phosphate synthase	4.1.1.48				
phosphoribosylanthranilate isomerase	5.3.1.24				
tryptophan synthase	4.2.1.20	AO090026000284	-1.16	-1.07	-
kynurenine 3-monooxygenase	1.14.13.9	AO090005001567	-1.22	-1.51	-
kynureninase	3.7.1.3	AO090003001247	-1.51	-	-
<b>Ubiquinone synthesis</b>					
4-hydroxybenzoate polyprenyltransferase	2.5.1.39	AO090023001001	-	-1.07	-
polyprenyldihydroxybenzoate methyltransferase/ 3-demethylubiquinol 3-O-methyltransferase	2.1.1.114/ 2.1.1.64	AO090003001180	-	-1.12	-
2-methoxy-6-polyprenyl-1,4-benzoquinol methylase	2.1.1.201	AO090001000559	-1.26	-2.03	-
<b>Terpenoid backbone synthesis and mevalonate pathway</b>					
hydroxymethylglutaryl-CoA synthase	2.3.3.10	AO090010000487	-	5.60	5.71
hydroxymethylglutaryl-CoA reductase	1.1.1.34	AO090038000218	-3.98	2.48	6.46
		AO090103000311	-	1.38	-
geranylgeranyl diphosphate synthase, type III	2.5.1.1 2.5.1.10 2.5.1.29	AO090009000093	-	1.95	-
<b>Pyruvate metabolism</b>					
D-lactate dehydrogenase (cytochrome)	1.1.2.4	AO090003001006	-	-	-1.75
D-lactate dehydrogenase	1.1.1.28	AO090023000577	-	-	1.11
hydroxyacylglutathione hydrolase (glyoxalase II)	3.1.2.6	AO090120000408	-	-1.07	-1.05
D-lactate dehydratase (glutathione independent glyoxalase)	4.2.1.130	AO090012000129	-	-6.63	-7.49



**Appendix 4:** Temporal change in pH value during the *A. oryzae* shake flask cultivation performed prior to transcriptome analysis. The data are means of three biological replicates, and the error bars represent the standard deviation.



**Appendix 5:** Temporal change in the pH value during 4 h overliming treatment at different temperatures using NaOH and Ca(OH)<sub>2</sub>. The data are mean values of duplicates and the error bars indicate the standard deviation